Groundwater and surface water interaction, Wairarapa valley, New Zealand

Michael Guggenmos

A thesis submitted in fulfillment of the requirements for the degree of Masters of Science in Physical Geography, at the Victoria University of Wellington, New Zealand

May 2010

Abstract

Physical and chemical interactions between surface and groundwater are complex and display significant spatial and temporal variability. However, relatively little is known about the chemical interaction between surface and groundwater; in particular the temporal scales at which this interaction occurs. The aim of this research was to determine if existing and/or potential water chemistry measurements could be used to investigate the interaction between surface and groundwater bodies in the Wairarapa valley, New Zealand and identify specific locations and timescales at which this interaction occurs. Analyses were undertaken at both regional and local scales.

The regional scale investigation utilised Hierarchical Cluster Analysis (HCA) to categorise 268 historic surface and groundwater sites from the 3000 km² Wairarapa valley into similar hydrochemical clusters in order to infer potential interaction. Six main clusters were identified, primarily differentiated by their total dissolved solids (TDS), redox potential and major ion ratios. Shallow aquifers, located in close proximity to losing reaches of the upper Ruamahanga, Waiopoua and Waiohine Rivers, were grouped with similar Ca^{2+}-HCO_3^- type surface waters, indicating (potential) recharge from these river systems. Likewise, rainfall-recharged groundwater sites that displayed higher Na^+ relative to Ca^{2+} and Cl^- relative to HCO_3^- were grouped with similar surface waters such as the Mangatarere and lower Waingawa streams. This suggests the provision of this rainfall-recharged signature to river base flow. Deep anoxic aquifers, high in TDS, were grouped together, but showed no statistical link to surface water sites. Results from the regional scale investigation highlight the potential use of HCA as a rapid and cost-effective method of identifying areas of surface and groundwater interaction using existing datasets.

A local scale investigation utilised existing quarterly and monthly hydrochemical data from the Mangatarere and Waiohine Rivers and nearby groundwater wells in an attempt to gain insight into temporal variability in surface and groundwater interactions. Time series analysis and HCA were employed, however, the coarse time scales at which data was available made it difficult to make reliable inferences regarding this interaction.

To overcome this issue, upstream and downstream surface and groundwater gauging stations were established in the Mangatarere Stream catchment for a 92 day period. Continuous electrical conductivity, water temperature and stage measurements were obtained at three of the four stations, along with one week of hydrochemical grab sampling. The fourth gauging station provided a more limited dataset due to technical issues. The downstream Mangatarere Stream received 30-60% of base flow from neighbouring groundwaters which provided cool Na^+-Cl^- type waters, high in TDS and NO_3^- concentrations. This reach also lost water to underlying groundwaters during an extended dry period when precipitation and regional groundwater stage was low. The upstream groundwater station received recharge primarily from precipitation as indicated by a Na^+-Cl^--NO_3^- signature, the result of precipitation passage through the soil-water zone. However, it appeared 2-4 m³/s of river recharge was also provided to the upstream groundwater station by the Mangatarere stream during an extended storm event on JD021-028. Mangatarere surface waters transferred a diurnal water temperature pattern and dilute Na^+-Ca^{2+}-Mg^{2+}-HCO_3^--Cl^- signature to the upstream groundwater station on JD026-028. Results obtained from the Mangatarere catchment confirm the temporal complexities of ground and surface water interaction and highlight the importance of meteorological processes in influencing this interaction.

Acknowledgements

There are a number of people and organisations that I would like to acknowledge and thank for their support and assistance in the completion of this research thesis:

- Firstly I would like to thank my supervisors Bethanna Jackson and Chris Daughney. You both provided an immense level of support, guidance and insight into this research and its various sub-projects. In particular I would like to thank Chris for pulling me out of the mountains and stimulating my interest in ground and surface water interactions.

- I would like to gratefully thank the Greater Wellington Regional Council for their financial assistance and logistical support. Without the council and its dedicated environmental team this project would not have been possible. Special thanks goes to Sheree Tidswell from the Masterton Office who provided an immense amount of her time to this project. I also wish to thank Edward Lee, Doug McAlister, Alton Perrie, Juliet Milne, Ted Taylor, and Laura Watts.

- Special thanks go to John Quinn and Reid's Piggery in the Wairarapa valley for allowing me to establish monitoring stations on their properties. In particular thanks must go to Andrew Hosken for his support and time.

- To GNS Science and all the team in the groundwater department for providing generous financial assistance and support.

- I would like to thank my office mates Conway Penne, Chris Gazley and Louise Gallard for answering all those stupid questions and putting up with my stinky gym gear.

- To all my friends and colleagues at Victoria University for your encouragement, proof reading and words of support. Special mention must go to Jan Thompson and Deb Maxwell – hydrology would not be nearly as sexy without you!

- Hamish McKoy, Gigi Woods and Andrew Rae for providing technical support and advice.

- Richard and the Willemsen family from the Taratahi Hotel in Carterton for hosting and entertaining me during my field work.

- Hill Laboratories in Hamilton for undertaking my chemical analyses.

- Lastly, the success of this research would not have been possible without my friends, flat mates, field assistants and family. I owe you all for your patients, support and belief.

Table of contents

List of Figures

List of Tables

List of Equations

Index of commonly used chemical species

Symbol	Definition
Al^{3+}	Aluminum
$C_6H_{12}O_6$	Glucose
Ca^{2+}	Calcium
$CaCO_3$	Calcite
$CaSO_4$	Calcium sulphate
CH_2O	Carbohydrates
CH_4	Methane
Cl^-	Chloride
CO_2	Carbon dioxide
CO_3^{2-}	Carbonate
Cu	Copper
F^-	Fluorine
Fe^{2+}	Iron
H^+	Hydrogen (proton)
H_2CO_3	Carbonic acid
H_2O	Water
H_2S	Hydrogen sulphide
HCO_3^-	Bicarbonate
K^+	Potassium
Mg^{2+}	Magnesium
Mn	Manganese
MnO_2	Manganese oxide
N_2	Nitrogen gas
Na^+	Sodium
NaCl	Halite
NH_4^+	Ammonium
Ni	Nickel
NO_3^-	Nitrate
O_2	Oxygen
OH-	Hydroxyl ion
P	Total dissolved phosphate
PO_4^3	Phosphate
SO_4^{2-}	Sulphate

Chapter 1
Introduction

Groundwater plays a crucial role in the global hydrological cycle making up approximately 89% of the world's fresh unfrozen water (Younger, 2007). As a result groundwater is of significant importance for human use and consumption. However, increased pressure from human activities can alter natural subsurface processes and rapidly change the quantity and quality of groundwater bodies and the surface water systems with which they interact. Groundwaters interact with surface waters in a variety of different ways, principally by gaining water from and providing water to river systems (Freeze and Cherry, 1979). These forms of river-aquifer interaction will be the main focus of this research.

In the past surface and groundwater bodies were largely treated individually, with little thought given to their interaction (Winter *et al.,* 1998). However, significant progress has been made in the last few decades to understand the physical mechanisms of their interaction. Recent hydrological approaches generally attempt to infer interaction by quantifying changes in water temperature (e.g. Silliman *et al.* 1993), discharge (e.g. Schmalz *et al.,* 2007), and/or chemistry (e.g. Burden, 1982; Kumar *et al.,* 2009) in both surface and groundwater bodies. It is now acknowledged that ground and surface waters interact at a variety of spatial and temporal scales, the degree of which is influenced by meteorological conditions, geological formations and anthropogenic and physiographic processes. This interaction influences the quantity and quality of both surface and groundwater as water moves across the stream-aquifer boundary (Dahm *et al.,* 1998; Winter *et al.,* 1998). It is recognised that chemical parallels between surface and groundwater bodies can be used to indicate potential processes and flow pathways with numerous studies suggesting similarities in water types, total dissolved solids (TDS) and ion ratios between interacting water bodies (e.g. Burden, 1982; Taylor *et al.,* 1989; Kumar *et al.,* 2009). However, relatively little is known about the chemical interaction between ground and surface water bodies and in particular the temporal scales at which this interaction can occur.

Numerous studies have shown the interaction between ground and surface waters is temporally variable with the transfer of water across the stream-aquifer interface varying over weekly or sub-daily time scales (e.g. Silliman *et al.,* 1993; Keery *et al.,* 2006; Schmalz *et al.,* 2007). Current local and global hydrochemical monitoring programmes may fail to capture the full extent of this interaction and potentially provide misleading or false inferences. To fully explore hydrochemical changes and to gain a greater understanding of current hydrological processes and theories new detailed field derived data are required (Kirchner, 2006; Schmalz *et al.,* 2007).

Current knowledge surrounding the chemical interaction between ground and surface waters in New Zealand is limited. Although studies have investigated potential interaction (e.g. Burden, 1982; Taylor *et al.,* 1989; Stewart *et al.,* 2003), few have investigated the temporal extent of this interaction and the wider processes that influence it. This knowledge gap likely stems from the treatment of each water body as an individual resource and the monthly, quarterly and yearly timeframes under which current local and nationwide hydrochemical monitoring is undertaken. Further, National State of the Environment (SoE) reporting is conducted by individual research institutions that fail to coincide sampling programmes with each other or to analyse concurrent hydrochemical changes in surface and groundwater bodies. Despite these issues, existing hydrochemical datasets may offer some insight into ground and surface water interaction within New Zealand and the locations at which this interaction occurs.

The main aim of this research was to determine if existing and/or potential water chemical measurements could be used to investigate the interaction between surface and groundwater bodies in the Wairarapa valley, New Zealand and to investigate specific locations and timescales at which this interaction occurs. In order to achieve this, a comparison of surface and groundwater water quality was undertaken at both regional and local scales. Regional scale interaction was assessed using historic hydrochemical medians from both surface and groundwater sites in the entire Wairarapa valley with the application of Hierarchical Cluster Analysis (HCA). This procedure aimed to link surface and groundwater sites into hydrochemical clusters or facies according to similarities in water chemistry, and to infer interaction based on these similarities.

A local scale temporal investigation of this potential interaction was also undertaken utilizing existing monthly and quarterly hydrochemical datasets from the Waiohine and Mangatarere Rivers in the Wairarapa valley and surrounding groundwater wells. This investigation aimed to offer insight into the temporal variability at which surface and groundwater interaction occur by focusing on temporal changes in existing water quality data from selected water bodies identified as potentially interacting through regional scale HCA. Again it was assumed that parallel changes in water quality could be used to infer potential surface and groundwater interaction.

However, as already mentioned, the interaction between surface and groundwater is known to show considerable temporal variability due to the influences of meteorological, fluvial, anthropogenic and geological processes. It is acknowledged that existing monthly and quarterly water quality monitoring undertaken by local and regional government may fail to capture this variability. Therefore, in order to assess the potential temporal scale at which ground and surface water interaction occurs, a high resolution (sub-daily) field investigation was undertaken at two reaches of the Mangatarere stream over a three month period during the summer of 2009-2010. This high resolution investigation focused upon temporal changes in chemical, hydrological and meteorological parameters from two surface and two groundwater gauging sites in the Mangatarere catchment. Quantification of these parameters enabled a systematic comparison of these systems and allowed links to be drawn between the water bodies to infer interaction. A full overview of the experimental design of this research and the steps it entails is provided in Figure 1.1.

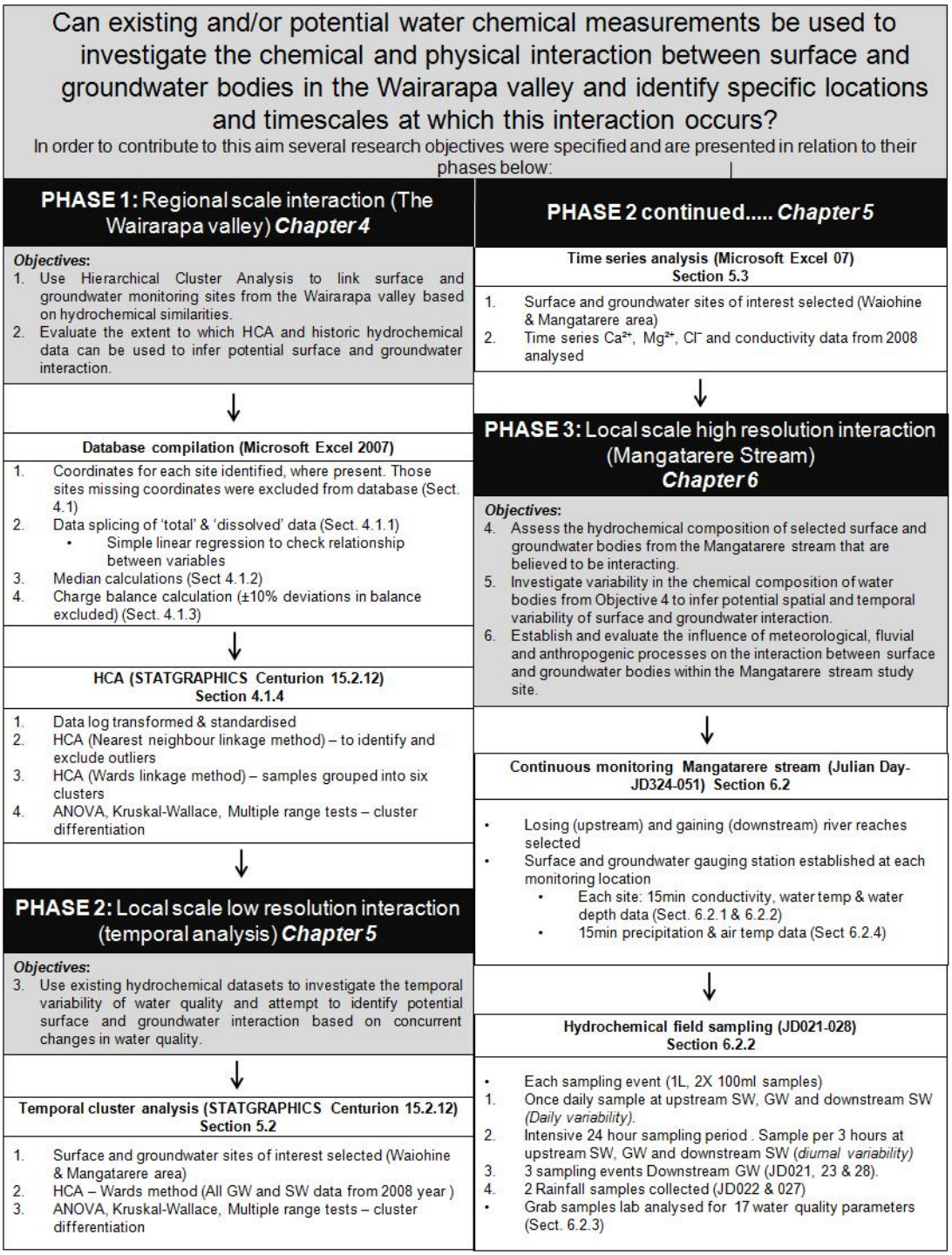

Figure 1.1. Schematic representation of the experimental design undertaken for this research. Each phase of the research (regional, local scale temporal and high resolution local scale) is related to specific research objectives pursued with methodologies.

Research was undertaken in the Wairarapa valley of New Zealand, an environment with a diverse and complex hydro-geological setting. Numerous river systems throughout the valley are thought to display strong hydraulic links to underlying groundwaters (Jones and Gyopari, 2006). Approximately 76% of the Wairarapa valley is occupied by pastoral agriculture, a practice that places significant pressure on surface and groundwater bodies (Jones and Baker, 2005). Agricultural run-off is known to accumulate in the region's groundwaters and therefore can potentially be transferred to surface water bodies. As agriculture continues to intensify, further information will be required about the interaction of ground and surface water in the area to foster effective environmental management of these resources.

In order to achieve the overall aim of this research a number of specific research objectives were outlined.

1. Use Hierarchical Cluster Analysis to link surface and groundwater monitoring sites from the Wairarapa valley based on hydrochemical similarities.
2. Evaluate the extent to which multivariate statistical methods (i.e. HCA) and historic hydrochemical data can be used to infer potential areas of surface and groundwater interaction.
3. Use existing hydrochemical datasets to investigate the temporal variability of water quality and attempt to identify potential surface and groundwater interaction based on concurrent changes in water quality.
4. Assess the hydrochemical composition of selected surface and groundwater bodies from the Mangatarere stream that are believed to be interacting.
5. Investigate variability in the chemical composition of water bodies from Objective four to infer potential spatial and temporal variability of surface and groundwater interaction.
6. Establish the influence of meteorological, fluvial and anthropogenic processes on the interaction between surface and groundwater bodies within the Mangatarere stream study site.

This research is divided into seven chapters. Chapter two introduces the broad theoretical concepts of ground and surface water systems and their physical and chemical interactions. This is followed by an overview of the specific geology, hydrogeology, climate and land use of the Wairarapa valley in Chapter three. Chapter four presents the methodologies and results from the regional scale investigation, while Chapter five focuses specifically on local scale temporal interaction from the Waiohine and Mangatarere streams using existing low resolution data. Chapter six provides a detailed account of the high resolution local scale field investigation undertaken on the Mangatarere stream, beginning with a detailed description of the field site, followed by the methodologies employed and analyses and interpretation of the results. This is followed in chapter seven with an overview of the main findings of this research and a range of recommendations and avenues for future research.

Chapter 2
Surface and groundwater interaction

Groundwater is a major component of the earth's hydrological cycle and displays strong hydraulic links with surface water bodies (Freeze and Cherry, 1979; Winter *et al.*, 1998). This interaction is important for surface water recharge and supply as 98% of the world's fresh unfrozen water is groundwater (Schwartz and Zhang, 2003) and significant quantities of this water are transferred across the stream-aquifer interface. The interaction between ground and surface water is complex and is influenced by the geological and climatic setting of an environment and a variety of physiographic processes. Knowledge of groundwater flow systems and the processes that influence them and their interaction with surface water bodies is essential for sustainable management of this natural resource.

This chapter begins with a broad overview of groundwater hydrology, introducing the principles of groundwater movement, groundwater flow systems and the topographic and geological phenomena that influence such systems. This is followed in section two with an outline of the physical mechanisms of surface and groundwater interaction and the spatial and temporal scales at which this interaction occurs. Section three presents an overview of hydrogeochemistry, groundwater chemical evolution and the specific chemical reactions and transport processes responsible for changes in water composition between and within surface and groundwater. Chemical interactions between ground and surface water bodies are also introduced. Finally, section four discusses current limitations and knowledge gaps in the literature.

2.1 Physical hydrogeology

Water occurs beneath the earth's surface in several primary zones (Winter *et al.*, 1998). The first of these, the soil-water zone, occurs directly beneath the earth's surface (Figure 2.1). The distribution and movement of moisture in this zone depend primarily on atmospheric conditions, recent exposure of the soil zone to moisture and boundary conditions between zones (Bear, 1979).

Thin films of moisture known as hygroscopic water are held to soil particles within the soil-water zone and the strong adhesive force by which this occurs renders this water unavailable for plant uptake. Upon the further addition of moisture to the soil-water zone through precipitation, flooding of the ground surface and irrigation, continuous films of water and menisci form around and between soil particles. This water, known as capillary water, is held by surface tension and is readily available to plants.

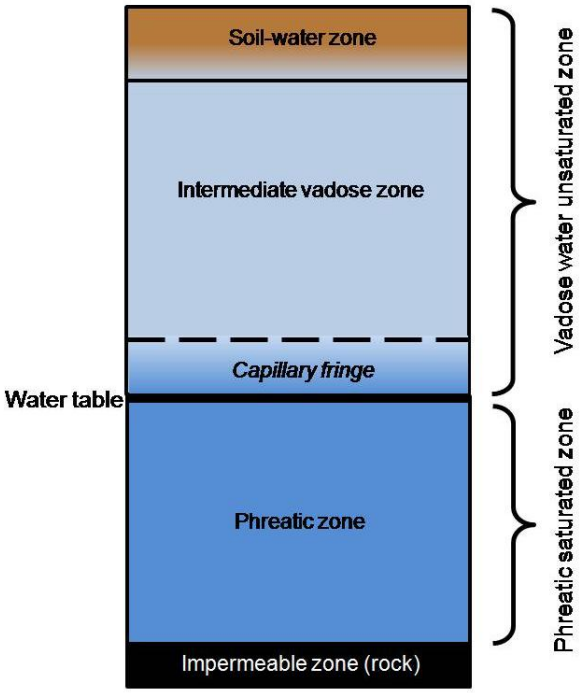

Figure 2.1. Simplified schematic representation of subsurface waters zones. Modified from Todd and Mays (2005).

During periods of excessive infiltration to the soil-water zone, field capacity, or the total amount of water which a soil column can hold against gravity, is exceeded. Assuming sufficient soil permeability, surplus waters are able to percolate downwards through soil voids created by the movement and decay of plant roots. This water moves due to gravitational forces through the soil-water zone into the intermediate vadose zone and/or phreatic zones (Figure 2.1). However, if soil permeability is low or the water table nears the surface these soils become saturated and the onset of overland flow conditions can occur.

The intermediate zone contains both water and air within its interstices and is therefore very similar to the soil-water zone. However, when the water table is within or directly below the soil-water zone, an intermediate vadose zone does not exist. The soil-water zone, intermediate vadose zone and capillary fringe make up the total vadose zone, an area of unsaturated sub-surface material (Figure 2.1).

Located directly below the vadose zone, the phreatic zone contains soil voids that are entirely filled with water under hydrostatic pressure (Figure 2.1). The two zones are separated by the water table, a surface at atmospheric pressure that marks the transition from unsaturated to saturated zones. Although the pressure boundary between these two zones is clearly defined, a capillary fringe of saturation can occur directly above the water table (Figure 2.1) (Bear, 1979; Freeze and Cherry, 1979). Within this capillary fringe negative pressure is experienced and capillary forces are able to draw water up from the water table (Hiscock, 2005). The thickness of the capillary fringe is dependent on soil properties and the heterogeneity of the soil. Moisture content generally decreases with distance above the water table under homogeneous soil conditions (Bear, 1979).

2.1.1 Groundwater movement

Groundwater is perpetually in motion within the natural sub-surface environment. This movement is governed by a set of well established hydraulic principles in which water moves through the porous media according to the availability of energy. The movement of groundwater through the sub-surface environment can be expressed by Darcy's flow law (Equation 2.1).

$$Q = -KA\frac{\mathrm{d}h}{\mathrm{d}l} \qquad (2.1)$$

Where:
Q = Groundwater flow (m^3/s)
K = hydraulic conductivity of porous medium (m/s)
A = cross sectional area of flow (m^2)
dh = change in hydraulic head ($h_1 - h_2$) (m)
dl = length or distance between hydraulic head measurements (m)

Empirically derived, Darcy's flow law states that flow through a porous medium is proportional to hydraulic conductivity (K) and changes in hydraulic gradient (dh/dl). Further, flow is inversely proportional to the length of the groundwater flow path

(Todd and Mays, 2005). Darcy's law can be applied to the majority of groundwater flow scenarios, however issues arise in turbulent, non-viscous flow (Reynolds number >10). The ease with which groundwater moves through a porous medium is described as the hydraulic conductivity. Hydraulic conductivity is influenced by a number of factors including fluid viscosity, porosity, particle size and their arrangement (Todd and Mays, 2005). In saturated conditions, high hydraulic conductivity values are directly associated with permeable units like sand and gravel, while poorly permeable materials such as clay yield low values (Schwartz and Zhang, 2003). Illustrative hydraulic conductivity values are provided by Schwartz and Zhang (2003) in Table 2.1.

Table 2.1. Illustrative saturated hydraulic conductivity values for a range of minerals.

Materials	Hydraulic Conductivity (m/s)
Gravel	$3 \times 10^{-4} – 3 \times 10^{-2}$
Coarse Sand	$9 \times 10^{-7} – 3 \times 10^{-3}$
Fine Sand	$2 \times 10^{-7} – 2 \times 10^{-5}$
Clay	$1 \times 10^{-11} – 4.7 \times 10^{-9}$
Sandstone	$1 \times 10^{-10} – 6 \times 10^{-6}$
Permeable Basalt	$4 \times 10^{-7} – 2 \times 10^{-2}$
Fractured metamorphic rock	$9 \times 10^{-9} – 3 \times 10^{4}$
Unfractured metamorphic rock	$3 \times 10^{-14} – 2 \times 10^{-10}$

Hydraulic gradient is the change in hydraulic head (d*h)* across a given distance (Freeze and Cherry, 1979). Groundwaters flow along a hydraulic gradient from an area of high hydraulic head to low hydraulic head. Hydraulic head (Equation 2.2) refers to the energy available for groundwater flow, and is a function of elevation and hydraulic pressure (Winter *et al.*, 1998; Schwartz and Zhang, 2003). Measurements of hydraulic head are given according to a common datum such as sea level and can be joined by equipotential lines according to areas of similar measurements. In groundwater hydrology, flowlines can be constructed perpendicular to the equipotential lines, indicating the movement of groundwater from areas of high to low hydraulic head (Figure 2.2).

$$h = \psi + z \qquad (2.2)$$

Where:
h = hydraulic head (m)
ψ = pressure head (m). Force per unit area based on elevation that water rises in the piezometer
z = elevation of the bottom of piezometer

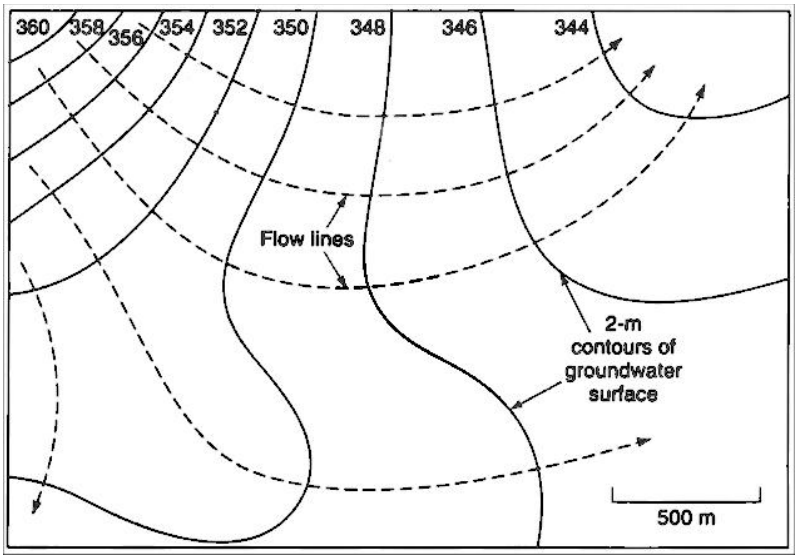

Figure 2.2. Groundwater flowlines constructed perpendicular to equipotential lines, indicating direction of groundwater movement. Modified from Todd and May (2005).

Groundwater flow moves from areas of recharge to areas of discharge (Figure 2.3). Recharge areas are zones where water flow is directed downwards away from the water table into the saturated zone. In contrast, a discharge area is a zone where water flow moves towards low pressure at the water table, and in which water can be lost from the groundwater system through seeps, springs, streams and evapotranspiration (Freeze and Cherry, 1979; Schwartz and Zhang, 2003). Generally, the water table lies at and/or is relatively close to zones of groundwater discharge (Figure 2.3) (Freeze and Cherry, 1979).

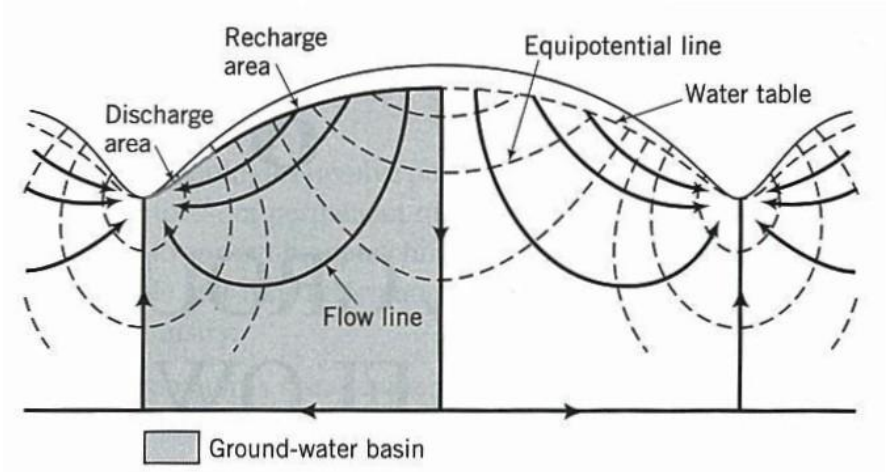

Figure 2.3. Simplified schematic representation of groundwater recharge and discharge areas. Presented without change from Schwartz and Zhang (2003).

2.1.2 Groundwater flow systems

Groundwater flow systems can be hierarchically classified according to the distribution and scale of recharge and discharge areas (Figure 2.4). At the macro scale a regional flow system occurs in which groundwater recharge areas occur along major topographic highs and groundwater divides. Resulting discharge areas are located at major draining divides or the bottom of the basin (Sophocleous, 2002). Regional groundwater flow systems often cover large distances and discharge to major rivers, lakes or the ocean (Sophocleous, 2002). An intermediate flow system occurs where smaller recharge and discharge zones are separated by one or more topographic highs or lows. This can be distinguished from a local flow system in which recharge and discharge points are immediately adjacent to each other with no topographic separation. Generally, highest volumes of water flow are associated with processes occurring at the local flow system level (Todd and Mays, 2004).

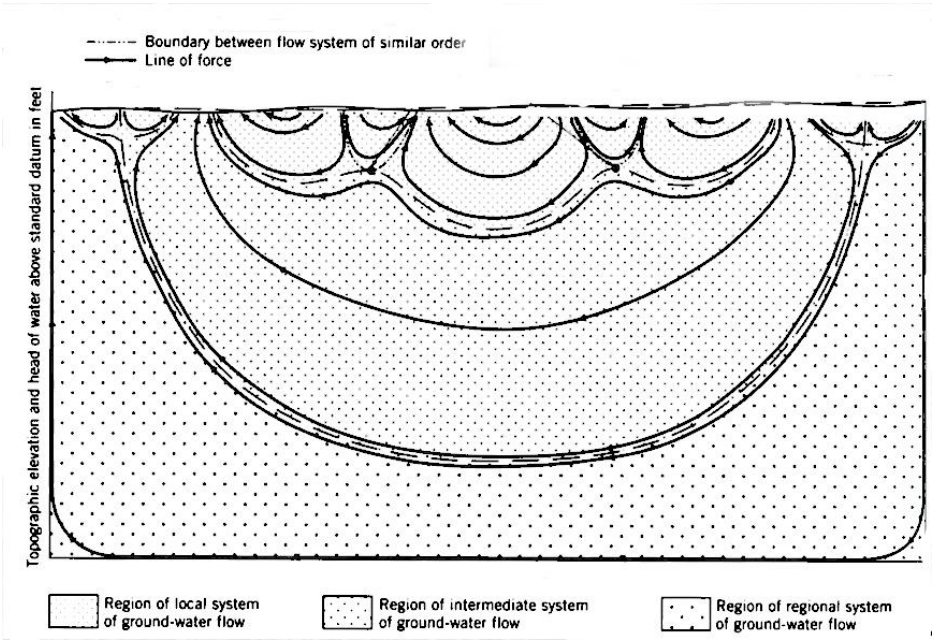

Figure 2.4. Simplified schematic representation of regional, intermediate and local groundwater flow systems. Presented without change from Schwartz and Zhang (2003).

2.1.3 Topographic and Geological influences

Topography and geology play significant roles in defining the location of groundwater recharge and discharge zones, and therefore groundwater flow systems. Generally, the water table follows and resembles surface topography (Figure 2.3), however heterogeneities in geology and depositional layers can complicate this scenario.

Topographic highs are usually associated with recharge zones, whereas the coinciding of topographic lows and the water table is likely to create discharge points (Schwartz and Zhang, 2003).

The importance of topography in determining these points is highlighted in Figure 2.5 by Freeze and Cherry (1979). Here two groundwater systems identical in depth and lateral extent are differentiated by surface topography. Figure 2.5a identifies a uniform single flow system (regional) in which groundwater flow mimics the gradual decline of the surface topography. In contrast, in Figure 2.5b local changes in topography create numerous recharge and discharge points, and therefore local flow systems within the major regional flow systems.

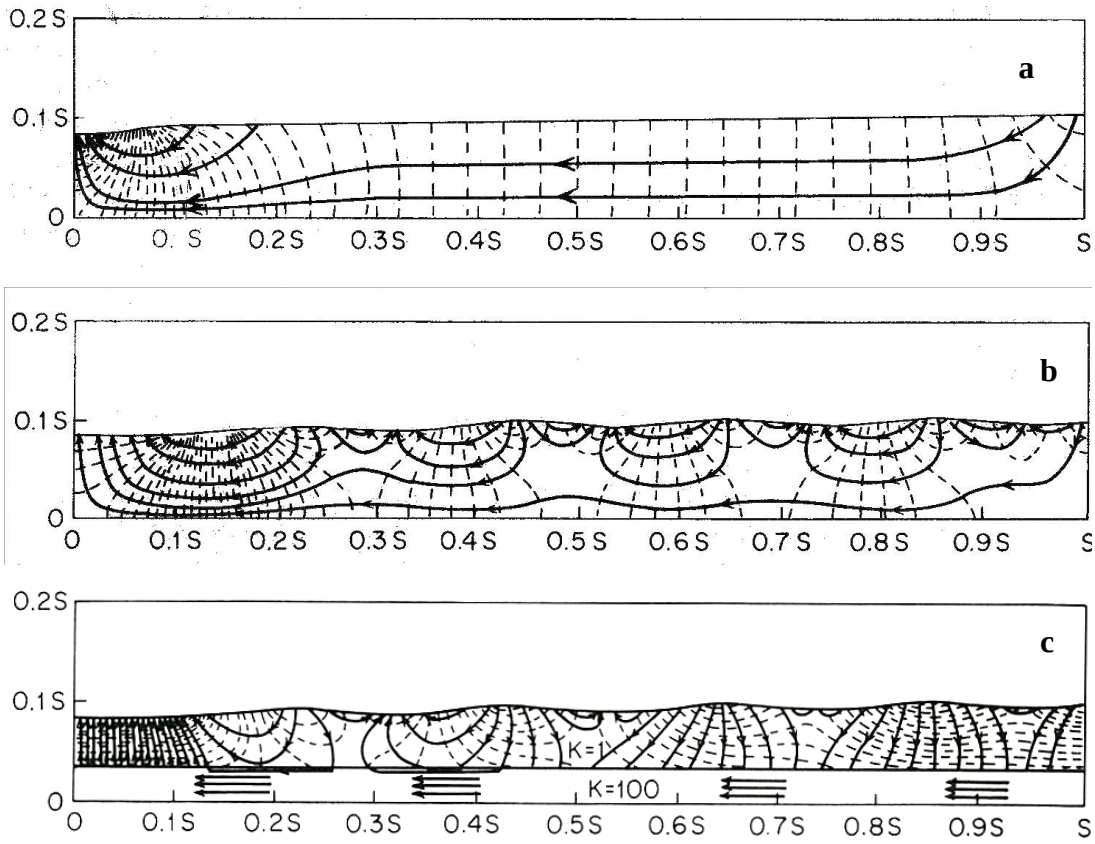

Figure 2.5. (**a**) Uniform single flow system, (**b**) numerous local flow systems that straddle a major regional flow system, (**c**) numerous local flow systems that are separated from a regional flow system by an impermeable medium. Presented without change from Freeze and Cherry (1979).

Geology also plays a significant role in the distribution and scale of groundwater flow systems. Subsurface media show considerable variation in their permeability, and display various hydraulic conductivities (Table 2.1) (Sophocleous, 2002). For example, layers of poorly sorted gravels have a high hydraulic conductivity in comparison to a homogenous layer of clay. Similarly, variability in permeability can also occur within a single medium, with the same layer or body of sediment (e.g. clay) displaying different hydraulic conductivities. These media are heterogeneous (Freeze and Cherry, 1979). The distribution of both homogenous and heterogeneous media therefore determines permeability layers, which in part restrict and channel groundwater flow patterns. Toth (1963) demonstrated that neighbouring layers of sediment allow multiple flow systems to occur side by side due to their diverse hydraulic conductivity. For example, several low permeability local flow systems can override a regional flow system consisting of a highly permeable basal aquifer (Figure 2.5c). Likewise the distribution of impermeable layers can further influence distribution of surface recharge and discharge areas, and the quantity of water discharged (Freeze and Cherry, 1979).

The natural distribution of geological formations and permeability also determines the location of aquifers, aquitards and aquicludes (Figure 2.6). Geological formations that are able to transmit and provide substantial quantities of water are known as an aquifer, and consist of one or more layers of subsurface material with high permeability (Pinder and Celia, 2006). An aquifer between two layers of impermeable material is confined, while unconfined aquifers have the water table as their upper boundary (Freeze and Cherry, 1979). The terms aquitards and aquicludes are applied to variety of different confining layers. An aquitard can also transmit water, however this transmission occurs at reduced quantities due to the lower permeability of the sub-surface medium. In contrast, an aquiclude is a saturated geological medium that is unable to transmit significant water under a normal hydraulic gradient and is generally a confining bed. Examples of aquicludes include clay which can act as a barrier to groundwater flow (Freeze and Cherry, 1979; Hiscock, 2005; Todd and Mays, 2005).

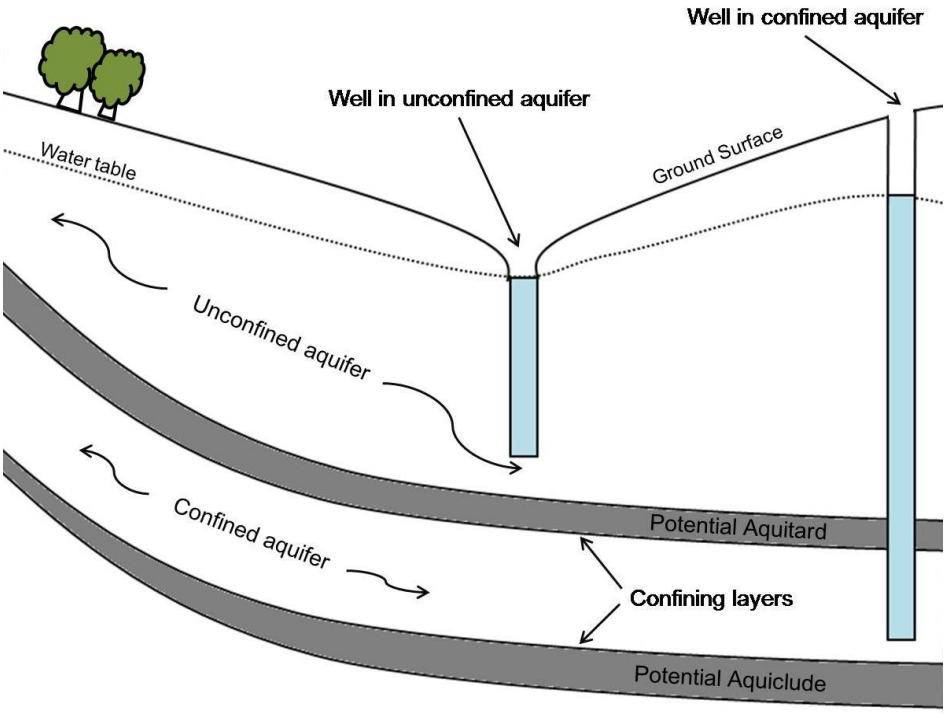

Figure 2.6. Role of geological formations (confining layers) in determining aquifer, aquitard and aquiclude locations.

2.2 Surface water and groundwater interaction

2.2.1 Stream and aquifer interaction

Ground and surface waters interact in a variety of different ways, principally through influent and effluent stream systems (Freeze and Cherry, 1979; Woessner, 2000). This mechanism of stream/aquifer interaction will be the main focus of this research and a variety of methods used to investigate this interaction will be presented in this section. An influent stream loses water through streambed seepage into underlying groundwater systems. This occurs when stream stage is higher than the water table, and streambed permeability allows a hydraulic connection to be made between the two water bodies (Figure 2.7a). An influent stream can also occur when stream and groundwater systems are not hydraulically connected and waters seep down through an unsaturated zone to the water table directly (Figure 2.7b). This downward movement occurs due to gravity and capillary pressures and is known as a disconnected influent stream. Groundwater systems also discharge water into nearby surface streams. Known as an effluent or gaining stream system, this occurs when the adjacent aquifer water table is at and/or higher than stream stage (Figure 2.7c) (Freeze and Cherry, 1979; Schmalz *et al.,* 2007).

In many streams base flow is provided by groundwater, through this effluent process, for most of the year (Brunke and Gonser, 1997). For the remainder of this study classification of ground and surface water interaction will be presented in accordance with an effluent or influent stream system.

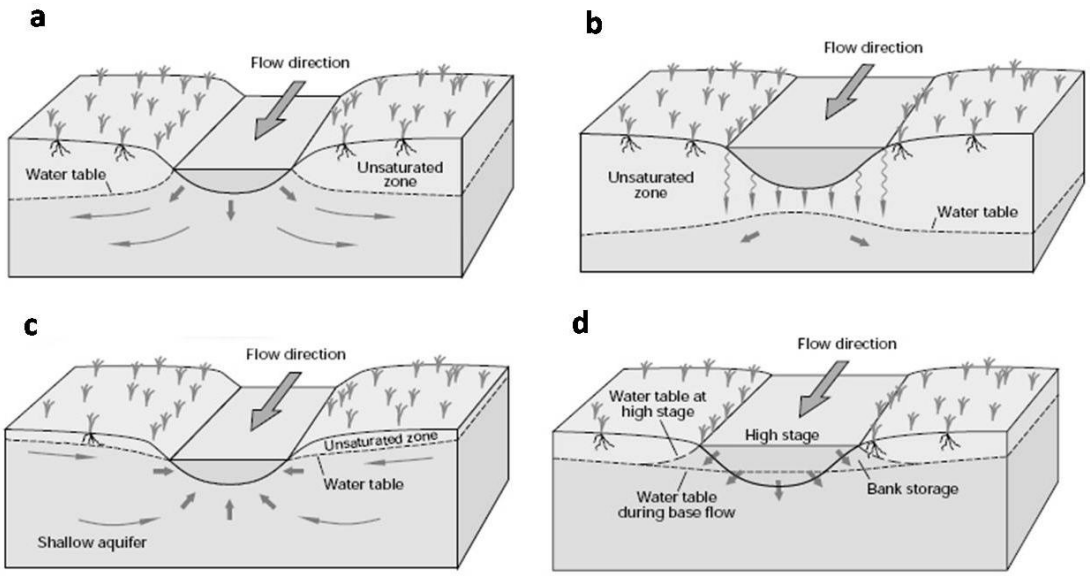

Figure 2.7. Schematic representation of (**a)** Influent (losing) stream, hydraulically connected to the groundwater system, (**b)** disconnected losing stream; **(c)** hydraulically connected gaining (effluent) stream system and (**d)** storage of excess water in neighbouring river banks. *Source:* Winter et al. (1998).

During high precipitation and flood events surplus waters may be introduced into stream banks as storage (Figure 2.7d). Following the flood peak a decline in river level occurs, and bank storage returns to the river system (Kondolf *et al.*, 1987). Likewise, as the water table recedes bank storage can infiltrate down to the groundwater system. The volume of water stored within the bank depends on the duration and intensity of the flood hydrograph as well as the transmissivity and storage capacity of the aquifer (Brunke and Gonser, 1997).

2.2.2 Spatial and temporal variability of stream-aquifer interaction

The interaction between stream and groundwater systems displays a wide degree of spatial and temporal variability, with individual streams displaying both influent and effluent reaches across various time scales (Winter *et al.*, 1998; Sophocleous, 2002). This interaction can change over a relatively short time period as climatic events and human induced pumping rapidly change stream stage and the water table.

Further, intense hydrological events and human modification of stream channels are able to change the geomorphologic setting of river systems (e.g. aggrading and degrading surfaces and stream bed hydraulic conductivity) and therefore the spatial distribution and extent of interaction with groundwater systems (Dahm *et al.*, 1998). Generally, under low precipitation, stream stage remains relatively low and receives recharge from groundwater sources (effluent). In contrast, during high precipitation events, an increase in river stage above the water table can lead to recharge of underlying aquifers (influent). This was highlighted in the Kielstau catchment, Germany by Schmalz *et al.* (2007) who investigated parallel changes in ground and surface water stage to infer interaction. During the period monitored, the Kielstau River typically received inflow from neighbouring groundwater wells as groundwater stage was *ca.* 20-40cm higher than the river stage. However, during high precipitation and flood events levels of the Kielstau River increased, reducing this difference to around 9cm and reversing the flow direction/gradient from the river to neighbouring groundwater systems.

Spatial and temporal variability in surface and groundwater interaction was also apparent on the river Tern in the United Kingdom (Keery *et al.*, 2006). Here variations in riverbed sediment temperature and water temperature were used to identify the transfer of water between surface and groundwater bodies. Results indicated that the upstream reaches of the Tern displayed a loss of surface water to underlying groundwater systems, whereas downstream the Tern received recharge from groundwaters as the water table approached surface topography. Further, this downstream effluent condition displayed a temporal pattern, with increased groundwater flux to the Tern during the summer months. This was attributed to high summer flow conditions removing settled bed sediments, enhancing permeability and increasing exchange at the stream/groundwater interface.

Human induced groundwater extraction can also influence the temporal phenomena of surface and groundwater interaction (Winter *et al.*, 1998; Sophocleous, 2002). Heavy extraction of groundwater may result in the lowering of the water table to a level below that of stream stage. This can induce influent conditions as surface waters move to replenish groundwater sources.

In contrast the application of irrigation water to the earth's surface can result in increased groundwater recharge, subsequently raising the water table and inducing effluent conditions and increased surface discharge (e.g. springs).

The spatial organisation of geomorphic environments and their associated geological formations and fluvial processes further influences the interaction between surface and groundwater systems. Dahm *et al.* (1998) and Brunke and Gonser (1997) present several hypothetical geomorphic stream environments and their various exchange scenarios with alluvial aquifers. The classification of these reaches is largely based on the works of Amoros *et al.* (1987) and Gregory *et al.* (1991) and is presented in Figure 2.8. In general, the headwaters of streams are relatively confined, single straight channels with high transport capacity and erosive energy. Lateral and vertical exchange of water at the stream-aquifer interface is of minor significance here, although exchange processes tend to display influent properties with waters lost to the groundwater system (Brunke and Gonser, 1997). As headwaters become unconfined and braided river patterns become dominant, rapid channel migration and the high permeability of sediments allow higher vertical and lateral exchange of water (D'Angelo, 1993; Brunke and Gonser, 1997). This exchange between the ground and surface water interface is believed to be greatest in aggrading reaches as the water table is further separated from the streambed (Dahm *et al.*, 1998). As a river progresses into a meandering stream it becomes characterised by one sinuous channel and continuous lateral migration over time. Strong exchanges of water can occur in this section, although fine particulate matter can cause clogging of the stream bed and a reduction in this interaction. Flood discharge conditions can remove siltation and reestablish infiltration (Brunke and Gonser (1997). Finally, human channelisation of fluvial environments largely reduces ground and surface water interactions due to the presence of impermeable barriers at both the bank and bed of the fluvial systems (Figure 2.8) (Dahm *et al.*, 1998).

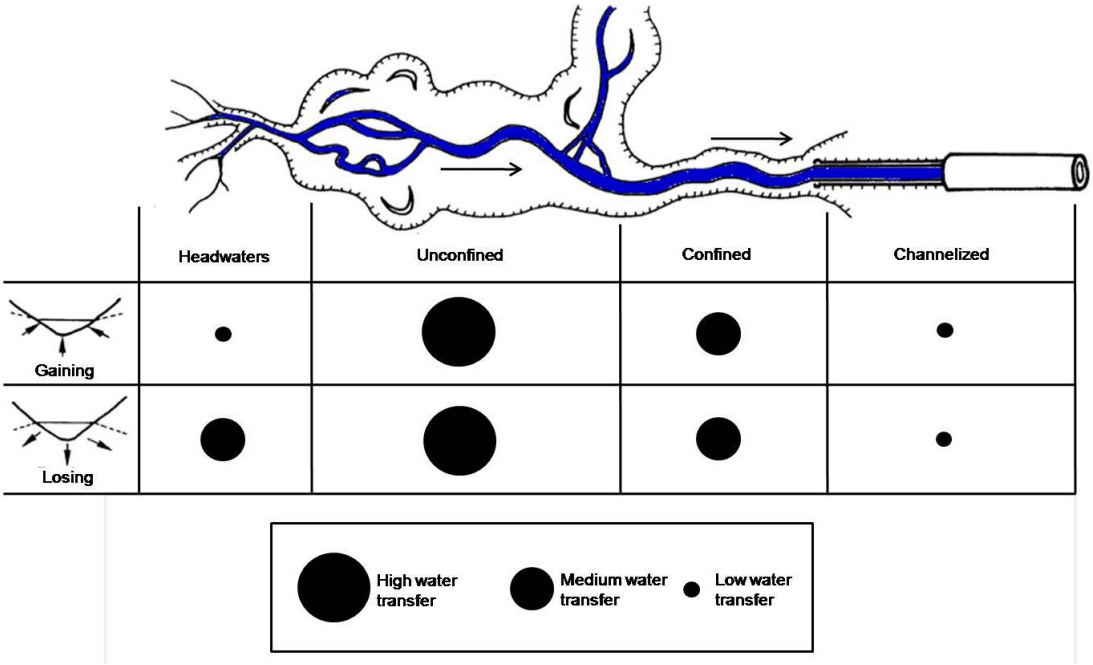

Figure 2.8. Simplified representation of hypothetical geomorphic fluvial environments and their associated degree of interaction (losing and gaining) with groundwater systems. Note: Arrow indicates flow direction. Modified from Dahm *et al.* (1998) and based on the works of Amoros *et al.* (1987), Gregory *et al.* (1991) and Brunke and Gonser (1997).

2.2.3 Lakes and Wetlands

Lakes interact with groundwater systems in a similar manner to streams, either losing or gaining water to groundwater systems through bank and bed infiltration. This works on the same principles as above, with water lost to the groundwater system when lake levels are higher than the water table and groundwaters feeding lakes when the water table is above the lake surface. Further information regarding groundwater and lake interaction is provided by Winter *et al.* (1998) and Tweed *et al.* (2009).

Groundwater also interacts with surface water in wetlands. Wetlands occur at the transitional interface between aquatic and terrestrial systems, where the water table is typically at or near surface topography. This results in the discharge of groundwater to the land surface (Figure 2.9a) (Mitsch and Gosselink, 2007). Wetlands generally form when surface waters fail to drain through the unsaturated zone due to the close proximity of the water table. This leads to an accumulation of water, however the duration and depth of accumulation displays significant seasonal and spatial variability (Freeze and Cherry, 1979; Schwartz and Zhang, 2003; Mitsch and Gosselink, 2007).

During high precipitation and overland flow events wetland stage may rise above the water table resulting in a direct recharge of wetland water to groundwater systems (Figure 2.9b). However, this recharge can be difficult to achieve due to the presence of low permeable organic matter on wetland floors that hinder downward water movement (Winter *et al.*, 1998). Further information regarding wetlands, their variability and interaction with groundwater systems is beyond the scope of this chapter, and is covered by Jolly *et al.* (2008).

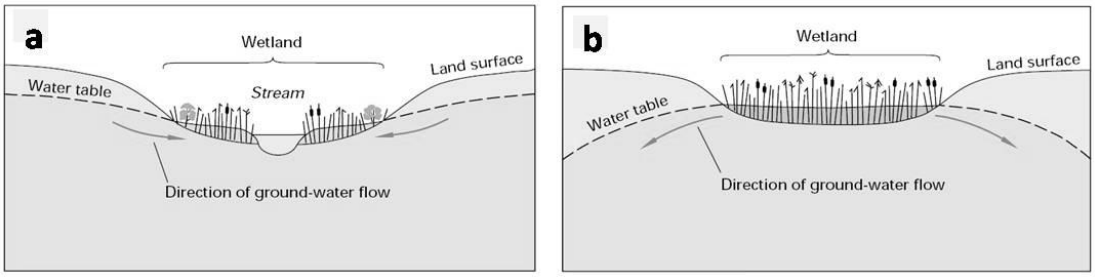

Figure 2.9. Schematic representation of groundwater-wetland interaction. (**a)** groundwater discharge to wetland bodies, (**b)** recharge of groundwater systems from wetland bodies. Replicated without change from Winter *et al.*, (1998).

2.2.4 Hyporheic zone

Further surface and groundwater interaction takes place in the hyporheic zone. This zone occurs at the stream and groundwater interface and is generally an area of elevated biogeochemical activity (Figure 2.10). Here oxygen rich surface waters flow into the streambed subsurface and create a zone of mixing with subsurface waters (Winter *et al.*, 1998; Sophocleous, 2002). Consequently this input of dissolved oxygen, often mixed with an abundant supply of reactive sediments and bacteria present in the subsurface, stimulates biogeochemical transformations. As a result, the hyporheic zone plays an extremely important role in the chemical transformation of water as it moves from the surface to groundwater systems (Gooseff *et al.*, 2002). For example, as water passes through the hyporheic zone dissolved metals may be removed from solution due to their adsorption to sediment surfaces (Winter *et al.*, 1998). Further information regarding this adsorption process is described in Section 2.3.5. Hyporheic exchange also displays spatial and temporal variability as identified by Storey et al. (2003), with exchange flows tending to be strongest at the sides of the stream channel.

The extent of vertical and horizontal mixing, quantity of water exchanged and length of water exchange are determined by the hydraulic conductivity of the streambed-groundwater interface and the hydraulic gradient between upstream and downstream areas of the exchange zone (Storey *et al.*, 2003).

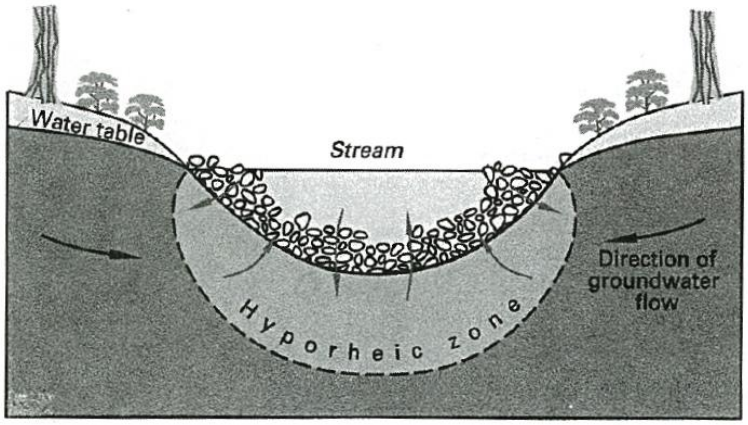

Figure 2.10. Simplified representation of the Hyporheic zone interface between groundwater and streambed. Presented without change from Todd and Mays (2005).

2.3 Hydrogeochemistry

The previous sections introduced the physical properties of groundwater movement and the dynamic physical nature of surface and groundwater interactions. This section will identify the distinct chemical compositions of natural water bodies and the chemical evolution of groundwater bodies. This will be followed by an overview of the spatial and temporal variability of chemical interactions between ground and surface water, before concluding with an outline of the specific chemical reactions and mass transport processes responsible for changes in the chemical composition of both ground and surface water. An index of chemical species used in this section and those that follow has already been presented on page *xii*.

2.3.1 Chemical composition of water bodies

In order to identify the chemical interaction between ground and surface water one must understand the chemical characteristics of each water body and how they influence one another. An understanding of the chemical composition of input water such as precipitation is also required. In general, the compositions of precipitation and surface and groundwaters are distinct and are known to show considerable global variability.

This variability is dependent on mineral weathering, geology, climate, solute sources and proximity to the ocean, and is commonly assessed in terms of the concentration of total dissolved solids (TDS), ion ratio and water type (Semkin *et al.,* 1994; Berner and Berner, 1996; Hiscock, 2005). Average global precipitation and surface and groundwater solute concentrations are presented in Table 2.2 and compared with New Zealand averages.

Precipitation

Typically, precipitation waters can be characterised as slightly acidic (pH 4-6) with low TDS (Table 2.2) and high concentrations of dissolved O_2 and CO_2 (Freeze and Cherry, 1979; Berner and Berner, 1996). Precipitation acquires solutes from particles in the air (Na^+, K^+, Ca^{2+}, Mg^{2+} and Cl^-) and those derived from atmospheric gases (SO_4^{2-}, NH_4^+ and NO_3^-). The dominance of selected ions in precipitation is highly dependent on proximity to the coast with precipitation from marine origins tending to experience higher concentrations of sea-salt derived Na^+ and Cl^- while inland precipitation is dominated by Ca^{2+} and SO_4^{2-} (Berner and Berner, 1996). The chemical composition of precipitation in New Zealand is largely marine (Na^+-Cl^- waters), a signature reflected in the average composition of New Zealand Rivers as they receive a high proportion of input waters from coastal weather systems (Table 2.2).

Table 2.2. Typical global composition and water types of marine and continental precipitation, shown in comparison with the average global and average New Zealand composition of rivers and groundwaters. Average water types are not displayed for groundwaters.

Source	**Location**	**Ca^{2+}**	**Mg^{2+}**	**Na^+**	**K^+**	**HCO_3**	**Cl^-**	**SO_4^{2-}**	**TDS**	**Water type**
Berner & Berner (1996)	Global continental precipitation	0.1-3.0	0.05-0.5	0.2-1	0.1-0.3		0.2-2	1-3	1-15	Ca-SO_4
Berner & Berner (1996)	Global marine precipitation	0.2-1.5	0.4-1.5	1-5	0.2-0.6		1-10	1-3	4-20	Na-Cl
Maybeck (1979)	Global river composition	14.7	3.7	7.2	1.4	53.0	8.3	11.5	110	Ca-HCO_3
Smith & Maasdam (1994)	NZ river composition	9.9	2.0	8.7	1.3	39	8.1	7.5	76	Ca^{2+}-Na^+-HCO_3
Hem (1985)	Global groundwater composition	50	7	30	3	200	20	30	350	-
Daughney & Reeves (2005)	NZ groundwater composition (NGWMP)	25	7.1	25	2.5	136.6	19	5	250	-

River waters

Globally, river compositions tend to be dominated by the elements Ca^{2+} and HCO_3^-, a pattern replicated but less pronounced in New Zealand Rivers. These analytes are commonly sourced through the dissolution of carbonate minerals and this Ca^{2+}-HCO_3^- water type is reflected in 98% of global river systems (Maybeck, 1979). The remaining 2% of rivers largely display a Na^+-Cl water type with higher Na^+ relative to Ca^{2+} and Cl^- relative to HCO_3^-. These waters are predominantly fed by marine rainfall and/or drain siliceous rocks that provide little carbonate material to solution. The average concentration of TDS for New Zealand river systems (76 mg/L) is significantly less than those presented on a global scale (110 mg/L), this is due to reduced anthropogenic contamination and high run-off (Berner and Berner, 1996). Anthropogenic contamination enters river systems from both point (e.g. direct sewage discharge) and non-point (e.g. groundwaters, leaching) sources and is able to provide additional solutes (e.g. Cl^-, SO_4^{2-}, NO_3^-, P) to river systems and subsequently increase and modify their TDS and chemical makeup. The chemical composition of a river is also influenced by groundwaters that provide solute rich base flow to effluent river systems (Rozemeijer and Broers, 2007). Due to their elevated TDS, these groundwaters usually increase the concentration of TDS in the receiving rivers and are able to transfer their chemical signature to surface water bodies (Figure 2.11). Typically, this results in the transfer of Na^+-Cl^- rainfall recharged groundwaters to a surface water body. Further, nutrients (e.g. NO_3^-, NH_4^+ and P) that accumulate in groundwaters are also able to be transferred (Taylor *et al.*, 1989; Hiscock, 2005).

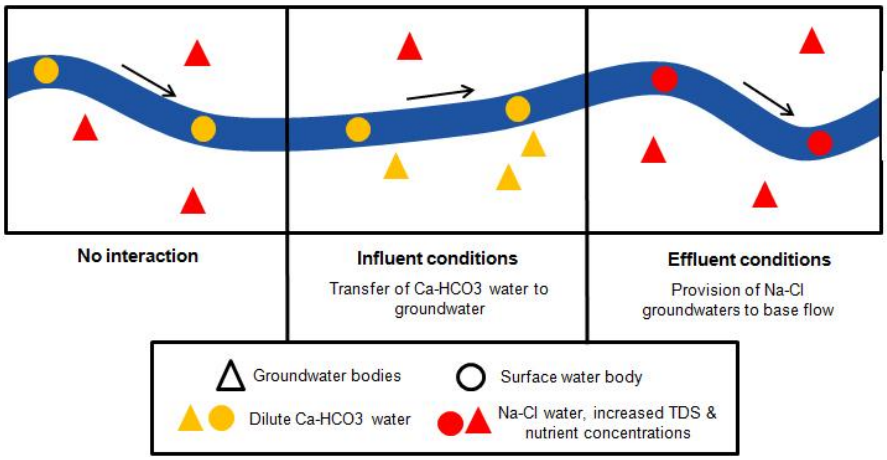

Figure 2.11. Simplified schematic representation showing ground and surface water types resulting from both influent and effluent interaction conditions. Water types are also shown when no interaction is occurring and groundwater systems are recharged by precipitation. Blue line represents the stream body while arrows indicate direction of stream flow.

Groundwaters

In comparison to river systems, groundwaters interact with a variety of subsurface geological materials that provide a range of inorganic and organic constituents to solution. As rock:water contact times are longer than those experienced by rivers, groundwaters tend to display a higher TDS than surface waters. This is reflected in both global average groundwater TDS (350 mg/L) and those from a New Zealand setting (250 mg/L) (Daughney and Reeves, 2005). The principal dissolved components of groundwater are the six major ions Ca^{2+}, Na^{+}, Cl^{-}, Mg^{2+}, HCO_3^{-} and SO_4^{2-} however, a variety of other ions and gases are also common and are presented in Table 2.3. Human activities are also able to modify the principal components of groundwater, in particular by elevating minor and trace ions to levels similar to that of major ions (Hiscock, 2005). For example, application of agricultural fertilizers is able to raise concentrations of NO_3^{-} and dissolved P in the soil zone and subsequent underlying groundwater bodies. In anaerobic groundwater bodies this NO_3^{-} is converted to NH_4^{+} due to microbial redox reactions (see section 2.3.4 for further information surrounding redox reactions).

The composition of natural groundwaters is commonly assessed using Piper diagrams that enable the cation and anion composition of specific waters to be identified and related to water types or hydrochemical facies (Freeze and Cherry, 1979). These facies can then be associated with environmental processes such as geology and water flow pathways (Güler *et al.*, 2002; Hiscock, 2005). The concept of hydrochemical facies was initially developed by Back (1966) and Morgan and Winner (1962), with facies generally identified within the subdivisions of a trilinear Piper diagram (Figure 2.12). Groundwater bodies show distinctive chemical compositions as they progress along subsurface flow paths and are influenced by various geological materials, recharge mechanisms and land use practices. These will be discussed in further detail in section 2.3.2.

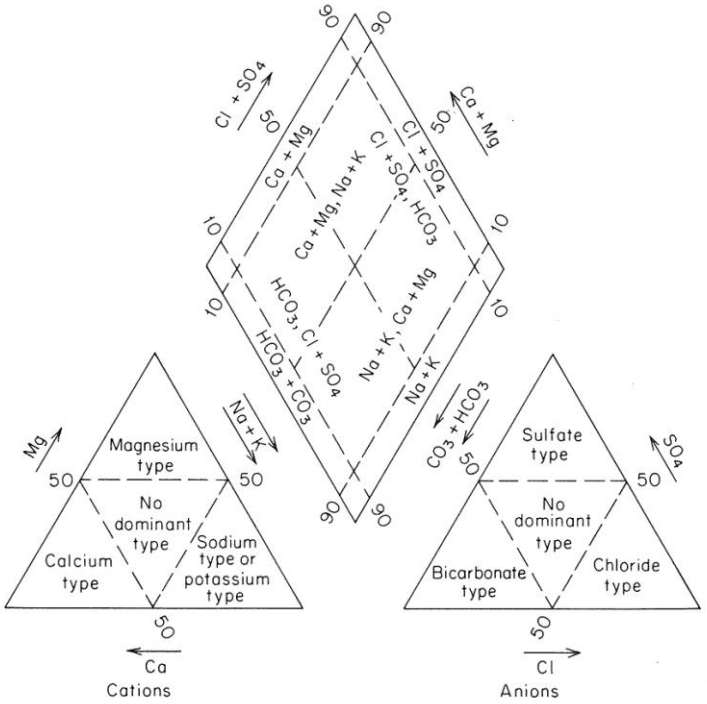

Figure 2.12. Trilinear Piper diagram of major hydrochemical facies or water types based on the composition of major cation and anions. The left triangle presents major cations while the right presents major anions. The center diamond represents the projected position based on both triangles. (After Morgan and Winner, 1962, and Back, 1966).

Table 2.3. Major and minor ions, trace constituents and dissolved gases commonly found in groundwaters. After Freeze and Cherry (1979).

Major ions (>5 mg/L)	
Bicarbonate (HCO_3^-)	Sodium (Na^+)
Chloride (Cl^-)	Calcium (Ca^{2+})
Sulphate (SO_4^{2-})	Magnesium (Mg^{2+})
Minor ions (0.01-10.0 mg/L)	
Nitrate (NO_3^-)	Potassium (K^+)
Carbonate (CO_3^{2-})	Strontium (Sr^{2+})
Fluoride (F)	Iron (Fe^{2+})
Phosphate (P)	Boron (B)
Trace constituents (<0.1 mg/L)	
Aluminium (Al^{3+})	Manganese (Mn)
Arsenic (As)	Nickel (Ni)
Barium (Ba)	Radium (Ra)
Bromide (Br)	Selenium (Se)
Cadmium (Cd)	Silica (Si)
Cesium (Cs)	Silver (Ag)
Chromium (Cr)	Thorium (Th)
Cobalt (Co)	Tin (Sn)
Gold (Au)	Titanium (Ti)
Iodide (Kl)	Uranium (U)
Lead (Pb)	Vanadium (V)
Lithium (Li)	Zinc (Zn)
Dissolved gases (trace to 10 mg/L)	
Nitrogen (N)	Methane (CH_4)
Oxygen (O_2)	Hydrogen sulphide (H_2S)
Carbon dioxide (CO_2)	Nitrous oxide (N_2O)

In New Zealand, 110 groundwaters from the New Zealand's National Groundwater monitoring programme (NGMP) were classified into six hydrochemical facies by Daughney and Reeves (2005). These facies were largely differentiated by their concentration of TDS, redox potential, underlying lithology, interaction with surface waters and degree of human impact and are summarised in Table 2.4 and Figure 2.13. In summary, the majority of sites in the programme (79 sites) shared chemical compositions similar to average global river waters with low TDS and a Ca^{2+}-Na^{+}-Mg^{2+}-HCO_3^{-} or Na^{+}-Ca^{2+}-Mg^{2+}-HCO_3^{-}-Cl^{-} signature. These sites were largely unconfined and oxidized and located in the South Island of New Zealand (Figure 2.13). Daughney and Reeves (2005) hypothesized that these aquifers receive recharge largely from precipitation and interaction with surface water bodies. The remaining groundwater sites, categorised into Facies 2A and 2B, were typically deeper and showed higher TDS and moderate to highly reduced conditions (Table 2.4). This chemistry likely reflects older groundwaters that have experienced longer rock:water interaction periods with little hydraulic link to surface water bodies.

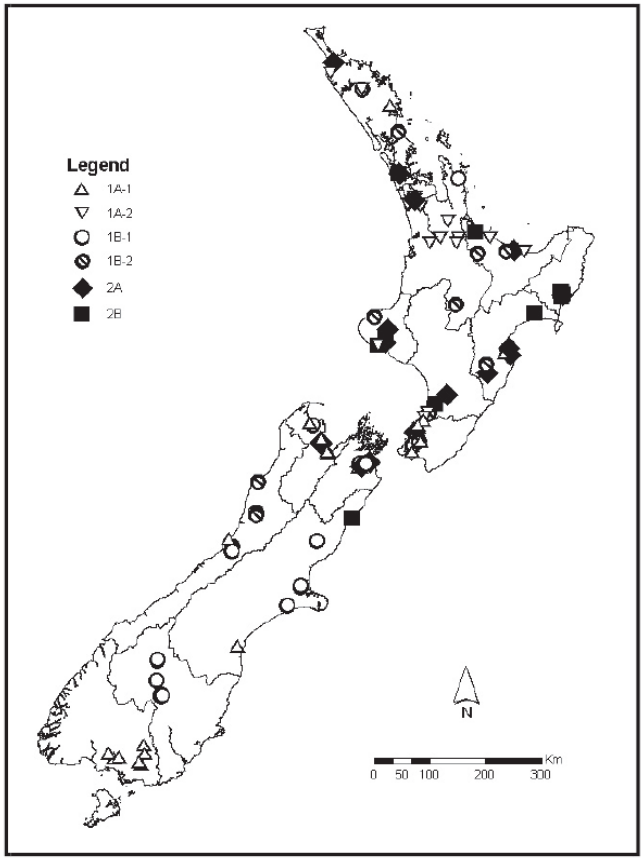

Figure 2.13. Location and hydrochemical facies of groundwater wells from the New Zealand Groundwater monitoring programme (NGMP). Sourced without change from Daughney and Reeves (2005).

Table 2.4. General characteristics of New Zealand hydrochemical facies from the New Zealand Groundwater monitoring programme (NGMP). Facies are described overall as Facies A and B and again as Facies 1A-1 to B2. 'HI' denotes Human Impacted. Source: Daughney and Reeves (2005).

	Overall facies description	Facies description continued	Facies	Individual Facies Description
Facies A (79 sites)	Surface dominated Oxidized unconfined aquifer. Low to moderate TDS, Ca-Na-Mg-HCO_3 water	Signs of HI Rainfall recharge Moderate TDS Na-Ca-Mg-HCO_3-Cl^- water	1A-1	Moderate HI Carbonate or clastic aquifers. Ca-Na-Mg-HCO_3-Cl
			1A-2	Most human impact Volcanic or volcaniclastic Na-Ca-Mg-HCO_3-Cl
		Little human impact River recharge Low TDS Ca-Na-HCO_3 water	1B-1	Carbonate or clastic aquifer, Ca-HCO_3 water
			1B-2	Volcanic or volcaniclastic Na-Ca-Mg-HCO_3-Cl
Facies B (29 sites)	Groundwater dominated Reduced Higher TDS Ca^{2+}-Na^+-HCO_3^- water		2A	Moderately reduced Majority unconfined High TDS
			2B	Highly reduced Majority confined Highest TDS

2.3.2 Groundwater evolution

Groundwater systems are recharged by infiltration from precipitation and snowmelt, discharge from overlying surface waters and percolation from neighbouring groundwater systems. Each mechanism of recharge provides water of a distinct chemical composition (see section 2.3.1) that has the ability to influence the chemical signature of underlying groundwater systems. The majority of groundwater originates at recharge areas as infiltration through the soil-water zone from precipitation and snowmelt (Figure 2.14). As mentioned in section 2.3.1, these Na^+-Cl^- waters initially display a relatively acidic chemical signature (pH 5-6), low in TDS and high in dissolved oxygen and carbon dioxide (Table 2.2). The chemical composition of infiltrating precipitation undergoes significant change as it percolates through the soil-water zone to underground flow systems and comes into contact with a diverse range of gases, rock minerals and organic and inorganic constituents of soil (Freeze and Cherry, 1979). Initially, infiltrating precipitation can acquire a range of accumulated salts (Na^+ and Cl^-) and fertilizer inputs (SO_4^{2-}, NO_3^-, P) as it moves through the soil-water zone (Figure 2.14).

This recharge pathway is reflected in the chemical composition of rainfall recharged groundwaters that typically display a Na^+-Cl^- water type with elevated concentrations of the nutrients NO_3^- and P (Taylor *et al.*, 1989). The soil-water zone also provides a range of inorganic and organic acids to infiltrating waters. An example of such an acid is carbonic acid, formed by the slow diffusion of atmospheric CO_2 into solution (Equation 2.3), and the oxidation of organic matter in the soil zone. Besides the additional input of CO_2, this oxidation process reduces the concentration of dissolved oxygen in solution, and can remove the majority of oxygen in infiltrating waters (Equation 2.4). Further sources of acidity are provided to the soil-water zone by organic acids (e.g. humic acids from biological activity) and the oxidation of minerals such as pyrite (Younger, 2007).

$$CO_2(g) + H_2O = H_2CO_3 \quad (2.3)$$

$$O_2(g) + CH_2O = CO_2(g) + H_2O \quad (2.4)$$

Upon their dissociation (resulting in free protons or H^+ ions) these acids promote the dissolution of minerals, notably soluble carbonate minerals such as calcite ($CaCO_3$). This dissolution increases the concentration of solutes within solution (Ca^{2+}, Mg^{2+}, HCO_3^- and K^+) and raises water pH. Generally, as groundwaters continue to move along shallow sub-surface paths into deeper systems, their concentrations of TDS increases and ion exchange processes play a significant role in controlling chemical composition (Section 2.3.5) (Ingebritsen, 2006).

Recharge is also provided to groundwater systems from overlying surface water bodies such as streams and rivers (Figure 2.11 – influent). Generally, this mechanism of recharge provides Ca^{2+}-HCO_3^- waters with a TDS range of 80-130 mg/L. However, these surfaces waters are generally under saturated in respect to calcite allowing further dissolution of shallow carbonate subsurface minerals to occur subsequently increasing groundwater TDS. Groundwaters tend to evolve from this dilute Ca^{2+}-HCO_3^- signature, towards a concentrated Na^+-Cl^- brine as they move into deeper flow systems and the dissolution of Cl^- rich minerals occurs.

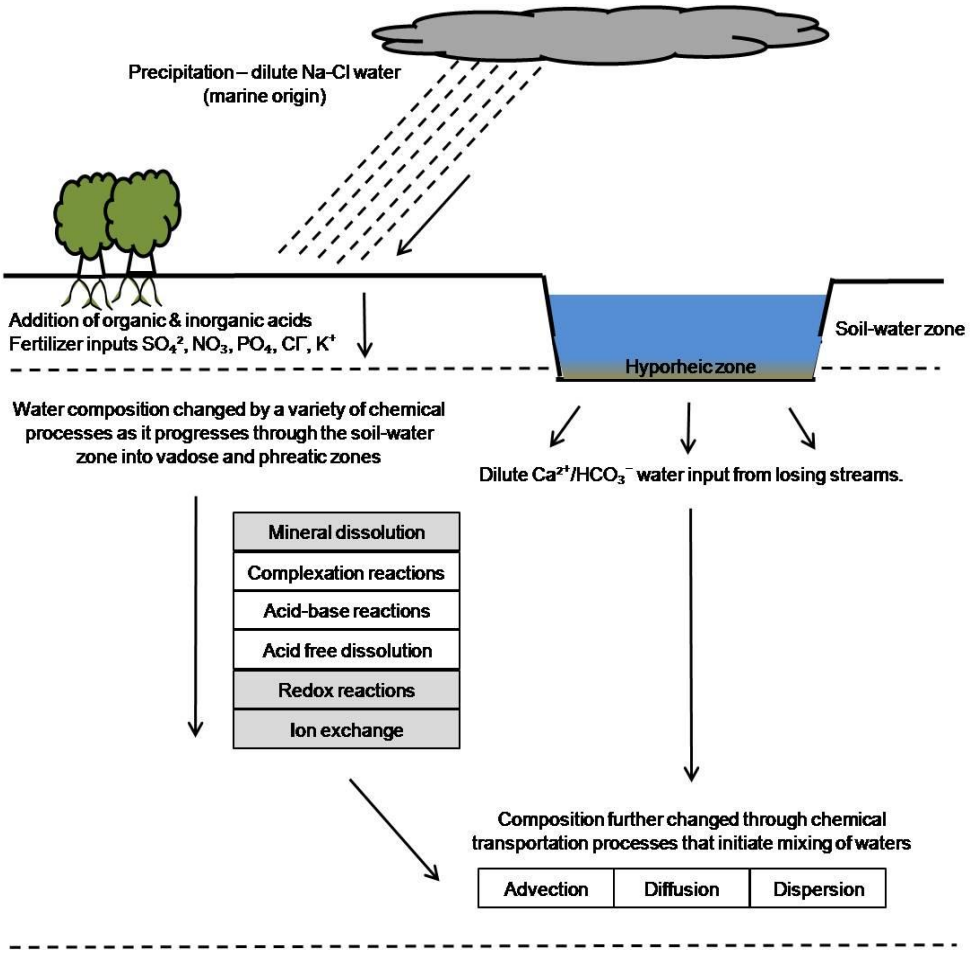

Figure 2.14 Simplified diagram of water entry and chemical evolution through a groundwater flow system. The processes shown are not necessarily sequential. Shaded chemical processes represent surface reactions

Following Chebotarev (1955), as is common, groundwater evolution in large sedimentary basins can be associated with three main zones, each of which correlate to a specific depth and groundwater age (Figure 2.15). Groundwaters in the *upper shallow zone* are typically low in TDS and show a Ca^{2+}-HCO_3^- water type. These groundwaters display high flow rates (of the order of m/day), with high connectivity to surface water and are dominated by dissolution of carbonate and silicate minerals. As these waters move into the deeper *intermediate zone* their concentration of TDS increases and SO_4^{2-} becomes the dominant anion due to the presence of gypsum ($CaSO_4$) and epsomite ($MgSO_4$) minerals. Groundwater circulation is reduced and chemical equilibrium is achieved between carbonate minerals and the groundwater (Younger, 2007). In the *lower zone*, deep flow systems are characterised by slow flow, high in TDS with a distinctive Cl^- anion signature.

This occurs when groundwaters access Cl^- minerals, high in solubility, that experience little groundwater flushing. As a result old groundwaters begin to show a chemical signature resembling that of salt water (High Cl^- and Na^+).

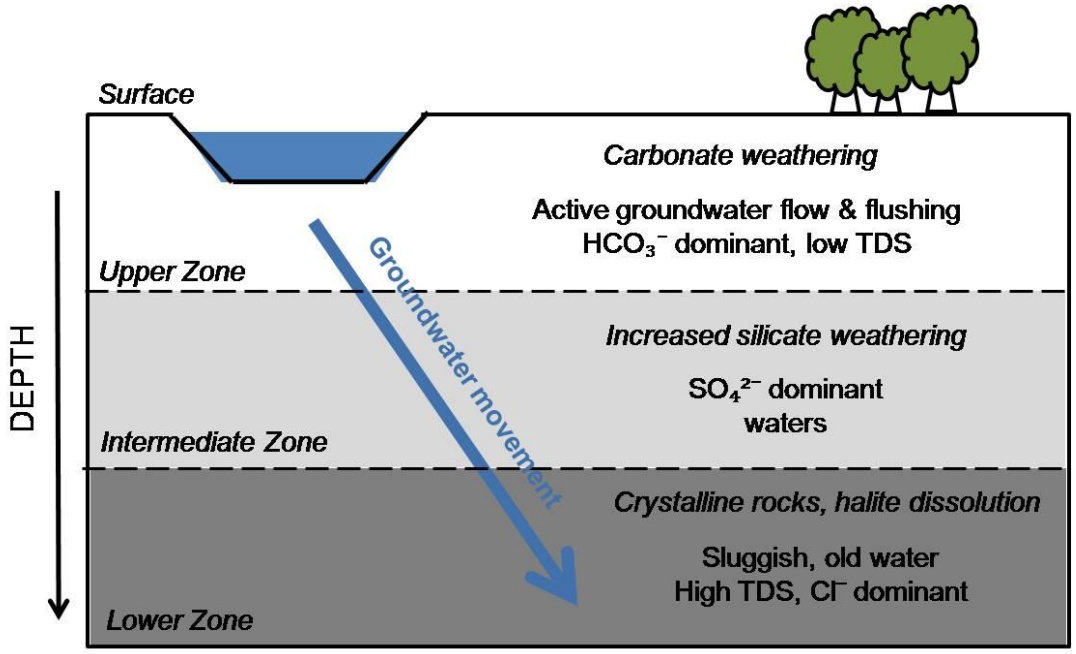

Figure 2.15. Simplified schematic representation of groundwater chemical evolution. Note: Diagonal movement of groundwater over time to represent both vertical and horizontal movement of water through the subsurface. Based on Chebotarev (1955).

2.3.3 Chemical surface and groundwater interactions

The movement of water between the surface and groundwater interface provides a major pathway for the transfer of chemicals and nutrients (Dahm *et al.,* 1998; Winter *et al.,* 1998). This transfer is known to affect the supply of carbon, oxygen, nutrients and other chemical constituents and it is recognised that chemical parallels between water bodies may indicate their potential interaction (Winter *et al.,* 1998; Taylor *et al.,* 1999). As mentioned in Section 2.2 the interaction between ground and surface water is known to show considerable spatial and temporal variability, which can be transferred to the chemical composition of either water body (Dahm *et al.,* 1998).

Seasonal variability in both surface (e.g. Holloway and Dahlgren, 2001; Vidon *et al.,* 2009) and groundwater (e.g. Jagannadha Sarma *et al.,* 1979; Eberts *et al.,* 2005) chemistry has been extensively documented in the hydrochemical literature. This chemical variability can be transferred across both water bodies as they interact and waters move through the stream-aquifer interface.

An example of such seasonal interaction and resulting changes in water composition has been documented at the Yumana River, India by Kumar *et al*. (2009). Here Kumar and his colleagues collected hydrochemical data twice a year for three successive years from ground and surface water sites along an 8km reach of the river. During the pre-monsoon season they found upstream ground and surface waters both displayed a Na^{+}-Ca^{2+}-Cl^{-} signature, indicating recharge of surface waters by the groundwater system. However, this signature showed a strong seasonal pattern with surface waters changing to Na^{+}-Ca^{2+}-HCO_3^{-} type waters and groundwater to Ca^{2+}-Na^{+}-HCO_3^{-} during the post-monsoon season. This temporal change was attributed to the greater input of high altitude precipitation to the Yamuna River and the diminished role of groundwater recharge to the river as head differences forced river waters to recharge the groundwater system. Further, the input of dilute precipitation during the post-monsoon resulted in an overall dilution effect to both ground and surface waters. Similar seasonal variations in water composition in response to surface recharge are also documented by Scanlon (1989), Rice and Bricker (1995) and Negrel *et al.* (2003).

The transfer of nutrients between the ground and surface water interface is also known to show strong seasonal variation in response to changes in temperature and organic matter (Dahm *et al.,* 1998; Winter *et al.,* 1998). An example is provided by von Gunten *et al.* (1991) at the River Glatt groundwater region, Switzerland. Here monthly hydrochemical sampling over a five year period showed a significant decrease in pH, O_2 and NO_3^{-} during the summer as waters infiltrated from the River Glatt into underlying groundwater systems. This reduction in chemical parameters, in particular NO_3^{-}, was believed to be a result of bacterial degradation of aquatic biota as water moved through the hyporheic zone. This process was stimulated during the summer due to increased water temperatures and increased sunlight (Ward and Stanford, 1982; von Gunten *et al.,* 1991). Further examples of variations in nutrient cycling across the ground and surface water interface are provided by Pekny *et al.* (1989) and Butturini *et al.* (2003) and in the review by Dahm *et al.* (1998).

The extent of surface and groundwater interaction also influences the attenuation of nutrients in stream waters (Dahm *et al.,* 1998). A variety of field investigations have shown that uptake of NH_4^+ and NO_3^- increases when surface and groundwater interaction is reduced and water residence times are greater (e.g. Lamberti *et al.,* 1989; Valett *et al.,* 1996). This is in part influenced by the geomorphic environment under which interaction occurs, with unconstrained river systems displaying greater interacting properties and therefore greater attenuation of nutrients (Lamberti *et al.,* 1989; D'Angelo *et al.,* 1993).

Spatial variability in solute concentrations and water composition is influenced by the interaction between ground and surface water (Dahm *et al.,* 1998). An example of this is also reported in the previously mentioned study by Kumar *et al*. (2009) from the Yumana River, India and surrounding groundwater sites. Here upstream groundwater sites displayed similar Na^+-Ca^{2+}-Cl^- type water to that of the surface water sites. However, following the introduction of an effluent drain to the river, both SW and neighbouring groundwater sites displayed a shift to contaminated NO_3^-, F and PO_4^3 waters. This indicated recharge of polluted surface waters to the underlying groundwater system. Further, Kumar *et al*. (2009) showed the strength of this surface-groundwater interaction and resulting changes in chemical composition diminished as the distance between the Yamuna River and groundwater sites increased.

Several New Zealand examples also provide evidence of the chemical interaction between ground and surface water bodies. Burden (1982) inferred potential interaction between the Rakaia and Ashburton Rivers and their underlying groundwater systems due to a similar low TDS, Ca^{2+}- HCO_3^- water signature present across all systems. Similarly, Taylor *et al.* (1989) inferred potential interaction due to indistinguishable ^{18}Oxygen ($\delta^{18}O$) values between waters of the Waimakariri River and neighbouring unconfined groundwater wells ($\delta^{18}O$ more negative than – 8.5‰). Further, Taylor *et al.* (1989) isolated groundwaters recharged entirely by precipitation infiltration ($\delta^{18}O$ *ca.* – 8.5‰, and elevated Cl^- and NO_3^- concentrations due to soil passage) and those representing a mixture of river and rainfall recharge ($\delta^{18}O$ range – 8.5 - 7‰).

In summary, chemical parallels between ground and surface water bodies are often used to infer potential interaction (e.g. Burden, 1982; Taylor *et al.*, 1989). Seasonal changes experienced in one water body are able to influence the other through recharge and discharge mechanisms (e.g. Scanlon, 1989). Likewise the chemical alteration to surface waters through contamination can lead to significant contamination of groundwater sources (e.g. Kumar *et al.*, 2009) and contamination of groundwater bodies can affect the surface waters to which they provide base flow. As a result an understanding of these complex interactions is crucial in order to monitor water and contaminant transport through fluvial systems and for sustainable water allocation (Winter *et al.*, 1998).

2.3.4 Chemical processes: ions and molecules within solution

Acid-base reactions

The hydrogeochemical literature identifies acid-base reactions as an important group of processes that influence the chemical composition of groundwater. These reactions involve the exchange of protons between aqueous ions and molecules in order to achieve neutralization of acids (Domenico and Schwartz, 1998; Schwartz and Zhang, 2003). This is shown by the dissociation of CO_2 gas into water (Equation 2.5) and subsequent neutralization of the resulting carbonic acid into HCO_3^- and H^+ (Equation 2.6).

$$CO_2(g) + H_2O = H_2CO_3 \qquad (2.5)$$

$$H_2CO_3 = HCO_3^- + H^+ \qquad (2.6)$$
(Acid) (Base)

An acid is a molecule that loses a H^+ ion (proton), while a base is the ion or molecule that can acquire the proton. Acid-Base reactions can also occur through the interaction of protons and the mineral surface of rocks or sediments. This mineral-acid dissolution will be discussed in further detail in Section 2.3.5.

Acid-Base reactions are extremely important due to their influence on groundwater pH. The addition of H^+ ions to solution (e.g. Equation 2.6) leads to an increase in acidity, while the removal of H^+ ions fosters more alkaline solutions. This is important as pH influences the solubility and state of ions and gases, and determines their precipitation and volatilization potential (Schwartz and Zhang, 2003). For example the type of carbonate species present in solution is highly dependent on water pH (Figure 2.16). Below pH 5, H_2CO_3 is the dominant species, with HCO_3^- dominant between pH 7-9 and CO_3^{2-} the most abundant during high pH (>10). Further, groundwaters of low pH are generally able to transport a large metal dissolved load, whereas metals tend to precipitate from solution between the pH 7-9 range.

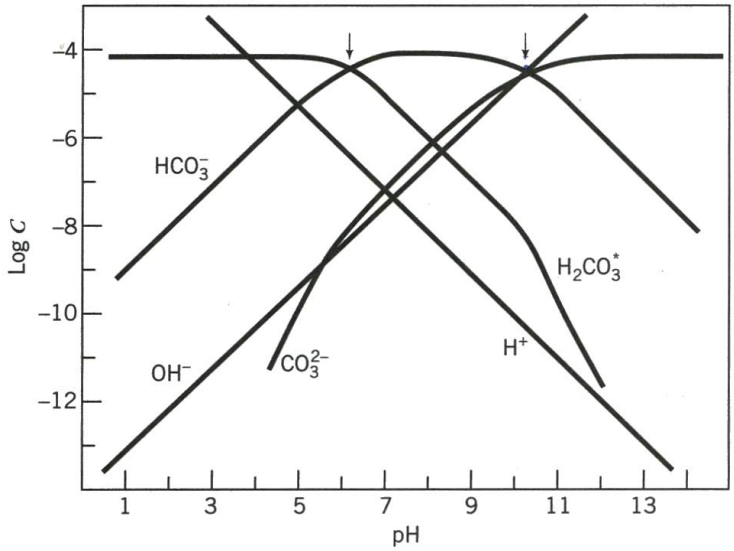

Figure 2.16. Forms of carbon within a groundwater system as a function of pH. *Log* carbon is displayed. Presented without change from Morel and Hering (1998).

Acid free dissolution

Acid free dissolution can also occur in a groundwater system. This reaction involves the simple dissolution of both inorganic and organic complexes into individual species. An example of this is provided by Freeze and Cherry (1979) in regards to the dissolution and precipitation of halite or common rock salt in solution (Equation 2.7).

$$NaCl = Na^+ + Cl^- \qquad (2.7)$$

Inorganic and organic molecules display a wide degree of variability in their dissolution and solubility. In general, charged species display a higher degree of solubility due to their ability to merge with polar[1] water molecules that hold an uneven distribution of electron density (Morel and Hering, 1998). This forces a change in the structure of water, in which polar molecules rearrange themselves to bind with cations. In contrast uncharged species are comparatively insoluble in water, due to their inability to merge easily with polar water molecules. This is commonly the case for organic molecules that usually display polar and uncharged compounds (Freeze and Cherry, 1979). Exceptions to this rule include methanol, which is highly soluble in water due to the presence of an OH- group that can readily bond with surrounding water molecules.

Complexation reactions

Complexation reactions involve the formation of complex ions through the combination of cations with ligands. Ligands are negatively charged molecules and can either be free anions (e.g. Cl^-, F^-), organic molecules (e.g. humic acid, amino acids) or other negatively charged complexes (e.g. HCO_3^-, SO_4^{2-}) (Merkel and Planer-Friedrich, 2008). Generally, a complex ion is composed of a metal cation paired with an anionic species with unpaired electrons (e.g. Cl^-, SO_4^{2-} and CO_3^{2-}). The two ions are bound together by discrepancies in their electrical charge; for example, the simple formation of a calcium sulphate ($CaSO_4$) complex (Equation 2.8) (Freeze and Cherry, 1979).

$$Ca^{2+} + SO_4^{2-} \leftrightarrow CaSO_4 \qquad (2.8)$$

Complexation reactions hold particular importance in the transportation of metal ions (Mills *et al.,* 1991). Free metal ions (e.g. Fe^{2+}) have restricted transport mechanisms due to their high sorption properties and the natural pH range of groundwater (pH 6.6-8.3). However, by forming complex ions with both organic and inorganic ligands, metals are able to be transported within the main dissolved constituent load.

[1] The oxygen atom of water displays a slight negative charge and therefore higher electronegativity than that of the neighbouring positively charged hydrogen ions (Maidment, 1993). This allows water to form a polar bond with other water molecules (through electrical dipole movement) to offset this charge deficit.

The importance of metal-organic ligand formation is particularly significant as identified by Glagoleva (1958). He found 50-70% of Fe^{2+}, Mn, Ni and Cu were transported in freshwaters as components of dissolved organic complexes.

Redox reactions

Redox reactions involve the chemical exchange of electrons between materials. They consist of a simultaneous oxidation reaction, in which electrons are lost, and a reduction reaction, in which electrons are gained. Mediated by microorganisms that acquire energy through the process, redox reactions can significantly modify groundwater chemistry (Schwartz and Zhang, 2003). As a result such reactions have significant implications for groundwater management practices (Hiscock, 2005).

Some redox reactions are highly dependent on the presence of organic matter and dissolved oxygen, therefore the groundwater environment and supply of these variables are major factors controlling redox potential (Kedziorek *et al.,* 2008). Stumm and Morgan (1996) provide an example of an oxidation-reduction reaction from an aerobic groundwater environment (Equation 2.9-2.11). Here Fe^{2+} oxidises to form Fe^{3+}, and subsequently loses electrons (*e*) which are donated to O_2, which is reduced or consumed in the reaction. Together the two reactions (Equation 2.9 and 2.10) create the full redox reaction (Equation 2.11) and reduce the concentration of dissolved Fe^{2+} in solution.

$$O_2 + 4H^+ + 4e = 2H_2O \quad \text{(reduction)} \quad (2.9)$$

$$4Fe^{2+} = 4Fe^{3+} + 4e \quad \text{(oxidation)} \quad (2.10)$$

$$O_2 + 4Fe^{2+} + H^+ = 4Fe^{3+} + 2H_2O \quad \text{(redox reaction)} \quad (2.11)$$

As water moves deeper into groundwater flow systems concentrations of dissolved oxygen become exhausted due to the reduction process (Equation 2.9) and a lack of oxygen replenishment. As a result, the electrons required to fuel redox reactions are sourced from the reduction of other compounds (e.g. NO_3, Mn and SO_4^{2-}). An example is provided by Kedziorek *et al.* (2008) in which manganese oxide is reduced into manganese and hydrogen ions, carbon dioxide and water (Equation 2.12). The occurrence of this particular reaction leads to elevated concentrations of Mn in groundwaters.

Further electron acceptors that are reduced and subsequently removed from solution in anaerobic environments include nitrate, iron oxyhydroxides, and sulfate (Kedziorek *et al.*, 2008). Therefore the presence of such ions in solution can offer valuable insight into the redox conditions of a groundwater environment, in particular whether waters are aerobic or anaerobic. Examples of ions commonly transformed in redox reactions and the sequence at which they are reduced are presented in Table 2.5. The presence of those elements listed in the oxidized column may indicate oxygen rich groundwaters while the presence of those elements listed in the reduced column may indicate oxygen poor groundwaters. Further, ions are reduced in a particular sequence with groundwater systems tending to reduce ions in the following order O_2, NO_3^-, Mn, Fe^{2+} and SO_4^{2-} as an environment becomes more anoxic. As a result concentrations of these ions in solution offer information on the state of oxidation for a particular system.

$$CH_2O + 2MnO_2\,(s) + 4H^+ = 2Mn^{2+} + 3H_2O_2 + CO_2 \qquad (2.12)$$

Table 2.5. Elements commonly transformed through redox reactions in groundwater. Elements are presented in their oxidized (oxygen rich groundwaters) and reduced forms (oxygen poor, anoxic groundwaters) according to the redox sequence.

Redox state	Oxidised (Oxygen available groundwaters)	Reduced (Oxygen poor groundwaters)
Oxidised	O_2	CO_2
↓	NO_3^-	N_2 gas, NH_4^+
	Mn minerals	Mn^{2+}
	Fe minerals	Fe^{2+}
	SO_4^{2-}	H_2S (sulphide)
Most reduced	CO_2	CH_4 (methane)

2.3.5 Chemical processes: surface reactions

Ion Exchange

This process involves the exchange of ions between mineral surfaces and solution due to charge imbalances in the crystal lattice of minerals (Schwartz and Zhang, 2003). Exchangeable ions in solution become absorbed to the colloidal surface of minerals to offset these charge imbalances (Figure 2.17). This results in elemental substitution, in which surface ions are replaced and bumped into solution by ions of a higher valence that are missing a greater quantity of electrons (e.g. Ca^{2+} can substitute Na^+ from colloidal surfaces).

In general the ability of ions to cling to the mineral surface is determined by their valence[2] or the number of chemical bonds that the ion is able to form (McLaren and Cameron, 1996). Trivalent ions (e.g. Al^{3+}) have the strongest surface bond, while Monovalent ions (e.g. Na^{+}, K^{+}) have the least strong bond. Further, an ion's degree of hydration[3] determines its bond to mineral surfaces, with high hydration radii (e.g. Na^{+}) being held more tightly. As an ion's degree of hydration is inversely proportional to its ionic size, smaller ions have a higher degree of hydration and have the strongest surface bond (Langmuir, 1997).

Ion exchange is of particular importance in controlling the chemical makeup of deep old sedimentary groundwater systems (Younger, 2007). This phenomenon is widely documented and involves the substitution of adsorbed Na^{+} ions on mineral surfaces with Ca^{2+} ions from fresh groundwaters. As fresh groundwaters access deep Na^{+} rich groundwater systems, mineral surfaces preferentially select their abundant Ca^{2+} ions, knocking Na^{+} into solution and increasing the total concentration of Na^{+} in deep groundwaters. As a result old groundwaters begin to show a chemical signature approaching that of salt water (High Cl^{-} and Na^{+}) (See Section 2.3.2).

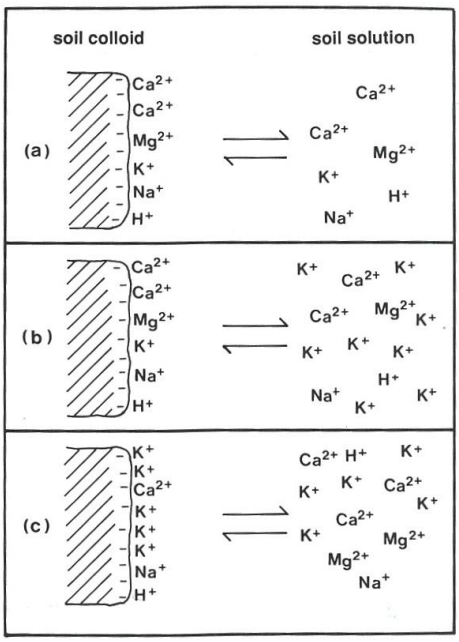

Figure 2.17. Simplified representation of ion exchange between soil colloid and K^{+} ions in solution. (**a**) Initial soil colloid and solution state, (**b**) addition of K^{+} ions to solution, (**c**) exchange of soil cations and K^{+} ions from solution to reach new equilibrium. Replicated without change from McLaren and Cameron (1996).

[2] Magnitude or size of the charge of an ion (Findlay, 1958).
[3] Effective size that determines how many water molecules will be attracted to the ion (Findlay, 1958)

Likewise, ion exchange processes are of particular importance in the soil-water zone, in particular when the clay mineral content is high. Clay minerals display significant negative charge allowing substantial interexchange of ions and percolating groundwater. Clay minerals also display preferential selection of ions absorbed to their surfaces with, for example, Ca^{2+} and Mg^{2+} preferred over Na^{+}. The capacity of minerals to exchange ions with solution can be evaluated using a *cation exchange capacity (CEC).* This CEC is highly dependent on pH which in turn determines a mineral's variable surface charge (Merkel and Planer-Friedrich, 2008). Under acidic conditions (pH < 4) protons are sorbed to a mineral surface, creating an overall positive charge capable of attracting anions from solution. When the pH increases the oxygen atoms of the surface functional group remain free and the mineral surface displays an overall negative charge. This allows the sorption of cations from solution as illustrated in Figure 2.17. Illustrative examples of minerals and their CEC are presented in Table 2.6.

Table 2.6. Various minerals and their typical cation exchange capacities (CEC). Source: McLaren and Cameron (2006).

Colloid	**CEC ($cmol_c\ kg^{-1}$)**
Humus	100-300+
Illite (hydrous mica)	10-40
Vermiculites	100-200
Smectites	60-150
Pedogenic chlorite	10-30
Kaolinite, halloysite	2-15
Fe and Al hydrous oxide	<1

Mineral Dissolution

As mentioned earlier, acid-base dissolution of mineral surfaces is another important chemical reaction affecting the chemical composition of groundwater. This reaction involves the chemical exchange of mineral cationic components with protons, supplied through the dissociation of hydrogen ions in solution (Tranter *et al.*, 1993). A set number of protons substitute for cations from mineral surfaces, subsequently setting them into solution as shown in Figure 2.18 for the substitution of K^{+} (Raisewell, 1984). This dissolution continues until chemical equilibrium with solution has been achieved or all the mineral has been dissolved (Freeze and Cherry, 1979).

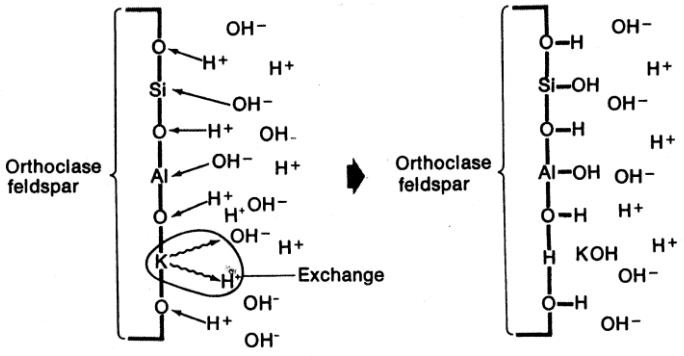

Figure 2.18. Simplified representation of acid-base dissolution of feldspar in which K^+ is substituted with H^+ ion, subsequently setting K^+ into solution. Replicated without change from Ritter (1978).

2.3.6 Mass Transport Processes

In the previous section the chemical processes that alter the chemical composition of surface and groundwater were identified. This section will introduce the transport processes that are responsible for the movement of solutes from one point to another. These processes initiate mixing of diverse water bodies, further changing the chemical composition of both surface and groundwaters and can be described by several processes; advection, diffusion and dispersion. The combination of the above is responsible for the mass transport of solute flux within, and between, surface and groundwater bodies.

Advection

The first order mechanism of groundwater mass transport is advection. This process is the movement of chemical solutes with the direction of groundwater flow (Freeze and Cherry, 1979; Steefel, 2008). In a simplified system with a constant fluid density, solutes move at the same mean linear velocity as the water body (Bear, 1979). The advective spread of chemical would remain linear and constant (Figure 2.19a) if not for the introduction of independent forces, described by the mechanisms of molecular diffusion and mechanical dispersion, that initiate the mixing of liquids of different chemical compositions (Bear, 1979; Steefel, 2008). As a result chemical constituents move in a spreading plume as opposed to a contained linear mass (Figure 2.19b).

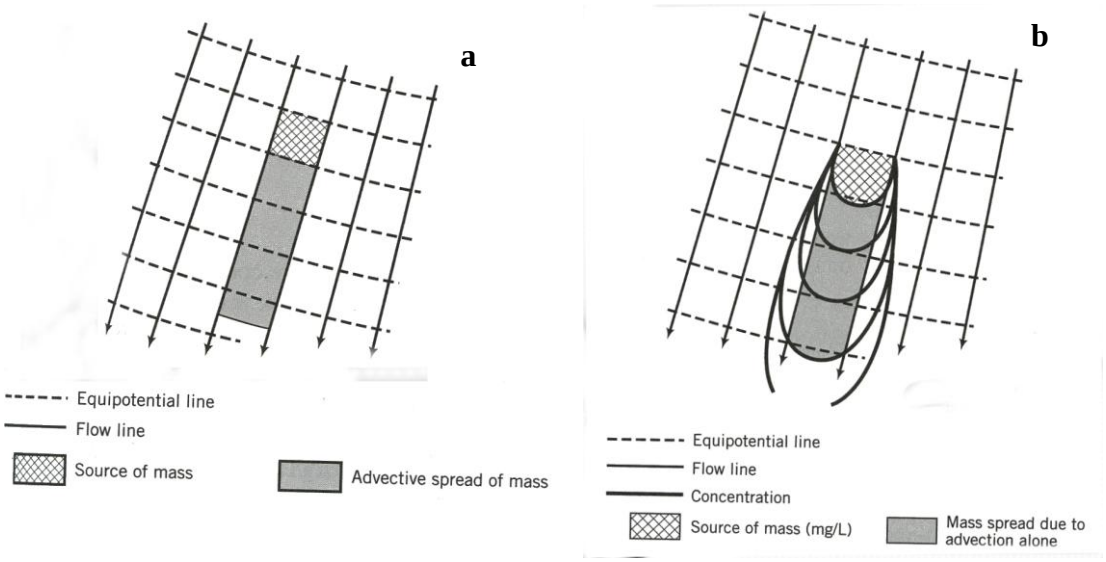

Figure 2.19. Simplified schematic representation of **(a)** advective and **(b)** dispersion transport. Replicated without change from Schwartz and Zhang (2005).

Molecular diffusion

Molecular diffusion occurs due to the presence of a chemical concentration gradient in which water of high solute concentration moves to water of a lower solute concentration in order to achieve chemical equilibrium (Freeze and Cherry, 1979; Schwartz and Zhang, 2003; Atteia *et al.*, 2005). Molecular diffusion occurs at a micro scale (e.g. µm to several metres) and therefore individually plays little part in chemical transfer of mass over regional scales. The chemical flux of this diffusion is commonly described in groundwater by a modified Ficks flow law (Equation 2.13).

$$J_i = \eta \tau D_i \frac{\partial C_i}{\partial x} \qquad (2.13)$$

Where.

J_i = Chemical mass flux

η = effective porosity

τ = tortuosity of the medium

D_i = Molecular diffusion coefficien t of an aqueous chemical

$\frac{\partial C_i}{\partial x}$ = concentrat ion gradient

This states that diffusion is proportional to a concentration gradient, the effective porosity of sediment, the tortuosity of the medium and the molecular diffusion coefficient of the individual ion of interest. A range of ion molecular diffusion coefficients are presented in Table 2.7.

However, in reality application of such coefficients can be difficult, as molecular diffusion is further influenced by the concentration of the diffusing ion and other ions in solution (Ingebritsen *et al.,* 2006). Further information regarding Ficks flow law and its individual components are beyond the scope of this review and are provided by Steefel (2008).

Table 2.7. Example cation and anion diffusion coefficients (D_i) provided by Steefel (2008).

Cation	D_i	Anion	D_i
H^+	9.31	OH^-	5.27
Na^+	1.33	Cl^-	2.03
K^+	1.96	NO_3^-	1.90
Mg^{2+}	0.705	HCO_3^-	1.18
Ca^{2+}	0.793	NO_2^-	1.91
Fe^{2+}	0.719	PO_4^{2-}	0.612

Dispersion

Local variations in flow velocity further initiate the mixing of groundwater chemistry. This process, known as mechanical dispersion, is caused by variability in the porous medium through which groundwater flows (DeWiest, 1965; Schwartz and Zhang, 2003). Such porous heterogeneities create channels of fast velocity in which individual fluid particles travel at variable velocities through the porous medium. This results in the breakdown of linear advective transport, the creation of plumes and the displacement of one fluid with another (Figure 2.20b).

Factors that cause variability in local velocities can occur at a variety of scales, ranging from the micro scale (pore size, porosity) (Figure 20a), to the macro scale (structural geology, faults) (Figure 20b) (Schwartz and Zhang, 2003; Steefel, 2008). Mechanical dispersion is commonly visualized through the injection of dyes into the fluid of interest. Generally the centre of the slug will travel at a constant mean velocity, increasing in volume and initiating mixing with surrounding fluid (DeWiest, 1965). Mechanical dispersion requires advection to operate and is dominant at high velocities (Ingebritsen *et al.,* 2006). Further, it enables mixing of large water bodies and the transfer of chemical mass across regional systems.

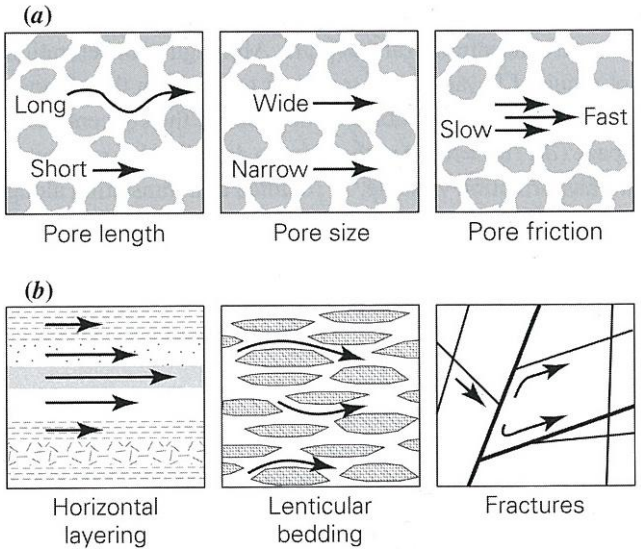

Figure 2.20. Factors that cause variability in local flow velocities at a micro-pore scale **(a)** and regional-field scale **(b).** Replicated without change from Ingebritsen et al. (2006).

2.4 Gaps in the literature and research justification

Research surrounding surface and groundwater interaction has progressed significantly through the concurrent monitoring of flow and water temperatures, analysis of chemical constituents and isotopes and the development of various subsurface empirical flow models and end member mixing models. However, large knowledge gaps still surround the degree of this interaction, in particular across dynamic and diverse environments. Progress in the use of chemical constituents, nutrients and isotopes to infer interaction is largely associated with the movement of anthropogenic contaminants (e.g. Chapman *et al.*, 2007; Kumar *et al.*, 2009) and water age dating (e.g. Ojiambo *et al.*, 2005). However changes in the natural composition of surface and groundwater due to their interaction and the spatial and temporal scale at which these changes occur are not well documented. A number of review papers from both ecological (e.g. Dahm *et al.*, 1998) and hydrological viewpoints (e.g. Winter *et al.*, 1998) suggest the need for a greater understanding of these interactions and the role hydrological processes play on biogeochemical processes at the aquifer-stream interface (Winter *et al.*, 1998). This is supported in the review by Sophocleous (2002) that calls for further quantification of the temporal dynamics of water and chemical flux between these water bodies.

Limited research has been undertaken investigating the physical or chemical interaction between surface and groundwater in New Zealand environments. Burden (1982) and Taylor *et al.* (1989) inferred potential interaction between groundwater aquifers and major river systems of the Canterbury plains using similarities in water chemistry and isotopes. Although these investigations link surface and groundwater bodies and suggest interaction they provide little information on the wider spatial and temporal patterns at which this interaction occurs and the processes that influence this phenomena. Concurrent flow gauging of river systems have also been undertaken by a number of regional councils to identify areas of water gain or loss between ground and surface water systems (e.g. Dravid and Brown, 1997, Jones and Gyopari, 2006). Again, although these investigations indicate the transfer of water between various systems they make little reference to the processes that influence this phenomenon and the spatial-temporal scales at which this interaction occurs. Further, initial observations are rarely supported or validated with new measurements.

In recent years detailed investigations surrounding New Zealand groundwater systems and their interaction with surface water have been undertaken by GNS Science (e.g. Stewart *et al.*, 2003; Daughney and Reeves, 2005; Reeves *et al.*, 2008). These investigations utilised a number of methods such as chemical and isotopic analysis, river flow gaugings and piezometric contour analysis to infer the transfer of water between surface and groundwater bodies. Results presented by Stewart *et al.* (2003) suggested that groundwater systems at Quinney's Bush and North Bridge near Nelson received 87% and 63% of their respective recharge from the Motupiko and Motueka Rivers. This assumption is based on a sensitivity analysis model that identified the relative influence of input variables (precipitation and river flow data) on groundwater levels to infer interaction. Further supporting evidence was provided through a comparison of isotopic and chemical data from the river and groundwater systems. Although this report attempted to quantify the extent of this interaction, model inputs were largely based on limited sample measurements that potentially failed to capture temporal variability of the systems of interest.

This simplification of a possibly dynamic interaction system may be sufficient for operational hydrology, however in order to gain an adequate understanding of ground and surface water interactions more detailed investigations must be undertaken that specifically investigate the complexity that these interactions and their associated processes may possess.

The lack of current research surrounding ground and surface water interaction in New Zealand can be attributed, in part, to the treatment of each water body largely as an individual resource. As mentioned in Section 3.5.2 current State of the Environment (SoE) monitoring programmes investigate hydrochemical changes in both groundwater and surface water monitoring sites across the country. However, these programmes are governed by separate research institutions (GNS Science and NIWA) that fail to coincide sampling programmes and frequently analyse and present results with little thought given to the possible interaction between water bodies and the influence this may have on their composition. This poses the question: if separate surface and groundwater data sets are available from various institutions then what can we learn about the chemical interaction between surface and groundwater if we systematically compare them? Hydrological investigation approaches generally attempt to quantify changes in discharge (e.g. Schwartz *et al.*, 2008), water temperature (e.g. Silliman *et al.* 1993) and/or chemistry (e.g. Burden , 1982; Kumar *et al.*, 2009) in both surface and groundwater bodies to infer interaction. If such SoE data are available can we classify surface and groundwaters into similar hydrochemical categories or facies and infer interaction from this? Although this conjures questions regarding the comprehensiveness and accuracy of such datasets, it provides a starting means by which the potential interaction between ground and surface water could be investigated.

Surface and groundwater monitoring (e.g. Regional council, SoE) and temporal investigations surrounding their chemical interaction are typically conducted at weekly to yearly timescales (e.g. Scanlon 1989 and Wollschlager *et al.*, 2007) or as one off samples (e.g. Taylor *et al.*, 1989). These temporal regimes are largely determined by monetary restrictions and the common perception that physical and chemical subsurface transformations occur over extended periods of time (Kirchner, 2006).

However, significant transfer of water between surface and groundwater bodies can occur within minutes, with exchange areas often small and easily missed (USEPA, 2000). Likewise solute transport can occur over these short time frames, and geochemical conditions and contaminant concentrations may change significantly over small spatial scales (e.g. centimeters) (Kirchner, 2006). Silliman *et al.* (1993) has shown that noticeable changes in sediment and water column temperature occur on a daily scale in response to influent and effluent river reaches. This highlights the importance of identifying surface and groundwater interaction occurring at sub-monthly and sub-daily timescales and the potential influence this may have on the chemical composition of water bodies. Further, the scientific community, as outlined by McDonnell (2003), is calling for the collection of more high resolution or "hard" data to gain a greater understanding of hydrological processes and to validate existing hydrological models. This is supported in the context of this investigation by Kirchner (2006) and Schmalz *et al.* (2007) who suggest that weekly or monthly monitoring of hydrological systems does not adequately capture potentially important hydrologic and chemical changes and therefore measurements need to be obtained at higher resolutions. Further, Kirchner (2006) believes new detailed hydrochemical datasets can provide enormous insight into our current understanding of hydrological processes and theories.

Chapter 3
The Wairarapa Valley

In order to evaluate ground and surface water interaction and the various geomorphic and geological processes that influence this phenomenon a sound understanding of the geological history and makeup of the Wairarapa valley is required. These historic geomorphic and geological processes have determined the distribution of permeable and impermeable material and therefore the location of aquifer bodies and transfer points between ground and surface waters. Further, the geological materials through which both surface and groundwater bodies flow heavily influence their chemical composition.

3.1 Geological history

The Wairarapa Valley is a large geological depression located in the south-east corner of the North Island of New Zealand (Figure 3.1). The valley extends approximately 80km north-east to south-west from Ekatahuna to Palliser Bay and largely overrides the locked subduction interface of the Australian and Pacific plates (Figure 3.1 and 3.2) (McConchie, 2000). Active plate margin tectonism, from as early as the Triassic-Jurassic era (280-150 million years before present), has resulted in the transfer of deformation stresses to the earth's surface through a range of active faults, folds and uplift blocks (Morgan and Hughes, 2001). Consequently, the valley is bounded by a series of axial greywacke ranges on its western periphery with the Rimutaka and Tararua Ranges and similarly the south-east periphery with the Aorangi ranges. These hard, heavily vegetated, Triassic-Jurassic greywackes form the highest relief in the area, reaching elevations of 1500m (Kamp, 1992). The north-east boundary of the valley is bound by soft, early Pleistocene/Late Tertiary marine sandstone, siltstone, mudstone and limestone ranges, the result of further compression, uplift and faulting of offshore marine sediments approximately 13-6 million years before present (MYBP) (McConchie, 2000).

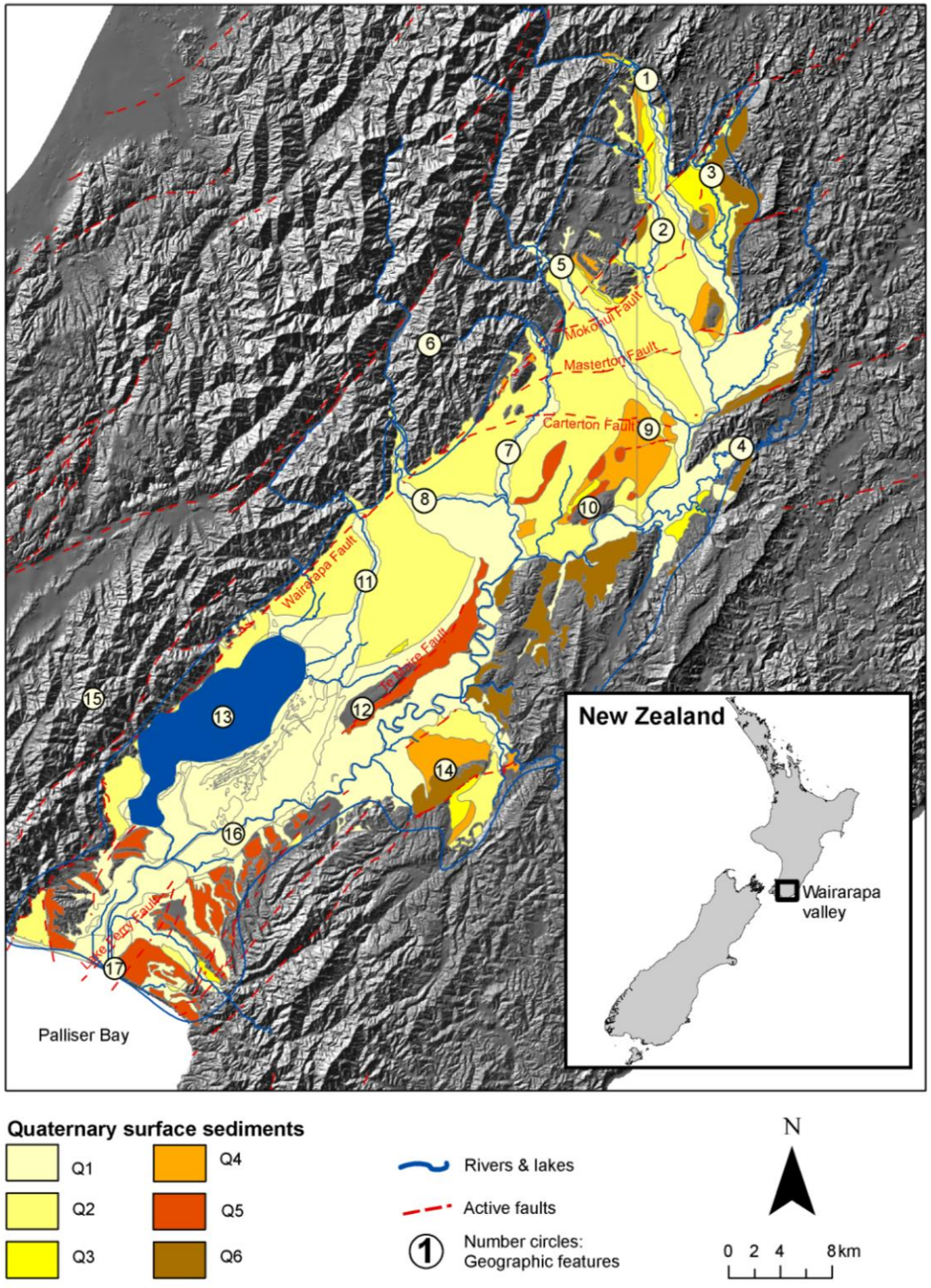

Figure 3.1. Location and geological map of the Wairarapa valley, New Zealand showing Quaternary surface sediments, active fault systems, major river and water bodies and a number of geographic features. Refer to Table 3.1 for Quaternary surface sediment ages. Circled numbers indicate major geographic features: 1) Ruamahanga River, 2) Waipoua River, 3) Whangaehu River, 4) Taueru River, 5) Waingawa River, 6) Tararua Ranges, 7) Mangatarere River, 8) Waiohine River, 9) Fernhill, 10) Tiffen Hill, 11) Tauherenikau River, 12) Te Maire Ridge, 13) Lake Wairarapa, 14) Martinborough Terrace, 15) Rimutaka Ranges, 16) Lower Ruamahanga River, 17) Lake Onoke.

During the Quaternary period (< 2 MYBP) substantial glacial and freeze thaw processes were operating in the high elevations of the Tararua and Rimutaka ranges (McLintock, 1966; Kamp, 1992). These processes, coupled with a lack of vegetation on the steep slopes, resulted in increased physical weathering and an overall smoothing of the ranges (Kamp, 1992). Resulting sediments were incorporated into fluvial systems and subsequently deposited in the Wairarapa basin as successive Quaternary fluvial fans (Q2 sediments Figures 3.1, Figure 3.3 and Table 3.1) (Morgan and Hughes, 2001). Large fan systems such as the Tauherenikau, Waipoua and Ruamahanga fans spread south-east pushing poorly sorted gravel, sand and silt glacial deposits (Q2) to the eastern margin of the valley (Kamp, 1992; Jones and Gyopari, 2006). Fine, highly sorted sedimentary deposits derived from the marine ranges of the Eastern hill country were also deposited on the eastern flanks of the valley.

Table 3.1. Timescale (Stage, Epoch, period and age) of common Quaternary surface sediments (oxygen isotope stages) from the Wairarapa valley, New Zealand.

Geological units	Stage	Epoch	Period	Age
Q1		Holocene	Quaternary	
				10 ka
Q2		Pleistocene		
Q3	Last Glacial			
Q4				
Q5				80 ka
Q5	Last interglacial			100 ka
Q5				130 ka
Q6				

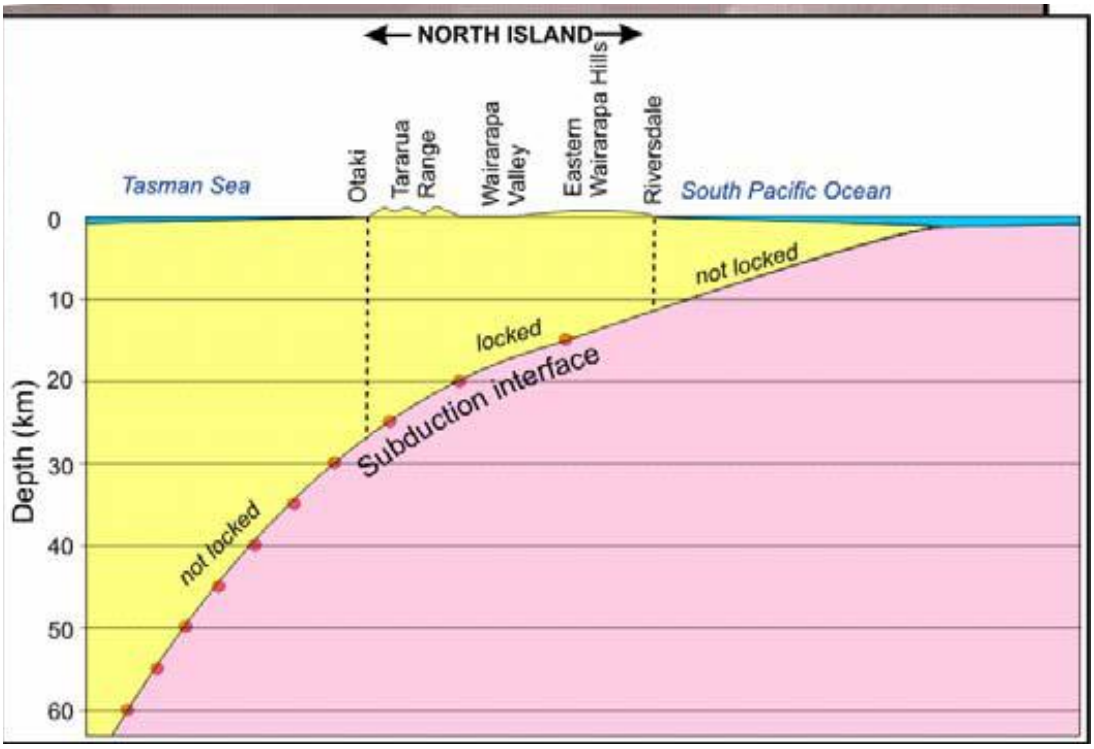

Figure 3.2. The Wairarapa region sits above the Pacific (pink) and Australian (yellow) tectonic plates. The Pacific plate is moving below the Australian plate at a rate of around 36-39mm/yr in this area, however the subduction zone is locked directly under the North Island. The resulting deformation stresses are transferred to the surface of the North Island resulting in the formation of the Wairarapa mountain ranges on the Australian plate. Source: Begg *et al. (*2005)

Global climate cycles and a shift to warmer inter-glacial temperatures resulted in the reworking of these fans and glacial deposits. The reworking of these depositional environments was assisted by a reduction in sediment supply to rivers, therefore increasing river erosive energy and ability to incise and rework depositional layers (Kamp, 1992). Further, substantial marine, estuarine and lacustrine depositional layers accumulated in the subsiding lower 25km of the Wairarapa valley due to global climate cycles and subsequent sea level fluctuations (Begg *et al.*, 2005). The lower basin contains 40-50 metres of postglacial estuarine mud, underlain by a sequence of lacustrine deposits that house at least six thin artesian gravel layers.

All of the described processes have resulted in substantial vertical and horizontal fluctuations in sediment deposition that heavily influence the distribution of aquifer bodies in the Wairarapa valley.

Figure 3.3. South facing photograph of the Wairarapa Valley. Taken from the onset of the Waiohine River gorge alluvial fan.

3.2 Hydrogeology

The complex mosaic of sedimentary layers within the Wairarapa basin has resulted in a dynamic regional groundwater basin that overrides a low permeability deposit of middle Quaternary clay and silt sediments (mQa) (Begg *et al.*, 2005). This layer of middle Quaternary sediments is likely the confining base of the groundwater system. The Wairarapa regional groundwater basin is compartmentalized into various sub-domain flow systems by the Mokonui, Masterton and Carterton faults that traverse the upper Wairarapa valley (Figure 3.1) (Jones and Gyopari, 2006). Here older, less permeable middle Quaternary sediment layers have been pushed towards the surface, creating barriers that restrict the movement of groundwater. Localised regions of subsidence and uplift, the result of tectonic fault movement, have also resulted in elevated basement and Quaternary sediments such as Tiffen Hill and Fernhill and localised depressions such as the Te Ore Ore Basin (Figure 3.4 and Figure 3.5). The distributions of such phenomena and the resulting hydrostratigraphic units have created various flow systems within the Wairarapa valley. These are presented in Figure 3.4.

The Greater Wellington Regional Council (GWRC) has classified the Wairarapa groundwater system into six broad hydrostratigraphic units (Jones and Gyopari, 2006). Identification of such units is based on lithology, aquifer yields and aquifer properties and is presented in Figure 3.4 and Table 3.2.

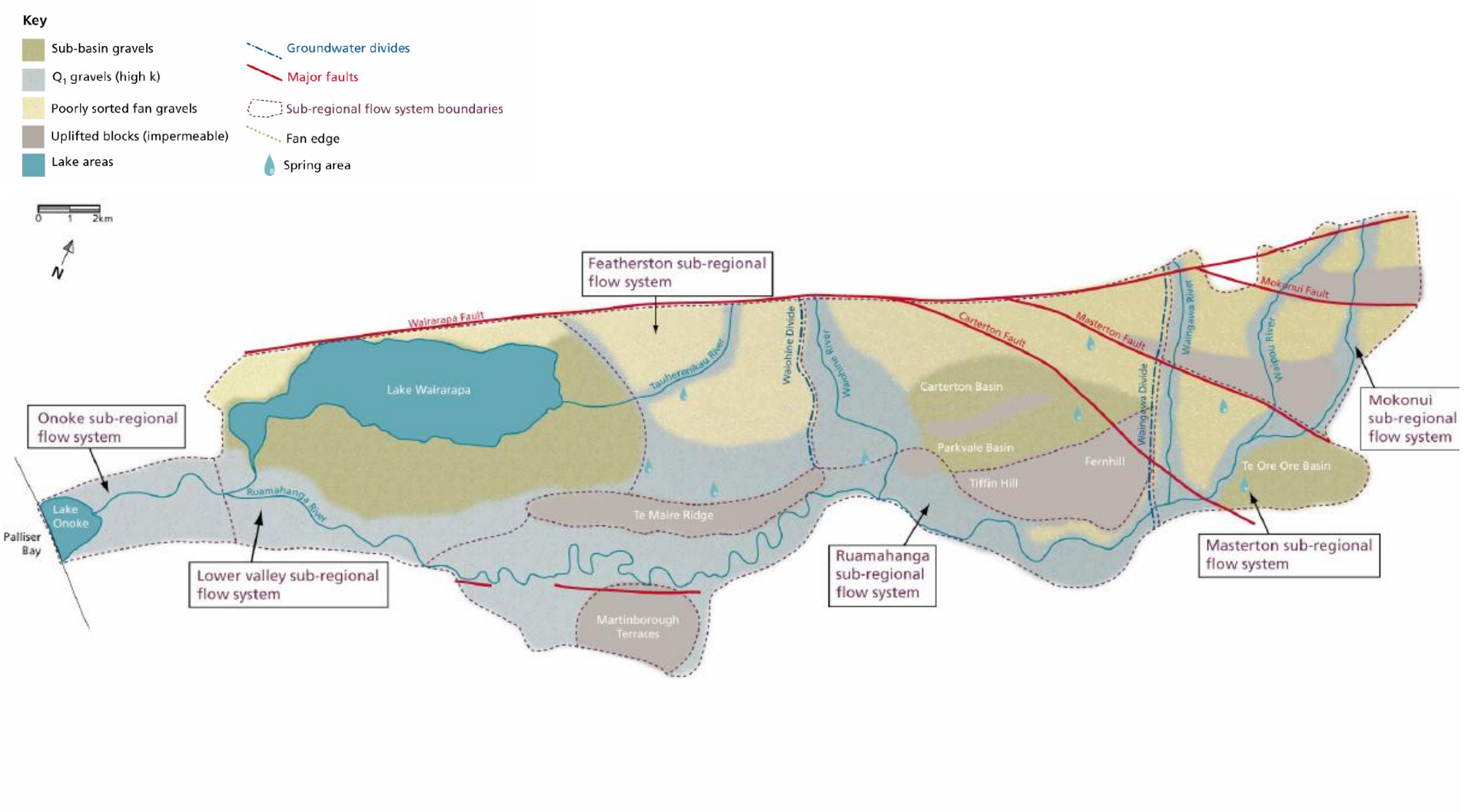

Figure 3.4. Sub-regional flow systems and hydrostratigraphic units of the Wairarapa Valley, New Zealand, including location of fault lines and major surface water features. Replicated without change from Jones and Gyopari (2006).

Table 3.2. Identified Wairarapa valley hydrostratigraphic categories, their general hydraulic nature and spatial distribution. '*K*' denotes hydraulic conductivity. Source: Jones and Gyopari (2006).

Unit	Name	General hydraulic nature	Spatial distribution
1	Alluvial fans/outwash gravels	Low *K*, poor yields	Major fan systems on western valley side of Tauherenikau, Waiohine, Waingawa, Waipoua rivers.
2	Q1 Holocene gravels	High *K*, reworked, strong connection with rivers	Main river channels, Waiohine floodplain, Ruamahanga floodplain, lower valley.
3	Reworked gravels	Medium to high *K*, generally thin localised zones.	Distal environment – lower valley, eastern side of valley, sub-basins (Te, Ore Ore, Parkvale).
4	Lower valley transition Zone	Med. to high *K*, intercalated permeable gravels and low *K* lacustrine/estuarine sediments.	Lower valley: lower Tauherenikau fan – northern lake area; Huangarua area.
5	Uplifted blocks	Very low or low *K*. Low bore yields. Form flow barriers.	Lansdowne, Tiffern, Fernhill, Te Maire ridge, Martinborough terraces.
6	Lower valley sub-basin estuarine and lacustrine deposits	Very low *K*; occasional thin high k gravel layers	Lower Valley, Lake Wairarapa.

3.2.1 Regional groundwater flow direction

Groundwaters within the Wairarapa valley follow a general regional flow direction, moving down valley in a south-easterly direction (Figure 3.5). This movement largely follows changes in topography but is also heavily influenced by the presence of impermeable barriers (Jones and Gyopari, 2006). Waters in the northern upper valley move through historic alluvial fan systems towards the Ruamahanga River and Te Ore Ore Plains. As these waters move down valley, flow is redirected by the impermeable Tiffen Hill and Fernhill and begins to move in a southerly direction parallel to the Parkvale and Carterton basins. The onset of Te Maire Ridge, mid-valley, forces regional flow to return toward a south-east direction as it is forced between the ridge and neighbouring Martinborough Terraces. Further, the Te Maire Ridge acts as a flow barrier, directing those groundwaters that flow south-east through the Tauherenikau outwash fans south. A number of springs discharge at the Te Maire Ridge as groundwater systems are forced upward due to the impermeable sediments (Jones and Gyopari, 2006).

In the lower valley the piezometric gradient is reduced as groundwaters flow into the subsiding valley (Figure 3.5) (Begg *et al.*, 2005). Flow tends to be directed toward the area beneath Lake Wairarapa and is prevented from reaching the ocean by an uplifted impermeable barrier below Lake Onoke (Jones and Baker, 2005).

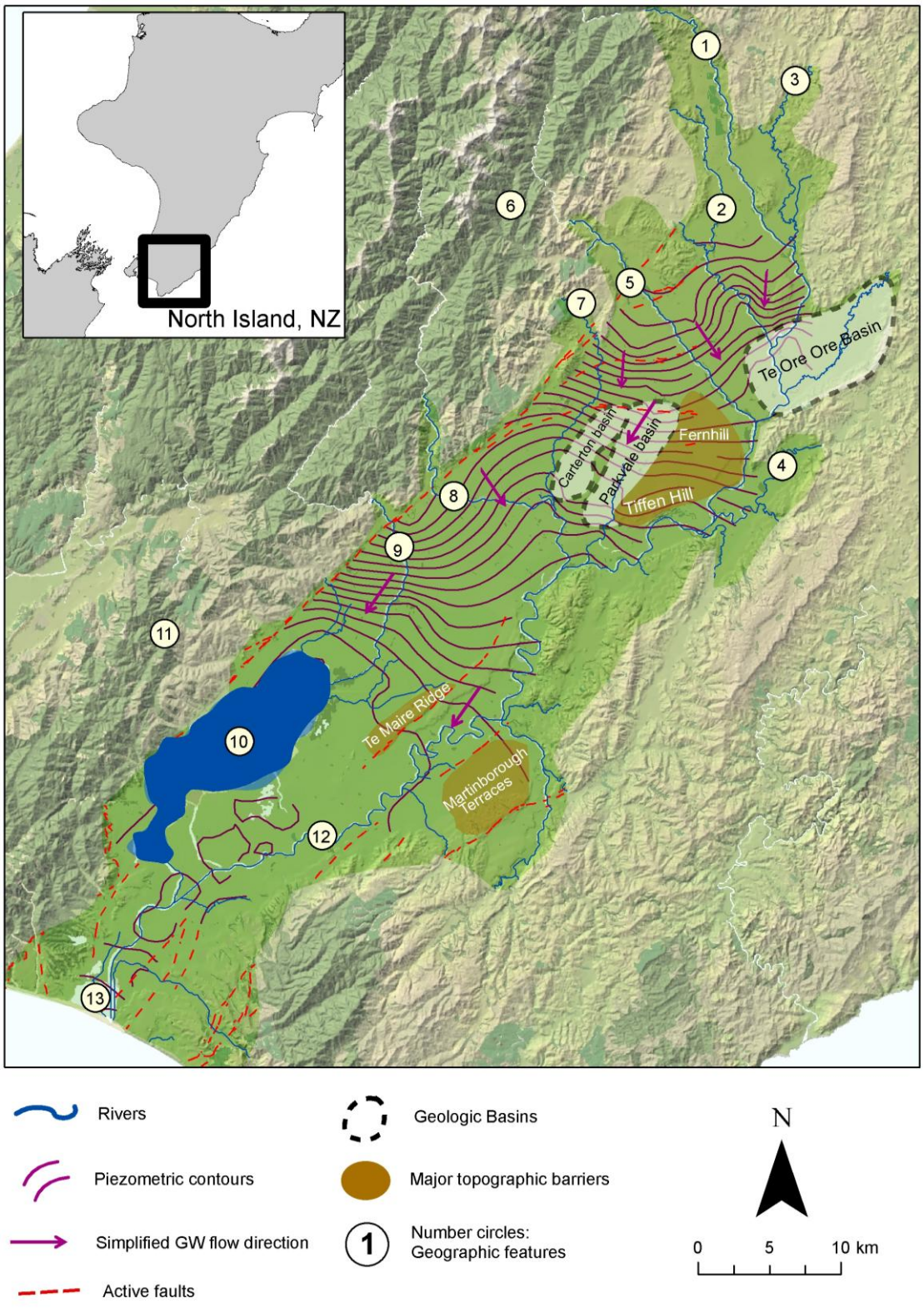

Figure 3.5. Piezometric contour map of the Wairarapa valley, New Zealand showing simplified groundwater flow direction, major topographic flow barriers, geologic basins, active faults and a number of geographic features and rivers. Circled numbers indicate major geographic features: 1) Ruamahanga River, 2) Waipoua River, 3) Whangaehu River, 4) Taueru River, 5) Waingawa River, 6) Tararua Ranges, 7) Mangatarere River, 8) Waiohine River, 9) Tauherenikau River, 10) Lake Wairarapa and 11) Rimutaka Ranges, 12) Lower Ruamahanga River, 13) Lake Onoke.

3.2.2 Groundwater recharge mechanisms

Groundwater systems in the Wairarapa Valley are recharged by two main recharge mechanisms (Jones and Gyopari, 2006). The distribution of these mechanisms is largely affected by Quaternary surface sediments and the Wairarapa fault system, and shows significant spatial variability (Figure 3.6). Groundwaters underlying Q1 river gravels are largely recharged by overlying river systems such as the upper Mangatarere, Tauherenikau and parts of the Ruamahanga. This mechanism of recharge provides the largest quantity of water to the groundwaters of the valley (Jones and Gyopari, 2006) and will be discussed in more detail in Section 3.3.

Rainfall recharge is also another major mechanism with *ca.* 35% of rainfall contributing to groundwater recharge (Jones and Gyopari, 2006). Zones with significant rainfall recharge dominate the majority of the Wairarapa Valley and in particular can be associated with deep aquifers in the lower flanks of the valley (Figure 3.6). Recharge can also be provided by a mix of these two mechanisms with rain/river recharge zones located around the Waiohine, lower Mangatarere, Waipoua and upper Ruamahanga Rivers (Jones and Gyopari, 2006). These zones are largely associated with Q1, Q2 and Q4 sediments (Table 3.1 and Figure 3.1).

3.3 Surface hydrology

A number of river systems flow across the Wairarapa Valley, with their headwaters in the low to mid altitude Rimutaka, Tararua and Eastern Wairarapa Hills. Water is largely provided to these systems by rainfall and snowmelt, however a significant proportion is also supplied from underlying groundwater systems. As a result of the numerous input sources, flow is known to display significant seasonal variability, with high flows generally experienced during the winter months May to August (Table 3.3). This is supported by high rainfall during this period as identified in the National Institute of Water & Atmospheric Research (NIWA) Climate database (Figure 3.8). In general, as these rivers exit the surrounding hills and cross historic permeable outwash plains they lose water to underlying groundwater systems. Further downstream these same rivers usually switch to effluent systems in which a proportion of base flow is provided by groundwater systems.

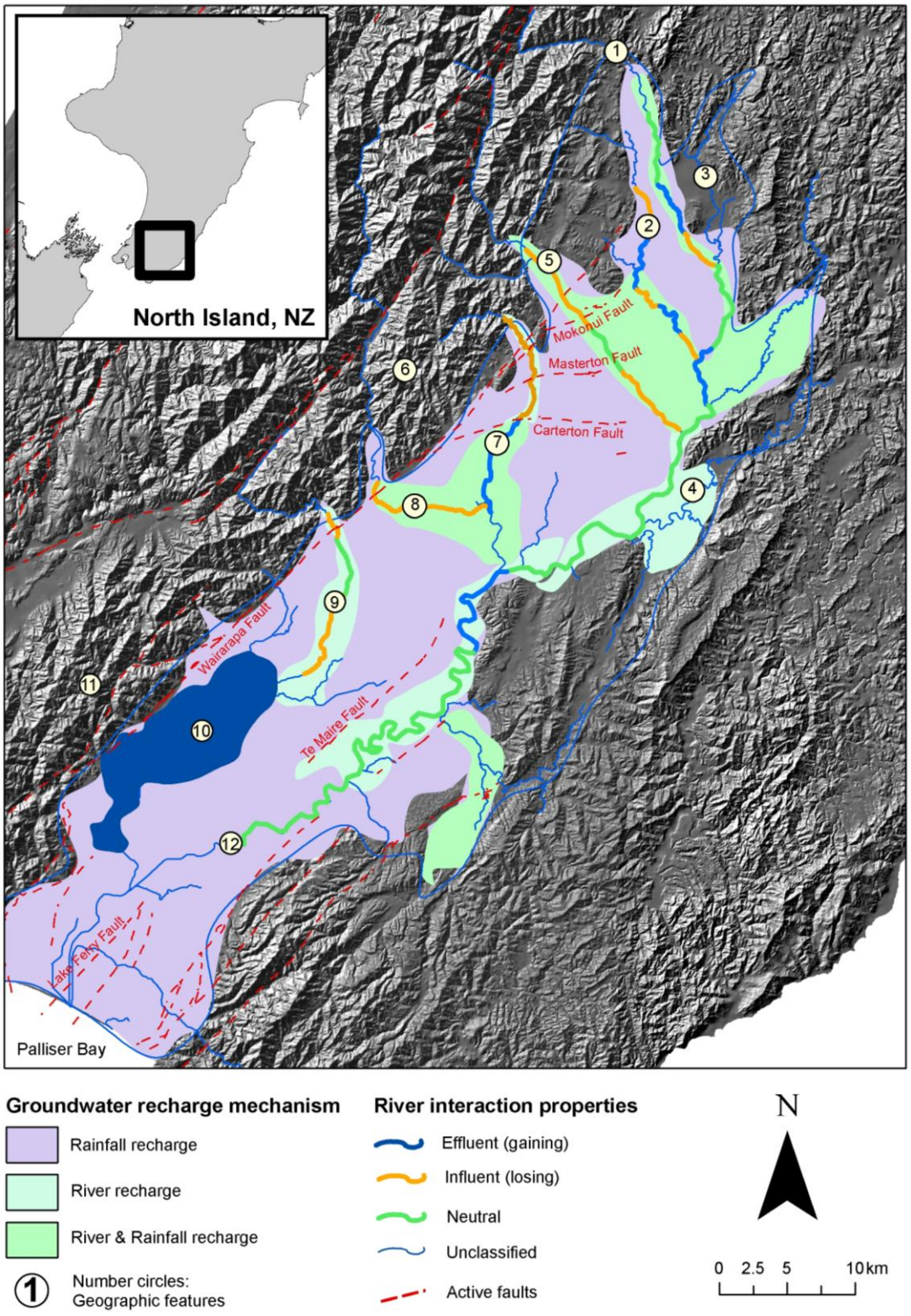

Figure 3.6. Identification of groundwater recharge zones and river interaction properties in the Wairarapa valley, New Zealand as classified by the Greater Wellington Regional Council. Major lakes and unclassified river systems are also identified. Circled numbers indicate major geographic features: 1) Ruamahanga River, 2) Waipoua River, 3) Whangaehu River, 4) Taueru River, 5) Waingawa River, 6) Tararua Ranges, 7) Mangatarere River, 8) Waiohine River, 9) Tauherenikau River, 10) Lake Wairarapa, 11) Rimutaka Ranges, 12) Lower Ruamahanga River. *Source:* Jones and Gyopari (2006).

Rivers within the Wairarapa valley are thought to display significant connectivity with underlying groundwater systems. This assumption is based on concurrent flow gaugings undertaken by the Greater Wellington Regional Council (GWRC) in 2006 that have resulted in the classification of river systems into three interacting categories; influent, effluent and neutral reaches. The direction of interaction is presented in regards to the river system (e.g. influent interaction refers to the river losing water to groundwaters, while effluent interaction refers to the river gaining water from groundwaters). An error of around ±10% is associated with the flow gaugings and is likely to be transferred to the classification of interacting properties.

The Ruamahanga River is one of the largest in the valley by flow quantity and experiences flow ranging from 11-20 m^3/s during the summer and 20-40 m^3/s in the winter. The river originates high in the Tararua ranges and flows south-east across poorly sorted alluvial gravels before straddling the eastern periphery of the valley and joining Lake Onoke. The Waipoua, Waingawa, Waiohine rivers and Lake Wairarapa provide flow to the river at various points throughout the valley. The Ruamahanga displays a high degree of interaction with underlying groundwater systems and has been identified as having both influent and effluent reaches through concurrent flow measurements (Jones and Gyopari, 2006). In the upper reaches it appears the degree of interaction is influenced by the Mokonui and Masterton fault lines that push impermeable sediments to the surface. As a result the system switches between an effluent and influent reach (Figure 3.6). A significant volume of water is also provided to the Ruamahanga from groundwater sources as it passes over the Te Ore Ore sub-basin and near the Greytown springs. The lower reaches of the river appear to show little interaction with groundwater systems.

The Waiohine is another major river system that drains the Tararua ranges with average flow ranging between 11-30 m^3/s. The river generally flows east across the valley before joining with the Ruamahanga River, and has an identified influent reach as the river exits the Ruamahanga gorge. Available flow gaugings show *ca.* 1800 m^3/s is lost to groundwater as the river flows across Q1 gravels and joins with the Mangatarere stream (Figure 3.6) (Jones and Gyopari, 2006).

Table 3.3. Mean monthly stream flow (m^3/s) for a range of major Wairarapa valley Rivers. Data range varies on a site by site basis and is displayed in the first column. Source: Keenan and Gordon (2008).

Site location and sampling date range	Jan	Feb	Mar	Apr	May	Jun	Jul	Aug	Sep	Oct	Nov	Dec
Ruamahanga at Wardells (1977-2008)	11.4	13.1	13.1	15.5	21.5	31.4	39.2	35.5	27.8	32.3	21.6	18.5
Waiohine at Gorge (1979-2008)	17.2	16.8	17.3	18.0	22.6	27.6	30.6	29.0	27.5	34.2	27.6	26.5
Mangatarere Stream at Gorge (1999-2008)	0.9	1.1	1.0	0.9	1.8	2.6	2.9	2.8	1.6	3.0	1.7	1.4
Whangaehu River at Waihi (1967-2008)	0.1	0.2	0.6	0.3	0.5	1.0	1.2	1.1	0.8	0.6	0.3	0.2
Waingawa River at Kaituna (1976-2008)	6.8	6.8	2.7	7.8	9.8	12.1	13.3	13.0	12.2	13.3	10.7	10.2
Tauherenikau River at Gorge (1976-2008)	5.3	5.1	6.0	6.6	9.1	11.8	13.4	12.1	10.7	12.0	8.5	8.6

The Waingawa and Waipoua Rivers, both medium sized rivers, also drain the Tararua ranges. Flowing south-east, these rivers dissect poorly sorted alluvial gravels and are known to interact with groundwater systems. As with the Ruamahanga, their degree of interaction is highly influenced by the Mokonui and Masterton fault lines (Jones and Gyopari, 2006). Both river systems display influent reaches that change as they cross the various fault lines (Figure 3.6).

The Tauherenikau and Mangatarere rivers flow south-east across the valley and join with Lake Wairarapa and the Waiohine River respectively. The Tauherenikau River has a considerably higher yearly flow range (5-13 m^3/s), in comparison to that of the much smaller Mangatarere stream (0.9-3 m^3/s). Both rivers largely dissect poorly sorted fan gravels and display various interaction properties with groundwater systems. The Mangatarere initially loses flow to groundwater, however upon crossing the Carterton fault it appears to switch and receive base flow from groundwater sources. Likewise, the Tauherenikau River initially loses flow as it leaves the Rimutaka ranges. This changes to a neutral reach for *ca.* 4.5km, before water once again is lost the underlying groundwater system. Remaining flow from the Tauherenikau is the principal inflow to Lake Wairarapa in the lower valley.

Lake Wairarapa is a 76 km^2 shallow lake located in the lower subsiding flanks of the Valley. It receives the majority of its inflow from the Tauherenikau River and shallow groundwater systems located within neighbouring Q1 gravels. Further input waters are provided by shoreline springs that tap deep confined aquifers located within the underlying lacustrine and estuarine sediments (Jones and Gyopari, 2006). A number of small streams also drain the eastern Wairarapa hills. The Whangaehu River and the Waingongoro and Huangarua streams flow across historic alluvial fans and join the Ruamahanga River. Little information is available regarding their interaction with groundwater systems however it is likely, in areas of Q1 river gravels, that interaction occurs. Continuous discharge and flow data are not readily available as these systems are monitored for flood control only.

3.4 Climate

The climate of the Wairarapa valley is heavily influenced by the neighbouring Rimutaka and Tararua ranges that straddle the valley on its western periphery (Figure 3.1). These ranges act as a topographic barrier, sheltering the valley and its plains from the predominantly westerly winds, and create a vast disparity in rainfall distribution (Figure 3.7) (Hawke, 2000). The Wairarapa valley is located on the leeward side of the ranges and as a result is reasonably dry, receiving between 800-1000mm of annual precipitation (Thompson, 1982; Watts, 2005). In contrast the ranges themselves and their surrounding foothills receive up to 6000mm per annum as moist westerly winds are forced to dump their moisture whilst traversing the ranges (Hawke, 2000). During the summer months rainfall is more variable, however these months are generally drier with higher intensity rainfall generally recorded during the winter (Figure 3.8). The Wairarapa valley experiences mean annual temperatures of 12-14°C and it is common for dry fohn winds to move across the valley during the summer months. As a result the region experiences the highest temperatures during the months November to March (*ca.* 16.6°C) (Figure 3.8) and can be affected by summer drought conditions (Hawke, 2000; NIWA, 2009).

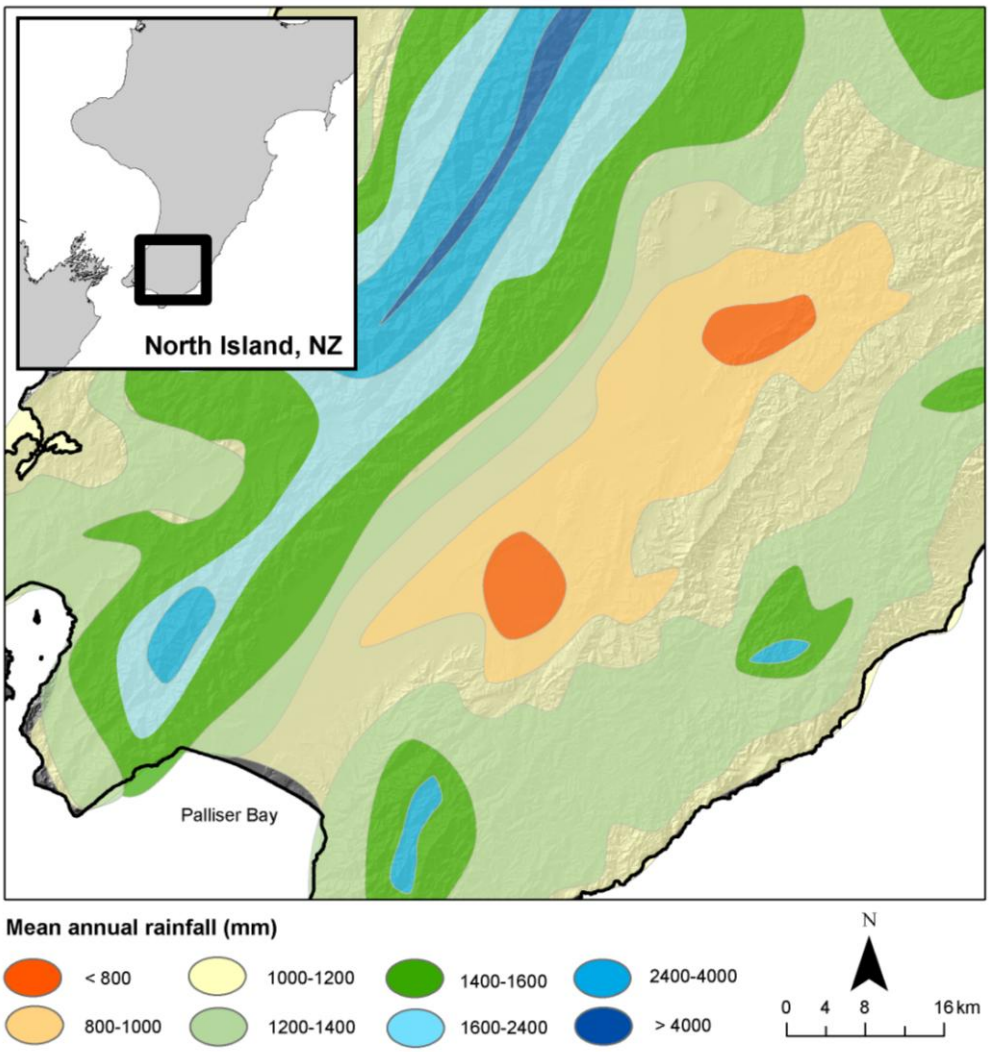

Figure 3.7. Distribution of mean annual precipitation in the Wellington region, including the Wairarapa valley. Modified from Watts (2005).

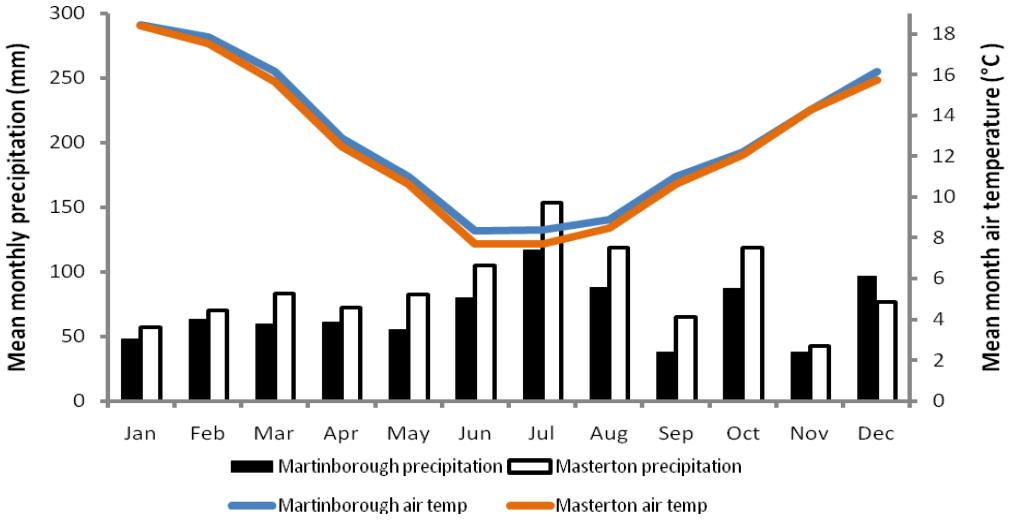

Figure 3.8. Mean monthly precipitation (mm) and air temperature (°C) for the townships of Martinborough (-41.252°S, 175.389°E) and Masterton (-40.957°S, 175.707°E). Based on 2004-2008 data. Source: NIWA (2009).

3.5 Human history and land use

As identified in Section 2 the interaction between ground and surface water is affected by a range of geomorphic and physiographic environmental processes. Therefore, human modification of vegetation, soil and hydrological systems must be acknowledged and understood to sensibly explore ground and surface water interaction in the Wairarapa valley.

Prior to human settlement much of the Wairarapa valley was covered in dense Podacarp-dominant forest such as *Podacarpus totara, Dacrycarpus dacrydioides* and *Prumnopitys taxifolia* (Beadel *et al.*, 2000). Maori arrival in the 17th century brought significant modification to the landscape with widespread controlled and unintentional fires clearing much of the native forest. This cleared land was quickly re-colonised by native grasslands, fernland, swamps and shrub. The arrival of Europeans to New Zealand shores in the 19th Century, and the abundance of grass and fernland, made the Wairarapa an appealing location for the establishment of farming (Beadel *et al.*, 2000). Extensive burning of native shrub, fern and tussock to promote fresh growth for stock was undertaken. Likewise, much of the remaining native forest was cleared and wetlands drained for more intensive land use. Exotic plant species such as Sweet vernal (*Anthoxanthum odoratum)*, timopth (*Pleum pretense*), Yorkshire fog (*Holcus lanatus*), and couch (*Elytrigia repens*) were also introduced and quickly re-colonised the Wairarapa valley.

Today land use in the Wairarapa is dominated by pastoral agriculture that covers approximately 76% of the valley (Figure 3.9) (Jones and Baker, 2005). Beef, sheep and dairy are the main forms of farming, and this is reflected in the vegetation with the valley being dominated by pastoral grasses and shelter belts of Macrocarpa, Pampas grass, Radiata pine and riparian willows. Small viticulture and market gardening projects are also present around Martinborough and other urban centers. Small pockets of native forest are scattered throughout the valley, with a significant cluster straddling the shores of Lake Wairarapa (Figure 3.9). The agriculture, viticulture and horticulture activities in the Wairarapa are known to add additional nutrients and chemicals to the land through fertilizers, soil cultivation and the discharge of effluent (Watts, 2005).

These analytes include NO_3^-, NH_4^+, P and the chemicals K^+ and Cl^-, and have the ability to be transported or leached into both surface and groundwater systems.

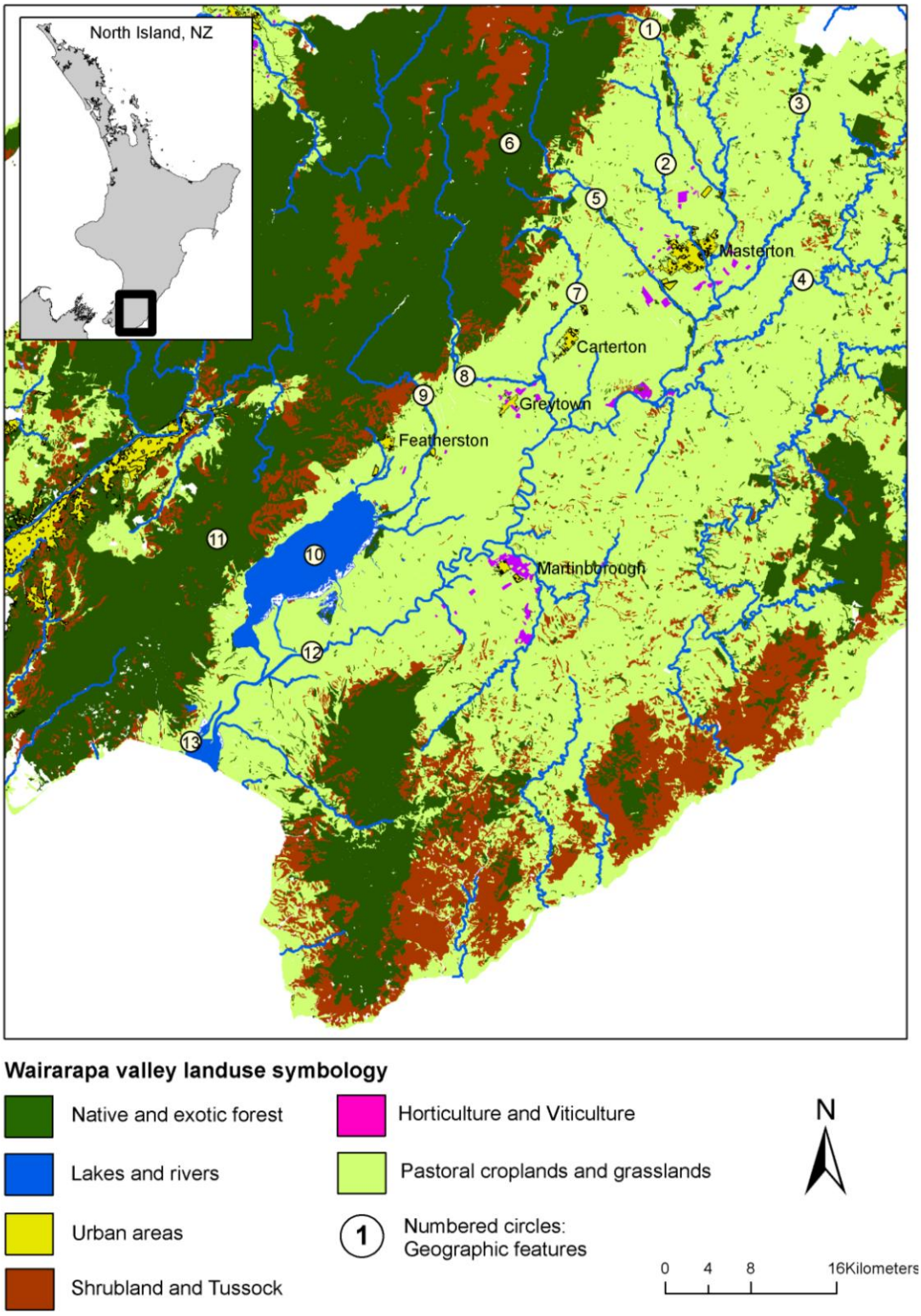

Figure 3.9. Landuse map of the Wairarapa valley and surrounding areas identifying main land use types and major geographic features. Circled numbers indicate major geographic features: 1) Ruamahanga River, 2) Waipoua River, 3) Whangaehu River, 4) Taueru River, 5) Waingawa River, 6) Tararua Ranges, 7) Mangatarere River, 8) Waiohine River, 9) Tauherenikau River, 10) Lake Wairarapa and 11) Rimutaka Ranges, 12) Lower Ruamahanga River, 13) Lake Onoke.

3.5.1 Surface and groundwater abstraction

Initially groundwater abstraction in the Wairarapa was for small-scale stock and rural domestic supply (Morgan and Hughes, 2001). The intensification of agriculture in the 1960's and the subsequent pressure placed on surface water extraction led to the establishment of the Wairarapa Catchment Board in 1970. This board aimed to achieve a greater understanding of water resources and their management in the area and undertook an extensive groundwater investigation between 1981 and 1986. Exploratory bores were established for long term automatic and manual monitoring that aimed to investigate groundwater depth, chemical composition and establish a network of piezometric contours (Morgan and Hughes, 2001). The investigation suggested that further comprehensive research was required to fully understand the dynamic nature of the Wairarapa groundwater system.

In 1989 groundwater allocation was 25million m^3/year, a value that almost doubled to 48million m^3/year by 1999 (Jones and Baker, 2005). Based on values provided by Morgan and Hughes (2001) it is likely nearly one third of rainfall recharge to the Wairarapa valley (*ca.* 150million m^3/year) is allocated for abstraction. Surface and groundwater abstraction has continued to increase substantially since the last decade in response to rising agriculture and horticulture needs (Jones and Baker, 2005). In December 2004 there were over 150 individual surface and 318 groundwater extraction permits, a number which is likely to have increased in recent years. Although the majority of such groundwater takes are less than 500m^3/day, several larger takes extract over 4000m^3/day. Further, large seasonal discrepancies in abstraction are present, with the majority of water abstracted for irrigation during the warmer months of October to March. Accurate quantification of these abstraction rates is difficult in the area as most takes are not metered (Jones and Baker, 2005). The extent to which abstraction influences surface and groundwater interaction in the Wairarapa valley is not well understood.

3.5.2 Current hydrological monitoring in the Wairarapa valley

GWRC undertake a variety of hydrological and hydrochemical monitoring programmes throughout the year to gain insight into environmental trends in water quality and quantity, provide information to guide resource consent decision making and convey information about natural resources to the wider community (Watts and Gordon, 2008). Water stage is continuously monitored (usually 15 minute intervals) within the majority of river systems and stage-discharge rating curves are used to continuously estimate discharge. Stage is also monitored at a number of selected groundwater bores (15 minute intervals) throughout the Wairarapa valley, with additional bores monitored by hand using bore dippers. This raw stage data from both ground and surface water sites are uploaded, via telemetry, to the council's database every 2 to 3 hours.

Hydrochemical monitoring of ground and surface water in the Wairarapa is generally undertaken by the council monthly for major river systems and every three months for major groundwater bores. Due to the sheer number of groundwater bores in the area the vast majority experience no chemical sampling. State of the Environment Monitoring (SoE) is also undertaken four times a year (March, July, September and December) at a selection of major river and groundwater systems (Watts and Gordon, 2008). Typically, groundwater sites are analysed for a full suite of parameters including the major ions and nutrients while analyses are largely restricted to water quality (e.g. *E.coli*) and nutrient indicators (e.g. NO_3^-, NH_4^+, P) for surface water bodies. Resulting data are used to document environmental change over time and can be compared with similar SoE monitoring data from other regions of the country. Results from all hydrochemical and hydrological monitoring programmes are summarised monthly and on an annual basis in hydrological summary reports compiled by GWRC.

3.6 Summary

The Wairarapa valley is a 90km structural depression that overlies the locked Pacific and Indo-Australian subduction zone. The valley is bound by the resistant Tararua and Rimutaka greywacke ranges on its western periphery and Pleistocene and late Tertiary sedimentary ranges on its eastern periphery. Successive glacio-fluvial layers have been deposited in the upper and middle section of the valley, while global climate cycles have resulted in deep layers of estuarine and marine sediment layers in the subsiding lower valley. This complex mosaic of sediments has created a diverse regional groundwater system that is further compartmentalized by the Masterton, Mokonui and Carterton faults that strike north east through the valley pushing impermeable sediments to the surface.

The valley is occupied by a number of significant river systems that largely overlie permeable Q1 alluvial gravels. These systems receive input from precipitation, snowmelt and groundwaters and tend to experience their highest flows during the winter when precipitation is greatest. Concurrent flow gaugings undertaken by the GWRC and the presence of permeable Q1 alluvial gravels suggest a number of these fluvial systems display strong interacting properties with groundwater systems. The extent of this interaction is not well documented or understood.

The Wairarapa has a strong history of agricultural use and today over 70% of the valley is occupied by pastoral agriculture. Subsequently, ground and surface water abstraction in the valley has increased over the last four decades to accommodate a surge in demand for irrigational waters. The impact of this extraction on ground and surface water interaction in the Wairarapa is not documented.

Chapter 4
Regional scale interaction

The main aim of this research was to determine if chemical measurements could be used to identify locations and timescales of interaction between surface and groundwater bodies in the Wairarapa valley, New Zealand. In order to achieve this, a comparison of surface and groundwater water quality was undertaken at both a regional and local scale within the Wairarapa Valley. This research strategy is formulated on the principle that the physical and chemical interaction between ground and surface water and the various physical pathways that water take influence the chemical composition of water (Dahm *et al.,* 1998; Winter *et al.,* 1998). The movement of water across the surface-groundwater interface is one of such pathways, and it is recognised that chemical parallels between the two water bodies can be used to indicate potential interaction (Taylor *et al.,* 1989). Regional scale interaction was assessed using historic hydrochemical medians and the statistical tool Hierarchical Cluster Analysis (HCA). This procedure aimed to link surface and groundwater sites into hydrochemical clusters according to similarities in water quality, and infer interaction based on these similarities. Further, the spatial distribution and overall regional extent of interaction was examined.

This chapter presents the results from the regional scale ground and surface water interaction investigation and is divided into seven main sections. The first section presents the methodology employed in this part of the investigation. This is followed by Section two which presents the findings of HCA using the Nearest Neighbour and Wards methods to identify sites with unusual chemistry (outliers), exclude them, and assign all remaining surface and groundwater sites to similar hydrochemical clusters. This is followed by a section that differentiates each individual cluster based on a range of statistical methods. In this section the spatial distribution of sites assigned to each cluster is also presented. Section four presents an overview of each assigned hydrochemical cluster and draws links between surface and groundwater sites in order to infer potential locations and styles of interaction.

Section five justifies the subjective nature in which clusters were determined by presenting an analysis of several alternative hydrochemical clusters and is followed by limitations surrounding this part of the investigation in section six. The final section presents a summary of potential ground and surface water interaction in the Wairarapa valley based on the results obtained from this regional scale investigation.

4.1 Regional scale methodology

In order to identify potential areas of regional scale surface and groundwater interaction a historic hydrochemical database (1965-2008) from the Wairarapa Valley was analysed and subjected to several statistical procedures. The database was provided by the Greater Wellington Regional Council (GWRC) and consisted of water quality data from 607 groundwater sites and 28 surface water sites (streams, rivers, lakes and springs). Groundwater sites were a mix of private boreholes, agricultural and domestic takes and long term water quality monitoring stations. Significant variability in sampling frequency was present between sites, with some locations sampled only once and others as often as monthly over two years. Variability also existed in regards to the number of parameters analysed at each site. For example some locations were only analysed for nutrients. Descriptive information regarding each monitoring site (e.g. site location, aquifer type and depth) was also obtained when available. Samples with unknown site locations (e.g. coordinates) were not included in the database due to their inability to be analysed spatially.

4.1.1 Dataset compilation

In total the database included over 6000 water samples that had been analysed for up to 50 variables (e.g. major and minor elements, pH, nutrients and electrical conductivity) over the 43 year sampling period. Concentrations were reported as mg/L, µS/cm for conductivity and pH units for pH. A complete list of parameters is presented in Appendix A. The dataset provided by GWRC included both 'dissolved' and 'total' concentrations of Na, K, Ca, Mg, B, Fe, P, Mn, SO_4, Cl and SiO_2. These referred to analyses conducted on field-filtered (dissolved) and unfiltered (total) water samples respectively.

Dissolved concentrations were selected for use, when available, as they were deemed less likely to be affected by post sampling chemical processes. When dissolved data were not available missing data were replaced with 'total' concentrations. Likewise both 'field' and 'lab' measurements of pH and conductivity were available for some sites. Field measurements were presented and supplemented with lab measurements when field data was unavailable. This approach was aimed to maximize the amount of data included in the database. Preference is given to field measurements as post sampling reactions (e.g. degassing) can influence conductivity and pH.

4.1.2 Calculation of medians

In order to improve the practical size of the workable database its size needed to be reduced. To achieve this, the log-probability method, based on the underlying theory of Helsel and Cohn (1988), was employed to allow the calculation of representative median values for each of the 50 analytes at each site. The log-probability method was deemed appropriate as it can account for up to 70% of the dataset being below a known detection limit (censored values) (Helsel and Cohn, 1988). This is a common occurrence in hydrochemical datasets and would usually reduce the number of input variables used in the calculation of the standard medians. The log-probability method calculates replacement censored values by plotting *Weibull plotting positions* for all uncensored data and using the slope and intercept of this regression to calculate values of concentration in regards to the censored data (Daughney, 2005). The log-probability method was conducted at each site, where data were available, using an automatic water quality processing program developed by Daughney (2005, 2006). For further information on the log-probability method and its algorithm refer to Helsel and Cohn (1988) and Daughney (2005). Following the calculation of new censored data the automatic water quality processing program (Daughney, 2005; 2006) was used to calculate median values for each of the water quality parameters. Median values were chosen, as opposed to averages, in order to reduce the influence of outlier chemistry and provided a more accurate snapshot of background water quality. The resulting output was a 50 analyte median x 635 site data array. When data was not available a median value could not calculated and the resulting analyte was left blank in the database.

4.1.3 Charge Balance errors

It was assumed that adequate sampling, control and analytical measures were performed at the time of original sampling. However it must be acknowledged that some error may compromise the quality of the existing hydrochemical dataset. In order to reduce these, charge balance error (CBE) was calculated to identify samples that are electrically unbalanced. At a macroscopic scale all water bodies are electrically neutral, with the sum of positive ionic charges (cations) equaling the sum of the negative ionic charges (anions) (Freeze and Cherry, 1979; Langmuir, 1997). As a result the calculation of CBE for each site can be used as an indication of data quality.

CBE were calculated at each site using Equation 4.1 and the median concentrations of the cations Na^+, K^+, Ca^{2+}, Mg^{2+} and the anions HCO_3^-, Cl^- and SO_4^{2-}. The use of such analytes is considered standard, as indicated by the hydrochemical literature (e.g. Freeze and Cherry, 1979; Güler *et al.,* 2002). Other analytes (e.g. Mn, NH_4^+, NO_3^-, Fe^{2+}) can usually be excluded from the CBE calculation due to their low concentrations. In an unconventional manner CBE were calculated for each monitoring location using site specific median concentrations. CBE were not calculated for each individual water sample, as is standard practice, as a large number of samples did not provide a full suite of individual parameters required to calculate CBE. In total CBE were calculated for 383 sites, with the remaining 252 sites excluded as two or more analyte median values were missing due to incomplete datasets. Subsequent CBE results are presented in Appendix B. Of the 383 CBE calculations, 56 had CBE above +10%, while 22 had CBE below -10%. The quality of data from these sites was therefore considered poor and they were excluded from further statistical analysis. A ± 10% CBE threshold was selected, as oppose to the industry standard ±5% (Freeze and Cherry, 1979), to exclude only those sites with severe charge imbalances. Although the calculation of CBE severely reduced the number of sites available it was necessary as it demonstrated severe errors in at least one analyte at some sites. It can be assumed these errors would also be present in some of the 252 non-calculated sites and therefore it was best to exclude them.

$$CBE \cong \frac{(Na^+ + Ca^{2+} + Mg^{2+} + K^+) - (Cl^- + HCO_3^- + SO_4^{2-})}{(Na^+ + Ca^{2+} + Mg^{2+} + K^+) + (Cl^- + HCO_3^- + SO_4^{2-})} \times 100 \quad (4.1)$$

Where analyte concentrations are presented as milli equivalents per litre (meq/L)

4.1.4 Hierarchical Cluster analysis

In order to link surface and groundwater monitoring sites, and infer locations of potential interaction, the hydrochemical database was subjected to HCA. The use of this procedure to link individual monitoring sites has been extensively applied in the hydrochemical literature (e.g. Alther, 1989; Güler and Thyne, 2004; Hussain *et al.*, 2008), and was conducted using the statistical package STATGRAPHICS Centurion (Version 15.2.12). HCA is a data reduction tool that works by partitioning a set of observations (e.g. monitoring sites) into a distinct number of clusters based on the statistical similarity of a given set of parameters (e.g. water quality medians) (Timm, 2002; Kumar *et al.*, 2009). Observations grouped together within the same clusters are statistically similar (at a 95% confidence level), while observations in different groups show little statistical similarity. This similarity is measured by the Squared Euclidian distance (SED) between two observations (x and y) (e.g. water quality parameters), as given in Equation 4.2. The SED is the geometric distance in multidimensional space between water chemistry at two specified sites (Kumar *et al.*, 2009).

$$d(x,y) = \sum_{i=1}^{n} (x_i - y_i)^2 \quad (4.2)$$

n = number of parameters considered

Following the calculation of the distance (similarity) between monitoring sites, each observation is placed automatically into an individual cluster. Clusters are then combined in a stepwise fashion, two at a time, based on their similarity measurement. This agglomerative process continues until all clusters have been joined and the user specifies an end target of clusters (e.g. five clusters) (Hair *et al.*, 2006).

Two methods of agglomerative HCA were employed. The first, the Nearest Neighbour linkage rule, was used to identify sites with outlier or unusual chemistry that may bias further statistical analysis. These outlier sites were excluded from the dataset and the remaining sites were subjected to further clustering using the Wards linkage method. Both linkage procedures are discussed further in the subsequent sections where they are applied.

Median values of Ca^{2+}, Mg^{2+}, K^{+}, Na^{+}, Cl^{-}, HCO_3^{-}, SO_4^{2-} and conductivity from surface and groundwater sites were included in the HCA algorithm. These analytes were selected as they were deemed likely to reflect changes in regional lithology and are the most common analytes present in the database. Further, these parameters are most likely to indicate ground and surface water interaction as they are known to differ substantially between surface and groundwater bodies (see section 2.3.1). In total 276 individual monitoring sites provided a full suite of these eight parameters and satisfied the CBE test, and so were included in the clustering algorithm. Prior to this process, data was standardized and log-transformed to meet the assumptions of homoscedasticity and normal distribution that are required for the cluster analysis procedure (Venugopal *et al.,* 2008; Woocay and Walton, 2008). Median values were standardised by subtracting their sample means and then diving the resulting value by its sample standard deviation.

A variety of other standard statistical techniques and procedures were employed to analyse resulting HCA outputs. These include ANOVA (Analysis of Variance), Kruskal-Wallis and Multiple range tests and were also conducted using STATGRAPHICS Centurion (Version 5.2.12). These procedures will be discussed further where they are applied.

4.2 Hierarchical Cluster Analysis outputs

4.2.1 Nearest Neighbour Linkage method - outlier identification

Figure 4.1 shows the result of HCA using the Nearest Neighbour linkage method. This single linkage method was used to identify outliers or residual sites that, if not excluded, might bias later stages of analysis. The Nearest Neighbour rule connects and compares all individual monitoring sites under one hierarchy (Timm, 2002). It defines the similarity or distance between two clusters as the minimum distance between any monitoring site of one cluster and a monitoring site of the other (Hair *et al.*, 2006). The resulting dendrogram (Figure 4.1) visually depicts the relationship between sites, with the terminus of each vertical line representing one monitoring station. Monitoring stations are linked by a horizontal line, of which a low position relative to the inter-cluster distance (*y-axis*) indicates similarity. From Figure 4.1 *ca.* 95% of all monitoring sites were deemed similar (inter-cluster distance or similarity < 4 on the *y-axis*) in terms of the eight variables considered in the clustering algorithm. The remaining 5% of monitoring sites on the right side of the dendrogram deviate in similarity as shown by the increasing *y*-axis distance. As a result these eight monitoring stations were visually identified, based on this distance, as outliers. A weakness to this approach is the subjective nature by which these outliers are visually identified (Romesburg, 1984), however to further support their identification the peculiarities in hydrochemistry of each outlier site were assessed. These are presented in Table 4.1 and Section 4.2.2. All eight residual sites are groundwater monitoring locations.

4.2.2. Outlier analysis

Table 4.1. Chemical median parameters for the eight outlier sites. Identified through HCA – Nearest Neighbour linkage method. Average median values from the remaining 268 monitoring sites are presented for comparison. All solute concentrations are presented as mg/L medians while conductivity is µS/cm median.

Site	Conductivity	Ca^{2+}	Na^{+}	K^{+}	Mg^{2+}	SO_4^{2-}	Cl^{-}	HCO_3
S26/0657	183	68	280	4	21	1	545	208
S26/0739	2250	48	411	5	11	25	640	306
S26/0793	5180	146	944	9	49	0.5	1690	264
S27/0442	643	8	125	1	3	0.5	101	197
S26/0001	330	25	740	12	18	38	1180	151
S26/0045	10	5	9	1	3	5	9	31
S27/0577	105	14	153	11	18	3	314	68
T26/0540	825	78	112	3	8	210	46	220
Average	313	18	35	2	7	7	46	96

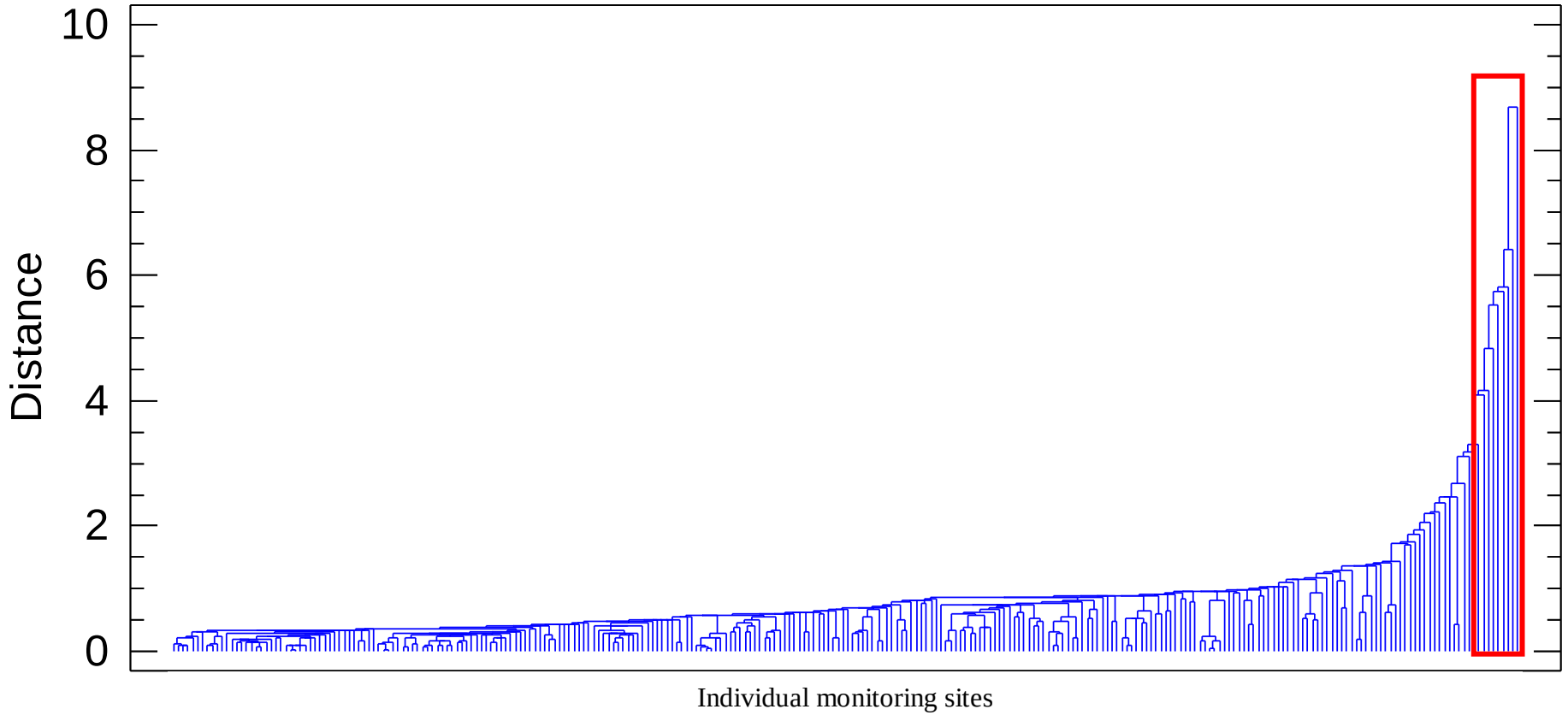

Figure 4.1. HCA Dendrogram determined using Nearest Neighbour linkage rule linking surface and groundwater monitoring sites from the Wairarapa valley, New Zealand under one hierarchy. The vertical *y*-axis indicates the relative similarity of individual monitoring stations or the inter-cluster distance. Each vertical blue terminus represents an individual monitoring site. Monitoring sites could not be individually labeled due to the large sample size. The red marked box identifies eight outlier (residual) sites.

S26/0657: Na^+-Cl^- water, suspiciously low conductivity (183 µS/cm) relative to high Na^+ (280 mg/L) and Cl^- (545 mg/L) concentrations. Well depth 62m. Low conductivity was not identified earlier as CBE does not include conductivity.

S26/0739: Na^+-Cl^- water with extremely high conductivity (2250 µS/cm) for a 6m well and in comparison to average conductivity (313 µS/cm).

S26/0793: Na^+-Cl^- water with extremely high conductivity (5180 µS/cm). Well depth 73m therefore likely highly evolved groundwater system.

S26/0442: 178m deep well with Na^+-HCO_3^--Cl^- waters and suspiciously low Ca^{2+} (8 mg/L). Reduced Ca^{2+} likely due to cation substitution with Na^+ ions.

S26/0001: Na^+-Cl^- rich waters with moderate conductivity (330 µS/cm) and high K^+ (12 mg/L) relative to average K^+ (2 mg/L). 3m deep well.

S26/0045: Extremely low conductivity (10 µS/cm) and individual ion concentrations for a 25m deep well. Likely to be an analytical error or rainwater sample (Verhoeven *et al.*, 1987).

S27/0577: Na^+-Cl^- water, low in Ca^{2+} (14 mg/L) and HCO_3^- (68 mg/L) and high in K^+ (11 mg/L). 137m deep well, Ca^{2+} likely substituted with Na^+ in solution.

T26/0540: 2m deep well with extremely high SO_4^{2-} (210 mg/L) concentration in relation to other variables. Likely to be measurement or recording error.

Outlier locations show no obvious pattern in spatial distribution (See Figure 4.2). This suggests the unusual chemistry displayed at these sites is not spatially dependent or influenced by a spatially distributed set of processes (e.g. regional lithology). Three sites (S26/0657, S26/0739 and S26/0793) are clustered in the Parkvale Basin, however they share little hydrochemical similarity (Table 4.1). It is likely these outlier sites are a result of human reporting error (e.g. T26/0540) or represent extremely old and evolved groundwaters (e.g. S26/0793).

CBE for each residual location was within limits deemed acceptable for this study (±10%), however reporting errors are largely associated with conductivity (e.g. S26/0657, S26/0739, S26/0045) and therefore were not identified in these calculations. The eight residual locations were excluded from further HCA.

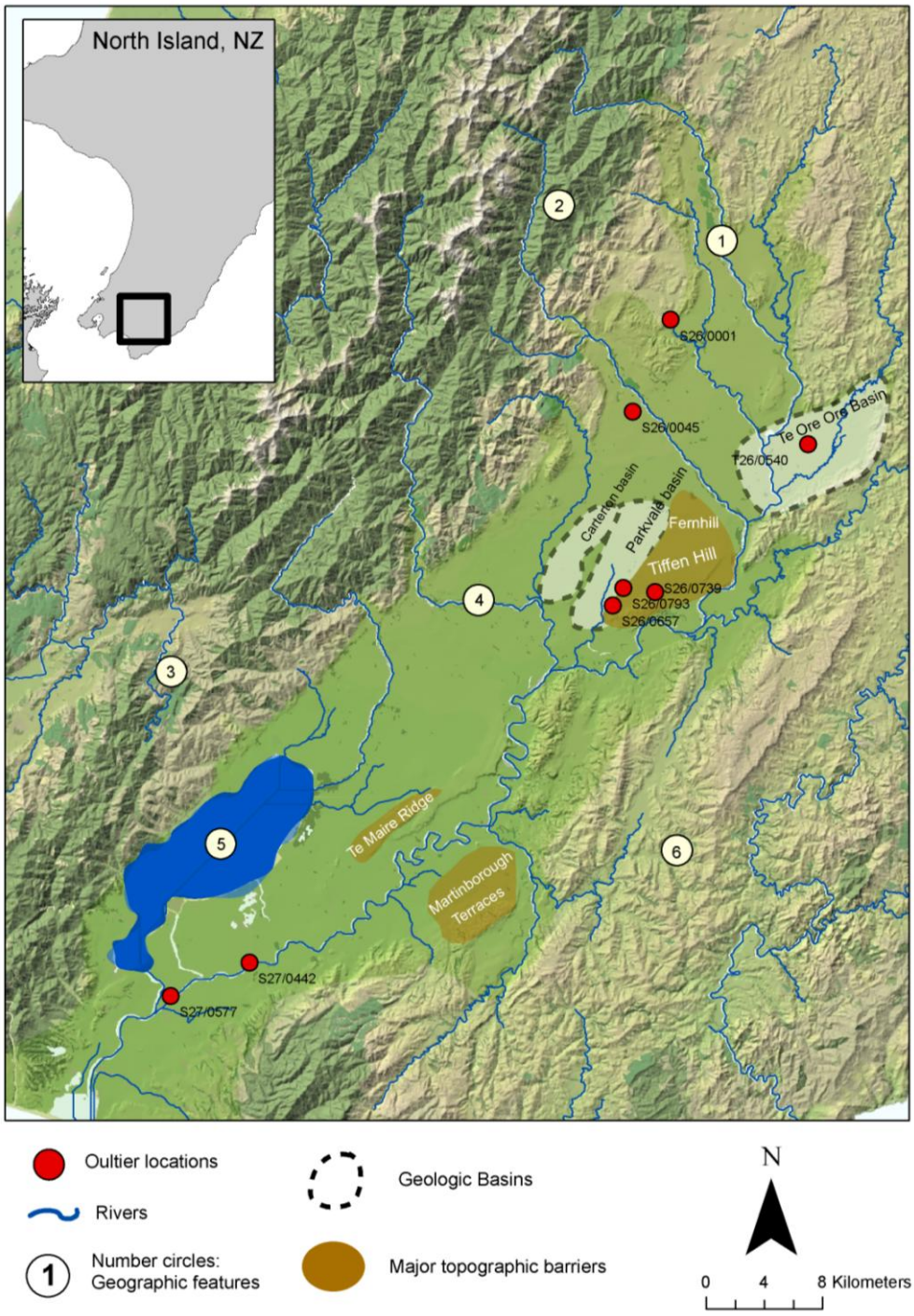

Figure 4.2. Spatial distribution of eight outlier or residual sampling locations in the Wairarapa Valley, New Zealand, identified through HCA – Nearest Neighbour linkage rule. Numbered circles indicate distinctive geographic features: 1) Ruamahanga River, 2) Tararua Ranges, 3) Rimutaka Ranges, 4) Waiohine River, 5) Lake Wairarapa and 6) Eastern Wairarapa Hills. *Note:* All locations are groundwater monitoring sites.

4.2.3 Wards Linkage method

Potential links between surface and groundwater monitoring sites were further investigated using HCA and Wards linkage method. The Wards method determines individual clusters and assigns the individual monitoring stations to each cluster based on the similarity of the eight chemical parameters considered as input to the algorithm. This method evaluates the distance between clusters using an analysis of variance procedure (Venugopal *et al.*, 2008). Monitoring sites with the lowest increase in the error sum of squares (SSE) are joined, two at a time, until all monitoring sites are assigned to a cluster (Hair *et al.*, 2006). This procedure aims to minimize the sum of squares of any two clusters that are obtained and achieves this through an analysis of any unexplained variation (SSE). More detail regarding this method is presented by Ward (1963). The resulting dendrogram, presented in Figure 4.3, allowed for the visual identification of six major clusters or hydrochemical facies at the 600 similarity distance (*y*-axis) threshold. Again, a weakness to this approach is the subjective nature by which the number of clusters is defined. However, this number of clusters is deemed appropriate in terms of a practical size for further analysis and the statistically significant difference between clusters. Further evidence supporting the appropriateness of this cluster threshold is provided in Section 4.5.

The number of monitoring sites assigned to each cluster is presented in Table 4.2. Surface water monitoring sites were assigned to three of the six arbitrarily named clusters (A1, A2 and B1), with the highest proportion grouped in cluster A2 (10 sites). Due to the larger number of groundwater sites considered in the algorithm, groundwater still accounted for a greater proportion of sites in these clusters with 26, 65 and 50 groundwater sites assigned to each respectively. Clusters B2, B3 and B4 consisted entirely of groundwater monitoring sites and therefore are likely to have different hydrochemistry to the surface water monitoring locations.

Table 4.2. Assignment of monitoring sites to six clusters determined by HCA – Wards Linkage method. Percentage (%) of ground or surface water sites assigned to each cluster presented in parenthesis. Full site names and their assignments to each cluster are presented in Appendix C.

Location	A1	A2	B1	B2	B3	B4	Total
Groundwater	26 (76%)	65 (87%)	50 (93%)	44 (100%)	30 (100%)	31(100%)	246
Surface water	8 (14%)	10 (13%)	4 (7%)	0	0	0	22
Total	34	75	54	44	30	31	268

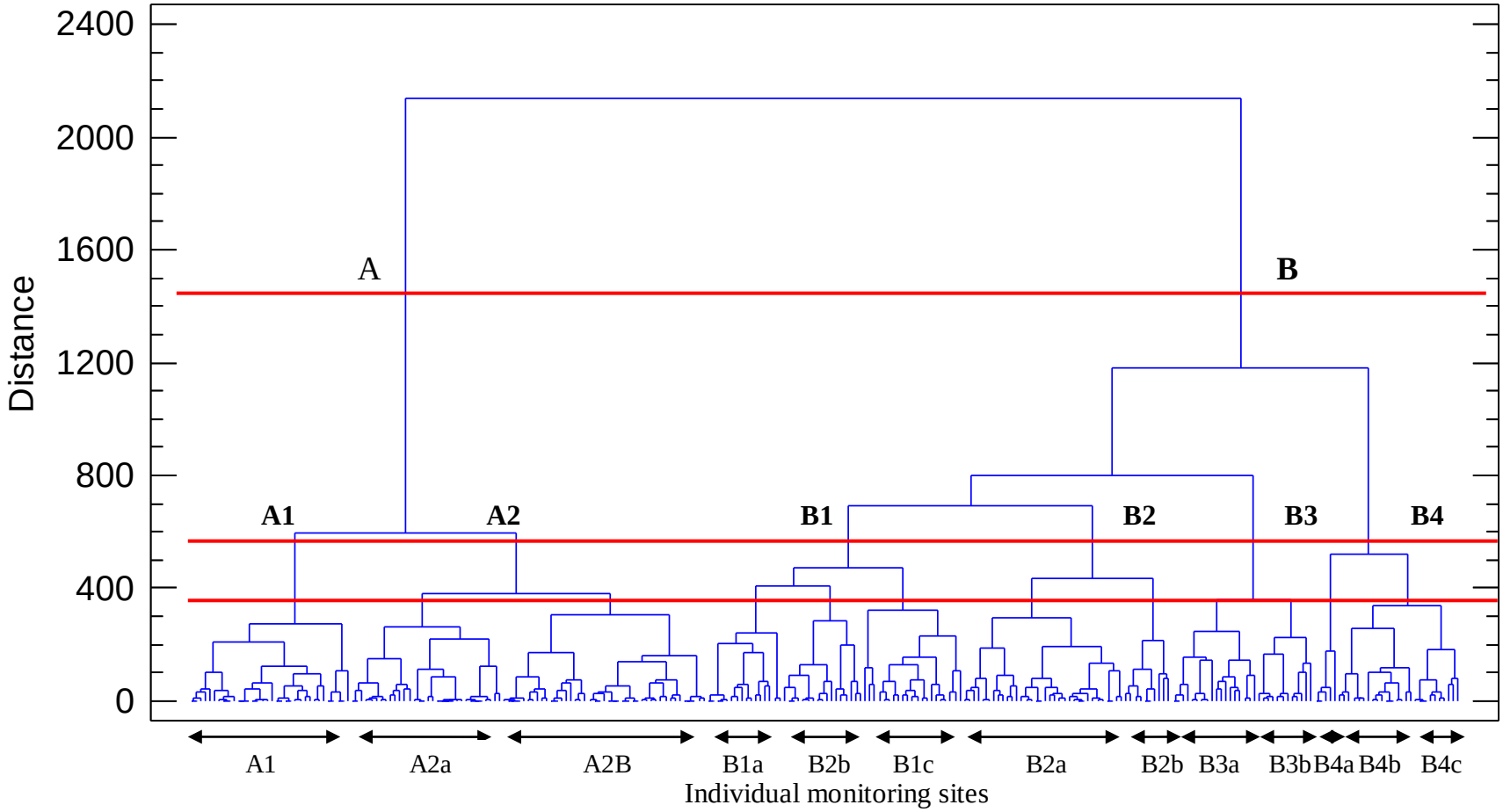

Figure 4.3. HCA Dendrogram determined using Wards linkage method classifying surface and groundwater monitoring stations from the Wairarapa Valley into clusters or hydrochemical facies. Vertical *y*-axis indicates the relative similarity of different monitoring stations, while each vertical blue terminus represents an individual monitoring site. Monitoring sites could not be individually labeled due to the large sample size. At a 1500 distance two main clusters (A and B) are identified, six clusters (A1-B4) at a *ca*. 500 distance threshold and 13 sub clusters (A1-Bc) at a *ca*. 300 distance threshold. Red horizontal lines indicate identification thresholds.

4.3 Cluster differentiation

Although HCA assigns monitoring sites to individual clusters based on similarity in their hydrochemical parameters, it provides little information on the specific water quality parameters that distinguish and differentiate each cluster (Daughney and Reeves, 2006). Therefore in order to determine these hydrochemical differences a variety of statistical and visual techniques were applied.

4.3.1 One-Way ANOVA (Analysis of Variance)

ANOVA was used to test the statistical and visual difference in sample means and medians between each cluster for each analyte. This approach has commonly been applied in analyses of HCA clusters (e.g. Kim *et al.*, 2003; Daughney and Reeves, 2005). Resulting ANOVA Box and Whisker plots and calculated mean values for each cluster are presented in Figure 4.4 and Table 4.3 for each of the eight log transformed parameters included in the HCA algorithm. Selections of additional parameters (e.g. nutrient levels, pH and well depth) were also subjected to ANOVA analysis and are presented in Figure 4.6. These variables were not included in the original HCA and therefore did not influence the assignment of individual monitoring sites to hydrochemical clusters. However, they may offer insight into chemical pathways and the potential processes that influence ground and surface water bodies (e.g. anthropogenic contamination) (Freeze and Cherry, 1979; Dahm *et al.*, 1998).

The six clusters identified in Figure 4.3 (separation threshold *ca.* 600) are largely differentiated by conductivity, TDS and ion ratios (Table 4.3 and Figure 4.4). Mean concentrations of the cations Ca^{2+}, Mg^{2+}, K^{+}, NH_4^{+}, Na^{+}, Fe^{2+} and Mn^{2+} and anions HCO_3^{-} and Cl^{-} increase along the following cluster sequence A1-A2-B2-B1-B3-B4. A similar trend is also shown in mean conductivity (77 µS/cm, 136 µS/cm, 198 µS/cm, 300 µS/cm, 421 µS/cm and 968 µS/cm) and mean calculated TDS concentrations (51.9 mg/L, 72.5 mg/L, 146.9 mg/L, 193 mg/L, 279.8 mg/L and 605.4 mg/L respectively), that follow this cluster sequence also. Concentrations of SO_4^{2-} and NO_3^{-} tend to show an inverse sequence to that of the other ions, with concentrations statistically highest in clusters B1, A1 and B3 (Figure 4.4). SO_4^{2-} concentrations are lowest in clusters B3 (1mg/L) and B4 (1.4mg/L).

The highest concentrations of dissolved reactive phosphorus were found in cluster B2 and B3, with levels similar in the remaining cluster (A1-A2, B1 and B4). The deepest groundwater sites tended to be assigned to cluster B3 and B4, with shallow wells assigned to clusters A1 and A2. An increase in well depth correlates with an increase in conductivity and TDS concentrations.

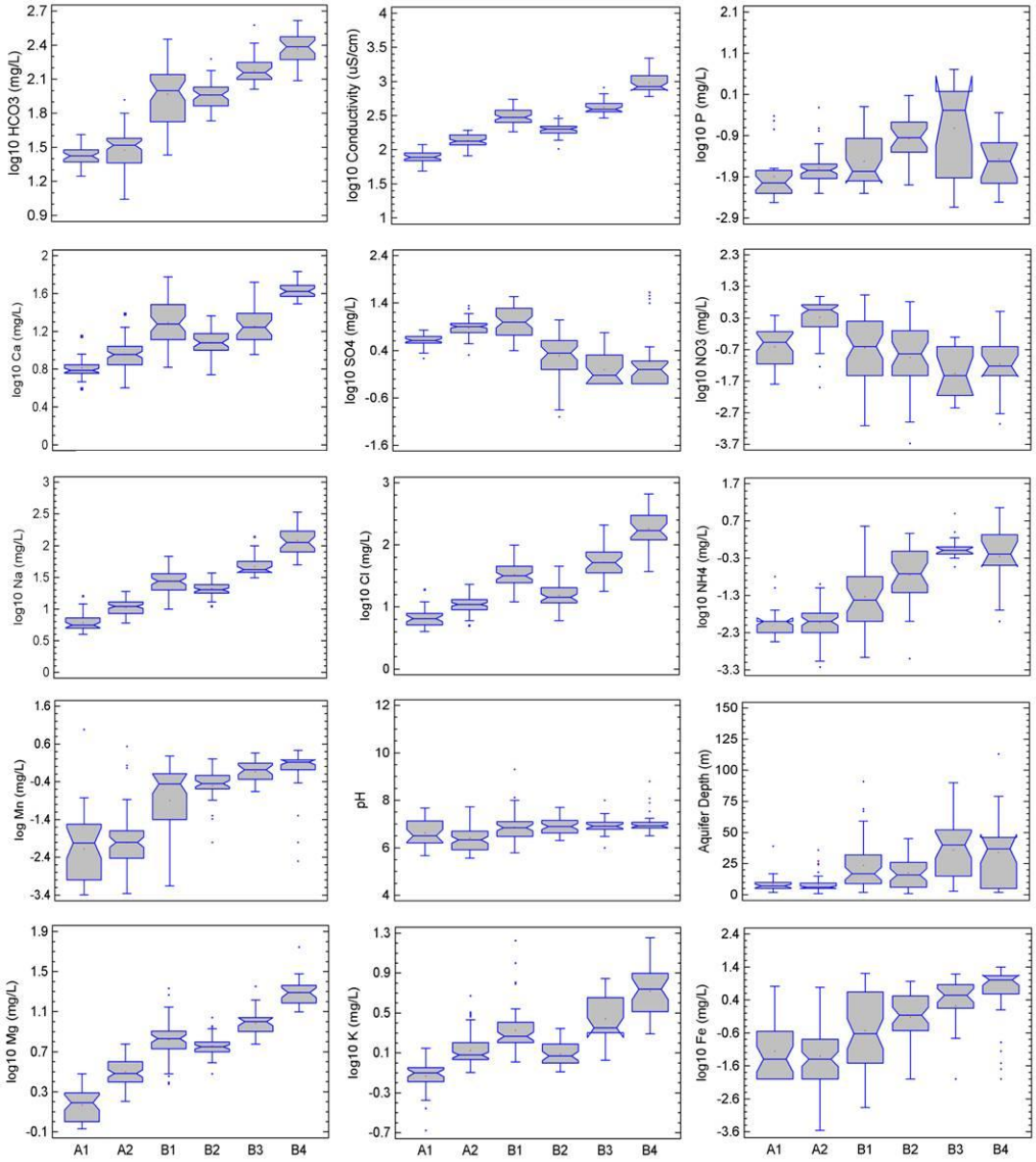

Figure 4.4. One-Way ANOVA Box-Whisker plots showing the variation across Clusters A1-B4 for selected parameters. Parameters include both those subjected to HCA and additional parameters selected for further investigation of cluster variation. The rectangular box identifies the first to the third quartile of the data, separated by a horizontal median line. Median notches are present around the median line identifying the margin of error surrounding sample median estimation. The vertical whisker lines identify the lowest and highest observations in the sample, except those deemed to be outliers as represented by the dots plotted outside these whiskers.

Table 4.3. Mean of each hydrochemical parameter for selected clusters. Defined by HCA (Ward's method, eight residual sites excluded). *Note*: Additional TDS column determined from the sum of other parameters (excluding conductivity), and *n* represents number of sites assigned to each cluster. All solutes are presented as mg/L, while conductivity is µS/cm.

Category	*n*	HCO_3	Ca^{2+}	Cl^-	Cond.	Mg^{2+}	K^+	Na^+	SO_4^{2-}	TDS
A1	34	26.6	6.5	6.5	77.1	1.5	0.7	6.1	4.1	51.9
A2	75	29.8	9.0	11.0	135.5	3.1	1.3	10.7	7.5	72.5
B1	54	93.5	19.8	33.3	300.9	6.5	2.1	27.7	10.1	193.0
B2	44	90.7	12.0	15.3	198.0	5.7	1.2	20.9	2.0	147.9
B3	30	149.3	18.0	52.2	421.2	9.6	2.8	46.9	1.0	279.8
B4	31	233.0	42.3	181.9	968.1	19.7	5.2	121.8	1.4	605.4

The parameters that differentiate each of the six clusters were further investigated using the Kruskal-Wallis and Multiple range tests, conducted at a 95% confidence interval. Both procedures are non-parametric tests that do not make assumptions regarding how the underlying data are distributed (Rogerson, 2006). The Kruskal-Wallis test investigates if a statistically significant difference is present between sample medians, while a Multiple Range tests if a statistically significant difference is present between sample means. Further information in regards to these tests and their methodologies are provided by Kruskal and Wallis (1952), Cheeney (1983) and Rogerson (2006). Subsequent results support those presented above and due to the large number of outputs are presented in Appendix D.

4.3.2 Piper diagrams

The hydrochemical composition of each assigned cluster was further assessed with the aid of Piper diagrams. Piper diagrams are used here to visually present the relative concentration of major ions for a given cluster, allowing the hydrochemical composition or water type to be inferred (Güler *et al.,* 2002). The hydrochemical mean for each cluster (Table 4.3) is presented in Figure 4.5a, while all monitoring sites are plotted in Figure 4.5b. The latter figure aims to show the overall spread of data within each cluster. Clusters A1, A2, B1 and B2 can largely be classified as Ca^{2+}-HCO_3^- waters according to the manner suggested by Back (1966), while B3 and B4 share characteristics more closely resembling Na^+- Cl^- waters. Further, B3 and B4 type waters show little SO_4^{2-} indicating highly reduced groundwaters, while clusters A1 and A2 display waters with a higher SO_4^{2-} signature. Figure 4.5(b) shows the significant spread of data within each cluster. For ease of interpretation the hydrochemical composition of each cluster mean will be referred to for the remainder of this chapter (e.g. Figure 4.5a).

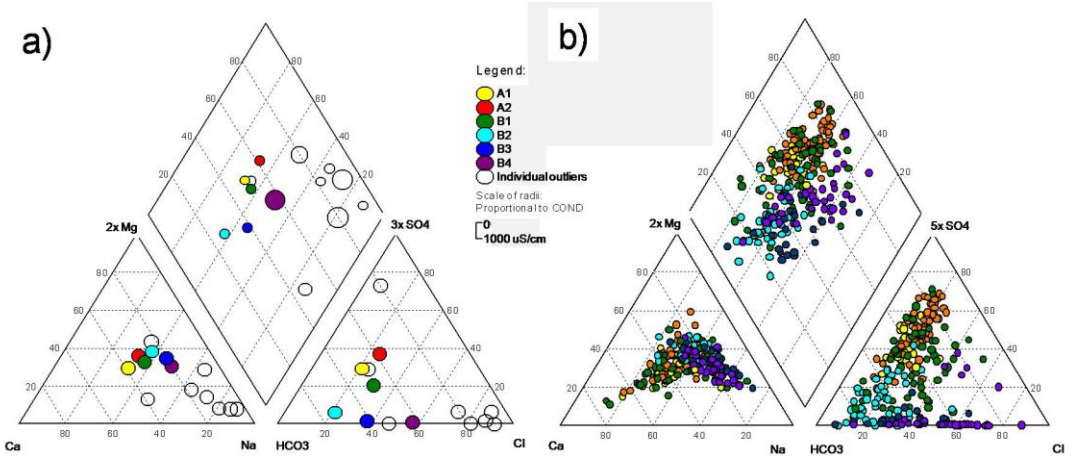

Figure 4.5. Piper diagram showing the variation of major ions (Ca^{2+}, Na^{+}, Mg^{2+}, Cl^{-}, HCO_3^{-}, SO_4^{2-} and Mg^{2+}) amongst the 6 defined clusters determined using HCA – Wards Linkage method. The left triangle presents major cations while the right presents major anions. The center diamond represents the projected position based on both triangles. **(a)** Hydrochemical mean for each defined cluster and outlier chemistry, **(b)** Plotted hydrochemistry of all monitoring sites within each cluster. *Notes*: Each individual circle represents an individual monitoring site in Figure 5.5 (b); Mg^{2} and SO_4^{2-} scales are exaggerated in both figures for ease of interpretation; circles in center diamond Figure 5.5 (a) are proportional to conductivity.

4.3.3. Spatial distribution of clusters

The spatial distribution of sites assigned to each hydrochemical facies is presented in Figure 4.6 and shows clear spatial patterns. Cluster A1 sites are located in close proximity to major river systems, with a significant agglomeration of A1 groundwater sites south-west of the Waiohine River, and smaller number of sites on the Tauherenikau, Waingawa and upper Waipoua and Ruamahanga Rivers. This may indicate potential interaction between these surface and groundwater monitoring sites. Rivers draining the resistant greywacke Tararua and Rimutaka ranges are classified in this category, while those draining the Eastern Pliocene ranges are largely assigned to cluster A2. Groundwater monitoring sites assigned to A2 are located from the upper to middle Wairarapa valley, however they become somewhat more dense around the Waipoua/Ruamahanga confluence and Waingawa River. Cluster B1 sites are scattered along the entire valley, however they are largely restricted to groundwater sites on the Eastern edges. An agglomeration of B2 groundwater sites occurs in the Parkvale basin, with a further handful scattered around the upper Wairarapa valley and the plains north-west of Lake Wairarapa. B3 and B4 monitoring sites are almost entirely restricted to the lower flanks of the Wairarapa, although a small cluster of both categories also occur mid valley in the Parkvale and Tiffen Hill areas.

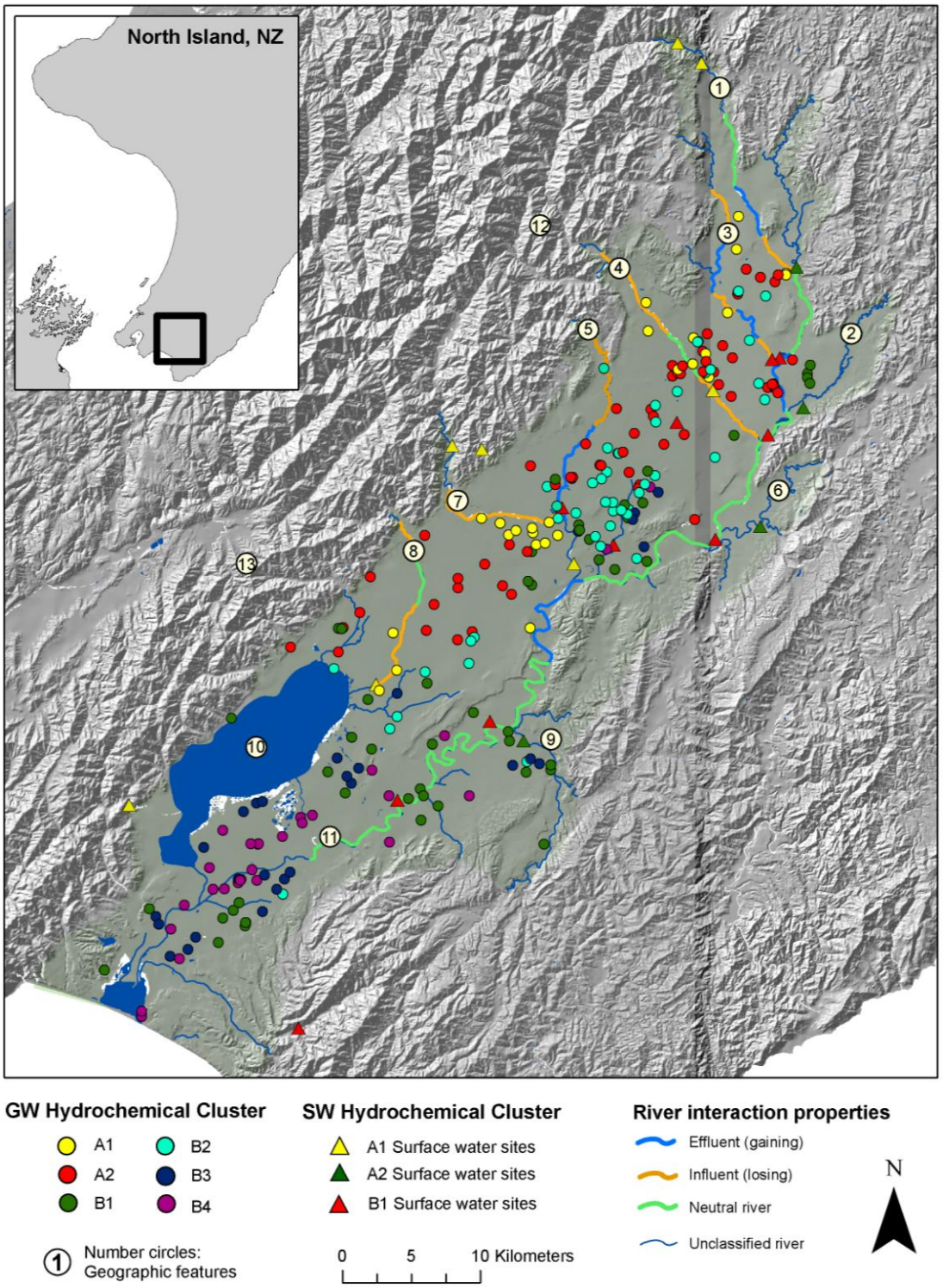

Figure 4.6. Spatial distribution of 276 groundwater and surface water (triangle symbol) monitoring stations assigned to six hydrochemical clusters in the Wairarapa valley, New Zealand. Determined with HCA – Wards linkage method. Distribution is shown in comparison to pre-determined river properties: influent, effluent or neutral stream systems. Circled numbers indicate major river systems of interest: 1) Ruamahanga River, 2) Whangaehu River, 3) Waingawa River, 4) Waipoua River, 5) Mangatarere River, 6) Waingongoro Stream, 7) Waiohine River, 8) Tauherenikau River, 9) Huangarua Stream, 10) Lake Wairarapa, 11) Lower Ruamahanga River, 12) Tararua Ranges and 13) Rimutaka Ranges.

4.4 Hydrochemical facies descriptions and discussion

Subjecting historic hydrochemical data to HCA allowed distinct hydrochemical clusters or facies to be identified, as previously described in Section 4.3. Individual groundwater and surface water monitoring sites from the Wairarapa valley were assigned to one of six clusters based on their hydrochemistry. Clusters A1, A2 and B2 contained both surface and groundwater sites suggesting a similar hydrochemical signature, and possibly indicating similar age, and potentially their interaction. These hydrochemical facies are presented and analysed in more detail below and are summarised in Table 4.4 and Figure 4.7.

Cluster A1 – Sites assigned to Cluster A1 are generally low in major solutes and conductivity (77µS/cm) and demonstrate a Ca^{2+}-HCO_3^- water type (Figures 4.5 and 4.7) typical of fresh surface waters (Berner and Berner, 1996). Eight surface water sites, that generally drain the resistant western Tararua and Rimutaka ranges, are associated with this cluster (e.g. Waiohine, Ruamahanga, Waingawa). Groundwater sites tend to be shallow (<10m), containing low concentrations of NH_4^+, Mn, and Fe^{2+} and are located in close proximity to losing reaches of the Waiohine, Waipoua and Tauherenikau Rivers (Figure 4.6). This may indicate they are fed by surface water systems, are oxygen rich and have strong hydraulic links with river systems. This is a similar result to that found by Burden *et al.* (1982) in which groundwaters of the Canterbury plains closely reflected the chemical composition (high proportions of Ca^{2+}-HCO_3^-, low Na^+, Cl^- and NO_3^-) of the adjacent Rakaia and Asburton Rivers. Burden *et al.* (1989) used this premise to link these water bodies and infer the importance of river recharge to underlying groundwater systems in the area.

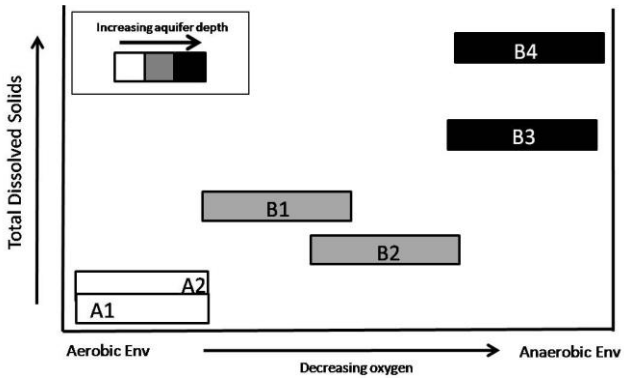

Figure 4.7. Simplified schematic representation of differences amongst the 6 hydrochemical clusters (A1-B4) in relation to their TDS, aquifer depth (when applicable) and aerobic environment. Scales of axes are simplified representations of increase only.

Cluster A2 – The hydrochemistry of sites assigned to cluster A2 is slightly higher in all major ions and conductivity (135µS/cm) when compared to cluster A1 and display higher Na^+ relative to Ca^{2+} and Cl^- relative to HCO_3^- (Figure 4.5). A2 sites displays similarly low concentrations of Mn, NH_4^+, and Fe^{2+} to those in A1 suggesting aerobic conditions, however concentrations of NO_3^- and SO_4^{2-} are higher. This increased concentration of NO_3^- highlights the probable importance of rainfall recharge to groundwaters assigned to this cluster with NO_3^- accumulation occurring as rainwater moves through the soil column. This is supported by elevated concentrations of Na^+ and Cl^- that also accumulate during the passage of infiltrating water through the soil column (Taylor *et al.*, 1989). Surface water sites assigned to Cluster A2 are located on the Ruamahanga, Mangatarere, Waipoua and Tauanui Rivers (Figure 4.6). As these rivers share similar hydrochemistry to groundwater sites in this cluster it may indicate they receive base flow from these underlying groundwater systems (effluent conditions). The presence of NO_3^- and low concentrations of Mn, NH_4^+ and Fe^{2+} indicate these waters are aerobic, further highlighting hydraulic links with the surface.

Cluster B1 – Surface and groundwater sites assigned to Cluster B1 are differentiated from those in Clusters A1 and A2 by an increase in major ions and conductivity (300µS/cm) as well as NH_4^+, Mn and Fe^{2+}. The four surface water sites assigned to this cluster largely drain the easily eroded eastern Pliocene ranges of the valley. As a result they have higher concentrations of major solutes and conductivity. Groundwater sites show an increase in well depth relative to A1 and A2 (Figure 4.7), and are also largely restricted to the eastern flanks of the valley. It is probable these groundwater systems receive recharge from those rivers draining the eastern hills, and therefore show a slightly increased concentration of solutes. Further, increased groundwater solute concentration may indicate older, more chemically evolved groundwaters with decreasing oxygen levels.

Cluster B2 – Sites assigned to Cluster B2 consist entirely of groundwater locations and share a similar hydrochemistry to sites in Cluster B1. However B2 groundwater sites tend to have slightly lower concentrations of all major ions and increased concentrations of NH_4^+, Mn, Fe^{2+} and SO_4^{2-}. Elevated concentrations of these ions suggest a reducing groundwater environment, with depleting oxygen supply (Kedziorek, 2008) (Figure 4.7). Sites assigned to this cluster are shallow to moderate in depth (5-30m) and show considerable spatial agglomeration in the Parkvale basin. The sequence of Q3, Q5, Q6 and Q8 sediments in the basin (Figure 3.14) may present various confining layers of silty gravels and clay that reduce oxygen supply to these B2 groundwaters. A handful of B2 sites are also scattered around the upper Wairarapa valley and plains north-west of Lake Wairarapa.

Cluster B3 – Sites assigned to Cluster B3 consist entirely of groundwater locations and have higher Na^+ relative to Ca^{2+} to those from B1 and B2. Similarly, sites show an increase in all major ions and conductivity, well depth and may indicate groundwaters that are older and more chemically evolved (Chebotarev, 1955). This is supported by lower concentrations (near or below the detection limit) of SO_4^{2-} and NO_3^- and elevated Mn and Fe^{2+} (Figure 4.7) which indicate anoxic conditions and potentially older waters exhausted of organic matter (Taylor *et al.,* 1989). B3 groundwaters are largely located in the lower Wairarapa valley, an area known to contain confined aquifers deep within its marine and estuarine deposits (Jones and Gyopari, 2006).

Cluster B4 – Cluster B4 consists entirely of moderate to deep groundwater sites located in the lower Wairarapa valley (Figures 4.6 and 4.7). Sites are differentiated from those in Cluster B3 by an increase in all major ions and conductivity, likely reflecting older groundwaters moving towards a Na^+-Cl^- brine (Figure 4.5) (Chebotarev, 1955). Increased concentrations of Mn, NH_4^+ and Fe^{2+} coupled with reduced NO_3^- and SO_4^{2-} indicate a heavily reducing anoxic environment with little connection to the atmosphere or overlying surface water systems. Recharge is likely provided from seepage from overlying groundwater units and extremely slow rainfall recharge.

Table 4.4. Summary of significant hydrochemical variations between six identified hierarchical clusters A1-B4. Based on Kruskal-Wallis tests and Multiple Range tests conducted at the 95% confidence level, *p*-value < 0.05 indicates statistically significant difference (e.g. higher or lower) between sample medians (Kruskal-Wallis) and sample means (Multiple Range).

	Cluster A1	**Cluster A2**	**Cluster B1**	**Cluster B2**	**Cluster B3**
Cluster A2	Compared to A1, A2 on average has slightly higher Na, K, Ca, Mg, HCO_3, Cl, SO_4, P, NO_3 and conductivity. There is no significant difference in Mn, Fe, NH_4 or depth. pH slightly lower.				
Cluster B1	Compared to A1, B1 is deeper and has higher Na, K, Ca, Mg, HCO_3, Cl, NH_4, Mn, Fe, depth and cond. B1 is lower in NO_3, and there is no significant difference in pH.	Compared to A2, B1 is deeper and has higher Ca, HCO_3, Cl, Na, Mg, K, NH_4, Fe, Mn, pH and cond. There is no significant difference in SO_4, or P, and B1 has lower NO_3.			
Cluster B2	Compared to A1, B2 is deeper and has higher Na, Ca, Mg, HCO_3, Cl, P, K, Mn, Fe, NH_4, cond. and lower SO_4 and NO_3. There is no difference in pH.	Compared to A2, B2 is deeper and has higher Ca, HCO_3, Cl, P, Na, Fe, Mn, NH_4, pH and cond. B2 has lower K, NO_3 and SO_4.	Compared to B1, B2 is shallower and has lower Ca, Na, Cl, cond, K, Mg, NO_3 and SO_4. There is no difference in pH or Mn, and B2 has higher NH_4, Fe and P.		
Cluster B3	Compared to A1, B3 is much deeper and has higher Na, Ca, Mg, HCO_3, Mn, K, NH_4, Cl, Fe and cond. B3 has lower NO_3 and SO_4, and there is no significant difference in pH.	Compared to A2, B3 is deeper and has higher Na, Ca, Cl, HCO_3, Mg, K, P, Fe, Mn, NH_4 and cond. and lower SO_4 and NO_3. There is no difference in pH.	Compared to B1, B3 is deeper and has higher HCO_3, Na, Cl, Mg, K, P, NH_4, Mn, Fe and cond. B1 has lower NO_3 and SO_4. There is no difference in Ca or pH.	Compared to B2, B3 is deeper and has lower SO_4. B3 has higher Ca, Na, Cl, HCO_3, K, Mg, Fe, Mn, NH_4 and cond. There is little difference in NO_3, P or pH.	
Cluster B4	Compared to A1, B4 is much deeper and has higher Na, K, P, Ca, Mg, Cl, pH, Fe, Mn, NH_4, HCO_3 and cond. B4 has lower SO_4 and NO_3.	Compared to A2, B4 is much deeper and has higher Na, K, Ca, Mg, Cl, pH, Fe, Mn, NH_4, HCO_3 and cond. B4 has lower SO_4 and NO_3, and there is no difference in P.	Compared to B1, B4 is deeper and has higher Na, K, Ca, Mg, Cl, Fe, Mn, NH_4, HCO_3 and cond. B4 has lower SO_4, and there is little or no difference in P, NO_3 or pH.	Compared to B2, B4 is shallower and has higher Na, Ca, Cl, HCO_3, Mg, K, P and cond. and lower P and SO_4 There is no difference in NO_3, Mn, pH or depth.	Compared to B3, B4 has higher Ca, Cl, Na, Mg, K, HCO_3 and cond. and lower SO_4 and P. There is no difference in NO_3, NH_4, SO_4, pH, depth, Fe or Mn.

4.5 Cluster validation

To explore any artifacts in the results caused by the large sample size, the inability to check these artifacts due to this sample size and the relatively arbitrary method used to determine cluster separation thresholds, two alternative cluster groupings were explored. At the 1500 distance threshold (*y-axis)* two main clusters (A and B) were identified and at a *ca.* 300 threshold 13 clusters (A1-B4c) were identified. These threshold levels are shown in Figure 4.3 and were used to assess the sensitivity of cluster assignments. ANOVA analysis, Kruskal Wallis and Multiple Range tests were also conducted for the alternative cluster groupings to determine any statistical difference in parameters between the clusters. Resulting ANOVA Box-Whisker plots for the log transformed parameters conductivity, Ca^{2+} and Cl^{-} are presented in Figure 4.8. These variables were selected for analysis as they were deemed representative of the main parameters that differentiate cluster groupings (Refer to Section 4.3). Analyses of all parameters at the two and 13 cluster threshold are presented in Appendix E and follow a similar pattern.

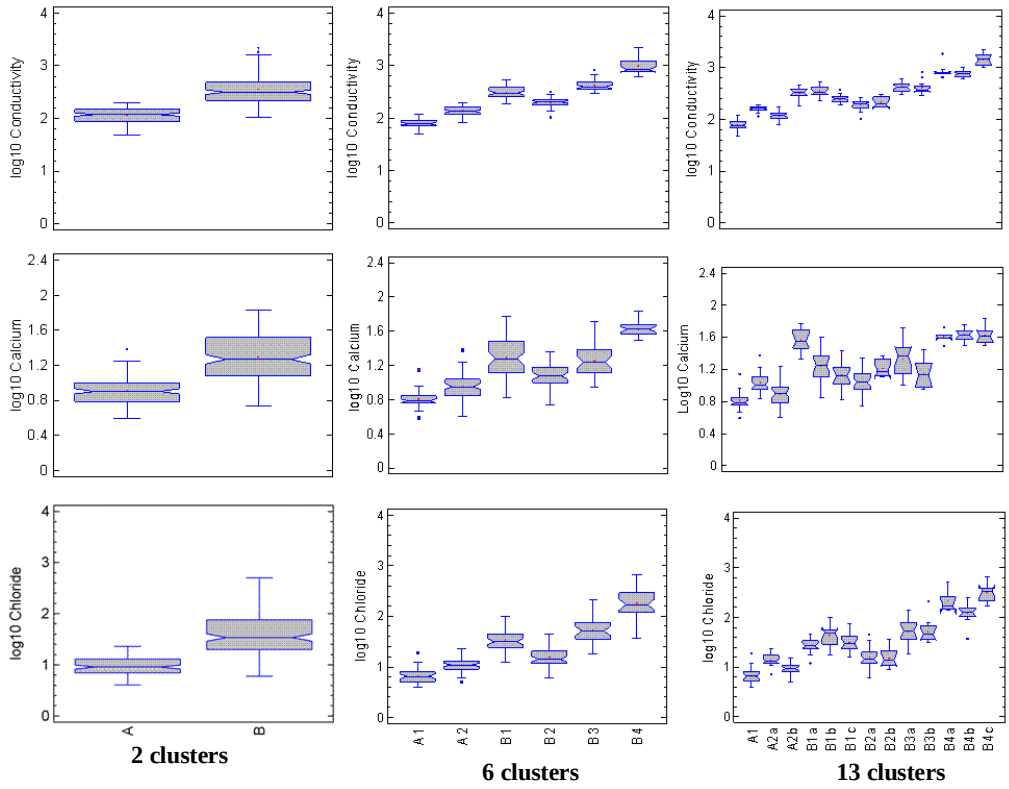

Figure 4.8. One-Way ANOVA Box-Whisker plots showing the variation in conductivity (µS/cm), Ca^{2+} (mg/L) and Cl^{-} (mg/L) across the two, six and 13 cluster thresholds. The rectangular box identifies the first to the third quartile of the data, separated by a horizontal median line. Median notches are also present around the median line indicating the margin of error surrounding the estimation of the sample median. The vertical whisker lines identify the lowest and highest observations in the sample, except those deemed to be outliers as represented by the dots plotted outside these whiskers.

At the two cluster threshold Clusters A and B are differentiated by conductivity, Ca^{2+} and Cl^{-}, with concentrations all highest in Cluster B (Figure 4.8). However this two cluster threshold fails to capture the hydrochemical variability amongst monitoring sites and therefore it is useful to separate Cluster A into A1 and A2 and Cluster B into B1-B4 as shown by Figure 4.8. All six of these clusters are significantly different across the three variables presented, a conclusion already discussed above in Section 4.3. At the lowest separation threshold, A1 remains undifferentiated, A2 becomes A2a-b, B1 becomes B1a-c, B2 becomes B2a-b, B3 becomes B3a-b and B4 becomes B4a-c. However, the significance of hydrochemical differences between clusters begins to diminish. Figure 4.8(c) shows little statistical difference for a range of parameters across the various sub-cluster groupings (e.g. Ca^{2+} cannot be statistically differentiated for Cluster B4b-c, B1a-c, B2a-b, B3a-b). This highlights the over-sensitivity of a 13 cluster threshold, and the lack of additional insight provided by such a large number of groupings. It is therefore deemed appropriate to remain with six clusters, due to the statistically significant difference between these clusters and feasible workload in terms of the analysis, interpretation and presentation required to process six groupings.

4.6 Regional scale limitations

A number of issues surround this regional scale investigation of surface and groundwater interaction in the Wairarapa valley and may affect the validity and significance of the reported findings. These issues are associated with the hydrochemical database and its construction, temporal variability in water quality, and the inferences made from HCA.

Several sources of error arise from the use of median values to reduce and summarise the hydrochemical dataset provided by the GWRC. A median value considers the ‘middle value’ of each dataset when they are ranked from highest to lowest and is generally used when datasets are skewed with the presence of significant outliers. However, a median value fails to represent the full range of data for a particular parameter (e.g. temporal changes in Ca^{2+} concentrations). This is a concern for monitoring sites in which water quality displays significant temporal variability (daily, seasonal, yearly, long term) as this variability will be ignored.

Issues surround the sampling frequency of each monitoring site with some locations only sampled once (see Section 4.1.1). These one-off samples may provide a poor representation of overall water quality at their locations, in particular if they were collected during specific hydrological or contamination periods (e.g. storm events or disposal of effluent). Further, historic one-off samples may no longer be representative of water quality at a given site due to land use change (e.g. shrub conversion to high intensity agriculture) that can significantly alter the natural composition of a water body (McLaren and Cameron, 2006). Information regarding land use change and sampling conditions (e.g. discharge, meteorological events) is limited, therefore, it is difficult to assess the representativeness of each water sample and their associated hydrochemical medians.

Issues surrounding temporal variations in water quality are amplified in the HCA process as median values were subjected to the algorithm. It was not possible to consider temporal variations in water quality in the determination of the hydrochemical median values and therefore in the definition of hydrochemical clusters. As noted in Section 2.2 the physical and chemical interaction between ground and surface water displays significant temporal variability. As this variability was not considered in this chapter the representativeness of these findings can be questioned.

Issues also surround the spatial variability of water quality. Rivers systems within the Wairarapa valley were consistently sampled at one location with subsequent water quality results applied to the entire river body. However, as identified in Section 2.2, the chemical composition of water bodies can show considerable spatial variability. Surface water monitoring sites may potentially fail to capture this spatial variability. This error is considered negligible as spatial variations in background river chemistry are minimal in the Wairarapa valley. This assumption is based on the relatively consistent hydrochemical signature experienced at the five monitoring locations of the Ruamahanga River. To further reduce the influence of this potential error surface water was analysed in regards to the specific location of the monitoring site as opposed to the entire river.

An unquantifiable uncertainty is also inherent in the collection and maintenance of the historic hydrochemical database (1940-2008) provided by the GWRC. Significant progress has been made in water quality extraction and laboratory methods over the last decade. For example chemical detection limits have been significantly lowered. It was assumed that adequate methods were performed at the time of sampling, analysis and data management, however, one cannot be completely certain of this. CBE were performed across the database (Section 4.1.3) in an attempt to identify samples that are electrically unbalanced due to these errors. Despite the calculation of CBE, and discarding of obvious erroneous samples, some errors are likely to remain and it is difficult to differentiate error from actual result. Despite this potential source of error, the median values presented in the hydrochemical database seem reasonable and closely resemble the overall background range of raw data values.

The main principle upon which this regional scale investigation is based is the assumption that similarities in hydrochemistry can be used to infer interaction between ground and surface water bodies. Although it is extensively noted in the literature that hydrochemical similarities suggest interaction (e.g. Burden, 1982; Taylor *et al.*, 1989; Kumar *et al.*, 2009), it is possible these similarities are due to other phenomenon such as similar flow paths, regional geology or contamination. In terms of this regional scale investigation this assumption is considered and a precautionary approach is taken when interpreting the associated findings.

The limitations identified above highlight the difficulties of using a widespread dataset that encapsulates significant timescales and the use of indirect methods and assumptions to infer locations of ground and surface water interaction. Despite these sources of error, the use of hydrochemical medians and HCA to identify areas of potential interaction and therefore achieve the aim of this method was relatively successful. Although these errors are limitations to the regional scale investigation they are acknowledged and results are treated as a stepping stone for the further analysis that is presented in Chapters five and six. In order to gain some insight into the temporal variability in ground and surface water interaction an investigation on local scale water quality changes from the Mangatarere and Waiohine Rivers and their neighbouring groundwater systems is undertaken in Chapter 5.

4.7 Regional scale interaction concluding remarks

This regional scale investigation of ground and surface water interaction aimed to classify ground and surface water bodies together based on hydrochemical similarities to infer interaction. The main principle on which this method is based is the assumption that similarities in water chemistry are the result of interaction. Regional scale results suggest ground and surface water interaction is occurring in several areas throughout the Wairarapa valley. The upper Ruamahanga, Waingawa, Waipoua, Waiohine and lower Tauherenikau Rivers are classified into cluster A1 and potentially provide recharge to neighbouring shallow (>10m) A1 groundwater bodies. These groundwater bodies share a similar low TDS, Ca^{2+}-HCO_3^- water type and are located in close proximity to the GWRC identified influent reaches of these river systems. Further, cluster A1 ground and surface waters are highly aerobic (as indicated by the presence of NO_3^- and SO_4^{2-}, and low Mn, NH_4^+, Fe^{2+} concentrations) and are located in permeable Q1 and Q2 alluvial gravels that foster high connectivity between ground and surface water bodies.

The Whangaehu, Huangarua and Taueru Rivers that drain the eastern Wairarapa foothills may also provide recharge to underlying groundwater systems. These rivers were classified into cluster B1 and have slightly elevated TDS in comparison to other surface waters in the valley. This increase in solutes is likely the result of a largely Pleistocene sedimentary geology of the eastern hills. Cluster B1 groundwater monitoring sites surround these river systems in Q1 and Q2 alluvial gravels in the Parkvale basin and eastern periphery of the Wairarapa valley. These groundwater sites share a similar hydrochemistry to these rivers systems suggesting the provision of recharge from surface water bodies.

A2 rainfall-recharged groundwaters appear to provide base flow to a number of surface water bodies. The Mangatarere, lower Waingawa, upper Ruamahanga and Parkvale streams are also assigned to cluster A2 and share elevated concentrations of Cl^-, Na^+ and NO_3^- to A2 groundwaters. These ions are known to accumulate during the passage of infiltrating precipitation through the soil column and can be transferred to surface water bodies by groundwater provided base flow.

Further, several of these surface water monitoring sites (e.g. Mangatarere and Upper Ruamahanga) have been classified by the GWRC as effluent reaches.

It appears the deep groundwater systems located in the lower flanks of the Wairarapa valley interact very little with river systems. Classified into clusters B3 and B4 these groundwater monitoring sites displayed high TDS and anoxic conditions that suggest little recharge from dilute Ca^{2+}-HCO_3^- surface waters. This is likely due to the significant depths at which these aquifer systems are present and the various mud and estuarine confining layers that have been deposited in the lower valley. The Na^+-Cl^- signature of these waters suggests a highly evolved groundwater system. Several B3 and B4 groundwater monitoring sites are also located in the Parkvale basin where the sequence of Q3, Q5, Q6 and Q8 sediments are likely to present various confining layers that promote anoxic conditions and separation from surface water bodies.

Although this regional scale investigation was able to infer interaction between ground and surface water bodies based on similarities in hydrochemistry, it does not acknowledge temporal variations in water chemistry and therefore potential interaction. Further, it is possible that similarities in water chemistry between ground and surface waters are not due to interaction, and are caused by other phenomenon such as similarities in flow paths, geology and contamination. Despite these uncertainties this regional scale investigation provides a potential method that support existing research (e.g. GWRC flow gaugings) in the identification of areas where potential ground and surface water interaction is occurring in the Wairarapa valley.

Chapter 5
Local scale low resolution temporal interaction

Two areas of particular interest, as inferred through the regional scale investigation, are the Waiohine and Mangatarere Rivers. It appears the Waiohine River provides recharge to several groundwater monitoring sites that lie south of the main Waiohine river channel. These groundwater sites, along with the Waiohine, were assigned to cluster A1 and share a similar low TDS, Ca^{2+}-HCO_3^- water type. In contrast, the downstream reaches of the neighbouring Mangatarere stream appear to receive solute rich base flow from several groundwater monitoring sites. These groundwater bodies and the downstream Mangatarere gauging station were classified together in cluster A2 and share a similar rainfall-recharged chemical signature (accumulated salts and NO_3^-). However, the interaction between surface and groundwater is known to show considerable temporal variability as determined by the changeability of the meteorological, fluvial, anthropogenic and geological processes that influence it (Section 2.2). The regional scale investigation employed in this research fails to account for the possibility of temporal variability. Therefore, the following sections aims to gain some insights on the temporal variability at which surface and groundwater interactions occur by focusing on temporal changes in water quality from only the Mangatarere and Waiohine Rivers and their neighbouring groundwater systems.

This chapter is divided into three sections. Section one presents the methodology and statistical techniques undertaken for investigation of potential local scale temporal interaction. Section two concerns the use of hydrochemical datasets and HCA to determine if temporal variation in chemical interaction can be inferred for the year 2008. The year 2008 was selected as it offered the most comprehensive dataset with the highest sampling frequency. In section three, time series analyses of water chemistry from several ground and surface water sites from the Waiohine and Mangatarere areas are presented, and potential links made between water bodies to infer interaction.

5.1 Local scale methodology

Local scale surface and groundwater interaction was investigated through an analysis of temporal water quality data for the 2008 year. Several monitoring sites from the Waiohine and Mangatarere stream areas were selected for this analysis. These sites are presented in Table 5.1. Two methods of temporal analysis were conducted. Temporal hydrochemical data from 2008 were subjected to HCA using the Wards linkage method. Unlike the regional scale HCA method, data were analysed as individual monthly or quarterly measurements in order to capture the temporal variability of water chemistry during the 2008 year. Median values were not calculated and a Nearest Neighbour Linkage method, to remove outlier data, was not performed to ensure all changes in water chemistry were analysed. This is because the Nearest Neighbour Linkage method may classify changes in water chemistry as outliers because they deviate from the hydrochemical norm. Ca^{2+}, Mg^{2+}, K^{+}, Na^{+}, Cl^{-}, HCO_3^{-}, SO_4^{2-} and conductivity measurements from the three surface water and four groundwater monitoring stations were included in the algorithm. Individual measurements (e.g. monthly or quarterly samples) were assigned to a cluster based on their hydrochemistry. The resulting outputs are presented in Section 5.2. Further information regarding HCA and the Wards linkage method is provided in Section 4.1.

Table 5.1. Surface and groundwater monitoring sites included in local scale temporal interaction investigation. Each monitoring site's regional scale interaction cluster assignment is presented also.

Surface water sites	Cluster	Groundwater sites	Cluster
Waiohine River at Gorge	A1	S26/0457	A1
Mangatarere Stream at SH2	A2	S26/0846	A1
Mangatarere at Bicknells	A1	S26/0439	A2
		S26/0467	A2

Time series analysis of Ca^{2+}, Cl^{-} and conductivity from the hydrochemical database was also carried out, and a systematic comparison of these parameters across the surface and neighbouring groundwater bodies was undertaken. The first two elements were selected as they are considered conservative and are unlikely to be affected by changing redox conditions (Kirchner *et al.*, 2001; Woocay and Walton, 2008). Conductivity is an exception to this, but provides a quantitative indicator of total ion concentration (Kegley and Andrews, 1998).

Data were selected from the years 2007 and 2008 as they provided the largest full dataset (monthly surface water and quarterly groundwater chemical sampling) and are the first years in which a full suite of water quality parameters were recorded at the all surface water sites.

5.2 Temporal cluster analysis

The temporal interaction between the Waiohine and Mangatarere streams and surrounding groundwater wells was investigated with the aid of HCA. Utilising the same principles as those presented in Chapter 4, surface and groundwater data from 2008 were subjected to HCA in a hope that similarities in hydrochemistry could be identified and interaction inferred. The resulting dendrogram, presented in Figure 5.1, allowed for the visual identification of three major clusters or hydrochemical facies at the 100 distance (*y-axis)* threshold. The number of monitoring sites assigned to each cluster is presented in Table 5.2. Surface water measurements are assigned almost evenly (11-13) across all three clusters, while measurements from groundwater sites are only assigned to cluster L2 (8 measurements) and L3 (9 measurements).

Table 5.2. Mean of each hydrochemical parameter for temporal clusters L1-L3 in comparison with clusters A1 and A2 from regional scale interaction HCA (Chapter 4). Determined using HCA - Wards linkage method. Additional TDS column determined from the sum of other parameters. *n* represents the number of individual surface water measurements assigned to each cluster. Groundwater measurements are presented in parenthesis. Sample size is not presented for regional scale clusters A1 and A2. Solute centroids are presented in mg/L while conductivity is presented as µS/cm.

Category	*N*	Cond	Ca^{2+}	HCO_3^-	Na^+	Cl^-	Mg^{2+}	K^+	SO_4^{2-}	TDS
L1	13(0)	49.2	4.2	18.0	4.2	5.7	0.8	0.4	2.7	33.3
L2	11(8)	78.4	6.9	29.1	6.0	7.1	1.5	0.7	4.4	51.3
L3	12(9)	136.0	8.0	33.5	12.1	14.3	3.1	1.5	9	72.5
A1		77.1	6.5	26.6	6.1	6.5	1.5	0.7	4.1	51.9
A2		135.5	9.0	29.8	10.7	11.0	3.1	1.3	7.5	72.5

ANOVA Box and Whisker plots were used to test the statistical difference in sample means and medians between each cluster for the analytes considered in the algorithm. Resulting outputs are presented in Figure 5.2. The three clusters are differentiated by conductivity and their concentration of major ions as indicated in Table 5.2.

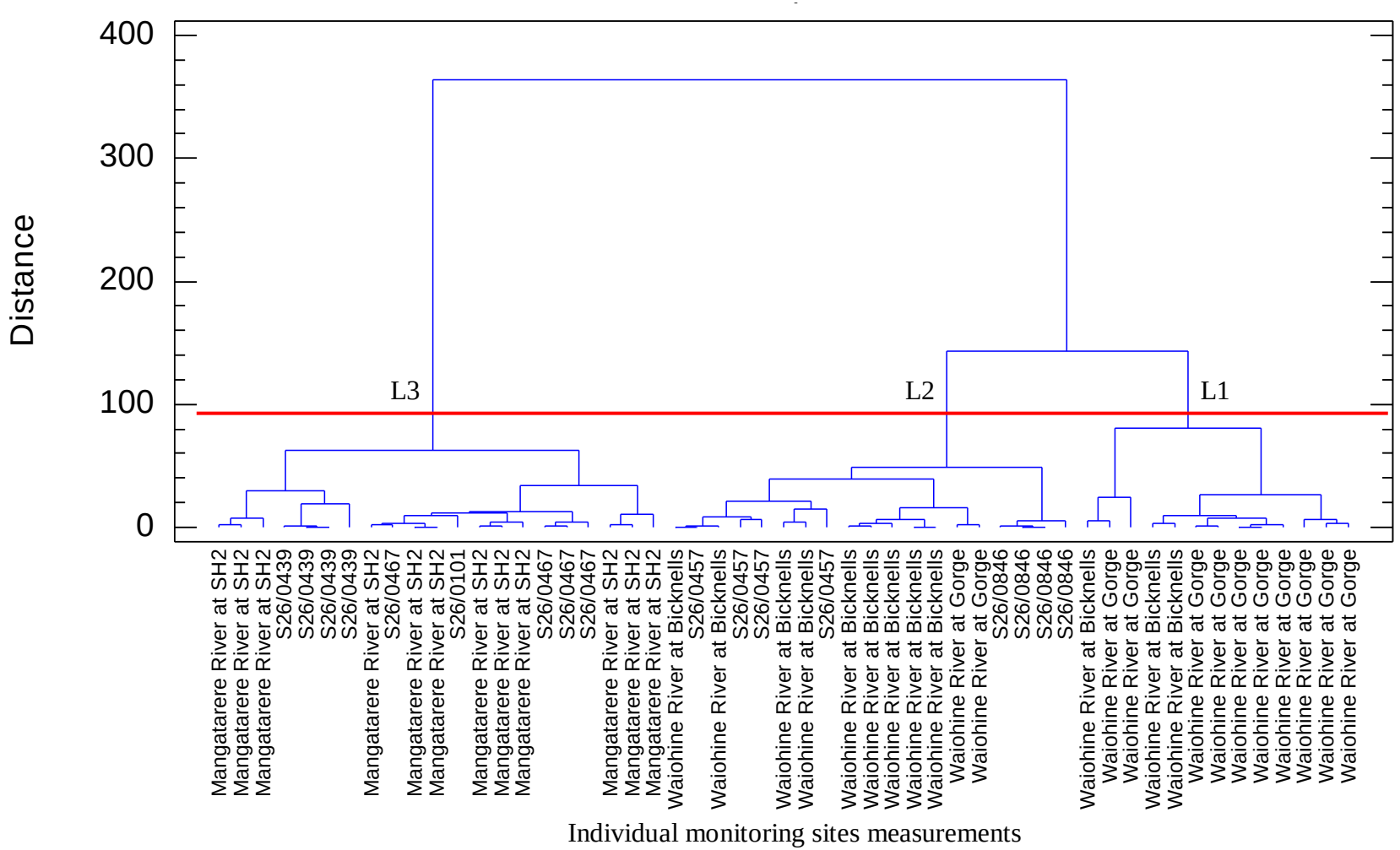

Figure 5.1. HCA Dendrogram determined using Wards linkage method classifying 2008 monthly surface water and quarterly groundwater water quality measurements from the Waiohine and Mangatarere River areas into hydrochemical clusters. *n* = 55 individual measurements across four surface water and four groundwater monitoring sites. Vertical *y*-axis indicates the relative similarity of different monitoring stations, while each vertical blue terminus (*x-axis*) represents an individual monitoring site measurement. At a 100 distance threshold three main clusters (L1 – L3) are identified.

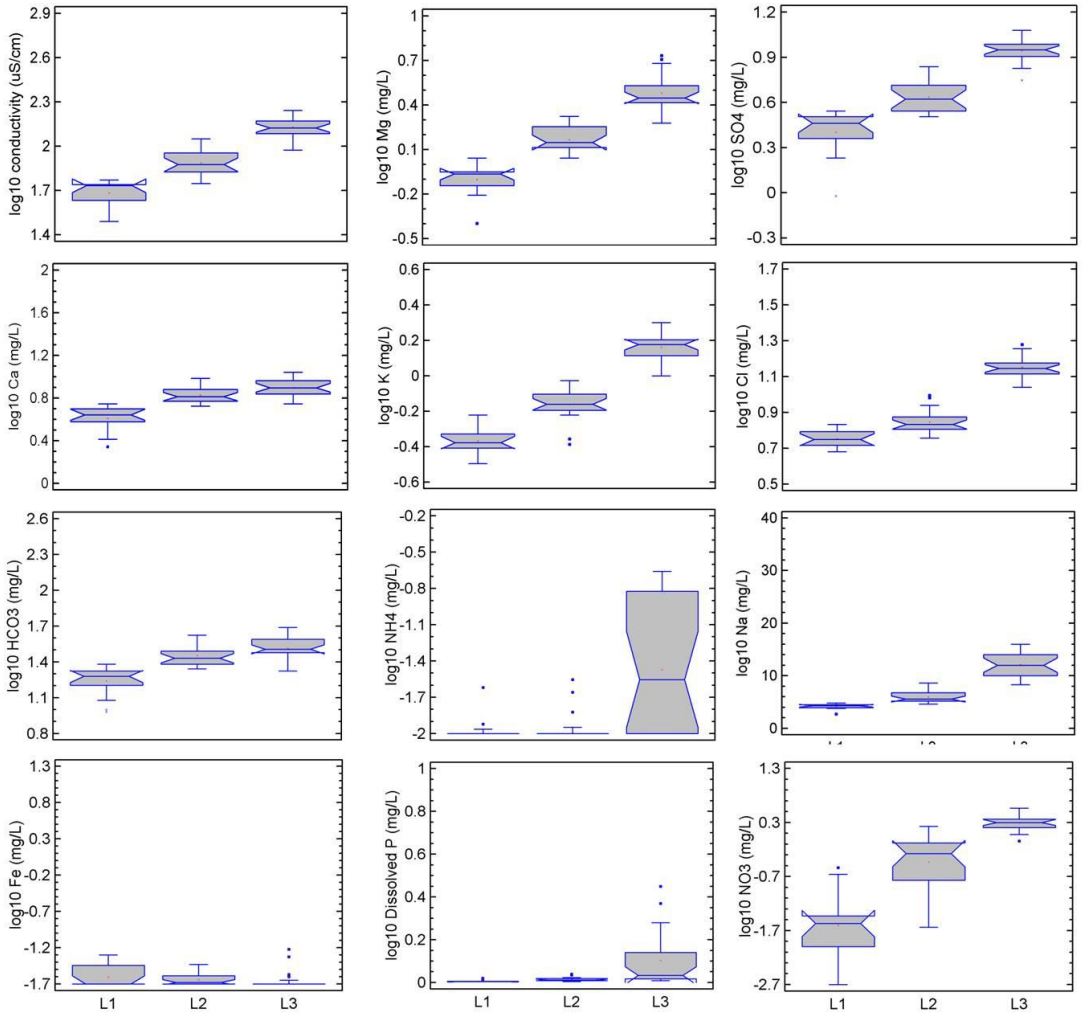

Figure 5.2. One-Way ANOVA Box-Whisker plots showing the variation across Clusters L1-L3 for selected parameters. Parameters include both those subjected to HCA and additional parameters selected for further investigation of cluster variation. The rectangular box identifies the first to the third quartile of the data, separated by a horizontal median line. Median notches are present around the median line identifying the margin of error surrounding sample median estimation. The vertical whisker lines identify the lowest and highest observations in the sample, except those deemed to be outliers as represented by the dots plotted outside these whiskers (Kim *et al.*, 2003).

All seven parameters considered in the algorithm increased along the following cluster sequence L1 – L2 – L3 (Table 5.2 and Figure 5.2). This is supported by calculated TDS values (33.3, 51.3 and 72.5 mg/L), that also follow this cluster sequence (Table 5.2). Concentrations of the major nutrients NO_3^-, NH_4^+ and total P are statistically highest in L3, however there is no statistically significant difference between concentrations of NH_4^+ and total P in clusters L1 and L2 (Figure 5.2). NO_3^- is an exception to this and has lower concentrations in cluster L1. There is no statistically significant difference in Fe^{2+} concentrations between the clusters. Additional parameters (e.g. pH and NO_2^-) could not be analysed due to an absence of these measurements within surface water data.

Clusters L2 and L3 display similar hydrochemical means for a number of parameters to those of clusters A1 and A2 presented in the regional scale interaction section (Section 4.3 and 4.4). These parameters include conductivity, Ca^{2+}, Na^{+}, Mg^{2+}, K^{+}, SO_4^{2-} and TDS. Cluster L1 (13 surface water measurements) has lower concentrations for all parameters than clusters A1 and A2 from the regional scale clustering (Section 4.3 and 4.4).

The chemical composition of each cluster is investigated in Figure 5.3 with the aid of a Piper diagram. Measurements assigned to cluster L2 show a Ca^{2+}-HCO_3^{-} water type while those of cluster L1 and L3 display a stronger Na^{+}-HCO_3^{-}- Cl^{-} signature. This may indicate potential rainfall recharge of L1 and L3 groundwaters as soluble salts accumulate during the passage of precipitation through the soil column (Freeze and Cherry, 1979; Taylor *et al.*, 1989).

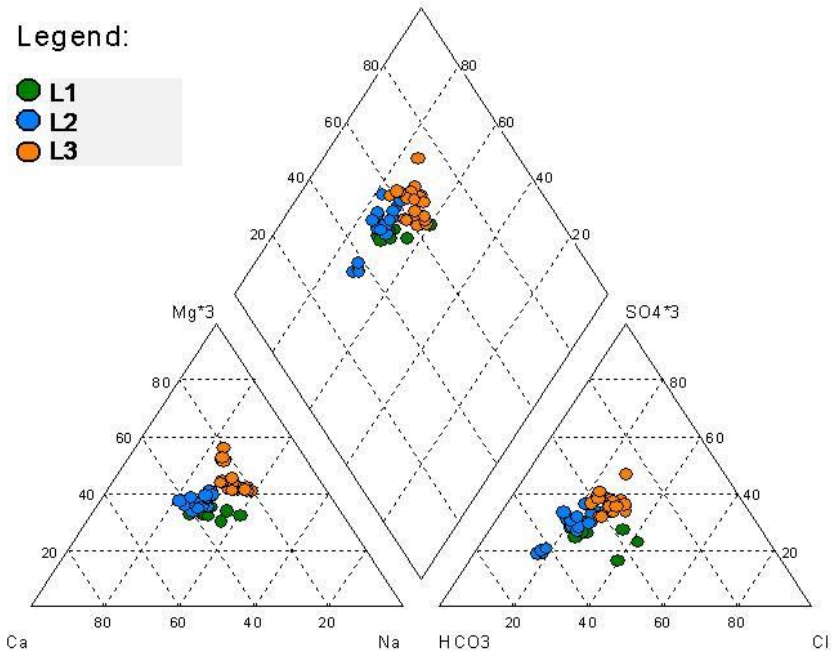

Figure 5.3. Piper diagram showing the variation of major ions (Ca^{2+}, Na^{+}, Mg^{2+}, Cl^{-}, HCO_3^{-}, SO_4^{2-} and Mg^{2+}) amongst the 53 individual measurements from the Mangatarere and Waiohine Rivers and neighbouring groundwater sites that were assigned to Clusters L1-L3. Clusters determined using HCA – Wards Linkage method. The left triangle presents major cations while the right presents major cations. The center triangle represents the projected position based on both triangles. Note the exaggerated Mg^{2} (x3) and SO_4^{2-} (x3) scales for ease of interpretation.

The assignment of individual water measurements to temporal clusters is presented in Figure 5.4. Each monitoring location is depicted by a circle consisting of 12 individual segments that represent months of the 2008 calendar year. Months of the year in which sampling was not undertaken are represented by white segments and were not included in the HCA process. This is the case for all four groundwater monitoring locations, at which sampling was only undertaken during the months of March, July, September and December. All three surface water locations were sampled monthly and show various temporal water chemistry responses.

The Mangatarere stream at State Highway 2 (SH2) displayed L3 type water for all 12 months of the entire 2008 year and was high in average TDS (72.5 mg/L) and conductivity (136 µS/cm). In contrast waters from the Waiohine River at Gorge were reasonably dilute for the majority of the year, with all months except April and May assigned to cluster L1. During April and May, waters were assigned to cluster L2, and exhibited higher than average conductivity (88.4 µS/cm) and TDS (51.3 mg/L). This may be explained by reduced Na^{+}-Cl^{-} rainfall input and increased residence times allowing for an increase in TDS.

Downstream at the Waiohine at Bicknells water generally tended to have higher solute concentrations (Table 5.2), and was assigned to cluster L2 for the majority of the year. Exceptions to this occurred during the months of June, November and December when L1 waters were experienced (average conductivity 33.3µS/cm). It is likely input from the more concentrated Mangatarere stream (100% L3 waters) elevated solute concentrations in the Waiohine at Bicknells, resulting in L2 waters for a longer duration of the year. The L1 waters experienced at Bicknells during July, November and December 2008 may indicate a greater input of diluted L1 waters from the Waiohine Gorge during certain periods of the year.

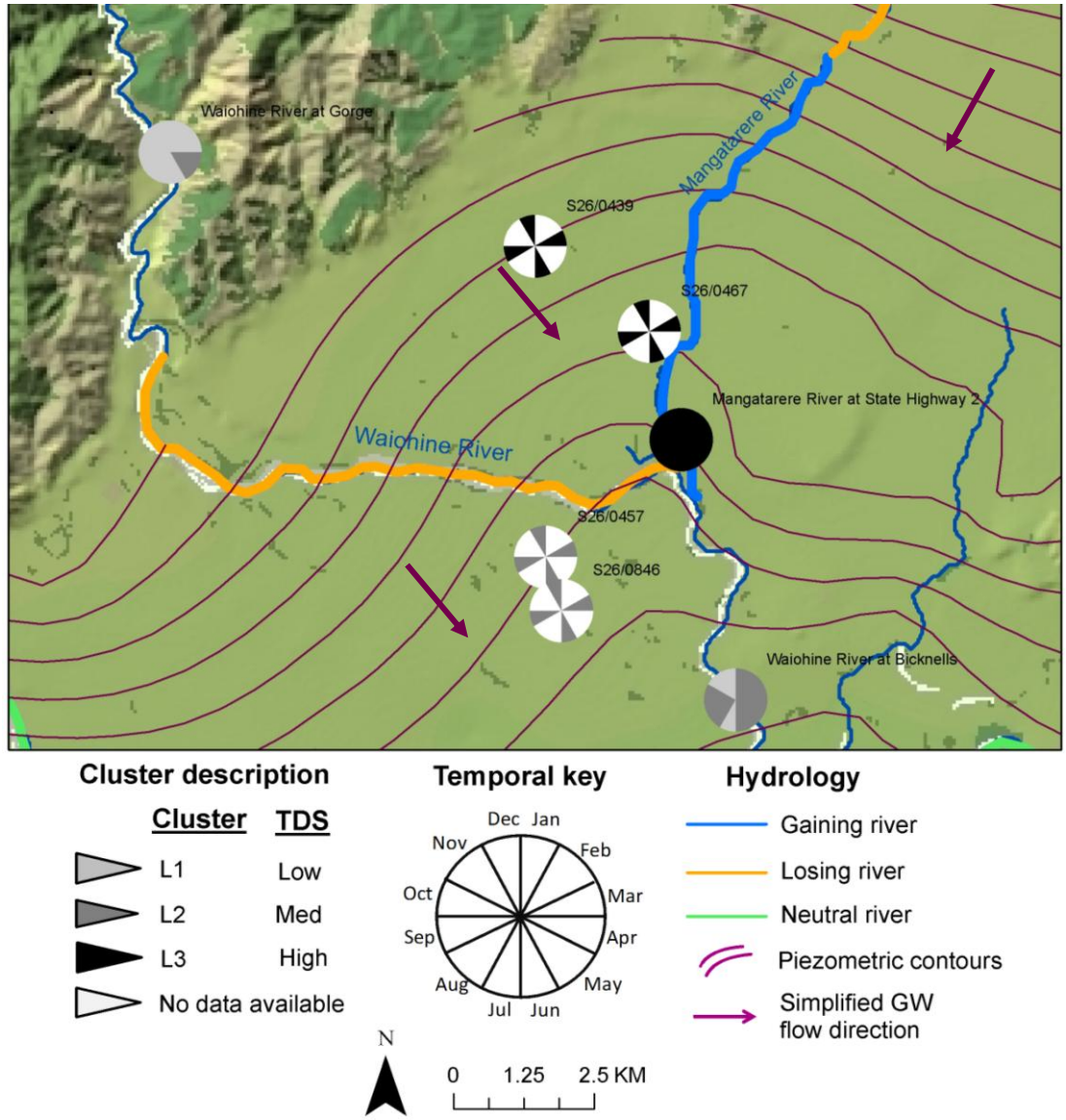

Figure 5.4. Assignment of individual monthly (surface) and quarterly (groundwater) water quality measurements to three hydrochemical clusters in the Waiohine and Mangatarere area. Determined using HCA – Wards linkage method. Distribution is shown in comparison to pre-determined river properties: gaining, losing or neutral stream systems.

Groundwater monitoring sites showed a more consistent hydrochemical pattern for the 2008 year. All measurements from wells S26/0439 and S26/0467 were assigned to cluster L3, while all those from S26/0457 and S26/0846 were assigned to the slightly less concentrated cluster L2. Due to the limited size of the groundwater dataset it is not possible to make robust inferences regarding temporal changes in water quality at these sites throughout the year.

Groundwater wells S26/0457 and S26/0846 show a consistent L2 signature for the four months where data is available. This may be due to the relatively consistent hydrochemistry displayed at the upstream Waiohine River at gorge (L1). These surface waters are thought to recharge underlying groundwater systems (Jones and Gyopari, 2006). The shift to L2 waters at these groundwater sites may be due to acquisition of solutes as dilute L1 waters from the Waiohine move through the hyporheic zone and subsurface medium. Dissolution of carbonate minerals during this passage may shift the chemical signature of waters towards Ca^{2+}-HCO_3^-.

Waters in the effluent reach of the Mangatarere at SH2 and the upstream wells S26/0439 and S26/0467 are consistently assigned to cluster L3. This may suggest S26/0439 and S26/0467 provide solute rich base flow, high in nutrients, to the Mangatarere stream. This assumption seems feasible as one can assume Mangatarere catchment headwaters would display a similar L1 water chemistry in line with those observed at the Waiohine at gorge (low TDS and nutrients). Further, the lower reach of the Mangatarere has been identified as receiving base flow from groundwater systems (Jones and Gyopari, 2006).

This method of temporal HCA aimed to group individual surface and groundwater hydrochemical measurements into similar clusters in order to infer potential interaction during the 2008 year. Further, it aimed to provide insight into the temporal variability and potential lag times at which this interaction occurs. Although temporal cluster analysis was able to link surface and groundwater sites based on hydrochemistry, the limited groundwater dataset (quarterly) makes it impossible to determine cause and/or significance of monthly variations in groundwater quality. As a result it is difficult to make solid inferences regarding the temporal variation in interaction between these surface and groundwaters bodies. More comprehensive datasets are required to validate these results and to fully understand temporal changes in groundwater chemistry.

5.3 Time series analysis

An analysis of existing hydrochemical time series data was undertaken to establish if surface and groundwater chemical interaction could be inferred by identifying if parallel changes in water chemistry occur concurrently across water bodies. This analysis focused on individual hydrochemical parameters, unlike the HCA described in Section 5.2 which dealt with all parameters simultaneously. Data were collected from the Waiohine River and Mangatarere stream and a selection of neighbouring groundwater sites (Table 5.1). Water quality tended to be similar across the majority of groundwater monitoring sites for this period, therefore, results are presented from two groundwater sites only (S26/0439 and S26/0467).

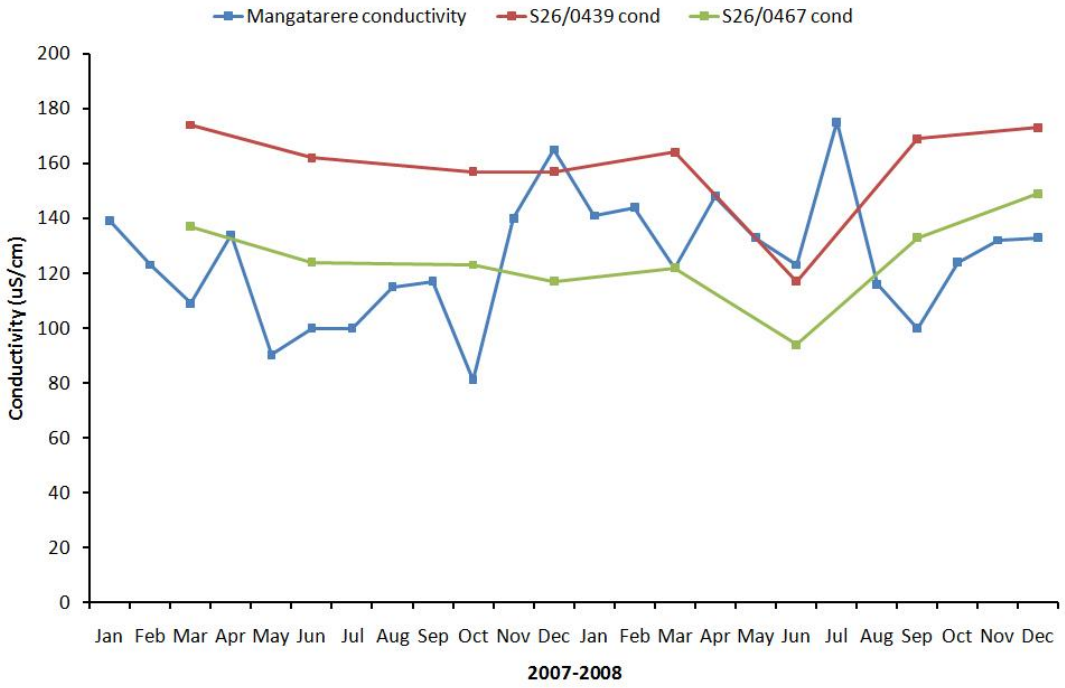

Figure 5.5. Temporal variations in conductivity (µS/cm) from the Mangatarere stream and S26/0439 and S26/0467 groundwater wells for the the period January 2007-December 2008. Individual measurements are identified by a marker point -Mangatarere stream measurements are conducted monthly while measurements at groundwater sites are conducted quarterly. Data provided by GWRC.

Monthly conductivity at the Mangatarere stream fluctuated significantly during the 2007-2008 period (Figure 5.5). There was no clear pattern to these fluctuations, however values appeared to be slightly lower during the 2007 year (80-140 µS/cm range), in comparison to 2008 (100-180 µS/cm range).

This may have been due to La Nina drought conditions experienced in the region from September 2007 until June 2008 that led to an overall reduction in discharge at the Mangatarere, resulting in potentially more concentrated flows and higher conductivity (Watts and Gordon, 2008). In contrast conductivity at the S26/0439 and S26/0467 groundwater sites remained relatively consistent for the duration of the study period. An exception to this occurred in June 2008 when a concurrent decrease in conductivity was experienced at both sites. The magnitude of this decrease was slightly lower (*ca.* 20 µS/cm) at the S26/0467 site. This may be due to S26/0467 being located closer to the Mangatarere stream. It is unlikely that this decrease in conductivity is a data or analytical outlier due to its concurrent occurrence at both groundwater sites. It does not appear that groundwater conductivity is influenced by the Mangatarere stream as changes in surface conductivity do not lead to a systematic response in groundwater. Likewise, it is hard to link the decrease in groundwater conductivity from June 2008 with a decrease in conductivity at the Mangatarere (e.g. Oct 2007) as no other responses are present prior or after this event. It is therefore relatively safe to conclude this phenomena is not a lag effect, or that if a lag effect exists, it is not detectable at the monthly or quarterly sampling frequency undertaken for monitoring presented in Figure 5.5.

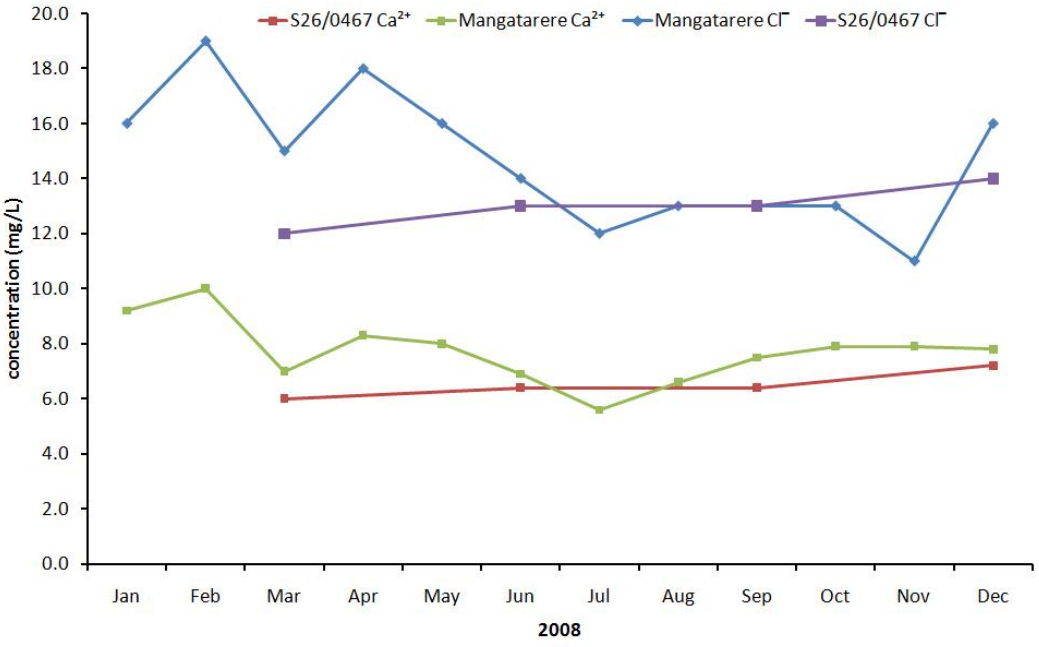

Figure 5.6. Temporal variations in Ca^{2+} and Cl^- concentrations (mg/L) from the Mangatarere stream and S26/0467 groundwater well for the the period January 2008 to December 2008. Individual measurements points are identified by a marker point - Mangatarere stream measurements are conducted monthly while S26/0467 samples are conducted quarterly. Data provided by GWRC.

An analyis of Ca^{2+} and Cl^- data from the Mangatarere stream and several neighbouring groundwater wells was also undertaken and representative results presented in Figure 6.6. Concentrations of the ions Cl^- and Ca^{2+} at the Mangatarere stream follow a similar pattern, fluctuating during the months of January to May (15-19 mg/L for Ca^{2+} and 5-10 mg/L for Cl^-) before decreasing and then remaining relatively consistent for the months of July to November. This decrease is likely a dilution effect, in which elevated winter rainfall events flush low solute waters into the Mangatarere stream. From November to Decemeber 2008 Mangatarere Cl^- concentrations increased from 11 mg/L to 16 mg/L, a pattern not shared by Ca^{2+}. This increase may have been due to increased evapotranspiration or a greater proportion of stream baseflow provided by rainfall recharged groundwaters (Taylor *et al.*, 1989). Concentrations of S26/0467 Ca^{2+} and Cl^- show a slight increase during 2008 with Ca^{2+} increasing 1.2 mg/L and Cl^- increasing 2 mg/L. This pattern of increase may be due to the dissolution of subsurface minerals as the year progresses or increased recharge from precipitation, the latter of which may elevate groundwater Na^+ and Cl^- concentrations, with Na^+ ions subsequently displacing Ca^{2+} ions from soil exchange sites and therefore increasing Ca^{2+} concentrations in solution (McLaren and Cameron, 2006). No clear relationship can be found between changes in Cl^- and Ca^{2+} concentration at the S26/0467 well and the Mangatarere stream. As already mentioned this may be due to the quarterly and monthly sampling that may fail to capture the full temporal variability in hydrochemistry. Data was only analysed for the 2008 year as monitoring of Ca^{2+} and Cl^- at the Mangatarere stream was only conducted during this period.

5.4 Local scale temporal interaction concluding remarks

In summary, the quarterly period at which groundwater sampling was undertaken offers little insight into the temporal nature at which hydrochemical changes in water quality may occur. This makes it difficult to ascertain whether deviations (e.g. conductivity in June 2008) are one off phenomena or consistent patterns (e.g. dilution during high rainfall). It is extremely difficult to associate parallel changes in water quality between ground and surface water sites and use this principle to infer potential interaction. This highlights the need for more frequent hydrochemical monitoring to establish the temporal extent of chemical change of these water bodies. Further, it is hard to make inferences regarding temporal changes in water quality without additional hydrological and metorological data (e.g. discharge, precipitation, evapotranspiration). This data would help one understand the possible drivers of patterns observed in hydrochemistry.

Chapter 6
Local scale high resolution interaction

Chapters four and five investigated regional and local scale surface and groundwater interaction in the Wairarapa valley using HCA, time series analysis and historic hydrochemical data. As identified in Section 2.2.2 significant transfer of water between surface and groundwater bodies can occur within minutes, a phenomenon that is also replicated in solute transport (USEPA, 2000). Investigations from this research at both a regional (Chapter four) and local scale (Chapter five) utilised existing low resolution (monthly, quarterly) datasets. These data sets may fail to capture the temporal variability at which surface and groundwaters interact and the impact this may have on water chemistry. Therefore, the potential high resolution (sub-daily, sub-hourly) interaction between ground and surface water was further investigated on the Mangatarere stream. This chapter aims to gain some insights on the temporal variability at which surface and groundwater interactions occur by focusing on temporal changes in chemical, hydrological and meteorological parameters from the Mangatarere stream and several neighbouring groundwater sites during the three month period 20th November 2009 until 20th February 2010 (JD324-051). For the remainder of this study these dates will be referred to as Julian Days (JD).

This chapter is divided into seven sections. Section one presents a detailed field site description from the Mangatarere stream and its catchment. This is followed in section two by an account of the methodologies employed for this high resolution investigation. The third section presents hydrological, chemical and meteorological time series data from the surface and groundwater gauging stations. Quantification of these parameters enabled a systematic comparison of the ground and surface water systems and allowed links to be drawn between the various systems to infer interaction. This is followed by an analysis of water quality changes from the various systems in Section four. Section five presents a quantification of water transfer between interacting systems while section six present the main findings and limitations of this local scale high resolution investigation.

6.1 The Mangatarere stream

The investigation of regional scale ground and surface water interaction within the Wairarapa valley (Chapter four) identified a number of water bodies thought to be interacting based on similarities in their hydrochemistry. One area of particular interest is the Mangatarere stream and its surrounding groundwater wells. These sites were identified as potentially interacting through regional scale investigations (Section 4.2.4 and 4.4) and were chosen for further investigation due to GWRC's desire to gain a greater understanding of hydrological systems within the Mangatarere catchment and their associated processes. Further, the Mangatarere catchment is of particular importance for agriculture production and therefore issues may surround the transport of agricultural contaminants between interacting water bodies. As a result, detailed field investigations were undertaken on the Mangatarere stream and two neighbouring groundwater wells and are detailed in this chapter.

The entire Mangatarere stream drains a low altitude (300-600m) 160 km^2 catchment in the Tararua ranges (Figure 6.1 and Figure 6.2). It is fed by precipitation, small tributary streams and groundwater as it flows through *ca.* 8 km of the Mangatarere valley. The headwaters of the stream are relatively unconfined, however the stream has incised a permanent passage as it meanders through the Mangatarere valley (Figure 6.3). Surrounding land use in the valley is low intensity agriculture and native bush (Figure 6.1). After exiting the valley the stream is primarily sinuous and moves south-west across the western alluvial fans of the larger Wairarapa valley before joining with the Waiohine River. A number of minor fluvial systems such as Beef Creek, Kaipatangata and Enaki streams provide waters to the Mangatarere along this *ca.* 15 km section. Approximate catchment areas and discharge ranges for these streams are presented in Table 6.1.

Table 6.1. Catchment size and summer and winter discharge ranges from the Mangatarere stream at State Highway 2 and various input streams. 'Summer discharge' denotes October-April, while 'Winter discharge' denotes May-September. Discharge ranges obtained by GWRC data 2008-2009.

Stream	Catchment size	Summer discharge (m^3/s)	Winter discharge (m^3/s)
Enaki	32km^2	0.4-0.33	0.30-2.74
Kaipatangata	23km^2	0.04-0.30	0.17-1.77
Beef Creek	30km^2	0.05-0.75	0.65-6.4
Mangatarere SH2	130km^2	0.36-2.69	2.64-15.4

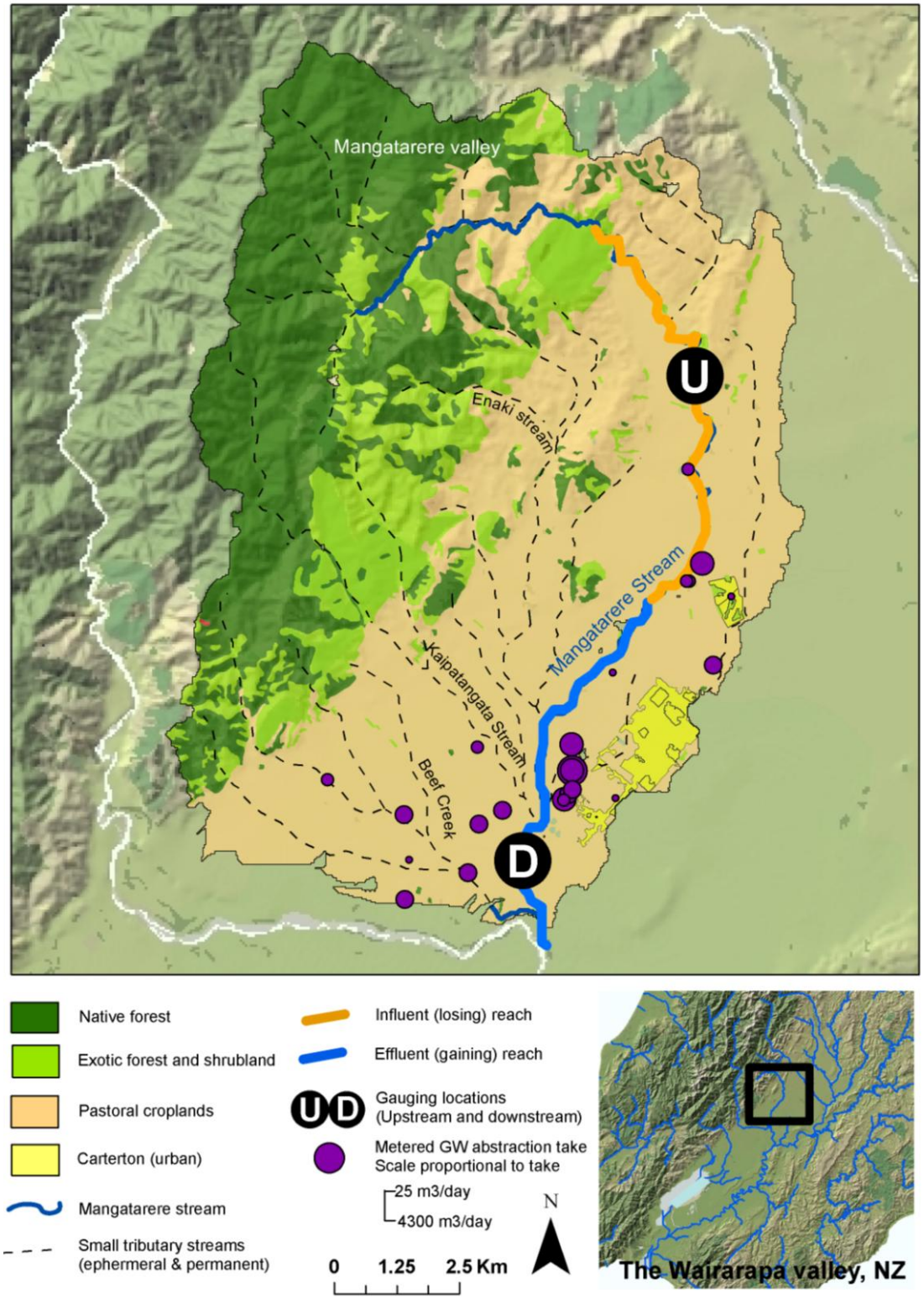

Figure 6.1. Location and land use map of the Mangatarere stream catchment, Wairarapa valley, New Zealand showing dominant land use, effluent and influent stream properties, location of small tributaries, metered daily groundwater abstraction takes and upstream and downstream gauging areas. Both upstream and downstream gauging locations consist of a surface and groundwater gauging station.

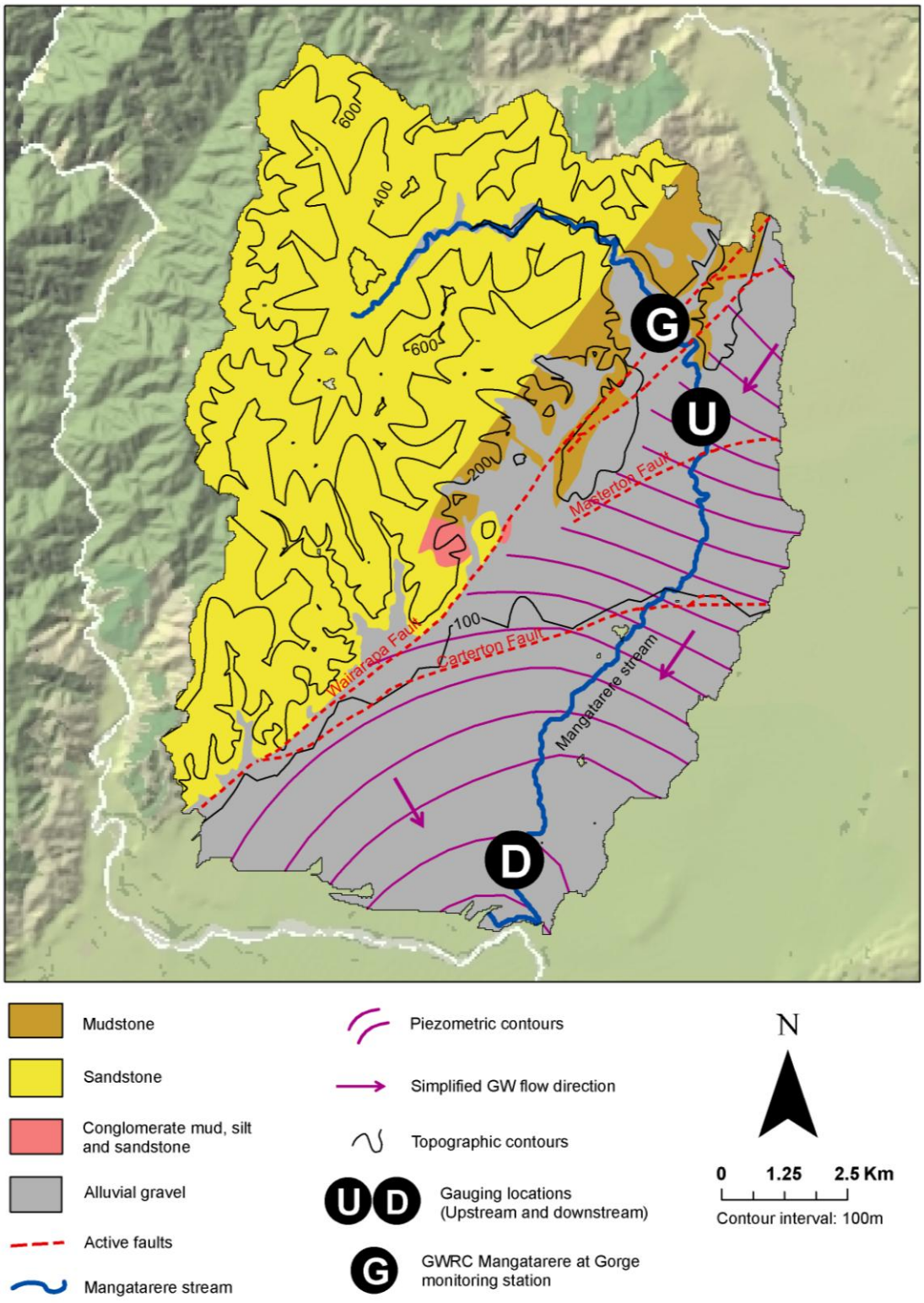

Figure 6.2. Geological map of the Mangatarere stream catchment, Wairarapa valley, New Zealand showing surficial geology, active tectonic faults, topographic contours, groundwater piezometric contours and groundwater flow direction and location of upstream and downstream gauging areas. Both upstream and downstream gauging locations consist of a surface and groundwater gauging station. The location of the Mangatarere catchment in regards to the Wairarapa valley is presented in Figure 3.10 and is applicable for this figure.

Figure 6.3. Easterly down valley view of the Mangatarere stream as it meanders through the Mangatarere valley in the Tararua Ranges, New Zealand.

The Mangatarere stream flows through a variety of different geological settings (Figure 6.2). Initial headwaters in the Tararua ranges are comprised of Torlesse greywacke, overlain with a variety of rock types such as mudstone and limestone. After exiting the ranges the stream incises poorly to moderately sorted alluvial gravels with minor sand or silt underlying terraces. These sedimentary layers are a result of various depositional periods and historic flood events, and can be seen in the banks of the Mangatarere as shown in Figure 6.4. Subsequent bore logs of the area (Figure 6.5) support this and further indicate layers of silty gravels and clay. Pockets of poorly sorted loess-covered fan gravels and lacustrine silt deposits are also present in the area surrounding the stream. Sediment directly below the stream largely consists of well sorted Q1 River gravels, however high flow events have resulted in the haphazard deposition of larger rocks (30-50cm) on the stream bed. The Mangatarere catchment is largely dominated by well drained brown soils such as Tauherenikau stony silt loam and Opaki brown stony loam. However, soils directly underneath and surrounding the upper half of the Mangatarere stream are poorly drained recent soils (Ahikouka and Otukura silt loam) while the lower reaches of the Mangatarere are underlain with well drained recent soils (Greytown silt loam) (Heine, 1975).

Figure 6.4. Sedimentary stratification of the Mangatarere stream bank, taken 100 metres downstream from the upstream surface water gauging station.

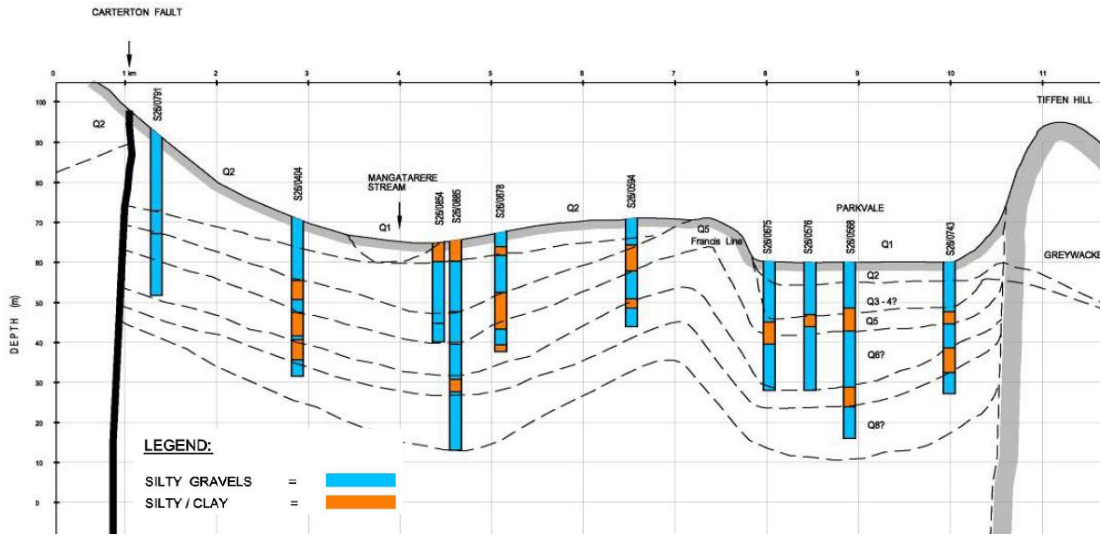

Figure 6.5. Hydrogeological profile of the Mangatarere stream running from the Carterton fault, through the Parkvale Basin to Tiffen Hill. Modified from Jones and Gyopari (2006).

The Mangatarere's flow displays a strong seasonal pattern with flow generally highest during the winter months of June to August (2-3 m^3/s) and lowest during the drier summer months (0.9-1.4 m^3/s) (Table 3.2 and Table 6.1). This flow pattern is principally governed by local precipitation, of which the greatest quantities are experienced in the region during the winter (Figure 3.8). The stream is known to interact with underlying groundwater systems as indicated by a range of recent flow measurements made by GWRC. It is assumed the stream loses flow as it moves through the Mangatarere valley, a trend that continues along its middle reaches. This system of interaction switches to an effluent reach as the Mangatarere passes over the Carterton fault line and groundwaters begin to supply base flow to the stream (Figure 6.1). As a result flow is highest in the lower reaches of the stream.

Groundwaters below the Mangatarere stream primarily flow in a south-easterly direction away from the Tararua ranges (Figure 6.1). These waters are part of the larger Carterton sub-regional flow system with boundaries set by the Wairarapa fault to the west and Tiffen Hill and Fernhill at the east. Recharge is provided to the Carterton flow system by both river and rainfall recharge mechanisms (Figure 3.6) and utilised unconfined shallow aquifers are placed at 5-15 metres deep (Morgan and Hughes, 2001). Shallow aquifer through-flow below the Mangatarere is estimated by the GWRC at 7.6 million m^3/year (Morgan and Hughes, 2001). In the middle reaches of the Mangatarere, after the stream exits the Tararua ranges, flow is lost to the underlying groundwater system. Direct recharge from precipitation becomes increasingly important as the distance from the Mangatarere increases. Darcy flow calculations indicate potential horizontal groundwater flow between 6-10 metres per day (Appendix F).

The Mangatarere catchment is largely dominated by native bush, shrub lands and agriculture on the valley flat (Figure 6.1). As the river exits the Tararua ranges land use is almost entirely medium intensity agriculture, with the small township of Carterton (population *ca.* 4014) located 500-900 metres east of the stream on the Wairarapa valley flat. A high intensity pig farm (10,000 sows) is located *ca.* 200 metres from the stream in its middle reaches. This operation sprays up to 200,000 m^3/year of effluent on neighbouring paddocks.

Treated sewage from the township of Carterton is also discharged into the Mangatarere stream near Belvedere (*ca.* 285,000-500,000 m³/year).

6.2 Local scale high resolution methodology

The resulting field programme was conducted during the 20th of November 2009 and the 20th February 2010 (JD324-051). This period of study was chosen due to the variability of precipitation experienced in the Wairarapa valley during the summer months. This variability provides both extended dry periods and intense precipitation events and would allow one to see how both surface and groundwater systems respond to these events. Upstream and downstream monitoring areas were established, both consisting of a surface and groundwater gauging station at each location. The location of each gauging station was determined by the identification of the sites as potentially interacting at a regional scale, the presence of an existing and currently operational groundwater well, and landowner approval. Further, the upstream location comprised an influent section of the Mangatarere River and the downstream an effluent section as inferred from GWRC analysis (Jones and Gyopari, 2006). This aimed to allow for a systematic comparison of two contrasting styles of interaction. The location of each monitoring area and their associated gauging stations are presented in Figure 6.6.

The upstream monitoring stations are located in the middle reaches of the Mangatarere, where the stream exits the Rimutaka ranges across a historic alluvial fan. This section of the Mangatarere is influent and the surrounding land use is agricultural (dairy and high intensity pig farming). The upstream groundwater gauging station (40°57'47.55"S, 175°31'44.01"E) is established on bore S26/0977 (Figure 6.6). This bore is used primarily for water quality monitoring and is summarised in Table 6.2. The stratigraphic makeup consists of a mixture of clay bound gravels, rock, sand and free sandy gravels (Figure 6.7). Top soil is present to a depth of *ca.* 50cm. The neighbouring surface water gauging station is located *ca.* 300 metres south-east on the banks of the Mangatarere Stream (40°57'51.82"S, 175°31'55.54"E).

The station was established on existing flood protection infrastructures that provide an anchor and adequate protection during high flow events (Figure 6.6). The upstream surface water gauging station drains an area of approximately 53km².

Table 6.2. Bore depth, aquifer type, use and casing material for groundwater monitoring station bores. 'US' denotes upstream well, 'DS' denotes downstream well, 'W.Q.M' denotes Water Quality Monitoring, 'N.U' denotes Not Used and 'N.D' denotes not described.

Bore name	Total bore depth	Aquifer type	Casing material	Diameter	Screen type	Top screen	Bottom screen	Use
S26/0977 (US)	10 m	Water table	PVC	50mm	Slotted PVC	9 m	10 m	W.Q.M
S26/0372 (DS)	6 m	Water table	PVC	40mm	N.D	N.D	N.D	N.U

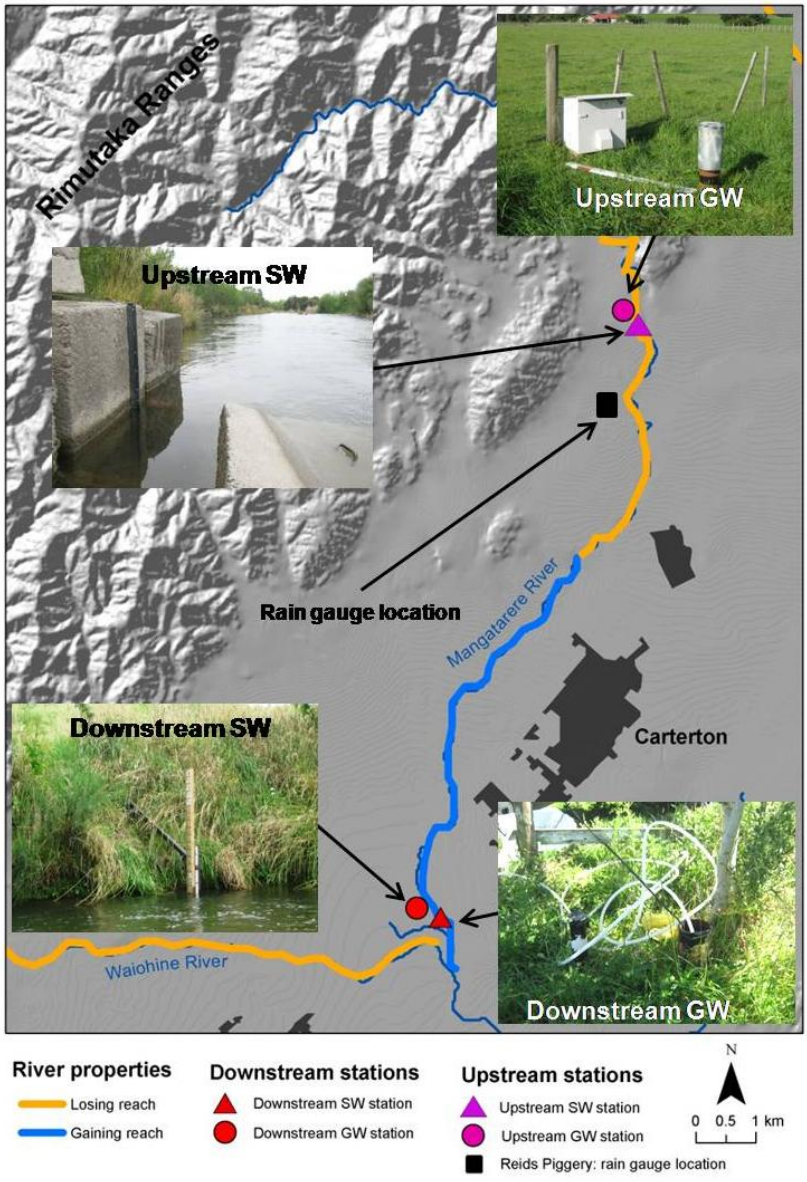

Figure 6.6. Location map and associated images of upstream and downstream surface and groundwater gauging stations. River and groundwater interaction properties (influent and effluent) are also displayed.

The lower gauging stations are *ca.* 10km downstream in the lower effluent reaches of the Mangatarere (Figure 6.6). The groundwater gauging station was established in bore S26/0372 *ca.* 34 metres from the Mangatarere stream. The bore has no current use and is summarised in Table 6.2. No stratigraphic information is available. The neighbouring surface water monitoring station is located *ca.* 300 metres south-west and utilises an existing downstream gauging station installed and operated by GWRC. The downstream surface water gauging station has a *ca.* 130km² catchment area that includes the upstream surface water catchment (*ca.* 52km²) and inputs from Enaki and Kaipatangata streams (*ca.* 32 and 23km² catchments respectively). Both S26/0977 and S26/0372 wells are not used for water abstraction and therefore are likely to display a natural behavior.

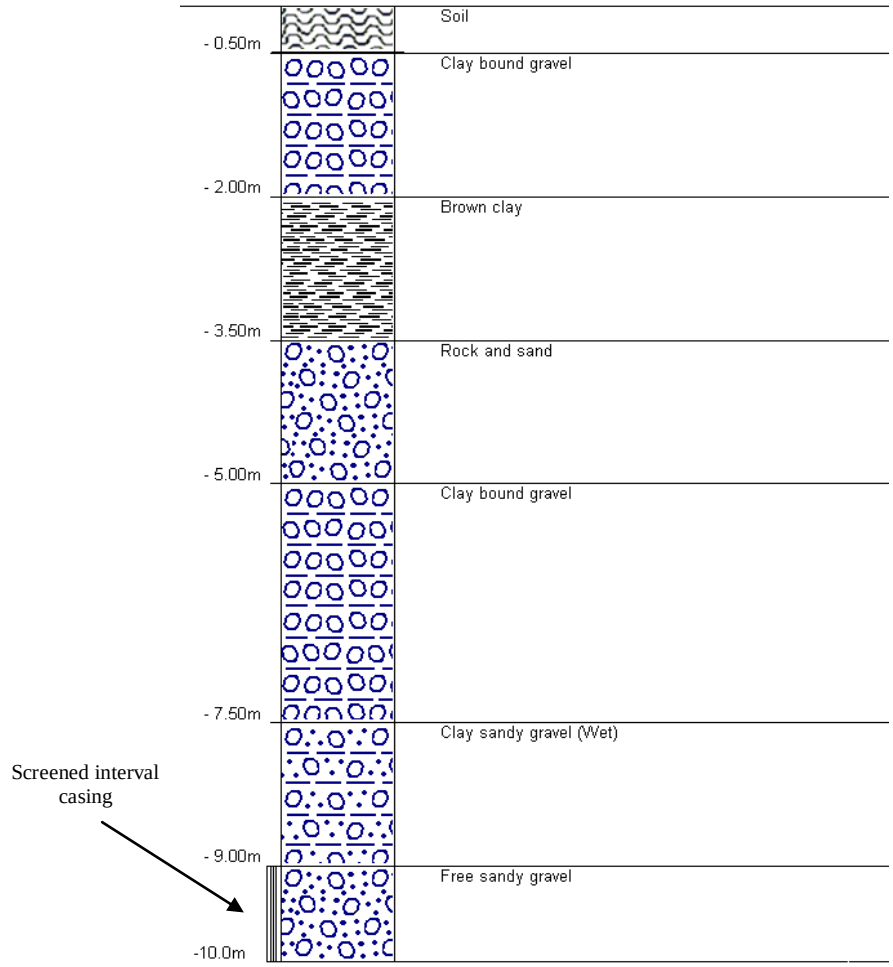

Figure 6.7. Borelog for well S26/0977 (40°57'47.55"S, 175°31'44.01"E) showing stratigraphic units associated with depth below ground surface. Well S26/0977 is cased with impermeable PVC from 0-9 metres while at 9-10 metres this casing is screened or slotted allowing the transfer of water. Sourced from GWRC files.

6.2.1 Physical hydrological parameters

In order to assess potential changes in ground and surface water quantity and infer interaction based on these changes water stage was recorded at the upstream ground and surface water sites and the downstream surface water site for the period JD324-051. The assumption was made that changes in water quantity are directly related to changes in water stage. For this assumption to hold true the cross sectional area of a stream needs to remain unchanged over time. Field observations from both surface water gauging stations confirmed the cross sectional area remained relatively stable during the study period, therefore changes in surface water stage were used as an indirect method of flow evaluation. Using water stage in this way is relatively common (e.g. Lewandowski and Nutzmass, 2008; Schmaltz *et al.*, 2008) and overcomes the practicalities and subsequent errors associated with determining continuous discharge measurements.

Water stage was recorded at all four gauging stations using miniTROLL SSP-100 absolute pressure transducers manufactured by InSitu, Inc. Although an SSP-100 was installed at the downstream groundwater station, technical problems in regards to power supply resulted in the loss of all data from this site. The loss of downstream groundwater data is a major limitation to this research and will be discussed in Section 6.7. The SSP-100 detects all changes in pressure exerted by a column of water and the atmosphere, and then determines stage through an adjustment with atmospheric pressure (Figure 6.8). Further, The SSP-100 PT automatically adjusts for changes in water temperature and fluid density, with an inbuilt temperature sensor. Stage was determined using the pressure difference between that measured by the SSP-100 (*a*) and atmospheric pressure (*b).* Atmospheric pressure measurements were obtained at the upstream groundwater gauging station using a InSitu Baro TROLL sensor located on the ground surface. Stage measurements were obtained every 15 minutes and recorded in the unit's inbuilt memory system. Power was provided to each SSP-100 by two internal AA lithium batteries.

Each SSP-100 pressure transducer was field calibrated by measuring the distance from the water surface to the stream or bore bed. Bore measurements were obtained using a bore dipper. These measurements were found to be accurate ±1cm of the distance provided by the SSP-100, consistent with the manufacturer's 0.2% accuracy range for 0-11m water level ranges.

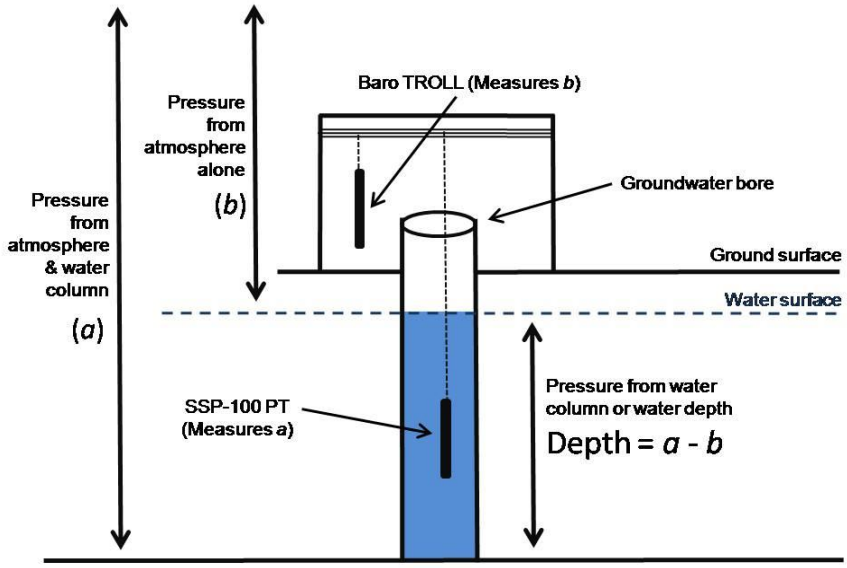

Figure 6.8. Schematic representation of miniTROLL SSP-100 absolute pressure transducer and the determination of water depth. The SSP-100 measures all changes in pressure forces (*a*) which are offset for changes in atmospheric pressure (*b*) to determine water depth.

6.2.2 Hydrochemical parameters

In order to assess hydrochemical changes in water quality, electrical conductivity and water temperature were monitored at all gauging stations. These parameters were chosen as they can be recorded using relatively cheap, real time sensors that provide information on the chemical systems of natural ground and surface water bodies. Measurements were collected at 15 minute intervals at both upstream gauging stations, while measurements were less frequent (hourly) at the downstream surface water station. This hourly measurement interval was due to a misunderstanding with GWRC who maintained the downstream surface water gauging station. Unfortunately, a loss of power to the downstream groundwater site resulted in the loss of all data at this site. Further, an erratic power supply over the period JD360-012 resulted in measurement gaps at the downstream surface water station. The CS547A probes were secured within the water column of each gauging station for the duration of the study period.

Surface water probes were installed in the thalweg of the stream, while groundwater probes were installed at a depth of 6.5 metres (upstream) and 4.5 metres (downstream) from the top of the surface bore casing. These installation depths are the approximate middle depth of each groundwater column and provide security against sudden changes in water depth and contamination from the aquifer base.

Electrical conductivity is a measure of the electrical charge of ions in solution (Kegley and Andrews, 1998). The total charge is proportional to the concentration of dissolved ions in solution and is, therefore, a quantitative indicator of total ion concentration. Electrical conductivity was measured as milli-Siemens per cm (mS/cm) and converted to micro-Siemens per cm (µS/cm) at each gauging station by multiplying mS/cm values by 1000. This was undertaken to remain consistent with international hydrochemical literature and data collected by the GWRC. Each CS547A had a conductivity measurement range of 0.5 to 700µS/cm and was automatically adjusted for temperature dependence by the inbuilt temperature probe. This adjustment is necessary because the conductance of ionic species in solution is influenced by water temperature (Smart, 1992). It was assumed that a linear relationship exists between conductivity and water temperature and therefore conductivity data was adjusted to a common temperature of 25 °C. This assumption is standard and supported in the hydrochemical literature (e.g. Jagannadha Sarma *et al.*, 1979 and Laudon and Slaymaker, 1997). Water temperature and EC measurements were collected at 15 minute intervals and stored in a Campbell Scientific 10X datalogger. Power was provided to the CS547A and associated data loggers by two parallel 12V NiCd batteries. Each CS547A probe was lab calibrated for accuracy prior to field installation and again upon removal to identify potential measurement drift. Results are presented in Table 6.3.

Table 6.3. Pre-field and post-field CS547A probe water temperature and electrical conductivity (EC) calibration results.

Location	Water temp (pre-field) 15 °C	Water temp (post-field) 15 °C	EC 180µS/cm standard (pre-field)	EC 180µS/cm standard (post-field)
Upstream SW	±0.2 °C	±0.2 °C	± 10%	± 10%
Upstream GW	±0.2 °C	±0.2 °C	± 10%	± 10%
Downstream SW	±0.2 °C	±0.2 °C	± 10%	± 10%
Downstream GW	±0.2 °C	±0.2 °C	± 10%	± 10%

6.2.3 Hydrochemical field sampling

A one week hydrochemical sampling programme was conducted during the period JD021 to JD028 in order to investigate daily and diurnal changes in water chemistry. Sampling was undertaken during this period as significant precipitation was forecast and this precipitation would likely stimulate change in hydrochemistry at both the surface and groundwater systems. The sampling scheme consisted of 45 sampling events, conducted at the upstream surface and groundwater gauging sites and the downstream surface water site only. The downstream groundwater site was largely abandoned from this hydrochemical sampling scheme as equipment failure prevented any grab sample data being put in the context of the high resolution monitoring. Therefore, in order to reduce sampling costs, this site was selectively sampled three times (JD021, JD023 and JD028 in 2010) during the sampling period to provide some insight into the chemical dynamics of this groundwater system. Six days (JD021-024 and 027-028) of once daily sampling was conducted at the three remaining sites in order to investigate daily changes in water chemistry. This was supplemented with an additional 24 hour period of sampling (from 1200h JD025 till 1200h JD026) in which samples were collected at three hour intervals in order to investigate changes throughout the day. All extraction locations and the date, time and meteorological conditions on the day of extraction are presented in Table 6.4. The period in which sampling was undertaken was planned to coincide with a range of meteorological and fluvial events in order to capture any variability in water chemistry that may result from these events and their associated processes. In addition, two rainfall samples were collected on JD022 and JD027 to assess the chemical composition of input waters. Rainfall was collected in a 40cm diameter, millipore[4] rinsed silica bowl.

Each sampling event included the collection of three individual water samples: a 100ml field filtered, un-preserved sample for the analysis of major anions (SO_4^{2-} and Cl^-); a 100ml field filtered, high purity nitric acid preserved sample for the analysis of major cations and total Ammoniacal nitrogen (NH_4^+) and reactive Phosphorous (P); and a 1L un-filtered, un-preserved sample for the analysis of nutrients and alkalinity.

[4] High purity filtered water

Further, the 1L unfiltered sample allowed determination of the influence of field filtering. Surface water samples were extracted using sterile TERUMO 60ml hand syringes from the thalweg of the stream, while groundwater samples were collected using a 12V battery power pump from a depth of 4.5m (upstream) and 6.5m (downstream) from the top of the bore casing. These depths were in line with existing water monitoring equipment and are deemed to have provided minimal contamination from the well base. Groundwater bores were purged for several minutes prior to sampling to remove *ca*. three casings of stagnant water and to prevent contamination between sites and samples.

Table 6.4. Hydrochemical grab sample events, date, time, meteorological conditions and upstream Mangatarere stream stage (m) on day of extraction. Three samples were collected for each extraction event (1L unfiltered, unpreserved, 100ml filtered, preserved and 100ml unfiltered, unpreserved). Extraction times (24hour) are presented in same order as sample location or type. Water stage is the average stage over the sampling event. Multiple event averages are presented next to the time of sampling event onset. Standard deviations for all averages were 0.0. Upstream Mangatarere stage data are provided only as deemed more reliable due to equipment malfunctions at the downstream Mangatarere site.

Date (JD)	Sample location or type	Extraction time	Meteorological conditions	Upstream Mangatarere stage (m)
021	Upstream SW, Upstream GW, Downstream SW, Downstream SW, Field blank	1230, 1300, 1200, 1130, 1300	Overcast and light rain	0.50m
022	Upstream SW, Upstream GW, Downstream SW, Rainfall	1230, 1300, 1200, 1130	Overcast, high precipitation event	0.50m
023	Upstream SW, Upstream GW, Downstream SW, Downstream SW	1230, 1300, 1200, 1130	Overcast and light rain	0.79m
024	Upstream SW, Upstream GW, Downstream SW	1230, 1300, 1200	High cloud	0.72m
025	Upstream SW Upstream GW Downstream SW	1230, 1530, 1830, 2130, 1300, 1600, 1900, 2200 1200, 1500, 1800, 2100	Overcast	1200 = 0.60m 1500 = 0.62m 1800 = 0.62m 2100 = 0.61m
026	Upstream SW Upstream GW Downstream SW	0030, 0330, 0630, 0930, 1230 0100, 0400, 0700, 1000, 1300 0000, 0300, 0600, 0900, 1200	Overcast, heavy early morning showers	0000 = 0.61m 0300 = 0.60m 0600 = 0.60m 0900=0.60m 1200= 0.59m
027	Upstream SW, Upstream GW, Downstream SW, Rainfall	1230, 1300, 1200, 1530	Fine and clear, with periods of heavy rain	0.57m
028	Upstream SW, Upstream GW, Downstream SW, Downstream SW, Field blank	1230, 1300, 1200, 1130, 1300	Fine and clear, with periods of light rain.	0.54m

All samples were stored in acid cleaned, sample rinsed, polyethylene bottles with air excluded to reduce post-sampling reactions. Samples were hand filtered through MILLIPORE 0.45µm Durapore membrane field filters and all 100ml filtered and preserved samples treated with 2ml of high purity nitric acid. Field blanks containing 100ml of high grade millipore H_2O and 2ml of nitric acid were exposed to the atmosphere on JD021 and JD028 to identify contamination from the nitric acid and field filters. Routine replicate samples and laboratory blanks containing filtered millipore H_2O were conducted in the laboratory to determine further contamination from the membrane field filters, storage bottles and laboratory equipment. All water samples were stored in the dark and refrigerated to 4 °C for overnight transportation to Hill Laboratories in Hamilton, New Zealand. Med-X Powder free Latex gloves were worn for all hydrochemical sampling and handling of equipment to reduce contamination. Further, sample bottles and sampling equipment was rinsed three times with sample water at the beginning of each sampling procedure to prevent contamination between locations.

6.2.4 Hydrochemical Lab analysis

Grab samples were analysed for the following 15 water quality parameters: major cations (Ca^{2+}, Mg^{2+}, K^{+}, Fe^{2+} and Na^{+}), anions (HCO_3^{-}, SO_4^{2-} and Cl^{-}), nutrients (Total NH_4^{+}, NO_3^{-}, NO_2^{-}, and dissolved reactive P), alkalinity, Manganese and pH. These parameters provide information regarding water age, drainage and aquifer lithology, redox state and the various pathways of water. All analytical analyses were conducted by Hill Laboratories Ltd in Hamilton, New Zealand using standard industry methods. Analytical method used, detection limit and accuracy for each chemical parameter are presented in Table 6.5.

6.2.5 Meteorological parameters

Precipitation and air temperature measurements were obtained for the duration of the study period JD324 to JD051 in order to investigate the influence of meteorological conditions on potential surface and groundwater interaction. Air temperature was monitored continuously at the upstream surface water gauging station using a Campbell Scientific 109-L temperature sensor. Measurements were obtained at 15 minute intervals and deemed applicable to all sites due to their close proximity.

The 109-L was factory calibrated and according to manufacturer specifications, was accurate to ±0.2 °C (Campbell Scientific Inc, 2007).

Table 6.5. Analytical method, detection limit and accuracy for 17 water quality chemical parameters. All analyses conducted by Hill Laboratories, Hamilton, New Zealand.

Chemical analyte	Analytical method	Detection limit	Accuracy
pH	pH meter. APHA 4500-H+ B 21st ed. 2005.	0.1 pH Units	±0.2
Total alkalinity	Titration to pH 4.5 (M-alkalinity), autotitrator. APHA 2320 B (Modified for alk <20) 21st ed. 2005.	1.0 mg/L	± 7%
HCO_3^-	Calculation: From alkalinity and pH	1.0 mg/L @ 25 °C	± 7%
Ca^{2+}	Filtered sample, ICP-MS, trace level. APHA 3125 B 21st ed. 2005.	0.05 mg/L	± 6 %
Fe^{2+}	Filtered sample, ICP-MS, trace level. APHA 3125 B 21st ed. 2005.	0.02 mg/L	± 7%
Mg^{2+}	Filtered sample, ICP-MS, trace level. APHA 3125 B 21st ed. 2005.	0.02 mg/L	± 7%
Mn	Filtered sample, ICP-MS, trace level. APHA 3125 B 21st ed. 2005.	0.0005 mg/L	± 9%
K^+	Filtered sample, ICP-MS, trace level. APHA 3125 B 21st ed. 2005.	0.05 mg/L	± 8%
Na^+	Filtered sample, ICP-MS, trace level. APHA 3125 B 21st ed. 2005.	0.02 mg/L	± 11%
Cl^-	Filtered sample. Ferric thiocyanate colorimetry. Discrete Analyser. APHA 4500 Cl- E (modified from continuous flow analysis) 21st ed. 2005.	0.50 mg/L	± 7-8%
NH_4^+	Filtered sample. Phenol/hypochlorite colorimetry. Discrete Analyser. (NH4-N = NH4+-N + NH3-N). APHA 4500-NH3 F (modified from manual analysis) 21st ed. 2005	0.010 mg/L	34-40%
NO_2	Automated Azo dye colorimetry, Flow injection analyser. APHA 4500-NO3- I (Proposed) 21st ed. 2005.	0.0020 mg/L	±0.0014 mg/L
NO_3^-	Total oxidised nitrogen. Automated cadmium reduction, flow injection analyser. APHA 4500-NO3- I (Proposed) 21st ed. 2005.	0.0020 mg/L	± 10%
Dissolved P	Filtered sample. Molybdenum blue colorimetry. Discrete Analyser. APHA 4500-P E (modified from manual analysis) 21st ed. 2005.	0.0040 mg/L	± 10%
SO_4^{2-}	Filtered sample. Ion Chromatography. APHA 4110 B 21st ed. 2005.	0.50 mg/L	± 7-12%

Precipitation was monitored using a Vaisala Weather Transmitter WXT520 and Harvest SPE-02 telemetry unit located at Reid's Piggery on Haringa Road (40°58'36.30"S, 175°31'44.14"E) (Figure 6.9). The location of the unit was deemed representative of all gauging locations due to their close proximity and consistency of the topography, however the station is located significantly closer to the upstream gauging sites (Figure 6.6). The WXT520 was factory calibrated and precipitation reported accurate to 0.5mm. Measurements were recorded at 15 minute intervals, however an error with the Harvest SPE-02 programming resulted in measurements being delivered at erratic intervals (e.g. 15, 30, 32, 45 minutes). As a result precipitation data are presented as daily totals (mm/day). The telemetry unit was maintained by Reid's Piggery who were unaware of this reporting error.

Figure 6.9. Vaisala Weather Transmitter WXT520 and Harvest SPE-02 telemetry unit installed at Reid's Piggery (40°58'36.30"S, 175°31'44.14"E) located between the upstream and downstream gauging locations.

6.2.6 Data processing (filtering)

In order to remove high frequency isolations and potential instrumentation noise water stage, conductivity and temperature data from all gauging stations were post-processed using a moving mean and Tukey-Hanning filter. Firstly, a five cell moving mean filter was applied to the data series with the resulting mean values exposed to three counts of the Tukey-Hanning filter as calculated by Equation 6.1. This filter takes a moving mean of three data points (X_1, X_2 and X_3) and gives the centre point (X_2) twice the weighting as the neighbouring points (X_1 and X_3) (Priestly, 1981).

$$X_{Filtered} = (X_1 \times 0.25) + (X_2 \times 0.50) + (X_3 \times 0.25) \qquad (6.1)$$

6.2.7 Scaling of conductivity data

At times electrical conductivity data from the upstream groundwater station was scaled in relation to upstream surface water conductivity to exaggerate changes in conductivity and to allow for easy interpretation of systematic changes between stations. Data were initially normalized to the first conductivity data point (78µS/cm) from the upstream surface water gauging station and then exaggerated by a factor of 20. The scaled conductivity is given by Equation 6.2.

$$EC_S = (20 + 78\mu S/cm) \times (GW_{EC} - 198\mu S/cm) \qquad (6.2)$$

Where:
EC_S = scaled upstream groundwater conductivity value (µS/cm)
20 = scaling factor (no units)
78µS/cm = initial upstream surface water conductivity value (JD021 at 0000h)
GW_{EC} = old upstream groundwater conductivity value
198µS/cm = initial upstream groundwater conductivity value

6.2.8 Mass balance calculations

Two simple mass balance calculations were employed in an attempt to quantify the interaction between surface and groundwater gauging stations. Similar mass balance methods have been used in the literature to separate storm flows into pre-event, event, soil and groundwater components (e.g. Hooper *et al.,* 1990; Mulholland, 1993; Laudon and Slaymaker, 1997).

The first of such calculations aimed to quantify the average daily river recharge (Q_r) provided to the upstream groundwater station by determining the loss of surface water between the GWRC Mangatarere Gorge monitoring station (Q_m) and the upstream surface water gauging station (Q_u) (Refer to Figure 6.2 for locations). Neglecting evaporation and water abstraction for consumptive use, which were deemed minimal, it was assumed that discharge (m^3/s) lost between these two stations was due to recharge of the underlying aquifer. The following equation was used to determine river recharge (Equation 6.3).

$$Q_r = Q_m - Q_u \qquad (6.3)$$

Where:
Q_r = recharge to upstream groundwater station (m^3/s)
Q_m = Mangatarere at Gorge discharge (m^3/s)
Q_u = upstream gauging station discharge (m^3/s)

Average daily discharge measurements were determined at both stations using average daily water stage (x) and a stage-discharge rating curve ($y = 6.5967x^{3.3547}$). This rating curve was determined for the Mangatarere at Gorge station (using interpolated GWRC data) and was deemed applicable to the upstream surface water gauging station due to cross sectional and environmental similarities (e.g. vegetation, stream bed sediment roughness and size) between the sites. Further, no major tributary inputs are present in the *ca.* 2km reach between the two gauging locations. Stage-discharge rating curves are commonly used to determine discharge (e.g. Orwin and Smart, 2004, Riihimaki *et al.,* 2005) as they overcome the practical dilemmas of sourcing continuous discharge measurements. The associate rating curve and the data used to determine it are graphically presented in Appendix G. Error estimates of ±15 and ±20% were placed on predicted discharge measurements from the Mangatarere at Gorge and upstream surface water station respectively. The higher error at the upstream surface water site reflects the application of a foreign rating curve to this site.

A second mass balance calculation was employed to quantify the proportion of daily base flow (GW_b) provided to the downstream surface water gauging station by groundwater sources. This model incorporated the parameter conductivity and assumed changes in average daily downstream surface water conductivity (EC_d) and discharge (Q_d) were due to changes in discharge and conductivity at the upstream

surface water gauging station (Q_{su} and EC_{su}) and the input of base flow of a known conductivity from the upstream groundwater gauging station (GW_b and EC_{gw}). The calculation is presented in Equation 6.4 and Figure 6.10. Upstream groundwater conductivity data were used to represent the downstream groundwater station as measurements were not available from this site due to the loss of power. Further, a lack of downstream surface water data during the period JD324-345 resulting in this period being excluded from the calculation.

$$GW_b = \frac{(Q_{su} \times EC_{su}) + (Q_d \times EC_d)}{EC_{gw}} \quad (6.4)$$

Where:
GW_b = groundwater input to downstream surface water station (m^3/s)
Q_{su} = Upstream surface water discharge (m^3/s)
EC_{su} = Upstream surface water conductivity (µS/cm)
Q_d = Downstream surface water discharge (m^3/s)
EC_d = Downstream surface water conductivity (µS/cm)
EC_{gw} = Downstream groundwater conductivity (µS/cm)

Daily discharge measurements were determined at the upstream gauging station using the Mangatarere Gorge stage-discharge rating curve equation ($Q_{su} = 6.5967x^{3.3547}$) while a separate rating equation ($Q_d = 9.2531x^{3.0892}$) was determined for the downstream gauging station using data provided by the GWRC. The upstream and downstream rating curves are presented in Appendix G. A number of assumptions were made for these calculations. These include:

- The application of the Mangatarere at Gorge discharge rating curves to the upstream surface water gauging station is sufficient.
- Upstream groundwater data can be used as a surrogate for the downstream groundwater gauging station. This is based on the assumption that both gauging stations are within the Carterton sub-regional flow system and respond in a similar manner.
- It is assumed that no additional input of water from tributary streams occurs along the *ca.* 10km reach between the upstream and downstream gauging locations. This assumption is flawed with several streams present (Figure 6.1), however input from these streams is deemed minimal over the period of interest, so is unlikely to influence the overall findings from these calculations.

This is formulated on the assumption, based on discharge data (Table 6.1), that inputs to the Mangatarere from these ephemeral streams during summer base flow conditions are extremely low (<0.1 m^3/s). However, it must be noted that these tributaries may contribute waters during large flow events when they become active. The extent of this input cannot be quantified as these catchments are largely ungauged during such events. It must also be noted that the total downstream gauging catchment (130km^2) is 60% larger than the upstream surface water gauging station catchment (52km^2) due to the Enaki (*ca.* 32km^2) and Kaipatangata (*ca.* 23km^2) stream catchments that it encompasses.

- Outputs from evaporation, plant uptake and water abstraction for consumptive use are deemed minimal.
- Direct inputs from precipitation are deemed minimal.

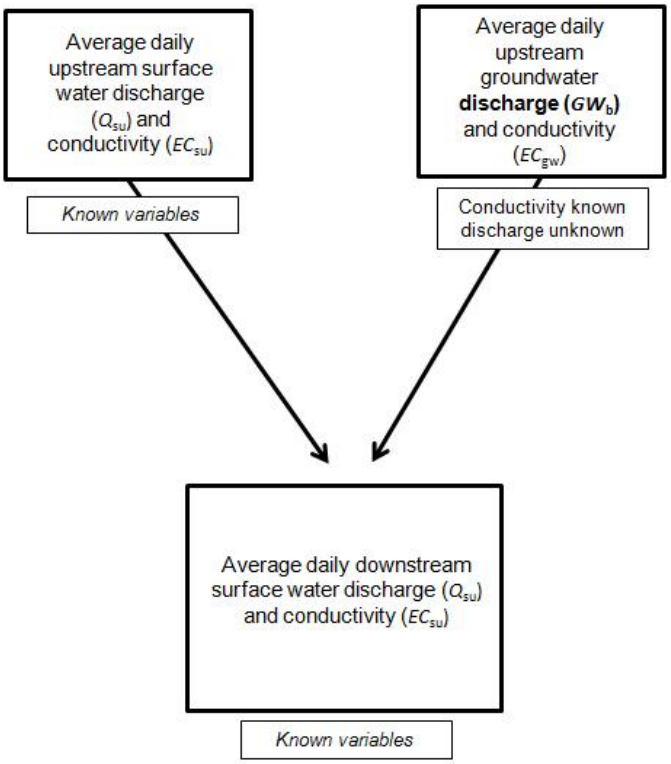

$$GW_b = \frac{(Q_{su} \times EC_{su}) + (Q_d \times EC_d)}{EC_{gw}}$$

Figure 6.10. Schematic representation of the chemical mass balance calculation employed to determine groundwater base flow inputs to the downstream surface water gauging station. The assumption is made that upstream and downstream surface and groundwater discharge determine downstream surface water discharge. Unknown variables, in this case the m^3/s of base flow provided by the upstream groundwater station to downstream surface water, is presented in bold. Discharge values are presented as m^3/s while conductivity is µS/cm.

6.3 High resolution time series analysis and results

Time series data of precipitation, air and water temperature, water stage and electrical conductivity (EC) from the upstream and downstream surface water monitoring stations and upstream groundwater monitoring station are presented in Figures 6.11-6.15. Figures 6.11-6.12 and 6.14-6.15 present data from across the entire study period (JD324-051), while Figure 6.13 concerns the one week period in which the hydrochemical sampling programme was undertaken (JD020-032). Data are presented at 15 minute intervals at both upstream gauging stations and one hour intervals at the downstream surface water gauging station. This one hour downstream sampling timeframe was the result of a misunderstanding with the GWRC in regards to the sampling frequency required at the downstream surface water station. Equipment failure resulted in the loss of all data at the downstream groundwater station, while significant data gaps are present at the downstream surface water station due to an erratic power supply. Precipitation values are presented as a total millimeter (mm) volume per day to overcome the Harvest SPE-02 telemetry unit's erratic recording interval. Further information surrounding these recording interval issues is presented in Section 6.7. Raw conductivity, water stage and temperature data were post processed using a smoothing filter to remove instrumentation noise and high frequency oscillations (see Section 6.2.5 for further details). All data are presented on a 15 min axis at their appropriate intervals.

6.3.1 Precipitation

Precipitation occurred during 39 days of the 94 day study period with significant events (>20mm/day) experienced on JD332, 335, 346, 022, 023 and 027 (Figure 6.11). High magnitude precipitation events were experienced on JD346, 022 and 023 in which 41, 54 and 34mm of rain were recorded each day respectively. These events all coincided with stage increases at both surface water gauging stations and groundwater stage increases were apparent in response to events on JD335, 346 and 022-023. The lack of groundwater response during these other events is likely due to low antecedent soil moisture conditions that resulted in precipitation filling the residual holding capacity of soil without additional drainage to the water table. Dry periods, in which little or no precipitation was experienced (< 10mm/week), occurred during JD324-332, 337-345, 347-365 and 034-044.

These dry periods are likely to have reduced soil moisture conditions allowing increased infiltration of precipitation. January 2010 (JD001-031) was the wettest (225mm) of the three months in which monitoring was undertaken (Table 6.6).

Table 6.6. Total precipitation and mean monthly air and water temperatures for the upstream ground and surface water gauging stations and downstream surface water gauging station. Mean monthly air temperature data are sourced from the upstream surface water gauging station, while precipitation data are sourced from Reid's Piggery (40°58'36.30"S, 175°31'44.14"E). The piggery is located closer to the upstream gauging stations (Figure 6.6). Data are not available from the downstream surface water station for the period November 2009 due to equipment malfunction.

Site	Nov 2009 mean (°C)	Dec 2009 mean (°C)	Jan 2010 mean (°C)	Feb 2010 mean (°C)
Air temp	15.6	15.8	16.7	17.4
Upstream GW	12.6	12.8	13.0	13.3
Upstream SW	15.8	15.8	17.0	17.4
Downstream SW	-	16.3	16.8	17.3
Total precipitation	38mm	110mm	225mm	43mm

6.3.2 Air and water temperatures

Air temperature measurements were obtained from the upstream surface water gauging station, and as expected, showed a clear diurnal pattern in which temperature decreased several degrees during the night (Figure 6.12). Air temperatures ranged between 6-27 °C for the study period (JD324-051) and on average warmer temperatures were experienced as the study period progressed. This is indicated by the progressive increase in mean monthly air temperature from November 2009 (15.6 °C) to February 2010 (17.4 °C) as presented in Table 6.6.

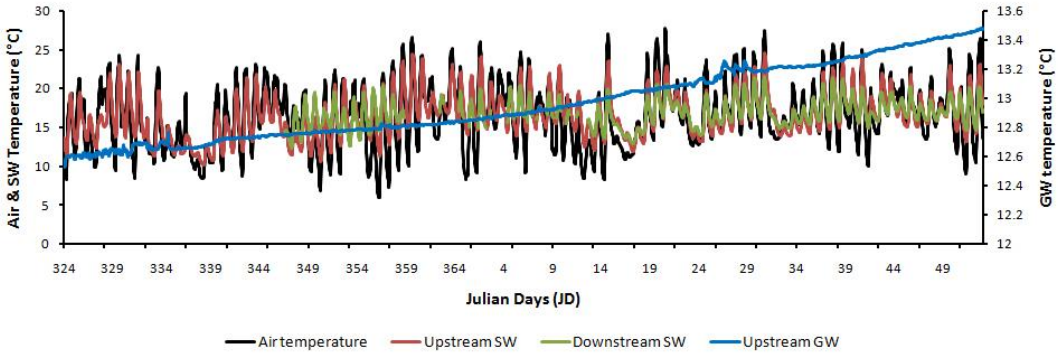

Figure 6.12. Temporal variations in air temperature, upstream surface (SW) and groundwater (GW) temperature and downstream surface water temperature, Mangatarere stream catchment, JD324-051. Air temperature was sourced from the upstream surface water gauging station and all data values are presented as one hour measurements. *Note:* Upstream groundwater temperatures are presented on the secondary axis.

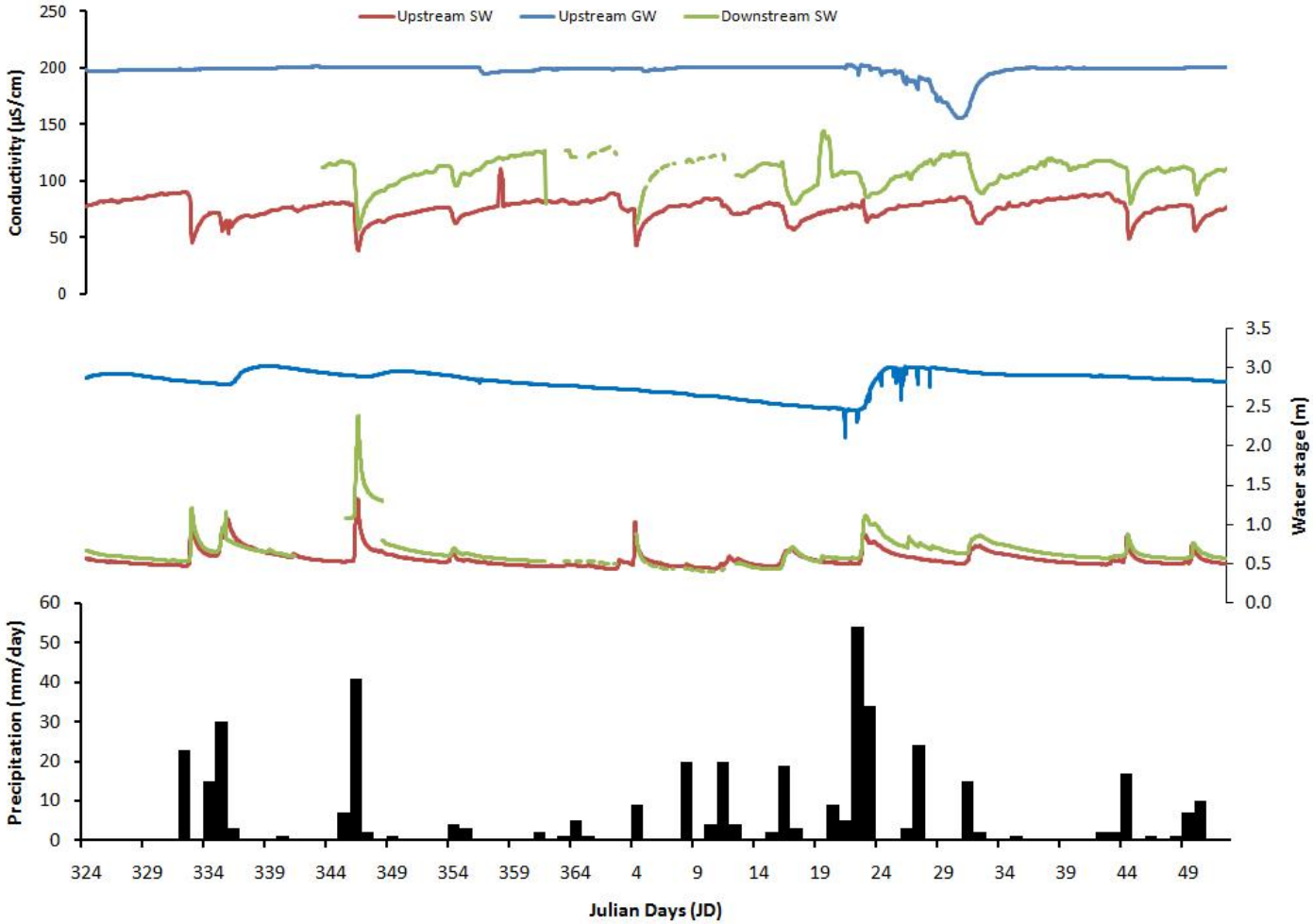

Figure 6.11. Time series data for total daily precipitation, water stage and electrical conductivity for the upstream surface (SW) and groundwater (GW) gauging stations and downstream surface water (SW) gauging station, Mangatarere stream, Wairarapa valley, New Zealand JD324-051. Water stage and conductivity data are presented as 15 minute measurements while precipitation is total mm per day.

The upstream groundwater gauging station showed a consistent increase in water temperature (12.4 °C to 13.5 °C) during the study period JD323-051. This increase is to be expected as groundwater temperatures generally vary according to long term mean air temperature (Brunke and Gonser, 1997). This statement is supported by the 1.8 °C increase in average monthly air temperature as the study period progressed (Table 6.6). Upstream and downstream surface water temperatures followed a similar diurnal pattern to that of air temperature, however diurnal variations were dampened at the downstream surface water site (downstream range 12-22 °C, upstream range 10-25 °C). Both surface water sites experienced an overall increase in water temperature as the study period progressed (1.6 °C upstream and 1 °C downstream November 09-Febuary 10) with mean water temperatures slightly colder downstream during the months of January and February 2010 (Table 6.6). This reduced downstream thermal signature suggests effluent conditions at the downstream surface water site in which a greater proportion of downstream base flow is provided by consistently cooler groundwaters. Meteorological energy inputs are subdued as advective inputs of groundwater are enhanced (O' Driscoll and DeWalle, 2006). If downstream surface water temperatures were dominated by upstream surface water inputs and solar radiation alone it would be likely these waters would be warmer due to additional solar heating as the waters travel across the valley. This dampening of diurnal water temperatures in response to groundwater inputs has also been reported by Constanz (1998) in a small alpine stream in the Colorado Rockies. Although downstream groundwater temperature data are not available, it can be assumed based on upstream groundwater data and examples from the literature (e.g. Constanz, 1998; Silliman and Booth, 1993; O' Driscoll and DeWalle, 2006), that these downstream groundwaters would also be substantially colder and display a more consistent temperature.

It must be noted that the banks immediately surrounding the downstream surface water station are heavily vegetated and may therefore have experienced reduced incoming solar radiation. This may have contributed to the colder downstream surface water temperatures. However, this shading effect is deemed insignificant as the *ca.* 10km reach between the upstream and downstream gauging stations is relatively open and exposed to solar radiation.

Slight fluctuations (*ca.* 0.2 °C) in groundwater temperature occurred during JD324-335 and JD021-028 (Figure 6.12). The first of these fluctuations on JD024-035 were erratic and therefore likely is a result of instrumentation noise following the initial installation of the CS547A temperature and conductivity probes. Fluctuations experienced during JD021-026 are the result of the hydrochemical sampling programme in which the CS547A probe was removed from the water column for *ca.* 15 minutes each day.

On JD026-028 upstream groundwater temperature displayed a weak diurnal pattern increasing *ca.* 0.1-0.2 °C during the day (Figures 6.12 and 6.13). This diurnal pattern was not experienced at any other time during the study and occurred concurrently with diurnal patterns in air and surface water temperatures. This suggests the transfer of diurnal temperature changes from the Mangatarere stream to the upstream groundwater aquifer and indicates a potential hydraulic link between the two systems during this three day period. The overall warming or cooling of groundwater temperatures in response to river recharge has been documented in the literature (e.g. Silliman and Booth, 1993; Constanz, 1998), however river recharge is not known to create diurnal patterns in groundwater temperature. Another explanation for this diurnal phenomenon is reported by Duque *et al.* (2010). This research suggests groundwaters may display a similar pattern to that of air temperature as the water table approaches the land surface and is influenced by radiant energy from the sun. It is unlikely this air temperature response is applicable for this current situation, as upstream groundwater temperatures did not show a diurnal response during other periods of the study when the distance between the water table and ground surface was similar (e.g. JD337-339) (Figure 6.11). Further, the conductive transport of heat from the atmosphere through the soil zone would have been heavily reduced by the presence of pastoral grass on the ground surface and the various layers of sand and silt which display low thermal conductance values (Baver, 1940; Campbell, 1985).

6.3.3 Ground and surface water stage

In order to assess potential changes in ground and surface water quantity, and infer interaction based on these changes, water stage was assessed from the upstream gauging stations and downstream surface water station in Figures 6.11 and 6.13-6.14. The assumption was made that if water stage increased at a particular gauging station that this increase would suggest the quantity of water at this station was also increasing. For example if upstream surface water stage increased one would assume upstream surface water discharge also increased.

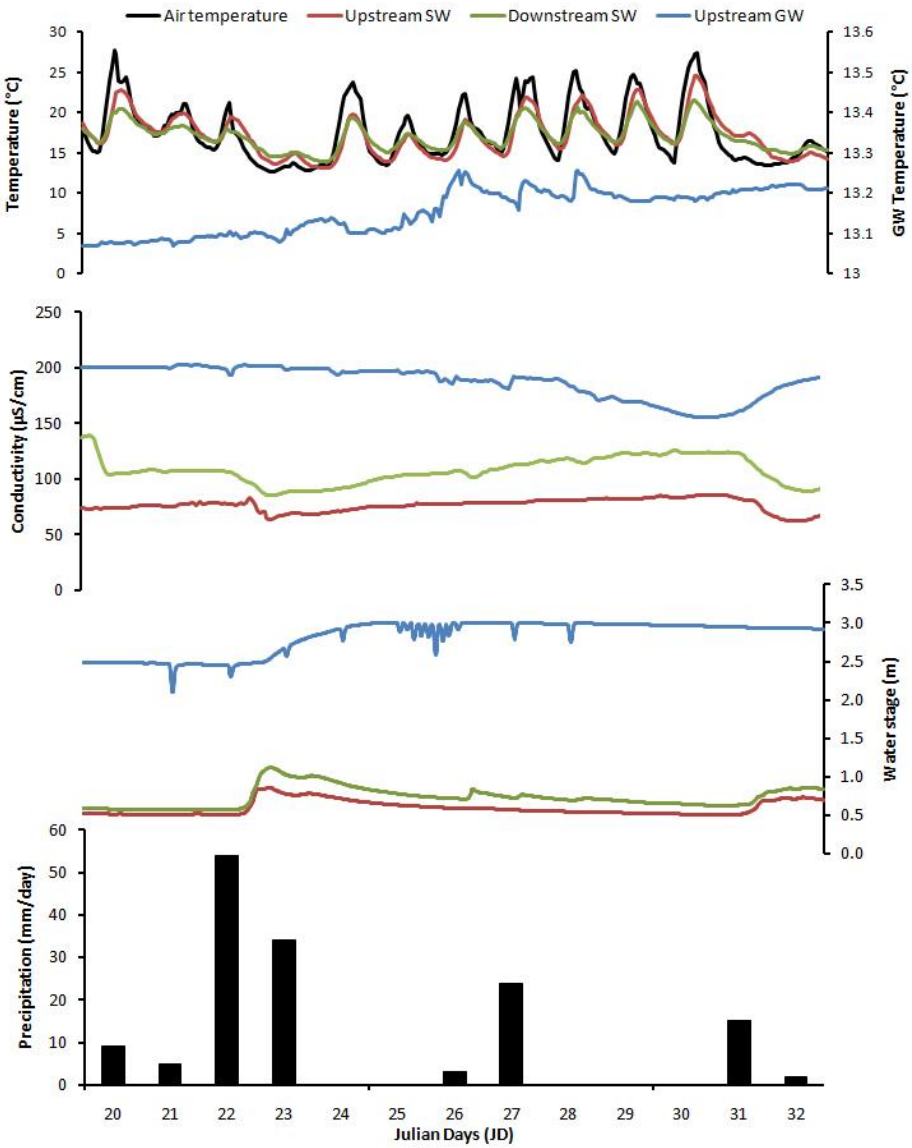

Figure 6.13. Time series data for total daily precipitation, water stage, electrical conductivity and air and water temperature for the upstream surface and groundwater gauging stations and downstream surface water gauging station, Mangatarere stream, Wairarapa valley, New Zealand JD020-032. Air temperature data were sourced from the upstream surface water gauging station. Water stage and conductivity data are presented as 15 minute measurements while precipitation is total mm per day.

A number of major stage increases occurred during the study period and were experienced at both surface water gauging stations (Figure 6.11). These events were concurrent with precipitation events and can be classified according to their magnitude. Major stage increases (> 40cm) occurred at both the upstream and downstream surface water gauging stations on JD332, 335, 346, 005 and 023 while less significant increases (< 40cm) occurred on JD 354, 012, 017, 032, 045 and 050. The extent to which precipitation affected river stage differed throughout the study period with significant precipitation events on JD008 and 011 initiating little surface water stage response. Further, the largest increase in upstream and downstream surface stage (JD336) did not coincide with the highest intensity precipitation period (JD020-024) in which 102mm of rainfall was experienced over four days. These differences in stage response suggest significant spatial variability in rainfall distribution within the Wairarapa valley (Figure 3.8) and/or temporal variations in catchment soil moisture conditions (Jenkins *et al.,* 1994).

Clear differences in river stage are present between the upstream and downstream gauging stations with downstream stage *ca.* 10cm higher for the majority of the study period (Figure 6.11). This stage difference suggests increased flow at the downstream gauging station and is likely due to the larger downstream catchment area (*ca.* 130km² including the *ca.* 53km² upstream gauging station catchment) and possible groundwaters influxes to the downstream surface water site. This surface water stage difference increased to *ca.* 20cm following the storm event experienced on JD021-024 as the downstream receding flood limb responded to precipitation on JD 027 and therefore required more time to return to base flow conditions (Figure 6.13). The extension of this receding limb is likely a result of the downstream gauging station's larger catchment area and therefore a delayed input of precipitation, subsurface and overland flow waters (Jenkins *et al.,* 1994).

During the period JD004-018 downstream surface water stage dropped *ca.* 10cm below that recorded upstream suggesting a loss of river flow at the downstream surface water gauging station (Figure 6.11). Surface water temperature data discussed earlier (Section 6.3.2) suggest effluent conditions at the downstream surface water site, therefore, it is likely this reduction in downstream stage is due to reduced base flow provision from the groundwater system.

This hypothesis is supported by upstream groundwater stage data that showed an overall decrease to its lowest levels (*ca.* 2.5m) during this period (JD004-018). As the upstream and downstream groundwater gauging stations are both within the larger Carterton sub-regional flow system it is almost certain downstream groundwater stage would also have declined to low levels, leading to a reduction in groundwater hydraulic head and the provision of base flow to the downstream surface water site. Further, the downstream surface water site may have provided recharge to the downstream groundwater system as groundwater levels were reduced leading to a reduction in downstream surface flow. As noted by Lewandowski and Nutzmass (2008) and Schmalz *et al.* (2007) surface and groundwater interaction can switch from effluent to influent as surface water stage rises above that of groundwater in response to storm events. It is hard to confirm the presence of influent downstream conditions without consistent downstream groundwater stage data.

Upstream groundwater stage appeared to decrease for the majority of the study period as shown in Figure 6.11. This decrease was offset at times by various recharge events that led to stage increases on JD335-339 (*ca.* 25cm), 348-350 (*ca.* 15cm) and 021-025 (*ca.* 60cm). Increases in groundwater stage occurred concurrently with major precipitation events and surface water stage increases. Further, they displayed a gradual rising limb in which stage increased slowly over several days. This indicates a buffer effect in which infiltrating waters take several days to percolate or to move new and old waters from the vadose zone to the water table. Similar delayed infiltration responses are reported by many authors (e.g. Dahan *et al.*, 2008 and Lu *et al.*, 2010) in regards to rainfall recharged groundwater systems. Groundwater stage did not always respond to precipitation with significant events (20mm/day) on JD008, 011, 016 and 044 having little influence on stage. The inability of these events to initiate groundwater stage response is likely due to high rates of evapotranspiration and low soil moisture conditions, a subsequent result of the low precipitation and warm air temperatures in the weeks prior (JD348-007). High intensity precipitation on JD 022 and 023 (54 and 33mm/day respectively) led to a substantial and almost immediate increase in groundwater stage (*ca.* 60cm) (Figures 6.11-6.12 and 6.14c).

It can be assumed the nine precipitation events (total 86mm) experienced during JD008-021 satisfied deficit soil moisture conditions, allowing field capacity to be reached and infiltration to recharge the groundwater system initiating an increase in stage.

Fluctuations and patterns in ground and surface water stage appeared to show some correlation. Major increases in upstream groundwater stage (JD 336-338, 350-353 and 021-025) coincided with similar increases at both surface water stations. However, increases in groundwater stage were more subdued and experienced longer receding limbs. These concurrent ground and surface water stage increases may indicate recharge of the groundwater system from the Mangatarere River. This is based on the theory that as surface water stage increases water may move through the stream bed to underlying groundwater systems resulting in a subsequent increase in groundwater stage. This is a relatively common phenomenon and is extensively documented in the literature (e.g. Dahan *et al.,* 2008; Schmalz *et al.,* 2007; Winter *et al.,* 2008), however it is hard to support this hypothesis based on water stage data alone. As identified earlier the presence of a diurnal air temperature pattern at the upstream surface water gauging station on JD026-028 suggests the transfer of stream waters to the groundwater system (Section 6.3.2). However, this diurnal groundwater pattern was not experienced at any other period of the study. This suggests, despite these three concurrent ground and surface water stage increases, that significant interaction between the upstream gauging stations was only occurring during the period JD026-028.

Research by Dahan *et al.* (2008) emphasizes the duration of peak flows as an important factor that determines river recharge flux to groundwater bodies. Therefore, in order to gain further insight into the potential ground and surface water interaction during these three events an analysis of storm hydrographs was undertaken (Figure 6.14). During the two events on JD334-340 (Figure 6.14a) and JD345-350 (Figure 6.14b) surface water stage showed a rapid response to rainfall as indicated by a sharp rising limb and relatively short falling limbs as water was quickly removed from the catchment.

The increase in groundwater stage during these two events was slightly delayed, suggesting slow infiltration of precipitation through the soil-water zone or recharge from far away sources such as the Mangatarere stream. In contrast, groundwater stage showed an almost immediate response to either precipitation or surface water stage during the event on JD022-027 (Figure 6.14c) suggesting initial high soil moisture conditions. Further, surface waters displayed a gradual and extended falling limb that incorporated the two day period in which the diurnal water temperature fluctuation was detectable at the upstream groundwater station. This suggests, as noted by Dahan *et al.* (2008), that an extended high duration flow event may be needed to initiate river recharge to the upstream groundwater station and that interaction may occur in the days following peak flows when surface water stage is reduced (e.g. JD026-028).

Although an increase in surface water stage may have increased upstream groundwater stage on JD022-028, this hypothesis holds little merit for the remainder of the study period in which increases in surface water stage on JD003, 004, 012, 017, 031, 034 and 050 did not initiate noticeable groundwater stage response. In general during these events groundwater stage was decreasing. This indicates that groundwater stage is dependent or influenced by other processes besides changes in surface water stage and/or the need for longer or higher magnitude surface water flow events to initiate surface water recharge. Both explanations seem plausible as similar magnitude increases in surface water stage (*ca.* 50cm) on JD332, 335 and 004 only resulted in a groundwater stage increase on JD335. Antecedent soil moisture conditions may explain this discrepancy in groundwater stage response with low soil moisture able to buffer against changes in groundwater stage (Cey *et al.,* 1998; Dahan *et al.,* 1998). Unfortunately soil moisture conditions and evaporation rates were not monitored, however inferences can be made using air temperature and precipitation data. It is likely soil moisture conditions were low during these events (JD332 and 004) due to the absence of significant rain in the days and/or weeks prior. Combined with the warm air temperatures experienced during the study period soil moisture conditions would likely have been low.

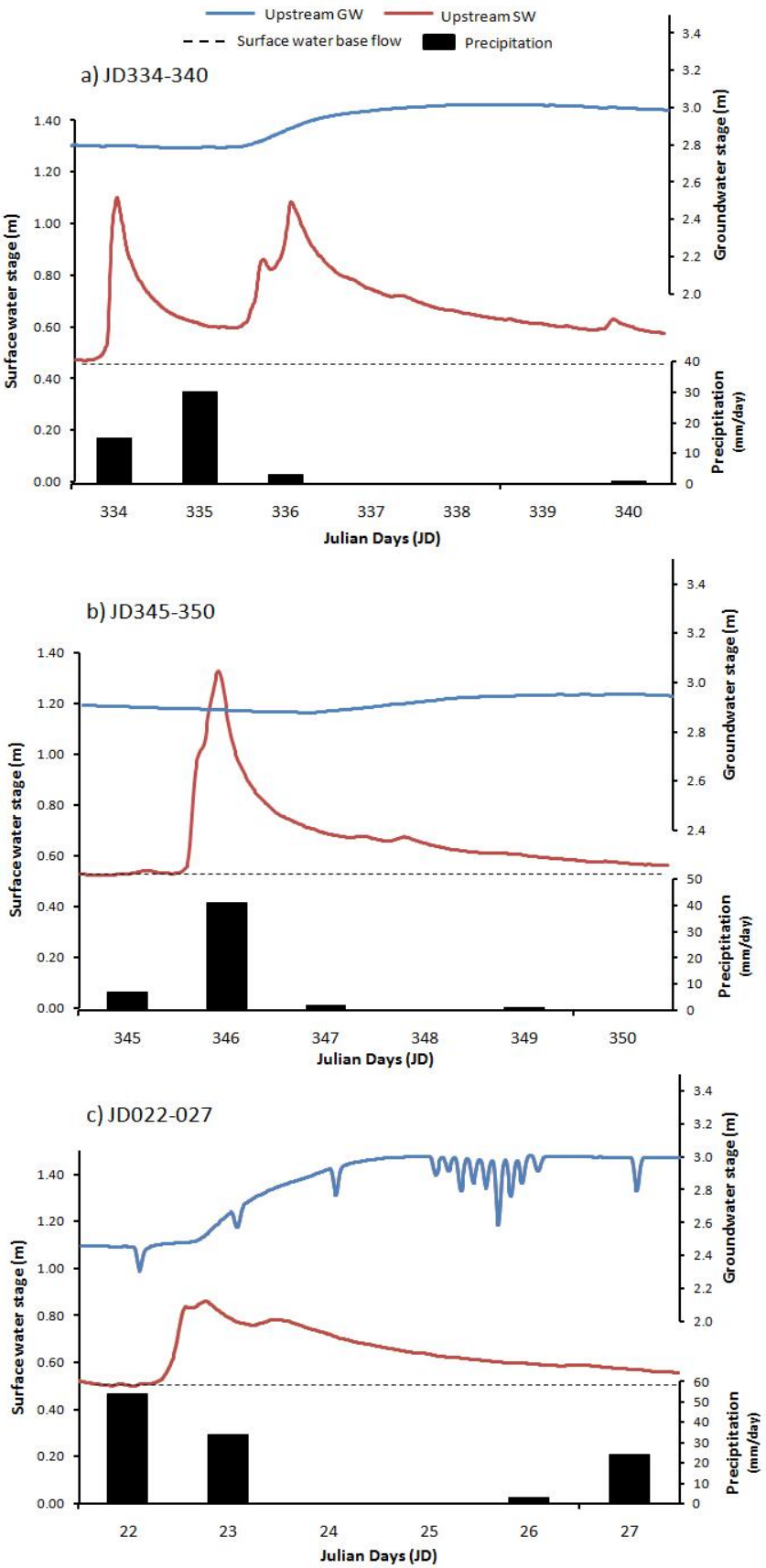

Figure 6.14. Storm hydrographs from selected upstream surface water events and concurrent groundwater stage response JD334-340 (**a**), 345-350 (**b**) and JD022-027 (**c**). Dotted horizontal line denotes approximate base flow conditions prior to the surface water stage response. Stage data are presented at 15 minute intervals, while precipitation data are presented as a daily total (mm/day).

6.3.4 Electrical conductivity

In order to assess the potential chemical interaction between ground and surface water stations, electrical conductivity data were assessed in Figures 6.11 and 6.13. The assumption was made that parallel changes in conductivity between the stations may indicate potential interaction. Scaled conductivity data from the upstream groundwater gauging station are also presented in Figure 6.15 to exaggerate changes in conductivity and allow for an easier interpretation of systematic changes.

It appears a proportion of downstream surface water base flow is provided by solute rich groundwaters as indicated by higher average downstream surface water conductivity (*ca.* 100-110 µS/cm) (Oxtobee and Novakowski, 2002). Conductivity at the upstream surface water station averaged 80µS/cm over the study period, while upstream groundwater conductivity averaged 198 µS/cm (Figure 6.11). The presence of effluent conditions at the downstream Mangatarere stream has already been inferred through water temperature and surface water stage data presented in Figures 6.11 and 6.12. Further sources of solutes, besides groundwater input, to the downstream surface water gauging station may include mineral dissolution and the input of point and non-point contaminants as the Mangatarere flows from the upstream to downstream stations (Figure 6.6). These inputs will be discussed further in Section 6.4.

Conductivity at the upstream and downstream surface water sites appeared to follow a similar pattern and experienced numerous concurrent dilution events. These events can be characterised according to their magnitude, with high magnitude dilution events (i.e. decrease in EC 40 µS/cm) experienced upstream on JD 332, 346, 005 and 045 and downstream on JD 346, 005, 016, 032 and 045. Small to mid magnitude events were experienced at either site on JD336, 354, 011, 023 and 050, when conductivity decreased by 10-30 µS/cm. The magnitude of dilution between the upstream and downstream surface water stations varies (e.g. 20 µS/cm decrease upstream and 40 µS/cm decrease downstream for JD032 event), however they generally follow a similar pattern.

During the majority of high flow events downstream surface water conductivity remains higher than that recorded upstream, suggesting that a high proportion of downstream storm flows are provided by solute rich groundwaters. An exception to this occurred on JD346 when both upstream and downstream conductivity decreased to *ca.* 40 µS/cm. It is likely the extremely high downstream surface water stage (*ca.* 2.5 m) during this event shifted the hydraulic gradient between the downstream surface and groundwaters severely reducing groundwater inputs to the downstream section of the Mangatarere. Following dilution events downstream conductivity tends to return to base levels faster than upstream indicating that the majority of runoff following the initial peak flow is provided by solute rich waters such as groundwater base flow (Oxtobee and Navakowski, 2002). All surface water dilution events coincided with increases in stream stage and precipitation and indicate a greater volume of low solute water in the river systems. The magnitude of dilution was largely proportional to changes in stage with peak stage events concurrent with high magnitude dilution events (e.g. JD 346, 332, 335 and 044).

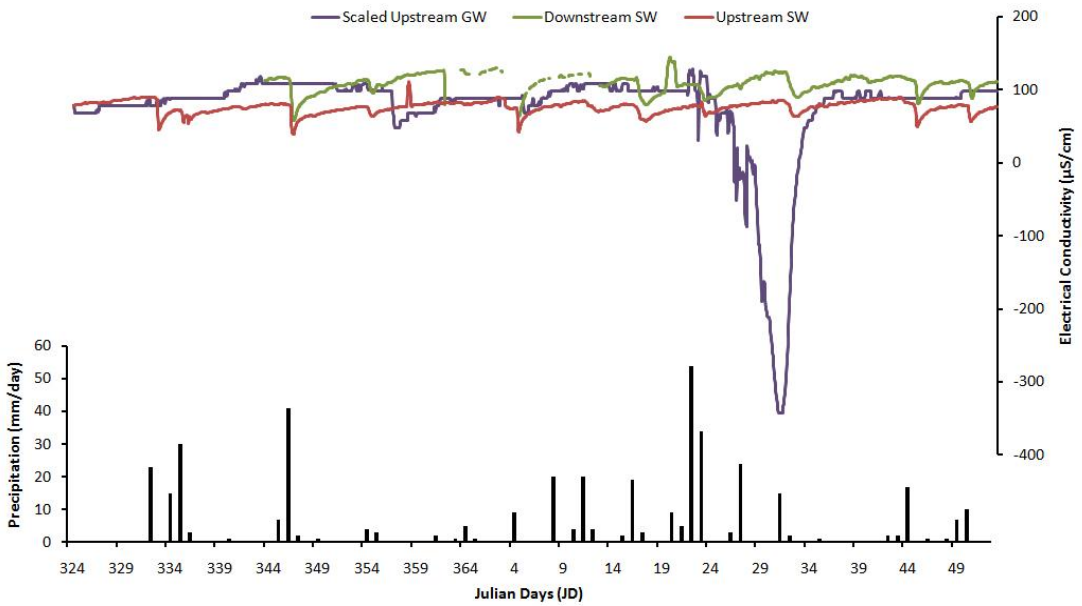

Figure 6.15. Scaled upstream groundwater conductivity time series data and normal upstream surface water and downstream surface water conductivity data, Mangatarere stream, JD324-052. Total daily precipitation data (mm/day) are also shown. Upstream groundwater data were scaled by a factor of 20 (Section 4.4.5) to exaggerate changes in conductivity in relation to the magnitude of change experienced at the upstream surface water gauging station.

Upstream groundwater conductivity remained relatively consistent for the duration of the study period (*ca.* 198 µS/cm). Three dilution events were experienced on JD356, 005 and 021-030 in which conductivity decreased *ca.* 5 µS/cm for the first two events and 50µS/cm for the last event (Figure 6.11). These dilution events occurred concurrently with increases in precipitation and during or slightly after increases in surface water stage. However, the extent to which precipitation and surface water stage affected groundwater dilution differed throughout the study period. For example, groundwater dilution events on JD357 and 004 occurred simultaneously with small precipitation events (*ca.* 5-10mm), while groundwater conductivity did not change during large precipitation events on JD 332-336 and 345. Further, significant upstream surface water dilution events on JD 332, 346, 045 and 050 did not coincide with changes in groundwater conductivity. This suggests, although these dilution events between ground and surface water may be linked, it is likely other parameters such as soil moisture conditions and the concentration of solutes within the vadose zone are influencing groundwater conductivity. The three dilution events will be explored in further detail below.

The first of these events on JD356 coincided with a minor groundwater stage decrease that occurred in response to well purging for hydrochemical sampling (Figure 6.11). This is likely to have caused a reduction in conductivity as more dilute waters from within the aquifer were drawn into the well casing to replace those extracted. This explanation seems plausible and is supported by the works of Wilson and Rouse (1983) and Reilly and Gibs (1993) who noted that concentrations of chemical constituents within a groundwater well can change during sample collection. However, groundwater conductivity took five days to return to base levels suggesting input of dilute waters continued for several days or the slow transport of solutes into the well casing through advection, dispersion and diffusion.

The second groundwater dilution event (JD005) followed 10mm of precipitation and a subsequent upstream surface water stage and conductivity responses on JD004 (*ca.* 40cm stage increase and 50µS/cm conductivity decrease). This suggests the decrease in groundwater conductivity may have been due to the 10mm input of infiltrating precipitation or potential recharge from the dilute upstream surface water station as surface water stage increased.

However, as groundwater stage showed a gradual and consistent decline during this period it suggests an influx of new water to the groundwater system did not occur. One would expect groundwater stage would increase if local or regional recharge was occurring (Freeze and Cherry, 1979; Winter *et al.*, 1998). Instead this decrease in conductivity may have been a manifestation of instrumentation error. Conductivity data were initially recorded as an mS/cm value and later converted to µS/cm (see section 6.2.2 for further details). This conversion may have exaggerated this change in conductivity which would have been a recorded as a 0.005 mS/cm change. This 0.005 mS/cm change falls within the ±10% accuracy values of the CS547A probe and therefore this change in conductivity may be an instrumentation error. Air and water temperature data offers little further insight into potential recharge mechanisms during this period.

A major extended dilution event also occurred at the upstream groundwater station from JD 021-031 in which conductivity gradually decreased from 200 µS/cm to 150 µS/cm (Figures 6.11 and 6.13). Upstream groundwater stage displayed a relatively fast response during this period, increasing from 2.5m to 3m over two days (JD023-024). This fast groundwater response indicates initial high soil moisture conditions and suggests recharging waters came from a relatively close distance such as local recharge from precipitation. This seems plausible as 102mm of precipitation was experienced during the period that could percolate through the vadose zone and provide dilute recharge waters to the water table. However, it is also possible this groundwater stage increase and the subsequent decrease in conductivity were caused by an input of dilute waters from the Mangatarere stream as surface water stage increased. This latter hypothesis is further supported by the upstream groundwater site displaying a weak diurnal temperature (*ca.* 0.1 °C) on JD026-028 and the magnitude of the groundwater stage increase. It is unlikely this *ca.* 50cm stage increase could be achieved by the 102mm (*ca.* 10cm) of precipitation experienced during this week, in particular as some precipitation would have been lost to surface runoff and evapotranspiration. Although antecedent soil moisture may have contributed some water to the water table it is unlikely, based on soil porosity (*ca.* 0.25-0.5 for silty gravels), that the holding capacity of the soil would allow water of such a quantity (*ca.* 40cm) to be provided. Therefore, it is likely water came from another source such as the Mangatarere stream.

However, as this diurnal temperature pattern only occurs on JD026-028 it suggests this interaction may not have occurred until these dates. Therefore, it may be possible that during JD021-030 the upstream groundwater gauging station received recharge from both precipitation and the Mangatarere stream.

Upstream groundwater conductivity fluctuated slightly throughout the ten day dilution period, with small (*ca.* 5-10 µS/cm) increases and decreases in conductivity detected (Figures 6.11 and 6.13). These fluctuations occurred in response to the hydrochemical sampling programme in which the upstream groundwater well was purged for several minutes prior to grab sampling. This purging resulted in an immediate decrease (*ca.* 5-35cm) in groundwater stage and a subsequent decrease (*ca.* 5-20 µS/cm) in conductivity. Both groundwater stage and conductivity readjusted themselves in the hour immediately following water extraction, indicating a quick response rate. This suggests although groundwater purging can influence the hydrological and hydrochemical properties of the upstream groundwater well, this influence is quickly counterbalanced by natural well processes. Therefore, it is unlikely groundwater purging influenced the chemical composition of the grab samples extracted during this week. It is assumed a similar stage and conductivity response to well purging would have occurred at the downstream groundwater station on JD021, 023 and 028 when samples were collected, however no data are available to confirm this. One must also consider that daily purging of the well for hydrochemical sampling may have influenced the magnitude of groundwater dilution (*ca.* 50 µS/cm) on JD022-30. This may be a similar phenomenon to that possibly experienced on JD356.

Significant increases in surface water conductivity upstream on JD358 (*ca.* 30 µS/cm increase) and downstream on JD019 (60 µS/cm increase) provide further evidence that the interaction between the Mangatarere stream and underlying groundwater systems shows considerable temporal variability (Figure 6.11). These events lasted *ca.* 12 and 23 hours respectively but did not result in changes to conductivity at the other gauging stations (surface or groundwater). This suggests interaction between the ground and surface water bodies is temporally variable or else these significant increases in conductivity would likely have been transferred through to the neighbouring groundwater body.

However, the magnitude and duration of these conductivity events may have been too small to be detected in the groundwater body. The length of these events suggests they are a real phenomenon (e.g. increased solute concentrations in the water column), rather than a result of instrumentation error or water temperature fluctuations. To further validate this statement the relationship between conductivity and water temperature during these two events was investigated as conductivity is known to show a positive correlation to temperature increases. The statistical correlation coefficients between the two parameters were weak (< 0.5) for both events, which suggest that these increases in conductivity were not caused by changes in water temperature. The resulting regression plots and statistical outputs are presented in Appendix H.

6.3.5 High resolution time series summary

From Figures 6.11-13 and 6.15 it appears fluctuations in groundwater conductivity and stage occurred in response to both precipitation and changes in surface water parameters. This suggests that the upstream groundwater site is recharged by two main mechanisms; rainfall recharge from infiltrating precipitation and river recharge or surface-groundwater interaction. From the current data presented it is difficult to differentiate between these two mechanisms as groundwater response occurs at the same time as both surface water stage increases and precipitation. Water temperature offered some insight into this potential interaction with the downstream surface water station displaying a dampened diurnal pattern suggesting input of cold groundwater sources. In contrast the upstream surface water station displayed a strong diurnal temperature that closely resembled air temperature suggesting influent conditions. Further, the upstream groundwater station displayed a weak diurnal temperature on JD026-028 which may indicate the transfer of upstream surface waters and its associated thermal regime to the upstream aquifer.

In order to gain further insight into the potential relationship between the variables depicted in Figures 6.11-6.14, data from the upstream surface and groundwater stations and total daily precipitation were subjected to the statistical technique Principal Components Analysis (PCA). Downstream data were excluded from this procedure due to the significant gaps in the data set.

PCA enables the simplification of large datasets by grouping data into components that explains variance in the original data set (Hagg and Westrich, 2002). These components can then be related to a set of know environmental processes (e.g. rainfall recharge). PCA results indicated moderate relationships (=0.5) between the ground and surface water parameters, but failed to offer additional insight into the relationship between parameters as depicted in Figures 6.11-6.15. This suggests that although these variables are related statistically in some way, this relationship is affected by other process and is temporally sensitive. Subsequent PCA results warrant little further discussion and are presented in Appendix I.

6.4 High resolution chemical sampling

To further investigate these recharge mechanisms and the potential interaction between ground and surface water stations detailed high resolution field data and hydrochemical grab samples obtained during the period JD021-028 were analysed. This period coincided with intense precipitation (JD022, 023 and 027) and subsequent responses at both surface and groundwater monitoring stations as presented in Figures 6.11 and 6.13. Hydrochemical grab samples were collected once daily at each site (at *ca.* 12:00-13:00) in order to investigate day-to-day variations in water chemistry and once every three hours over a 24 hour period (025-026) to investigate sub-daily variations. Sampling times are presented in Table 6.4.

The hydrochemical composition of water samples from the four gauging stations was assessed using average solute concentrations obtained from the eight days of hydrochemical sampling (Table 6.7). Average concentrations were deemed sufficient due to the small data range and the presence of no obvious outlier values or samples of unusually chemistry. Two rainfall samples were also collected during this period and are presented in Table 6.7. Water samples were analysed for 17 water quality parameters of which only some will be discussed here due to similarities across analytes. The remaining analytical results are presented in Appendix J. Solute concentrations varied across the four gauging stations and Na^+ was the only detectable ion of those measured in precipitation (0.065 mg/L). Similarities did exist between the ground and surface water sites with Na^+ and Ca^{2+} the dominant cations and HCO_3^- and Cl^- the dominant anions in solution (Table 6.7).

Table 6.7. Mean solute concentrations, pH and Total Dissolved Solids (TDS) for the upstream and downstream surface and groundwater stations and precipitation, Mangatarere stream catchment, Wairarapa valley, New Zealand, JD021-028. Number of observations (*n*) and standard deviations (in parentheses) are also presented. All solute values are presented as mean mg/L concentrations. Dash (-) indicates analyte was not tested. TDS column determined from the sum of main ions (Ca^{2+}, HCO_3^-, Cl^-, Mg^{2+}, K^+, Na^+ and SO_4^{2-}).

Location	***N***	**pH**	**TDS**	**HCO_3^-**	**Cl^-**	**Ca^{2+}**	**Mg^{2+}**	**K^+**	**Na^+**	**SO_4^{2-}**	**As**	**Fe^{2+}**	**Mn**	**P**	**NO_3^-**	**NH_4^+**
Upstream SW	15	7.3 (0.1)	49.9	24.8 (1.4)	8.6 (0.6)	4.3 (0.2)	1.4 (0.1)	0.8 (0.1)	7.2 (0.4)	2.8 (0.3)	<0.001 (0.000)	0.044 (0.029)	0.002 (0.001)	0.006 (0.001)	0.04 (0.02)	0.010 (0.001)
Upstream GW	15	7.2 (0.2)	128.2	72.6 (5.0)	11.9 (0.3)	12.27 (1.2)	5.7 (0.4)	1.2 (0.11)	14.8 (1.0)	9.7 (0.6)	<0.001 (0.000)	0.093 (0.049)	0.142 (0.019)	0.007 (0.003)	2.09 (0.45)	0.038 (0.015)
Downstream SW	15	7.2	65.7	31.0 (2.2)	10.7 (0.7)	6.2 (0.3)	2.0 0.2)	1.3 (0.1)	8.7 (0.6)	5.8 (0.6)	<0.001 (0.000)	0.054 (0.037)	0.003 (0.001)	0.072 (0.003)	0.48 (0.08)	0.100 (0.04)
Downstream GW	3	6.7 (0.2)	145.8	66.3 (2.9)	25.7 (0.6)	15.0 (1.7)	6.4 (0.4)	1.4 (0.2)	18.7 (1.2)	12.3 (1.2)	<0.001 (0.000)	3.400 (2.307)	0.036 (0.019)	0.069 (0.031)	2.60 (0.52)	0.095 (0.09)
Precipitation	2	-	-	-	<0.5	<0.05	<0.02	<0.05	0.065 (0.042)	<0.50	-	-	-	-	-	-

The dominance of these ions suggests precipitation derived Cl^- and Na^+ and the dissolution of carbonate and silicate minerals within the sedimentary and metamorphic lithology of the Mangatarere catchment (Schmalz, 1972). As the concentration of solutes in precipitation are extremely low, and only Na^+ was detected, it can be assumed the majority of these solutes are acquired through mineral dissolution. The upstream and downstream surface water sites shared a Na^+-Ca^{2+}-HCO_3^--Cl^- water type for the one week sampling period (Table 6.8), however downstream waters displayed slightly higher Na^+ relative to Ca^{2+} and higher Cl^- relative to HCO_3^- (Figure 6.16).

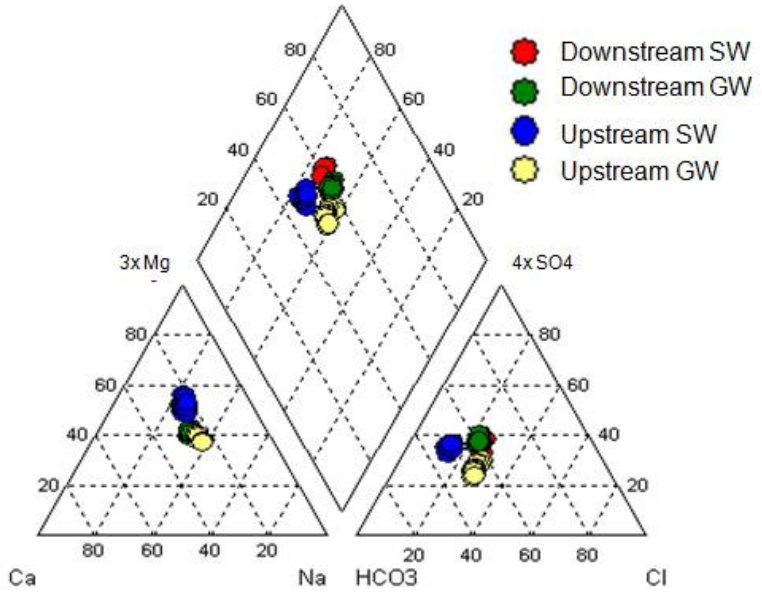

Figure 6.16. Piper diagram showing the variation of major ions (Ca^{2+}, Na^+, Mg^{2+}, Cl^-, HCO_3^-, SO_4^{2-} and Mg^{2+}) from the upstream and downstream surface and groundwater monitoring sites during the intensive hydrochemical sampling programme JD021-028. The left triangle presents major cations while the right presents major anions. The center diamond represents the projected position based on both triangles. *Note:* Mg^2 and SO_4^{2-} scales are exaggerated for ease of interpretation.

It appears the downstream surface water gauging station receives a significant proportion of base flow from neighbouring groundwaters as indicated by a higher TDS (49.9 mg/L upstream and 65.7 mg/L downstream) and elevated concentrations of NO_3^-, NH_4^+, Na^+ and Cl^- (Table 6.7 and Figures 6.17-6.19). These elements accumulate in the soil-water zone and are likely to have been transferred to the downstream surface water site by concentrated downstream rainfall-recharged groundwaters that provide base flow to this river system.

Similar results, in which a selection of these solutes (e.g. NO_3^- and Cl^-) are transferred to stream base flow, have been extensively documented in the literature by Burden (1982), Taylor *et al.* (1989) and Rozemeijer and Broers (2007). This hypothesis of effluent downstream surface waters conditions is further supported by the subdued downstream surface water temperature discussed earlier. If the downstream groundwater site was not providing base flow to the downstream surface water site or if this interaction was influent it would be assumed that downstream solute concentrations and TDS would more closely resemble those of the upstream surface water site. Other explanations for this increased downstream surface water TDS include similar groundwater base flow proportions but increased mineral dissolution and/or the input of point or non-point contaminants. Neither of these suggestions are particularly plausible as significant mineral dissolution is unlikely to have occurred in the short distance between the two gauging locations (*ca.* 10km) and the geology between the two gauging catchments is relatively uniform (Figure 3.11). Further, the increase in solutes is not ion specific as would be expected from point source inputs (e.g. only elevated P and NO_3^- as presented by Saffigna and Keeney, 1977).

A similar pattern in solute concentrations was apparent at the groundwater gauging stations with all downstream solutes elevated (Table 6.7). This is supported by groundwater TDS values which were 128.2 mg/L upstream and 145.8 mg/L downstream (Table 6.7). Elevated downstream solute concentrations likely reflect older, more chemically evolved groundwaters that have experienced longer rock:water contact periods and dissolution of minerals (Chebotarev, 1955). Further, the downstream groundwater site is likely a continuation of the upstream groundwater flow system as both are within the Carterton sub-regional flow system (Figure 6.1) which suggests upstream groundwaters would have travelled down valley to this site acquiring additional solutes through mineral dissolution and rainfall recharge. Concentrations of Mg^{2+} were higher at both the upstream and downstream gauging stations (5.7 mg/L and 6.4 mg/L respectively) in relation to those observed at the surface water sites and are likely acquired due to dissolution of subsurface carbonate minerals.

Table 6.8. Sample date, time, TDS, Cl^-/HCO_3^- and Ca^{2+}/Na^+ ratios and water type for the upstream and downstream surface and groundwater hydrochemical samples, Mangatarere stream catchment, JD021-028.

Location	Sample date & time	TDS	Cl/HCO_3	Ca/Na	Water type
Downstream SW	JD021 @ 11:00 am	67	2.82	0.74	Na-Ca-HCO3-Cl
	JD022 @ 12:00 pm	70	3.00	0.70	Na-Ca-HCO3-Cl
	JD023 @ 12:00 pm	56	2.83	0.77	Na-Ca-HCO3-Cl
	JD024 @ 12:00 pm	58	2.78	0.73	Na-Ca-HCO3-Cl
	JD025 @ 12:00 pm	64	3.10	0.75	Na-Ca-HCO3-Cl
	JD025 @ 3:00 pm	63	3.00	0.70	Na-Ca-HCO3-Cl
	JD025 @ 6:00 pm	66	2.73	0.73	Na-Ca-HCO3-Cl
	JD025 @ 9:00 pm	67	2.82	0.70	Na-Ca-HCO3-Cl
	JD026 @ 12:00 am	67	2.91	0.70	Na-Ca-HCO3-Cl
	JD026 @ 3:00 am	67	2.91	0.71	Na-Ca-HCO3-Cl
	JD026 @ 6:00 am	66	2.82	0.70	Na-Ca-HCO3-Cl
	JD026 @ 9:00 am	66	2.82	0.71	Na-Ca-HCO3-Cl
	JD026 @ 12:00 pm	66	2.91	0.73	Na-Ca-HCO3-Cl
	JD027 @ 12:00 pm	69	3.00	0.70	Na-Ca-HCO3-Cl
	JD028 @ 12:00 pm	73	2.92	0.72	Na-Ca-HCO3-Cl
Downstream GW	JD021 @ 11:30 am	141	2.52	0.78	Na-Ca-Mg-HCO3-Cl
	JD023 @ 11:30 am	153	2.62	0.85	Na-Ca-Mg-HCO3-Cl
	JD028 @ 11:30 am	145	2.62	0.78	Na-Ca-Mg-HCO3-Cl
Upstream SW	JD021 @ 12:30 pm	50	2.55	0.58	Na-Ca-HCO3-Cl
	JD022 @ 12:30 pm	54	2.60	0.56	Na-Ca-HCO3-Cl
	JD023 @ 12:30 pm	44	2.84	0.64	Na-Ca-HCO3-Cl
	JD024 @ 12:30 pm	40	2.95	0.59	Na-Ca-HCO3-Cl
	JD025 @ 12:30 pm	48	2.89	0.61	Na-Ca-HCO3-Cl
	JD025 @ 3:30 pm	48	2.89	0.62	Na-Ca-HCO3-Cl
	JD025 @ 6:30 pm	51	3.10	0.61	Na-Ca-HCO3-Cl
	JD025 @ 9:30 pm	50	2.94	0.62	Na-Ca-HCO3-Cl
	JD026 @ 12:30 am	51	2.84	0.62	Na-Ca-HCO3-Cl
	JD026 @ 3:30 am	50	3.01	0.64	Na-Ca-HCO3-Cl
	JD026 @ 6:30 am	51	3.02	0.64	Na-Ca-HCO3-Cl
	JD026 @ 9:30 am	51	3.02	0.63	Na-Ca-HCO3-Cl
	JD026 @ 12:30 pm	50	2.98	0.61	Na-Ca-HCO3-Cl
	JD027 @ 12:30 pm	51	2.95	0.55	Na-Ca-HCO3-Cl
	JD028 @ 12:30 pm	52	2.86	0.56	Na-Ca-HCO3-Cl
Upstream GW	JD021 @ 1:00 pm	140	6.67	0.88	Ca-Na-Mg-HCO3
	JD022 @ 1:00 pm	142	6.83	0.76	Na-Ca-Mg-HCO3
	JD023 @ 1:00 pm	132	6.33	0.87	Na-Ca-Mg-HCO3
	JD024 @ 1:00 pm	126	6.00	0.86	Na-Ca-Mg-HCO3
	JD025 @ 1:00 pm	130	6.17	0.80	Na-Ca-Mg-HCO3
	JD025 @ 4:00 pm	132	6.17	0.93	Ca-Na-Mg-HCO3
	JD025 @ 7:00 pm	132	6.08	0.88	Ca-Na-Mg-HCO3
	JD025 @ 10:00 pm	129	6.00	0.87	Na-Ca-Mg-HCO3
	JD026 @ 1:00 am	126	5.83	0.80	Na-Ca-Mg-HCO3
	JD026 @ 4:00 am	130	6.17	0.80	Na-Ca-Mg-HCO3
	JD026 @ 7:00 am	130	6.25	0.86	Na-Ca-Mg-HCO3
	JD026 @ 10:00 am	126	6.00	0.79	Na-Ca-Mg-HCO3-Cl
	JD026 @ 1:00 pm	119	5.42	0.79	Na-Ca-Mg-HCO3-Cl
	JD027 @ 1:00 pm	117	5.42	0.79	Na-Ca-Mg-HCO3-Cl
	JD028 @ 1:00 pm	115	5.91	0.77	Na-Ca-Mg-HCO3-Cl

Concentrations of the nutrients NO_3^-, NH_4^+ and P were relatively low at the upstream surface water station (0.04, 0.01 and 0.006 mg/L respectively), while high concentrations of NO_3^- and NH_4^+ were present in the upstream (2.09 and 0.038 mg/L) and downstream groundwaters (2.6 and 0.095 mg/L). Low concentrations of these nutrients at the upstream surface water station reflect the low intensity land use of the upstream drainage catchment (e.g. Mangatarere valley), while elevated groundwater concentrations indicate the flushing of agricultural nutrients through the soil profile into the groundwater wells from rainfall recharge (Saffigna and Keeney, 1977). NO_3^- and NH_4^+ concentrations were slightly elevated in the downstream surface water site (0.48 and 0.1 mg/L) further suggesting the transfer of rainfall recharged groundwaters to this downstream station. It is also likely some nutrients were transferred to the downstream gauging station by point-source discharge of treated sewage into the Mangatarere between the upstream and downstream gauging locations. Dissolved P and Fe^{2+} concentrations were highest in the downstream groundwaters (0.069 and 3.4 mg/L), again reflecting land use (in the case of dissolved P) and the stirring of iron rich minerals from the well base during groundwater purging.

Temporal fluctuations in ground and surface water solute concentrations during the period JD020-028 are presented in Figures 6.17-6.19. Upstream ground and surface water conductivity is also included in these figures to provide an overview of general chemical change in each system during the sampling period and to tie back to results and discussion in Section 6.3. Generally, upstream and downstream surface water solute concentrations followed a similar pattern throughout the week in which concentrations of Ca^{2+}, Cl^-, Na^+, Mg^{2+} and SO_4^{2-} decreased slightly on JD 023 in response to increased precipitation and river stage (Figures 6.17-6.19). Following this dilution, solute concentrations showed a general increase as the receding limb of the storm hydrograph eased and base flow conditions resumed. The analytes total dissolved P and NH_4^+ were exceptions to this decrease. Both analytes showed a steady increase in their concentrations at the downstream surface water station, while concentrations remained relatively consistent at the upstream surface water gauging station.

It is likely increased downstream concentrations have been transferred from rainfall recharged groundwaters that have acquired these nutrients during the passage of precipitation through the soil water zone. Further, a number of tributary streams that enter the Mangatarere between the upstream and downstream gauging locations (Figure 3.10) may have contributed further nutrient inputs. The relatively consistent upstream NH_4^+ and dissolved P concentrations likely suggest the reduced impact of agricultural activity upstream and the lack of base flow provided by rainfall recharged groundwaters.

Chemical parameters showed considerable variability at the upstream groundwater gauging station and this is reflected in the associated upstream groundwater water types (Table 6.8). Concentrations of the ions Ca^{2+}, HCO_3^-, SO_4^{2-} and Na^+ showed an overall decrease at the upstream groundwater site, while Cl^- concentrations remained consistent at 12 mg/L (Figures 6.17-6.19). NO_3^- concentrations increased to 2.6mg/L on JD025 before decreasing for the remainder of the sampling period to 1.5 mg/L on JD028. These chemical dynamics suggest the input of dilute waters to the groundwater system, subsequently reducing Ca^{2+}, HCO_3^-, SO_4^{2-} and Na^+ concentrations. As Cl^- concentrations remain consistent, and an initial pulse of NO_3^- is experienced, this suggests these two solutes are acquired by the passage of dilute precipitation waters through the vadose zone (Taylor *et al.*, 1999; Rosen *et al.*, 1999). This indicates rainfall recharge to the groundwater system resulting in the significant groundwater stage increase and a reduction in groundwater conductivity (Figure 6.13). However, the overall decrease in Na^+ and NO_3^- concentrations from JD026 suggests the input of low NO_3^- and Na^+ waters from a different source such as the Mangatarere stream or an exhaustion of NO_3^- sources. The former is supported by the overall decrease in Ca^{2+}, HCO_3^-, SO_4^{2-} and Na^+ and constant NO_3^- concentration that is also experienced at upstream surface water station during this period (Figures 6.17-6.19). Further, this hypothesis is supported by the diurnal temperature pattern recorded at the upstream gauging station from JD026-028 that suggests the transfer of upstream surface waters to the upstream groundwater station. However, denitrification may also have caused this decrease in NO_3^- in which NO_3^- is reduced to nitrogen gas as anoxic conditions prevail and anaerobic bacteria use NO_3^- as an electron acceptor (Equation 6.5) (McLaren and Cameron, 1996).

$$C_6H_{12}O_6 + 4\ NO_3^- \rightarrow 6CO_2 + 6H_2O_2 + 2N_2 \qquad (6.5)$$

This hypothesis is also supported by the overall increase in Mn concentrations at the upstream groundwater gauging station (Figures 6.18) and the likelihood that the soil column became saturated in response to the 120mm of rainfall experienced (JD021-028). A substantial increase in iron (0.078-0.18 mg/L), also a redox sensitive ion, was experienced during this period. However, it is likely this elevated Fe^{2+} concentrations was due to the large iron pan that runs through the area and the disturbance of iron rich minerals from well purging, as oppose to changing redox conditions. SO_4^{2-} concentrations remained relatively consistent at the upstream groundwater station during this period suggesting that highly reduced conditions were not present. Typically, as waters become extremely anoxic concentrations of SO_4^{2-} are expected to decrease as O_2, NO_3^- and Mn are already exhausted (Dahm *et al.*, 1998; Kedziorek *et al.*, 2008). This suggests upstream groundwaters may have been slightly reduced, but were not highly anoxic.

The substantial changes in solute concentrations at the upstream groundwater station are also reflected in the diversity of water types and Cl^-/HCO_3^- and Na^+/Ca^{2+} ratios. These hydrochemical parameters are useful for comparing different water types and provide some insight into the geochemical evolution of water bodies (Rosenthal, 1987). Upstream groundwaters were generally Na^+-Ca^{2+}-Mg^{2+}-HCO_3^- (Figure 6.16), however on JD021 and 025 this switched to Ca^{2+}-Na^+-Mg^{2+}-HCO_3^- indicating a higher proportion of Ca^{2+} ions. This signature again changed for the last three days of the hydrochemical sampling programme (JD026 at 10.00am until JD028 at 13:00) to a Na^+-Ca^{2+}-Mg^{2+}-HCO_3^--Cl^- water type. This indicates the increased importance of Cl^- during this period and is also reflected in lower Cl^-/HCO_3^- (0.77-0.79) as shown in Table 6.8. Further this Na^+-Ca^{2+}-Mg^{2+}-HCO_3^--Cl^- water type is very similar to that presented at the upstream surface water station (Na^+-Ca^{2+}-HCO_3^--Cl^-) suggesting the transfer of surface waters to the aquifer during this period.

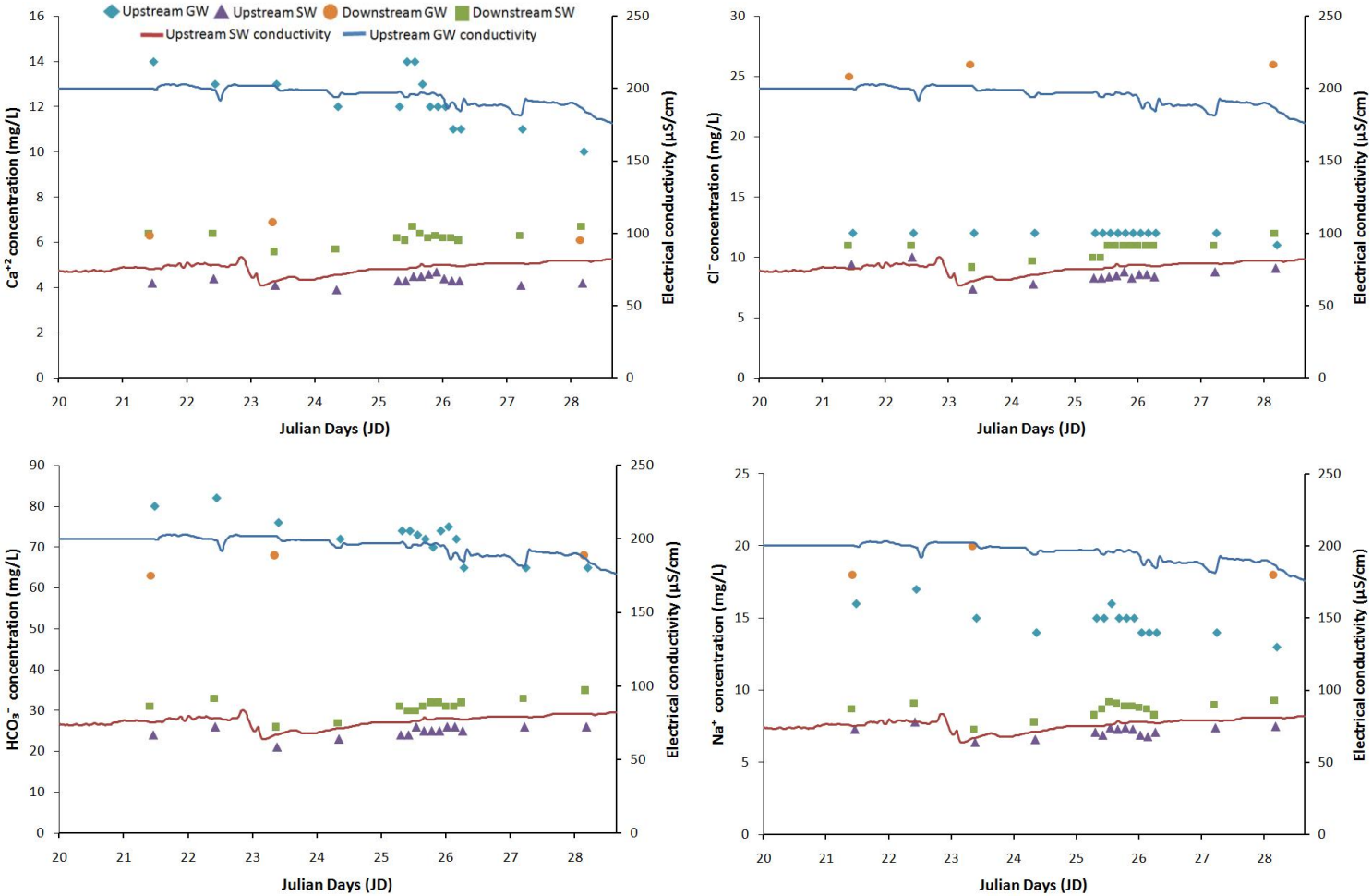

Figure 6.17. Temporal variations in water quality parameters Ca^{2+}, Cl^{-}, HCO_3^{-} and Na^{+} at the upstream surface and groundwater gauging station and downstream surface and groundwater gauging stations JD020-029. Upstream surface and groundwater conductivity data for the period are also presented on the secondary axis for comparison. Downstream conductivity data are not shown due to the substantial gaps present in the dataset.

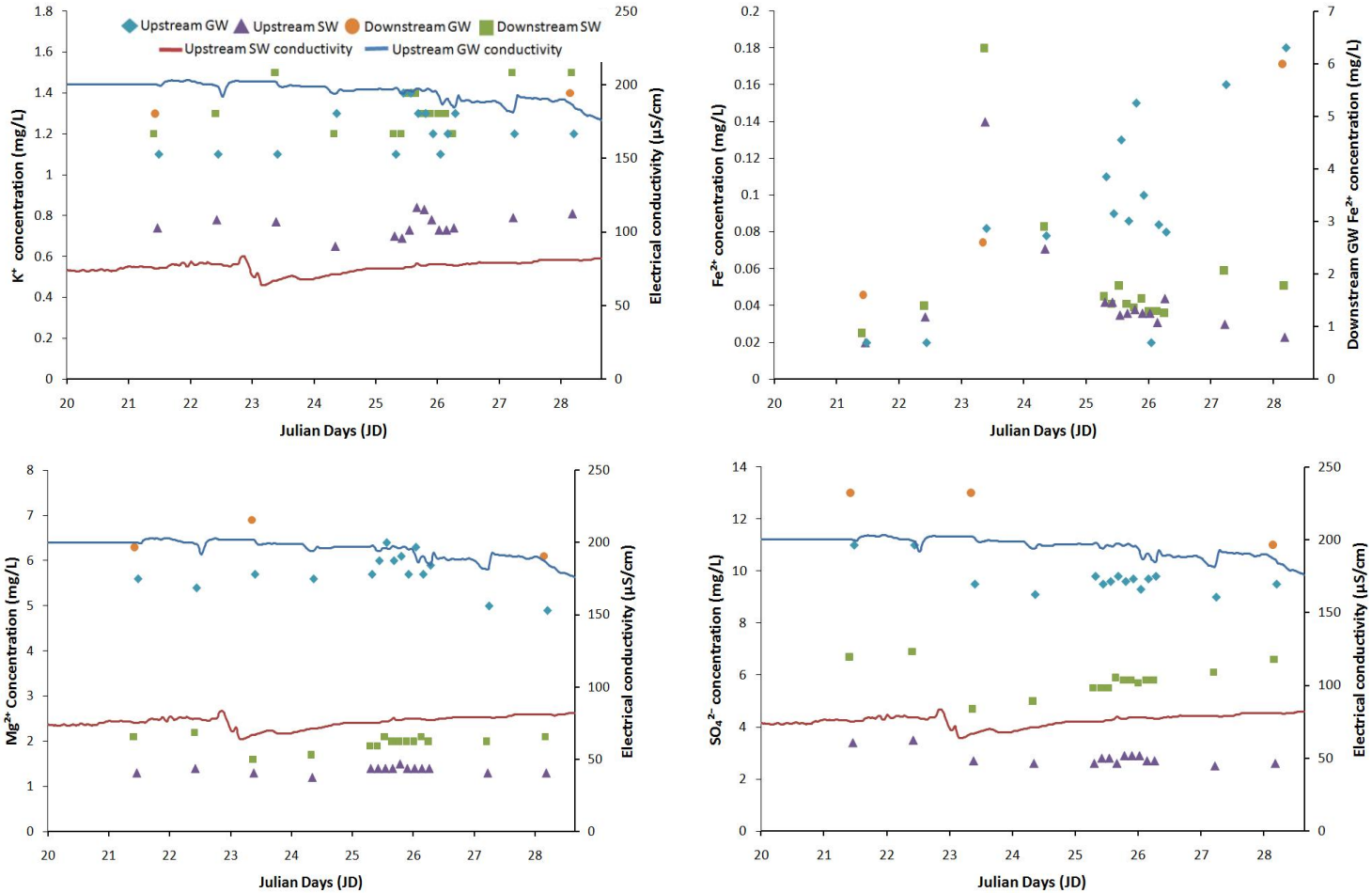

Figure 6.18. Temporal variations in water quality parameters K^+, Fe^{2+}, Mg^{2+} and SO_4^{2-} at the upstream surface and groundwater gauging station and downstream surface and groundwater gauging stations JD020-029. Upstream surface and groundwater conductivity data for the period are also presented on the secondary axis for comparison. Downstream conductivity data are not shown due to the substantial gaps present in the dataset. Note the Fe^{2+} concentration figure does not show upstream surface or groundwater conductivity data. The secondary *y*-axis presents downstream groundwater Fe^{2+} concentrations.

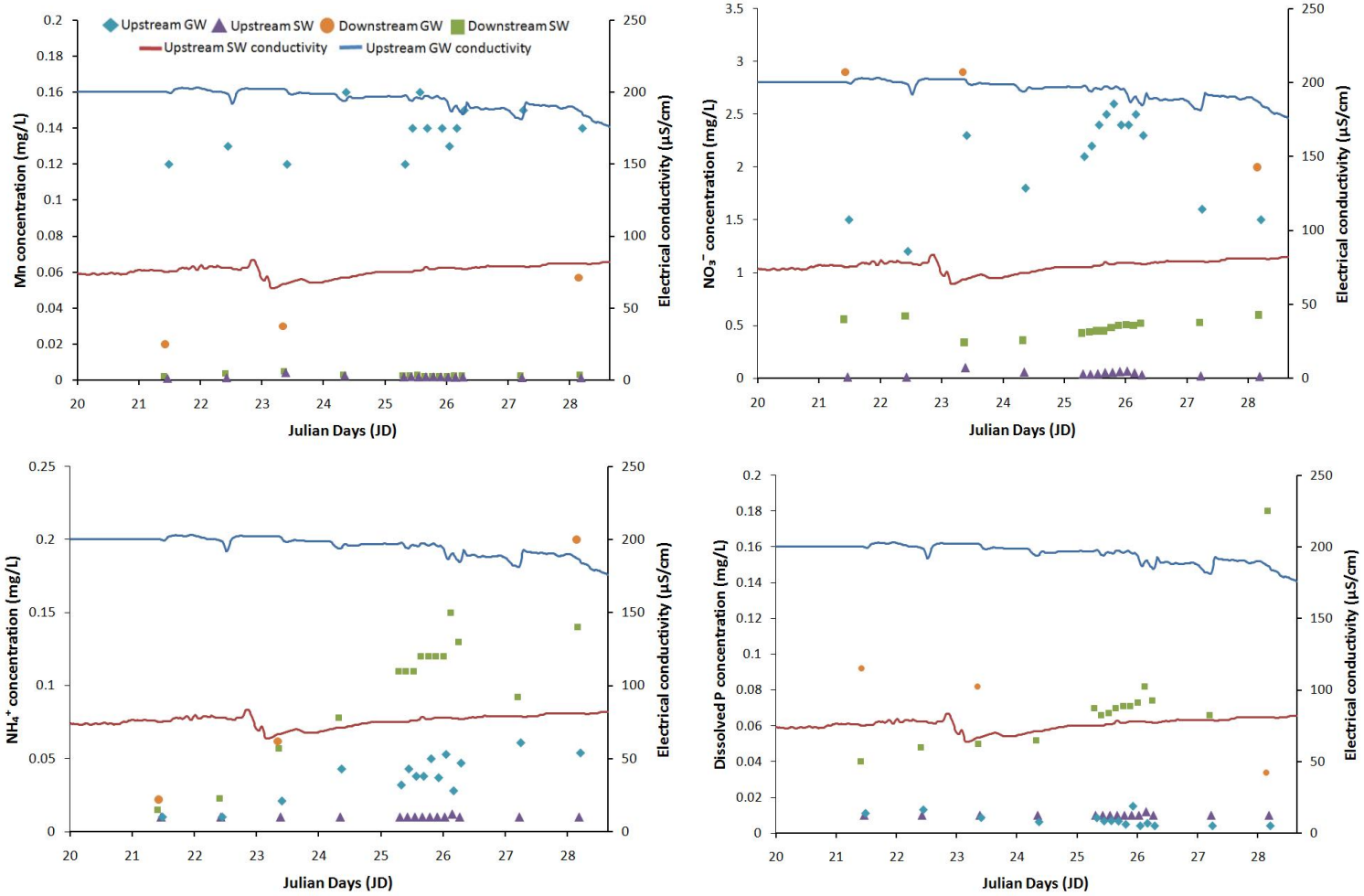

Figure 6.19. Temporal variations in water quality parameters Mn, NO_3^-, NH_4^+ and dissolved P at the upstream surface and groundwater gauging station and downstream surface and groundwater gauging stations JD020-029. Upstream surface and groundwater conductivity data for the period is also presented on the secondary axis for comparison. Downstream conductivity data is not shown due to the substantial gaps present in the dataset.

Upstream groundwater Ca^{2+}/Na^{+} ratios also decreased during these last three days from 6-6.83 to 5.41-5.91, which together with the Cl^{-}/HCO_3^{-} ratios, suggest the increased importance of Na^{+} and Cl^{-} in the sample waters (Table 6.8). Due to the extremely low concentrations of all ions in precipitation (Table 6.7) it is likely this Na^{+} was sourced from river waters and the dissolution of sedimentary rocks in the Mangatarere's catchment. These ratios would likely be higher at the upstream groundwater station if waters were sourced entirely from rainfall recharge as precipitation would provide more Ca^{2+} and HCO_3^{-} to solution from the dissolution of Q1 and Q2 alluvial gravels through which these waters pass. Another explanation surrounds the input of additional Ca^{2+} ions from carbonate dissolution, that subsequently bump Na^{+} into solution therefore increasing their concentration and proportionality (McLaren and Cameron, 2006).

The analytes K^{+}, Mg^{2+}, NO_3^{-} and Mn fluctuated at the upstream groundwater site during the hydrochemical sampling period (Figures 6.18-6.19). In particular, K^{+} and Mg^{2+} showed considerable variation during the 24 hour intensive sampling program, with K^{+} fluctuating *ca.* 0.4 mg/L and Mg^{2+} *ca.* 0.7 mg/L (Table 6.7). This variability in K^{+} and Mg^{2+} concentrations may be a factor of cation exchange (Rosenthal, 1987; McLaren and Cameron, 2006) and highlights the significant temporal variability of these analytes within a sub-daily time period. This variability may be further explained by purging of the groundwater well that resulted in dilute waters being drawn into the well casing. This water may have mixed with existing well waters, creating temporal variations in all measured parameters. This variability may have implications for current water quality monitoring programmes and will be discussed in further detail in Section 7.2

Water chemistry also showed significant variation at the downstream groundwater gauging station as depicted from the three samples collected on JD021, 023 and 028. Overall, concentrations of SO_4^{2-}, NO_3^{-} and P decreased during the sampling week while concentrations of NH_4^{+}, Fe^{2+} and Mn increased to 0.178 mg/L, 4.4 mg/L and 0.037 mg/L respectively. Increased concentrations of these three analytes, coupled with an overall 0.9 mg/L reduction in NO_3^{-} suggest a possible shift to anoxic groundwater conditions at the downstream gauging station.

This may be due to saturation of the soil water zone due to the 129mm of precipitation experienced during the week and/or the efficient removal of NO_3^- due to biogenic[5] respiration that would also reduce O_2 concentrations. It is hard to confirm this statement without more information regarding the dissolved oxygen concentration of the water. However some inference regarding redox states can be made from an analysis of these analytes that are sensitive to changing redox conditions. The downstream groundwater station displayed a consistent Na^+-Ca^{2+}-Mg^{2+}-HCO_3^--Cl^- water type for the three samples collected. The Ca^{2+}/Na^+ ratio was 0.78 for JD021 and JD028 but increased to 0.85 for the JD023 sample. This indicates higher Ca^{2+} relative to Cl^- during this sample and therefore suggests increased mineral dissolution during this period as precipitation passes through the Q1 and Q2 alluvial gravels.

6.5 Quantifying ground and surface water interaction

To further explore the potential interaction between surface and groundwater gauging stations two simple mass balance calculations were undertaken. These calculations allowed for the quantification of water transfer between the various ground and surface water stations and are outlined, with their assumptions, in Section 6.2.8. The first of such calculations aimed to quantify the amount of river recharge provided to the upstream groundwater station by determining the loss of surface water between the GWRC Mangatarere Gorge monitoring station and the upstream surface water gauging station. The resulting output is presented in Figure 6.20 and shows the predicted average daily discharge (m^3/s) for the two gauging stations during the period JD324-038. Stage data was not available from the Mangatarere at Gorge station from JD039-051 and therefore this period was excluded as discharge could not be determined.

[5] Surrounding living organisms or biological processes

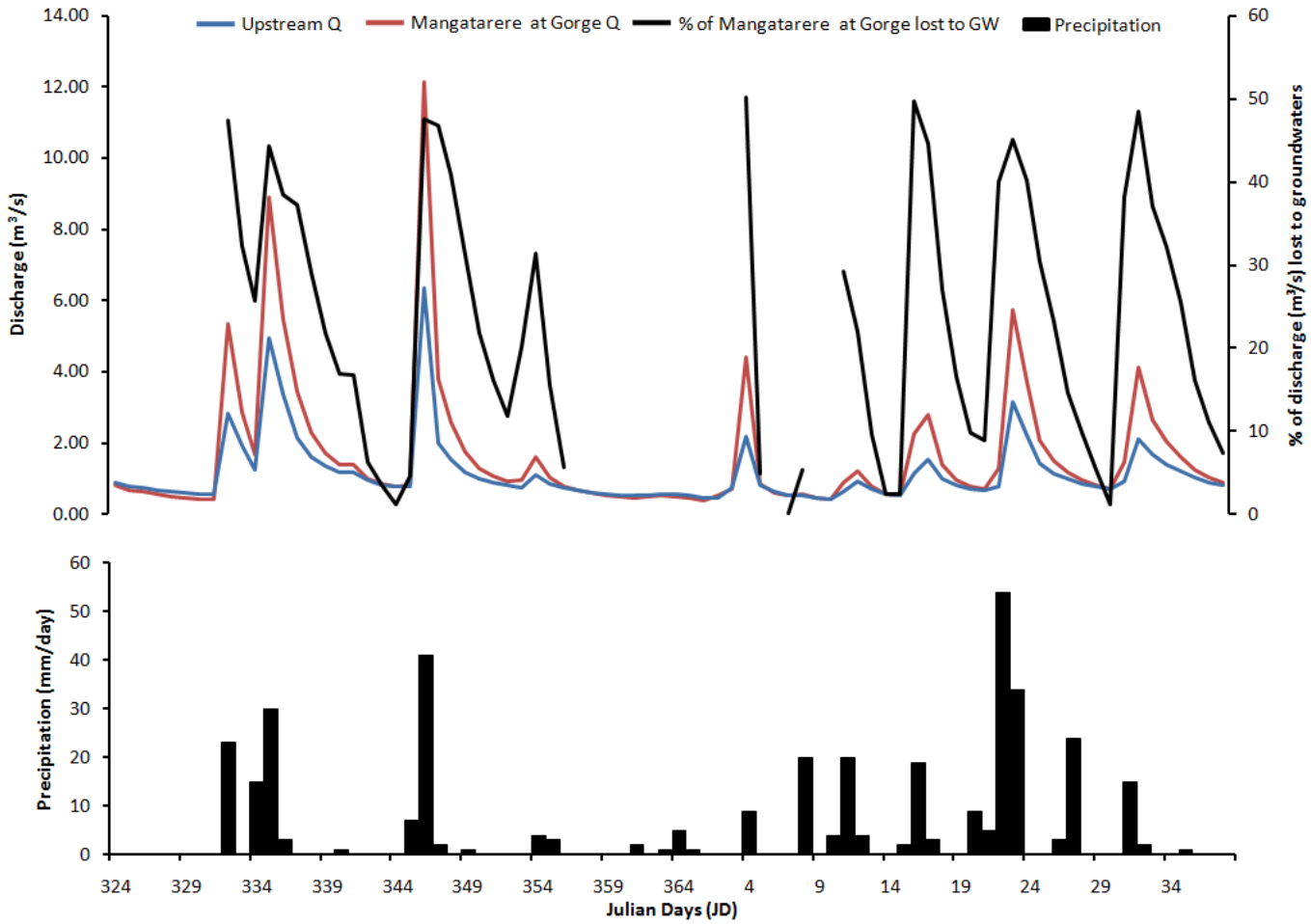

Figure 6.20. GWRC Mangatarere at Gorge monitoring station and the upstream surface water station average daily discharge measurements JD324-039. The difference in discharge between the Mangatarere at Gorge site and upstream station is deemed lost to underlying groundwater. Precipitation and the % of Mangatarere at Gorges discharge lost to groundwater system are also shown.

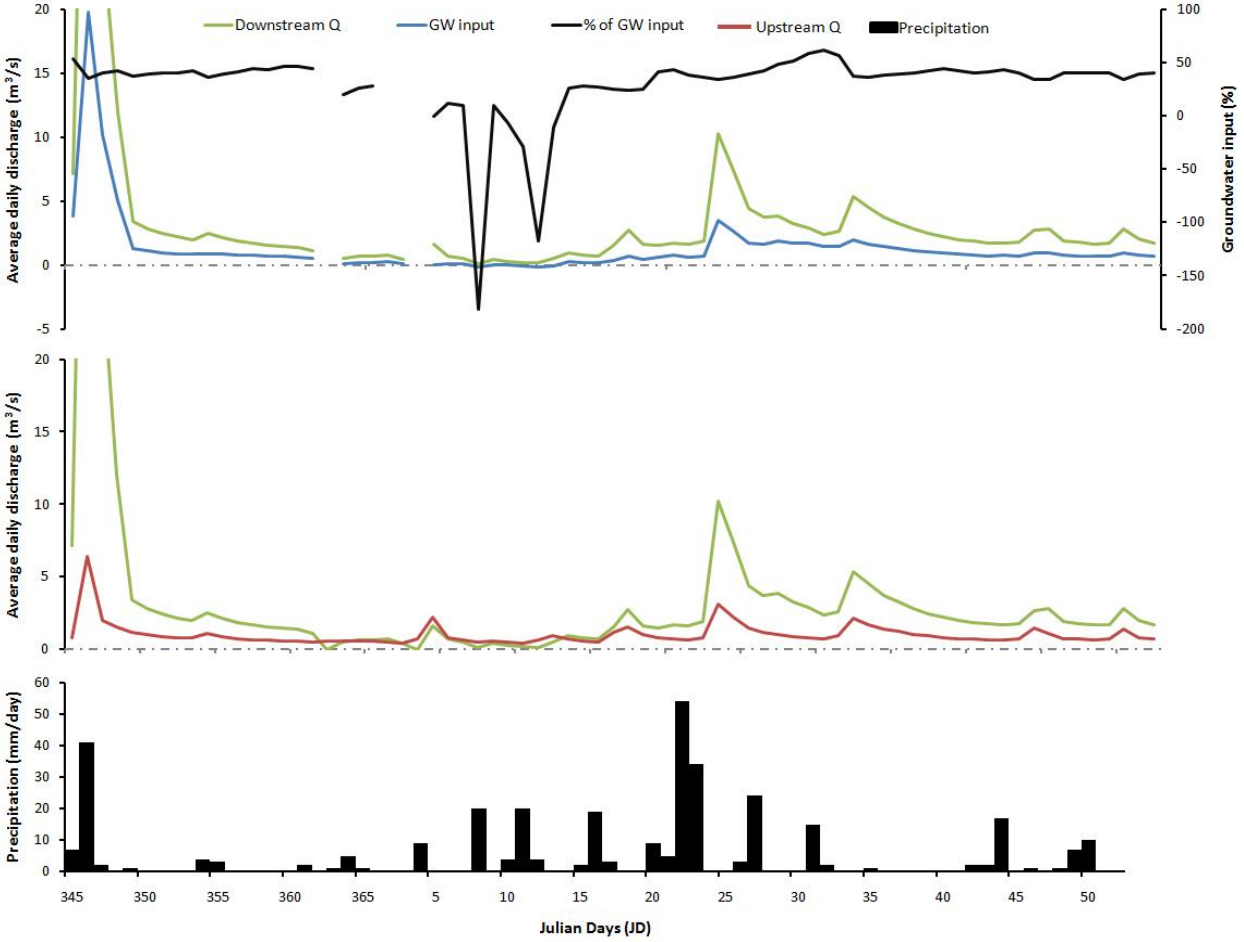

Figure 6.21. Average daily upstream and downstream surface water discharge (Q) and groundwater input to downstream surface water gauging station. Precipitation and the percentage of downstream base flow provided by groundwater sources are also presented. *Note:* Average daily discharge (primary *y-axis)* has been fixed at 20 m³/s to allow for the interpretation of small changes in discharge despite the high flow event on JD345 peaking at 55 m³/s.

159

Despite several anomalies within the timeframe, in which discharge was higher at the upstream surface water station than the Mangatarere at Gorge, it appears the majority of recharge to the upstream groundwater system was provided during high flow events (Figure 6.21). This is indicated by the loss of flow between the Mangatarere at Gorge and the upstream surface water gauging station on JD332-336, 348, 354, 004, 012, 017, 023 and 031-34. It is likely during these events as discharge increased water was able to move through the stream bed and banks and into underlying groundwater systems. Analyses from Figure 6.11 showed that upstream groundwater stage only responded to possible recharge on JD335, 348 and 021-025. This supports initial assumptions that although water may have been lost to the groundwater system during other periods a certain magnitude of recharge or high antecedent soil moisture conditions is required to initiate a groundwater stage response. This was earlier inferred from stage data in Section 6.3. Figure 6.20 suggests *ca.* 2-4 m^3/s of flow from the upstream Mangatarere stream was lost to the underlying groundwater system during the three groundwater stage response events on JD335, 348 and 021-025.

From Figure 6.21 it appears *ca.* 30-60% of downstream surface water base flow was provided by the neighbouring groundwater aquifer during the period JD345-051. This proportion varied significantly over the 72 day modeled period and on average changed on a day to day basis. Generally the proportion of groundwater provided base flow decreased during high flow events, despite higher input quantities, when the majority of discharge was provided to the downstream Mangatarere from direct rainfall runoff and the upstream surface water gauging station. For the majority of the modeled study period downstream surface water discharge was *ca.* 60% higher than that experienced upstream. This difference in surface water discharge was already inferred from stage data in section 6.3.3 and is likely due to the downstream stations larger catchment area (130 km^2) and input from groundwaters. During the period JD004-012 downstream discharge dropped *ca.* 0.3 m^3/s below upstream projections and the provision of groundwater base flow to the downstream station ceased.

This discharge discrepancy suggests downstream surface waters were lost to the underlying groundwater system and supports the previously stated hypothesis that low groundwater levels during this period switched the downstream surface water station from an effluent to influent system. Following several days of precipitation (JD010-012) and possible river recharge to the groundwater system it appeared this gradient switched back (JD012) and groundwaters once again provided base flow to the downstream surface water station. Following significant precipitation on JD020-023 up to 62% of downstream base flow was provided by the groundwater system (Figure 6.21). These input waters (*ca.* 1.5-3 m^3/s) extended the downstream gauging station's receding flood limb while upstream flood waters were quickly removed from the upstream catchment. The increased provision of base flow during this period is likely due to increased downstream groundwater stage as suggested by the *ca.* 50cm increase in upstream groundwater stage (Figure 6.11). It is hard to confirm this hypothesis without downstream groundwater data; however, the increased importance of groundwater base flow during this period is further supported by a gradual increase in NO_3^-, NH_4^+ and P concentrations at the downstream surface water station from JD023-028 (see Section 6.4).

Although a number of major limitations and assumptions surround these mass balance calculations, they provide further evidence to support hypothesis already stated in Sections 6.3 and 6.4. It is likely significant uncertainty surrounds the calculation of discharge, in particular where foreign rating curves are applied to the upstream surface water gauging station. Therefore, a precautionary approach is taken when interpreting the magnitude of interaction and findings from this section are only used to support initial assumptions outlined in Sections 6.3 and 6.4.

6.6 Comparison with current environmental monitoring

Current hydrochemical monitoring undertaken by the GWRC in the Wairarapa valley consists of monthly sampling for major river systems and quarterly sampling for major groundwater bores. Both the upstream groundwater station (S26/0977) and the downstream surface water station (Mangatarere at State Highway 2) are included in these sampling programmes and recent results obtained by the GWRC during the 2008 year are compared with data from this study in Tables 6.8 and Figure 6.22.

Unfortunately long term data sets from these locations are not available. Comparison of data from this study and from GWRC monitoring allows for an evaluation of current monitoring programmes and their ability to capture variability in water quality parameters. The conditions under which water sampling was undertaken for this study (JD021-028) include extended precipitation and high flow events. These events may have had an impact on water quality (e.g. dilution events) and baseline conditions and therefore should be acknowledged. It is likely sampling undertaken by GWRC would not have been conducted during such conditions.

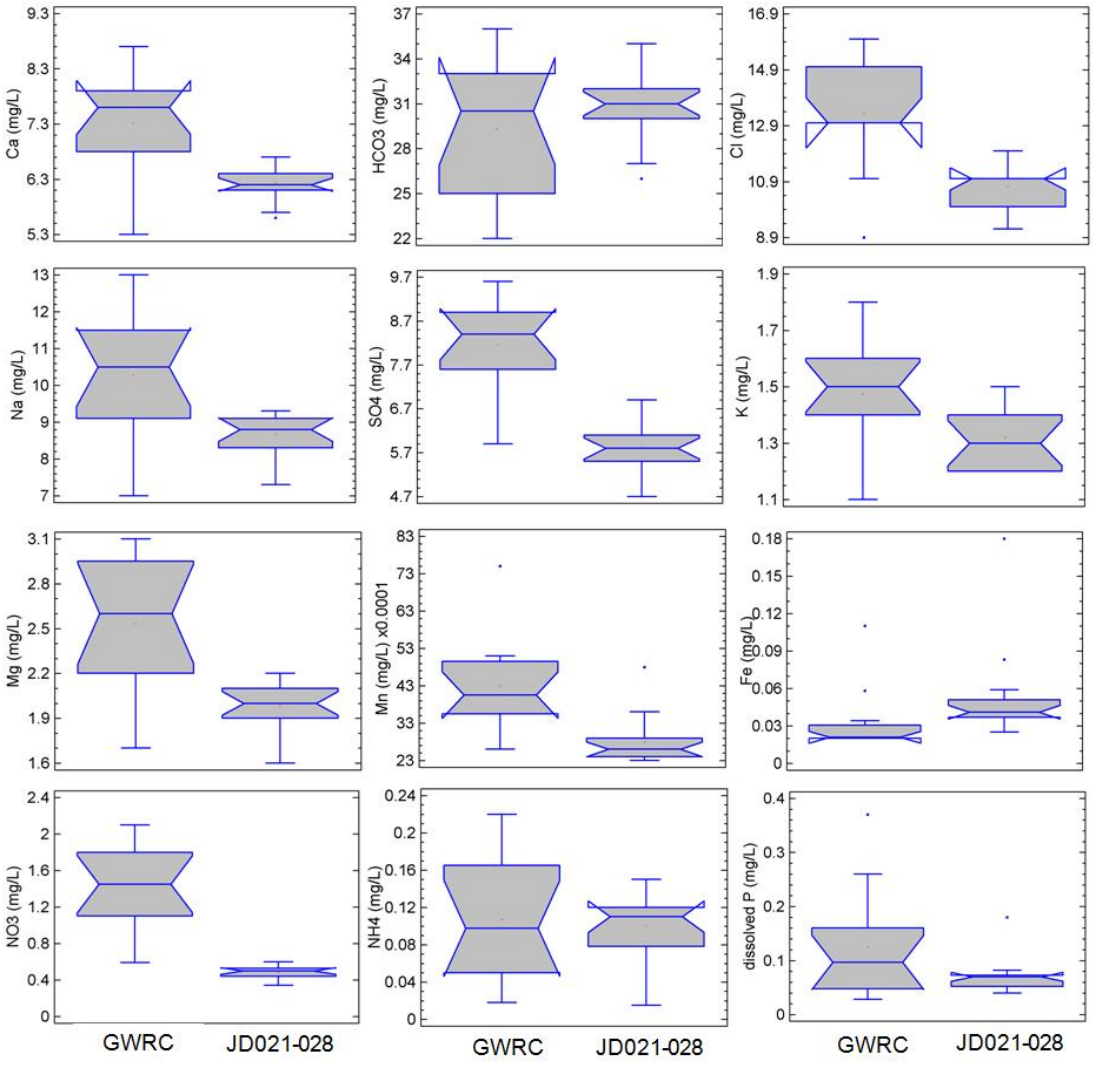

Figure 6.22. Range of individual solute concentrations from the downstream gauging station, Mangatarere stream, comparing concentrations obtained by the GWRC monthly monitoring program (September 2008-September 2009) and results from this study (JD021-028). Number of observations for GWRC monitoring is 12, while 15 observations were collected for this study. The rectangular box identifies the first to the third quartile of the data, separated by a horizontal median line. Median notches are present around the mean line identifying the margin of error surrounding sample mean estimation. The vertical whisker lines identify the lowest and highest observations in the sample, except those deemed to be outliers as represented by the dots plotted outside these whiskers.

Figure 6.22 compares the range of downstream surface water solute concentrations obtained by GWRC environmental monitoring with results from this study. GWRC data were obtained from monthly sampling over the period September 2008-September 2009. This is the most recent data that have undergone data quality control. The range of solute concentrations obtained at the downstream surface water gauging station during this study generally fell outside the 25^{th} to 75^{th} quartile of GWRC monitoring programme and displayed significantly lower average median concentrations. This suggests two possible scenarios. Firstly, high precipitation and water flows during the intensive sampling programme (JD021-028) may have resulted in a dilution effect at the downstream station. Secondly, solute concentrations, in general, may be lower during this period of the year. Solute concentrations obtained during this study still fall within the highest and lowest observations from the GWRC programme. Exceptions to this rule included NO_3^- and Fe^{2+} which had concentrations significantly lower (NO_3^-) and higher (Fe^{2+}) than the range of concentrations obtained by the GWRC programme. This suggests that the GWRC monthly sampling programme fails to capture the complete range of concentrations present at the downstream gauging station and highlights the need for more frequent sampling to capture this variability. This has implications for environmental reporting in which parameters may be overstated, leading to potentially misleading or false inferences.

Solute concentrations at the upstream groundwater station were similar to those obtained by GWRC monitoring during the last year (Table 6.9). Fe^{2+} was an exception to this with GWRC concentrations significantly higher (0.49 mg/L) than those experienced during the intensive sampling week (0.093 mg/L). This elevated Fe^{2+} concentration may have been caused by poor sampling practices in which extended purging of the well stirred up iron rich sediments (e.g. peat) within the groundwater bore. The similarity of solute concentration obtained from this study and those from GWRC monitoring reaffirm the range of values obtained in this research.

As shown in Figures 6.17-6.19 the surface and groundwater solute concentrations displayed noticeable variability during the one week intensive sampling programme (JD021-028). However, this variability was relatively subtle with the majority of solutes displaying a relatively small range of values. Exceptions to this include Na^+, SO_4^{2-}, Mn, Fe^{2+}, K^+ and the nutrients NO_3^- and NH_4^+, all of which fluctuated significantly at one or more sites (Figures 6.17-6.19). This highlights the temporal variability displayed by these solutes within a relatively short time period (e.g. sub-daily) and suggest current monthly and quarterly sampling regimes undertaken by GWRC may fail to capture this variability. However, the inability to capture such variability is not necessarily a problem, in particular for solutes that have little applicability for operational hydrology and/or influence on human health (e.g. Na^+). In contrast, the temporal variability of parameters such as NO_3^-, NH_4^+ and dissolved P, that have known human health and ecological impacts should be identified and acknowledged. Further, these nutrients offer valuable insight into contaminant transport and the impact of land use practices (e.g. agriculture) on water quality. However, concentrations of these nutrients in the Mangatarere stream catchment measured to data are all significantly lower than those 'deemed harmful to human health' as set out in the New Zealand Drinking Water Standards 2005 (e.g. NO_3^- should not exceed 11.3 mg/L).

Table 6.9. Individual solute concentrations from the upstream groundwater gauging station obtained during the intensive monitoring programme (JD021-028) and from the GWRC quarterly monitoring programme for 2008-2009. GWRC monitoring consisted of four samples of which at times only several parameters were measured. Solute concentrations are presented as mg/L and standard deviations are presented in parentheses.

Source	***N***	**HCO_3^-**	**Cl^-**	**Ca^{2+}**	**Mg^{2+}**	**K^+**	**Na^+**	**SO_4^{2-}**
Upstream GW	15	72.6 (5.0)	11.9 (0.3)	12.27 (1.2)	5.7 (0.4)	1.2 (0.11)	14.8 (1.0)	9.7 (0.6)
GWRC monitoring	2-4	78.5 (12.0)	12.0 (1.4)	12.00 (0.00)	6.15 (0.21)	1.2 (0.00)	15.5 (2.1)	8.5 (0.85)
Source		**As**	**Fe^{2+}**	**Mn**	**P**	**NO_3^-**	**NH_4^+**	
Upstream GW	2-4	<0.001 (0.000)	0.093 (0.049)	0.142 (0.019)	0.007 (0.003)	2.09 (0.45)	0.038 (0.015)	
GWRC monitoring	15		0.49 (0.00)	0.23 (0.06)	0.01 (0.00)	2.45 (0.23)	0.032 (0.020)	

6.7 Limitations

A number of problems arose during the high resolution monitoring programme and as a result there are several limitations surrounding this research. The results presented in this research highlight the difficulties in determining high resolution interaction between ground and surface water bodies using chemical data alone. Subsequent interpretations of interaction were based on a range of chemical and physical parameters (e.g. water temperature).

A major limitation surrounding the high resolution field monitoring and interpretation of subsequent results was the loss of downstream surface and groundwater data. On JD356 faulty wiring resulted in the loss of power to the downstream groundwater gauging station. All stored data were lost and the issue was not identified until JD004 when a site inspection was undertaken. Due to the significant costs and length of time required to repair this fault the downstream groundwater gauging station was abandoned. As a result, besides chemical grab samples obtained on JD021, 023 and 028, no data were obtained from this system. Equipment malfunction was also a problem at the downstream surface water gauging station maintained by the GWRC. An erratic power supply resulted in significant gaps in the downstream surface water data set. As a result the downstream gauging location was heavily underrepresented in the analysis of ground and surface water interaction in the Mangatarere catchment. Although inferences were made about the downstream system using available data, the response of these systems in particular the downstream groundwater site, is still not well understood. The lack of downstream groundwater data meant little systematic comparison could be made between this station and the downstream surface water site.

Issues surround the interpretation of soil moisture conditions and the influence these conditions have on stream flow and groundwater response. Low soil moisture conditions were inferred during extended dry periods in which ground and surface water response was slow, while high soil moisture conditions were inferred during periods preceding significant rainfall. Although soil moisture could be inferred from precipitation, for future research it would be ideal to collect soil moisture and evapotranspiration data *in situ* within the field.

This would allow greater confidence to be achieved surrounding soil moisture conditions and their impact on ground and surface water response.

Further issues surround the various timescales at which high resolution data were reported and subsequent comparison of these data. The downstream surface water gauging station recorded temperature and electrical conductivity data at ten minute intervals and presented these data as one hour averages. This timescale was due to a misunderstanding with the GWRC in regards to required recording intervals. However, these downstream hourly averages seemed representative of natural changes in the system and were therefore not deemed a significant limitation. Further, both upstream surface water gauging stations maintained full 15 minute recording intervals that allowed a systematic comparison between these two sites. Precipitation data were presented as daily totals (mm/day) to overcome issues surrounding an erratic recording interval. The Harvest SPE-02 telemetry unit presented data at 15 minute intervals, however, an erratic pattern switched this recording interval every hour by several minutes. The telemetry unit was maintained by Reid's Piggery who was unaware of this reporting error. The presence of this erratic recording interval prevented systematic comparison between 15 minute stage and conductivity data and precipitation data. This prevented potential lag durations between precipitation and stage and conductivity response from being determined.

Issues surround the use of electrical conductivity to assess chemical changes in groundwater parameters and therefore infer ground and surface water interaction. As noted by Reilly and LeBlanc (1998) significant spatial and temporal variability of solute concentrations within an aquifer can occur even when typical field parameters such as electrical conductivity, pH and dissolved oxygen display no change. Conductivity was continuously measured at three gauging locations in order to infer changes in chemistry and therefore interaction. However, this parameter may have exhibited little change even though significant changes in water quality were occurring within the water body. As a result potential chemical interaction between the ground and surface water gauging station in the Mangatarere catchment may have gone unnoticed.

Extended purging of the groundwater well for grab sampling may have affected the hydrochemical composition of well waters. Continuous conductivity data showed a clear decrease in conductivity immediately following purging as new dilute aquifer waters were drawn into the well casing. This may have affected solute compositions and subsequent hydrochemical grab sample results. However, as well purging was undertaken for each grab sample, any error due to this purging was consistently introduced to all sampling events. This error highlights potential issues surrounding nationwide hydrochemical sampling as industry standard measures (purging of three well casings) may influence hydrochemical compositions resulting in unrepresentative results.

6.8 Summary and conclusions

Results from the high resolution field monitoring period suggest ground and surface water interaction was occurring in the Mangatarere stream catchment during the period JD324-051. This interaction displayed a wide degree of spatial variability with the upstream surface and groundwater stations showing an overall influent (losing) system of interaction while the downstream gauging areas displayed an overall effluent (gaining) system of interaction. Further, these systems of interaction showed aspects of temporal variability.

1. The downstream surface water gauging station likely received a significant proportion of base flow from the neighbouring groundwater aquifer. This was indicated by a subdued diurnal water temperature and overall colder water temperatures at the downstream gauging station. In contrast, upstream surface water temperatures strongly followed diurnal variations in air temperature, indicative of solar meteorological energy inputs. Downstream surface water conductivity and solute concentrations were significantly higher than those experienced at the upstream surface water station, again indicating a supply of solute rich groundwaters to stream base flow. This hypothesis was further supported by elevated NO_3^-, Na^+ and Cl^- concentrations in downstream surface waters, analytes known to accumulate in rainfall-recharged groundwaters. Downstream mass balance calculations suggested 30-60% of downstream surface water base flow was provided by the groundwater system.

2. The provision of groundwater base flow to the downstream surface water gauging station appeared to show temporal variability as indicated by a reduction in downstream surface water stage (to *ca.* 40-50cm) and discharge during the period JD004-016. This period of low surface waters occurred during a relatively dry period of the study when groundwater levels were very low (*ca.* 2.5m). This is likely to have led to a reduction in groundwater hydraulic head and therefore reduced transfer of groundwaters to the downstream Mangatarere stream. Mass balance calculations further support the premise that the downstream surface water system shifted to influent conditions during this period as surface waters were lost to underlying groundwaters.

3. Na^+ and Ca^{2+} were the dominant cations in solution at all four gauging stations while HCO_3^- and Cl^- were the dominant anions in solution. This water signature reflects the largely sedimentary lithology within the Mangatarere stream catchment and the input of Na^+ and Cl^- from precipitation. Both the upstream and downstream groundwater locations receive recharge primarily from precipitation as indicated by elevated NO_3^-, Cl^- and Na^+ concentrations. Solute concentrations were significantly higher in groundwaters in comparison to surface water stations, reflecting increased rock:water contact time and rainfall recharge.

4. Both the upstream and downstream surface water gauging stations showed a marked response to precipitation, with subsequent stream stage increases and conductivity dilution events. The magnitude of these stage and conductivity responses varied and was influenced significantly by the magnitude of precipitation and antecedent soil moisture conditions. Downstream surface water conductivity returned to base levels faster than upstream, indicating that the majority of runoff was provided by solute rich groundwaters as opposed to surface water runoff.

5. The upstream groundwater gauging station likely receives recharge primarily from precipitation, but also from interaction with the Mangatarere stream. Gradual increases in groundwater stage occurred concurrently with major precipitation events and surface water stage increases on JD335-339, 348-350 and 021-025. However, using stage data alone it is extremely difficult to differentiate between the two recharge mechanisms. Concentrations of NO_3^-, Cl^- and Na^+ concentrations were significantly higher in the upstream groundwaters than those experienced in surface waters suggesting their accumulation during passage of precipitation through the soil-water zone. This suggests recharge is dominated by precipitation. Groundwater stage response was highly dependent on antecedent soil moisture conditions with stage response minimal during extended dry periods.

6. The intensive sampling programme undertaken during JD021-028 offered further insight into recharge mechanisms at the upstream groundwater station. High precipitation on JD022-023 led to an immediate groundwater stage response (*ca.* 60cm) and a subsequent decrease in groundwater conductivity and solute concentrations as dilute rain waters recharged the groundwater aquifer. Exceptions to this were the NO_3^- and Cl^- ions that increased or stayed constant as infiltrating waters flushed them through the soil water zone into the aquifer body. However, on JD026 it appeared recharge was also provided by inflows from the Mangatarere stream. Groundwater NO_3^- concentrations decreased and the dominant water type became Na^+-Ca^{2+}-Mg^{2+}-HCO_3^--Cl^- as *ca.* 2-4 m^3/s of dilute, low NO_3^- surface waters recharged the aquifer. Further, a diurnal water temperature pattern was transferred from the Mangatarere stream to the upstream groundwater station during the period JD026-028. It appears the onset of river recharge to the upstream groundwater station during this period may have been controlled by the duration of the surface water high flow event experienced during JD022-028 in which an extended falling limb was present.

7. The upstream groundwater gauging station responded to well purging undertaken on JD356 and 021-028. This purging resulted in an immediate stage and conductivity decrease (*ca.* 10-50 cm and *ca.* 3-10 µS/cm respectively) as waters were removed from the well and new dilute waters from within the aquifer were drawn into the well casing to replace those extracted. Extended periods of purging undertaken during JD021-028 may have impacted on ground and surface water interaction with the upstream gauging station receiving recharge from the Mangatarere stream on JD026-028. It appears this may have been the only time during the study period in which this mechanism of recharge occurred. As a result it may be possible that extended pumping of the well influenced recharge mechanisms.

Chapter 7
Conclusions and recommendations

The overall aim of this research was to determine if existing and/or potential water chemistry measurements could be used to investigate the interaction between surface and groundwater bodies in the Wairarapa valley, New Zealand and identify specific locations and timescales at which this interaction occurs. In order to achieve this, a comparison of surface and groundwater water quality was undertaken at both a regional and local scale within the Wairarapa valley. A number of research objectives were specified in Chapter one and were met throughout this research. A schematic representation of the main findings of this research is presented in Figure 7.1.

7.1 Overall conclusions

- Results from this research suggest significant ground and surface water interaction is occurring in the Wairarapa valley, New Zealand. Regional scale investigations, employed in Chapter four, utilised HCA and hydrochemical medians from the entire Wairarapa to link ground and surface water bodies, based on similarities in hydrochemistry to infer interaction. Six main clusters were identified, primarily differentiated by their TDS, redox potential and major ion ratios. Results indicated both local and regional coupling between surface and groundwater sites. Shallow aquifers, located in close proximity to losing reaches of rivers such as the Waiohine and Waipoua, were grouped with similar Ca^{2+}-HCO_3^- type surface waters, indicating potential recharge from these river systems. Likewise, rainfall-recharged groundwater sites that displayed higher Na^+ relative to Ca^{2+} and Cl^- relative to HCO_3^- were grouped with similar surface waters such as the Mangatarere and Parkvale streams. This suggests river base flow, and this chemical signature was provided to these streams from underlying groundwaters. Deep anoxic aquifers, high in total dissolved solids, were grouped together in distinct clusters, but showed no hydrological link to surface water sites. These groundwaters were largely restricted to the lower Wairarapa valley, an area dominated by various estuarine confining layers.

Regional scale results highlight the potential use of HCA and existing datasets as a rapid and cost-effective method of identifying regional ground and surface water interaction. However, although this regional approach was successful, the methodology employed does not account for temporal variability in water chemistry and thus temporal variability in ground and surface water interaction.

- Local scale temporal investigations, presented in Chapter five, utilised exisiting low resolution data from the Waiohine and Mangatarare streams in an attempt to link ground and surface water bodies using HCA and similarities in hydrochemistry. However, this investigation offered little insight into the temporal nature of ground and surface water interaction due to the monthly and quarterly timescales at which sampling was undertaken. It was extremely difficult to identify parallel temporal changes in water quality between ground and surface water bodies using the available data. This highlighted the need for more frequent hydrochemical monitoring to establish the temporal extent of chemical change in surface and groundwaters.

- Chapter six presented a high resolution temporal field investigation from the Mangatarere stream and neighbouring groundwater bodies. Results indicate ground and surface water interaction was occuring during the period JD324-051. This interaction was spatially variable with the upstream Mangatarere showing overall influent properties while the downstream Mangatarere showed an overall effluent system. Reduced downstream surface water temperatures and elevated NO_3^-, Cl^- and Na^+ concentrations suggest the provision of a higher proportion of base flow to the downstream surface water gauging station from groundwater sources. Mass balance calculations suggest *ca.* 30-60% of downstream surface water base flow is provided by the neighbouring groundwater system. The proportion of this groundwater provided base flow can vary signficantly and over short timescales (e.g. daily). This interaction between downstream surface and groundwater bodies appeared to display temporal variability with the downstream system switching to an influent system during the period *ca.* JD004-018.

This occurred during a relatively dry period (low precipitation) when groundwater stage levels were heavily reduced. This highlights the importance of meteorological conditions in controlling the interaction of surface and groundwater interaction in the downstream reaches.

- The upstream groundwater station received recharge primarily from rainfall as indicated by elevated NO_3^-, Cl^- and Na^+ concentrations. However, concurrent ground and surface water stage increases suggest recharge may also have been provided by the upstream Mangatarere stream during high flow events on JD336-338, 350-353 and 021-028. It is very hard to differentiate between rainfall and river recharge using stage and precipitation data alone. The occurance of river recharge to the upstream groundwater system during the period JD026-028 is supported by the transfer of the upstream Mangatarere's diurnal temperature pattern and chemical signature to the groundwater station. Further, it appeared the extended high flow event during this period may have resulted in the transfer of surface waters to the groundwater system, highlighting the importance of flow duration as opposed to magnitude, in initiating potential ground and surface water interaction. Mass balance calculations suggest 5-50% of upstream surface water discharge is lost to the underlying groundwater system, the majority of which is lost during high flow events.

- Results obtained from the four gauging stations showed solute concentrations displayed noticeable variability during the intensive sampling programme (JD021-028). In particular Na^+, SO_4^{2-}, Mn, Fe^{2+}, K^+ and the nutrients NO_3^- and NH_4^+ fluctuated significantly at one or more sites. This highlights the temporal variability of solute concentrations in both surface and groundwaters in the Mangatarere catchment and suggests current monitoring programmes conducted by the GWRC may fail to capture this variability.

Further, the range of solute concentrations obtained from the downstream surface water gauging station generally fell outside the 25^{th} to 75^{th} quartile of concentrations obtained by the GWRC during their monthly sampling programme for the 2008 year. This further highlights the potentially misrepresentative results obtained by the GWRC monitoring programme for the Mangatarere stream.

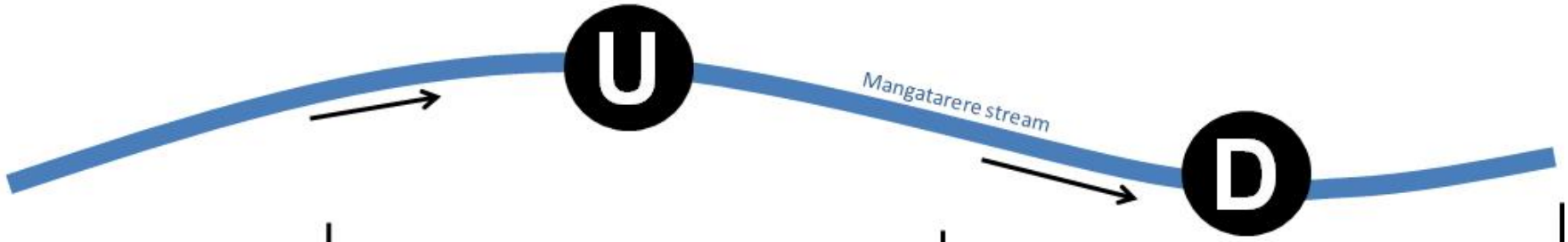

Method or variable	Upstream Mangatarere (influent)		Downstream Mangatarere (largely effluent)	
Regional scale (Chap 4)	✗	No upstream surface water site analysed	✓	Downstream surface water station grouped with similar Na-Cl-NO3 groundwaters
Local scale temporal (Chap 5)	✗	Monthly & quarterly data hard to interpret	✗	Monthly & quarterly data hard to interpret
Water temp (Chap 6)	✓	Diurnal water temperature JD026-028 suggest GW recharge from SW	✓	Subdued diurnal water temp, input of colder waters from groundwaters
Water stage (Chap 6)	–	Concurrent GW-SW stage increases but hard to differentiate from precipitation driven increase	✓	Downstream SW stage decreased below upstream stage suggesting a switch to influent conditions
Conductivity (Chap 6)	–	Concurrent GW-SW conductivity decreases but hard to differentiate from precipitation inputs	✓	Higher downstream surface water conductivity suggests input of solute rich groundwaters
Water chemistry (Chap 6)	✓	During events JD021-028 dilute waters enter upstream GW station, chem signature resembles SW	✓	Na, Cl, NO3 transferred from groundwaters to downstream surface water station

✓ **Strong inferences can be made** – **Some inferences can be made** ✗ **No inferences can be made**

Figure 7.1. Simplified schematic representation of the main findings surrounding the Mangatarere stream and neighbouring groundwaters from the three methods (regional, local scale temporal and high resolution local scale) employed in this research. The local scale high resolution investigation is assessed in terms of the variables water temperature, stage, conductivity and water chemistry. Each method or variable is assessed in terms of the information and/or inferences it provided to this investigation and the determination of ground and surface water interaction in the Mangatarere stream catchment. Arrows indicate the flow direction of the Mangatarere stream while 'U' and 'D' symbols denote upstream and downstream gauging locations respectively.

7.2 Avenues for future research

Although this research provided some insight into the interaction between ground and surface water bodies and presented a potential method (HCA) for identifying this interaction in the Wairarapa valley and other regions throughout New Zealand, there are still a number of avenues for future research. These avenues are presented in the following two sections. This research investigated ground and surface water interaction over a three month period during the summer, however the processes surrounding this interaction and the spatial and temporal scales at which this interaction occurs is still not fully understood.

A number of research topics and question that were only briefly touched on in this research and that require further attention include:

- This investigation attempted to identify the interaction of ground and surface water through solute dynamics of entire water bodies. However, solute concentrations are known to change as water moves across the stream-aquifer boundary. Two research questions are: 1) How do solute concentrations change as they move across this boundary? 2) How do solute concentrations vary spatially within an aquifer, in particular with distance from recharge source?
- Further insight regarding ground and surface water interaction in the Mangatarere stream catchment could be obtained with water age dating techniques (e.g. isotope data). 1) How old are waters in the Mangatarere stream and neighbouring groundwater bodies and 2) Can water age be used to infer the origins and pathways of different interacting water bodies within the Mangatarere catchment?
- HCA analysis identified areas of potential chemical interaction in the Wairarapa valley. Can this method be applied across other individual regions within New Zealand or at a nationwide scale?
- Future research is required to investigate high resolution temporal variations in ground and surface water interaction over longer time periods such as seasons or years. This research was undertaken during the summer months when ground and surface water levels are known to be lowest.

How do temporal dynamics surrounding this interaction change during the winter when surface water levels are substantially higher? Are strong seasonal patterns present in this interaction within the Mangatarere stream?

A similar methodology to that undertaken during the high resolution field investigation (Chapter six) plus additional monitoring (e.g. soil moisture) could be employed for a longer duration to investigate these questions.

- The distance between the upstream ground and surface water gauging stations was *ca.* 200 metres. Is it possible that this distance was too great and that significant changes in water chemistry, the result of interaction, were buffered by the natural system? To investigate this questions one could establish a monitoring network of piezometers that evaluated spatial changes in groundwater chemistry from the stream to the groundwater gauging station.

7.3 Recommendations

Results from the regional scale investigation (Chapter four) and high resolution local scale investigation (Chapter six) suggest the provision of base flow to the downstream Mangatarere stream from neighbouring groundwater bodies and the transfer of nutrients to this river system. This interaction has potential implications for water quality at the downstream Mangatarere site; in particular as agriculture continues to intensify in the Mangatarere catchment. Currently the concentrations of nutrients in both surface and groundwaters in the Mangatarere catchment are relatively low and comply with New Zealand drinking water standards, however as land use continues to intensify these concentrations are likely to increase. High resolution hydrochemical monitoring undertaken during the period JD021-028 showed concentrations of these nutrients can change within daily and hourly periods, a result likely influenced by the interaction between ground and surface water bodies. Therefore, environmental management decisions, in regards to agriculture runoff, need to account for the relatively fast transfer of these nutrients through the downstream system and the implication this may have on long term water quality issues.

Purging of the groundwater wells prior to hydrochemical sampling resulted in an immediate decrease in groundwater conductivity as new dilute waters were drawn from within the aquifer into the well casing (see Section 6.3.4). This research did not investigate the potential impact this pumping may have on the chemical composition of subsequent grab samples, however, it is possible that collected grab samples were affected. As a result further research is needed to elucidate the impact of well purging on hydrochemical sampling, in particular for current environmental monitoring programmes undertaken by the GWRC and for national SoE monitoring. Do solute concentrations change within the timeframe that a groundwater well is purged? In order to investigate this limitation continuous purging of a well could be undertaken with extracted waters analysed to determine temporal changes in solute concentrations.

Results from this research suggest the Mangatarere stream displayed both influent and effluent interacting properties that vary with time due to temporal variability in meteorological and hydrological parameters. There is still much to learn about the Mangatarere system and its interaction with underlying groundwaters. Can the boundary between these interacting systems be defined and does this boundary display a temporal regime that shifts with the seasons or meteorological conditions? In order to investigate these questions further ground and surface water gauging stations could be installed along the entire length of the Mangatarere stream, in particular the middle reaches. Further, the potential temporal variability in ground and surface water interaction in the area needs to be investigated to a greater extent and incorporated into the Wairarapa regional flow model currently being developed by the GWRC. Daily and sub-daily variations in precipitation, soil moisture conditions and water stage should be included in such a model in order to predict possible temporal scenarios in ground and surface water interaction and the variables that influence it.

The loss of the downstream groundwater gauging station was a major limitation to this project and highlights the need to factor instrumentation redundancies into any real-time monitoring network. It is recommended that future monitoring programmes include a greater number of gauging stations to allow for the loss of some stations and therefore datasets.

Further, monitoring programmes such as that undertaken in this research should be applied to a number of catchments where ground and surface water interaction is thought to be occurring in order to increase one's understanding of such interacting systems. A wider set of meteorological parameters (e.g. evaporation, soil moisture conditions, etc) should also be investigated and included in such monitoring programmes as it appears these parameters play a major role in influencing ground and surface water interactions.

Ground and surface water interaction is likely to be occurring in a number of regions throughout New Zealand, in particular in areas containing highly permeable alluvial sediments and large fluvial systems such as the Canterbury and Otago plains. These areas are of particular importance for agricultural production and therefore issues surround the transfer of agricultural contaminants between ground and surface water bodies. The regional scale methodology, employed in Chapter four, could be used to identify potential areas of ground and surface water interaction in these regions using existing data. Upon their identification these areas could be further investigated with high resolution monitoring such as that undertaken in Chapter six. This would allow regional councils and national research institutions (e.g. NIWA and GNS) to gain a greater understanding of these interacting systems and the spatial and temporal extent of their operation. This would benefit the design, implementation and outcome of both current and new environmental monitoring programmes and facilitate more informed environmental management decisions.

References

Alther, G.A., 1989. A simplified statistical sequence applied to routine water quality analysis: A case history, *Ground water,* 17**,** 556-561.

Amoros, C., Roux, A.L., Regrobellet, J.L., Bravard, J.P. & Pautou, G., 1987. A method for applied ecological studies of fluvial hydrosystems, *Regulated rivers,* 1**,** 17-36.

Atteia, O., Andre, L., Dupuy, A. & Franceschi, M., 2005. Contributions of diffusion, dissolution, ion exchange, and leakage from low-permeability layers to confined aquifers, *Water Resources Research,* 41.

Back, W., 1966. Hydrochemical facies and groundwater flow patterns in northern part of Atlantic Coastal plain. *in U.S. Geol. Sur. Prof. Paper* pp. 42.

Baver, L.D., 1940. *Soil Physics* edn, Vol., pp. Pages, John Wiley & Sons, Inc, London.

Beadel, S., Perfect, A., Rebergen, A. & Saywer, J., 2000. Wairarapa Plains Ecological District Report,Department of Conservation, Wellington

Bear, J., 1979. *Hydraulics of Groundwater,* edn, Vol., pp. Pages, Dover Publications, Mineola

Begg, J.G., Brown, L.J., Gyopari, M. & Jones, A., 2005. A review of Wairarapa geology - with a groundwater bias,Institute of Geological and Nuclear Science Wellington.

Berner, E.K. & Berner, R.A., 1996. *Global environment: Water, air and geochemical cycles,* edn, Vol., pp. Pages, Prentice-Hall, Inc, New Jersey.

Brunke, M. & Gonser, T., 1997. The ecological significance of exchange processes between rivers and groundwater *Freshwater Biology,* 37**,** 1-33.

Burden, R.J., 1982. Hydrocemical variation in a water-table aquifer beneath grazed pastureland *Journal of Hydrology (NZ),* 21**,** 61-75.

Butturini, A., Bernal, S. & Nin, E., 2003. Influences of the stream groundwater hydrology on nitrate concentration in unsaturated riparian area bounded by an intermittent Mediterranean stream, *Water Resources Research,* 39**,** 1-12.

Campbell, G.S., 1985. *Soil Physics with basic transport models for soil-plant systems,* edn, Vol., pp. Pages, Elsevier Scientific Publishing Company Inc., New York.

Campbell_Scientific, I., 2007. Model 107 Temperature probe. *in Instruction Manual,* pp. 1-12.

Cey, E.E., Rudolph, D.L., Parkin, G.W. & Aravena, R., 1998. Quantifying groundwater discharge to a small perennial stream in southern Ontario, Canada, *Journal of Hydrology,* 210**,** 21-37.

Chapman, S.W., Parker, B.L., Cherry, J.A., Aravena, R. & Hunkeler, D., 2007. Groundwater-surface water interaction and its role on TCE groundwater plume attenuation,, *Journal of Contaminant Hydrology,* 91**,** 203-232.

Chebotarev, I.I., 1955. Metamorphism of natural waters in the crust of weathering,, *Geochemica et Cosmochimica Acta,* 8**,** 22-48.

Cheeney, R.F., 1983. *Statistical methods in Geology* edn, Vol., pp. Pages, George Allen & Unwin Ltd London.

Constanz, J., 1998. Interaction between stream temperature, streamflow and groundwater exchanges in alpine streams., *Water Resources Research,* 34**,** 1609-1615.

Dahan, O., Tatarsky, B., Kulls, C., Seely. M. & Benito, G., 2008. Dynamics of flood water infiltration and groundwater recharge in Hyperarid Desert, *Ground Water,* 46**,** 450-461.

Dahm, C.N., Grimm, N.B., Marmonier, P., Valette, H.M. & Vervier, P., 1998. Nutrient dynamics at the interface between surface waters and groundwaters, *Freshwater Biology,* 40**,** 427-451.

D'Angerlo, D.J., Webster, J.R., Gregory, S.V. & Meyer J.L., 1993. Transient storage in Appalachian and Cascade mountain streams as related to hydraulic characteristics, *Journal of North American Benthological Society,* 12**,** 223-235.

Daughney, C.J. & Reeves, R.R., 2005. Definition of hydrochemical facies in the New Zealand National Groundwater Monitoring Programme, *Journal of Hydrology (NZ),* 44**,** 104-130.

Daughney, C.J. & Reeves, R.R., 2006. Analysis of temporal trends in New Zealand's groundwater quality based on data from the National Groundwater monitoring Programme., *Journal of Hydrology (NZ),* 45**,** 41-62.

DeWiest, R.J.M., 1965. Dispersion and salt water intrusion, *unknown***,** 39-44.

Dravid, P.N. & Brown, L.J., 1997. Heretaunga Plains Groundwater. Study volume 1: Findings,Hawkes Bay Regional Council., Napier.

Duque, C., Calvache, M.L. & Engesgaard, P., 2010. Investigating river-aquifer relations using water temperature in an anthropized environment, *Journal of Hydrology,* 381**,** 121-133.

Eberts, S.M., Jones, S.A., Braun, C.L. & Harvey, G.J., 2005. Long term changes in groundwater chemistry at a Pytoremediation demonstration site, *Ground Water,* 43**,** 178-186.

EPA, U.S.E.P.A., 2000. Proceedings of the Ground-Water/Surface-Water Interactions Workshop. *in Ground-Water/Surface-Water Interactions Workshop*, Washington, DC.

Findlay, A., 1958. *Introduction to physical chemistry*, 3rd edn, Vol., pp. Pages, Longmans London.

Freeze, R.A. & Cherry, J.A., 1979. *Groundwater*, edn, Vol., pp. Pages, Prentice-Hall. Inc, New Jersey.

Glagoleva, M.A., 1958. Forms of trace element migration in river waters *Doklady AN SSSR*, 121**,** 1052-1055.

Gooseff, M.N., McKnight, D.M., Lyons, W.B. & Blum, A.E., 2002. Weathering reactions and hyporheic exchange controls on stream water chemistry in a glacial meltwater stream in the McMurdo Dry Valleys, *Water Resources Research*, 38.

Gregory, S.V., Swanson, F.J., McKee, W.A. & Cummins, K.W., 1991. An ecosystem perspective of riparian zones *Bioscience* 41**,** 540-551.

Güler, C., Thyne, G.D. & McCray, J.E., 2002. Evaluation of graphical and multivariate statistical methods for classification of water chemistry data *Hydrogeology Journal*, 10**,** 455-474.

Haag, I. & Westrich, B., 2002. Processes governing river water quality identified by principal component analysis, *Hydrological Processes*, 16**,** 3113-3130.

Hair, J.F., Black, W.C., Babin, B.J., Anderson, R.E. & Tatham, R.L., 2006. *Multivariate Data Analysis*, 6th edn, Vol., pp. Pages, Prentice Hall, Inc New Jersey.

Hawke, R., McConchie, J. & Trueman, T., 2000. *Wairarapa irrigation study: moisture availability as a result of the climate* edn, Vol., pp. Pages, Victoria

University of Wellington, Wellington.

Heine, J.C., 1975. Interim report on soils of Wairarapa valley, New Zealand *in New Zealand Soil Bureau Record,* Department of Scientific and Industrial Research, New Zealand

Helsel, D.R. & Cohn, T.A., 1988. Estimation of descriptive statistics for multiply censored water quality data, *Water Resources Research,* 24**,** 1997-2004.

Hiscock, K., 2005. *Hydrogeology: Principles and practice,* edn, Vol., pp. Pages, Blackwell Science Ltd, Oxford.

Holloway, J.M. & Dahlgren, R.A., 2001. Seasonal and event-scale variations in solute chemistry fro four Sierra Nevada catchments, *Journal of Hydrology,* 250**,** 106-121.

Hooper, R.P., Christophersen, N. & Peters, N.E., 1990. Modelling streamwater chemistry as a mixture of soil water end members - an application to the Panola Mountain Catchment,, *Journal of Hydrology,* 116**,** 321-343.

Hussain, M., Ahmed, S.M. & Abderrahman, W., 2008. Cluster analysis and quality assessment of logged water at an irrigation project, eastern Saudi Arabia, *Journal of Environmental Management* 86**,** 297-307.

Ingebritsen, S., Sanford, W. & Neuzil, C., 2006. *Groundwater in Geologic Processes* 2nd edn, Vol., pp. Pages, Cambridge University Press, Cambridge.

Jagannadha Sarma, V.V., Prasad, N.V. & Prasad, R., 1979. The effect of hydrogeology on variations in electrical conductivity of groundwater fluctuations *Journal of Hydrology,* 44**,** 81-87.

Jenkins, A., Norman, P.E. & Rodhe, A., 1994. Hydrology *in Biogeochemistry of small catchments: A tool for environmental research,* eds. Moldan, B. & Cerny, J. John Wiley & Sons, Ltd, Chichester

Jolly, I.D., McEwan, K.L. & Holland, K.L., 2008. A review of groundwater-surface water interactions in arid/semi-arid wetlands and the consequences of salinity for wetland ecology, *Ecohydrology,* 1**,** 43-58.

Jones, A. & Baker, T., 2005. Groundwater monitoring technical report.Greater Wellington Regional Council., Wellington

Jones, A. & Gyopari, M., 2006. Regional conceptual and numerical modelling of the Wairarapa groundwater basin, Greater Wellington Regional Council,, Wellington.

Kamp, P.J.J., 1992 Landforms of Wairarapa: A Geological Perspective. *in Landforms of New Zealand,* eds. Soons, J. M. & Selby, M. J. Longman Paul Ltd, Auckland.

Kedziorek, M.A., Geoffriau, S. & Bourg, A.C.M., 2008. Organic matter and modeling redox reactions during river bank filtration in an alluvial aquifer of the Lot River, France, *Environmental Science and Technology,* 42**,** 2793-2798.

Keenan, L. & Gordon, M., 2008. Annual hydrology monitoring report for the Wellington Region, 2008/2009,Greater Wellington Regional Council Wellington.

Keery, J., Binley. A., Crook, N. & Smith, J.W.N., 2007. Temporal and spatial variability in groundwater-surface water fluxes: Development and application of an analytical method using temperature time series, *Journal of Hydrology,* 3**,** 1-16.

Kegley, S.E. & Andrews, J., 1998. *The chemistry of water,* edn, Vol., pp. Pages, University Science Books, Sausalito.

Kim, J., Yum, B., Kim, R., Koh, D., Cheong, T., Lee, J. & Chang, H., 2003. Application of clusters analysis for the hydrogeochemical factors of saliine groundwater in Kimje, Korea., *Geosciences Journal* 7**,** 313-322.

Kirchner, J.W., 2006. Getting the right answers for the right reasons: Linking measurements, analyses and models to advance the science of hydrology, *Water Resources Research,* 42.

Kirchner, J.W., Feng, X. & Neal, C., 2001. Catchment scale advection and dispersion as a mechanism for fractal scaling in stream tracer concentrations, *Journal of Hydrology,* 254**,** 82-101.

Kondolf, G.M., Maloney, L.M. & Williams, J.G., 1986. Effects of bank storage and well pumping on base flow, Carmel River, Monterey County, California *Journal of Hydrology,* 91**,** 351-369.

Kruskal, W.H. & Wallis, A.W., 1952. Use of ranks in one-criterion variance analysis, *Journal of American Statistical Association,* 47**,** 583-621.

Kumar, M., Ramanathan, A. & Keshari, A.K., 2009. Understanding the extent of interactions between groundwater and surface water through major ion chemistry and multivariate statistical techniques, *Hydrological Processes,* 23**,** 297-310.

Lamberti, G.A., Gregory, S.V., Ashkenas, L.R., Wildman, R.C. & Steinman, A.D., 1989. Influence of channel morphoogy on retention of dissolved and particulate matter in a Cascade mountain stream. *in Californian Riparian Systems Conference: Protection, Management, and Restoration for the 1990's,*, pp. 33-39, ed Abell, D. L. U.S. Department of Agriculture, Berkeley

Langmuir, D., 1997. *Aqueous Environmental Geochemistry* edn, Vol., pp. Pages, Prentice-Hal, Inc., New Jersey.

Laudon, H. & Slaymaker, O., 1997. Hydrograph separation using stable isotopes, silica and electrical conductivity: an alpine example *Journal of Hydrology,* 201**,** 82-101.

Lewandowski, J. & Nutzmann, G., 2008. Surface water-groundwater interactions: hydrological and biochemical processes at the lowland River Spree (Germany). *in Groundwater-Surface Water Interaction: Process Understanding, Conceptualization and Modelling*, pp. 30-38, eds. Abesser, C., Wagener, T. & Nuetzmann, G. International Association of Hydrological Sciences, Oxford.

Lu, X., Jin, M., van Genuchten, M.T. & Wang, B., 2010. Groundwater recharge at five representative sites in the Hebei Plain, China, *Ground Water,* Accecpted, awaiting publication

Maidment, D.R., 1993. Hydrology *in Handbook of Hydrology,* ed. Maidment, D. R. McGraw-Hill, Inc, New York.

Maybeck, M., 1979. Concentrations des eaux fluviales en elements majeurs et apports en solution aux oceans, *Rev. Geol. Dyn. Phys.*, 21**,** 215-246.

McConchie, J., 2000. From shaky beginnings. *in Dynamic Wellington: A contemporary synthesis and explanation of Wellington*, eds. McConchie, J., Winchester, D. R. & Willis, R. Institute of Geography: Victoria University of Wellington, Wellington.

McLaren, R.G. & Cameron, K.C., 1996. *Soil Science* edn, Vol., pp. Pages, Oxford University Press Melbourne.

McLintock, H.A., 1966. Geology - land districts of New Zealand. *in The Encyclopedia of New Zealand*.

Merkel, B.J. & Planer-Friedrich, B., 2008. *Groundwater Geochemistry: A practical guide to modeling of natural and contaminated aquatic systems,* 2nd edn, Vol., pp. Pages, Springer, Berlin.

Mills, W.B., Liu, S. & Fong, F.K., 1991. Literature Review and Model (COMET) for Colloid/Metals Transport in Porous Media, *Ground Water,* 29**,** 199-208.

Mitsch, W.J. & Gosselink, J.G., 2007. *Wetlands,* edn, Vol., pp. Pages, John Wiley & Sons, Inc, Hoboken.

Morel, F.M.M. & Hering, J.G., 1998. *Principles and Applications of Aquatic Chemistry,* edn, Vol., pp. Pages, John Wiley & Sons, New York.

Morgan, C.O. & Winner, M.D., 1962. Hydrochemical facies in the 400 foot and 600 foot sands of the Baton Rouge Area, Louisiana,. *in US Geological Survey Professional Paper 450-B.,* pp. 120-121, US Geological Society.

Morgan, M. & Hughes, B., 2001. Wellington. *in Groundwaters of New Zealand*, pp. 397-410, eds. Rosen, M. R. & White, P. NZ Hydrological Society, Wellington.

Mulholland, P.J., 1993. Hydrometric and stream chemistry evidence of three storm flow paths in Walker Branch Watershed, *Journal of Hydrology,* 141**,** 291-316.

Negrel, P., Petelet-Giruad, E. & Gautier, E., 2003. Surface water-groundwater interactions in an alluvial plain: Chemical and isotopic systematics, *Journal of Hydrology,* 227**,** 248-267.

NIWA, 2008. Cliflow- The National Climate Database New Zealand. National Institute of Water and Atmospheric Research, New Zealand.

O'Driscoll, M.A. & DeWalle, D.R., 2006. Stream-air temperature relations to classify stream-groundwater interactions in a karst setting, central Pennsylvania, USA., *Journal of Hydrology,* 329**,** 140-153.

Ojiambo, B.S., Poreda, R.J. & Berry Lyons, W., 2005. Groundwater/surface water interactions in Lake Naivasha, Kenya *Ground water* 39**,** 526-533.

Orwin, J.F. & Smart, C.C., 2004. Short-term spatial and temporal patterns of suspended sediment transfer in proglacial channels, Small River Glacier, Canada, *Hydrological Processes,* 18**,** 1521-1542.

Oxtobee, J.P.A. & Novakowski, K., 2002. A field investigation of groundwater/surface water interaction in a fractured bedrock environment *Journal of Hydrology,* 269**,** 169-193.

Pekny, V., Skorepa, J. & Vrba, J., 1989. Impact of nitrogen fertilisers on groundwater quality- some examples from Czechoslovakia, *Journal of Contaminant Hydrology,* 4**,** 51-67.

Pinder, G.F. & Celia, M.A., 2006. *Subsurface hydrology,* edn, Vol., pp. Pages, Wiley-Interscience, Hoboken, New Jersey.

Priestly, M.B., 1981. *Spectral Analysis and Time Series,* edn, Vol., pp. Pages, Academic Press, unknown.

Raiswell, R., 1984. Chemical models of solute acquisition in glacial melt waters *Journal of Glaciology* 30**,** 49-57.

Reeves, R.R., Morgenstern, U., Daughney, C.J., Stewart, M.K. & Gordon, M., 2008. Identifying leakage to groundwater from Lake Rerewhakaaitu using isotopic and water quality data, *Journal of Hydrology (NZ),* 47**,** 85-106.

Reilly, T.E. & Gibs, J., 1993. Effects of physical and chemical heterogeneity on water quality samples obtained from wells, *Ground Water,* 31**,** 805-813.

Reilly, T.E. & Leblanc, D.R., 1998. Experimental evaluation of factors affecting temporal variability of water samples obtained from long-screened wells, *Ground Water,* 36**,** 566-576

Rice, K.C. & Bricker, O.P., 1995. Seasonal cycles of dissolved constituents in streamwater in two forested catchments in the mid-Atlantic region of the eastern USA, *Journal of Hydrology,* 170**,** 137-158.

Riihimaki, C.A., MacGregor, K.R., Anderson, R.S., Anderson, S.P. & Loso, M.G., 2005. Sediment evacuation and glacial erosion rates at a small alpine glacier, *Journal of Geophysical Research,* 110**,** 1-17.

Ritter, D.F., 1978. *Process Geomorphology* edn, Vol., pp. Pages, Wm. C. Brown Company Publishers Iowa.

Rogerson, P.A., 2006. *Statistical methods for Geography: A student guide,* edn, Vol., pp. Pages, SAGE Publications Ltd London.

Romesburg, C., 1984. *Cluster analysis for researchers,* edn, Vol., pp. Pages, Lulu Print, North Carolina

Rosen, M.R., Bright, J., Carran, P., Stewart, M.K. & Reeves, R.R., 1999. Estimating rainfall recharge and soil water residence times in Pukekohe, New Zealand by combining geophysical, chemical and isotopic methods, *Ground Water,* 37**,** 836-844.

Rosenthal, E., 1987. Chemical composition of rainfall and groundwater in recharge areas of the Bet Shean-Harod Multiple aquifer system, Israel, *Journal of Hydrology,* 89**,** 329-352.

Rozemeijer, J.C. & Broers, H.P., 2007. The groundwater contribution to surface water contamination in a region with intensive agricultural land use (Noord-Brabant, The Netherlands),, *Environmental Pollution,* 148**,** 695-706.

Saffigna, P.G. & Keeney, D.R., 1977. Nitrate and Chloride in Groundwater under irrigated agriculture in Central Wisconsin, *Ground Water*, 15**,** 170-177.

Scanlon, B.R., 1989. Physical controls on Hydrochemical variability in the Inner Bluegrass Karst Region of Central Kentucky *Ground Water*, 27**,** 639-646.

Schmalz, B., Springer, P. & Fohrer, N., 2007. Interactions between near-surface groundwater and surface water in a drained riparian wetland. *in Groundwater-Surface Water Interaction: Process Understanding, Conceptualization and Modelling*, pp. 21-29, eds. Abesser, C., Wagener, T. & Nuetzmann, G. International Association of Hydrological Sciences, Oxford.

Schmalz, R.F., 1972. Calcium Carbonate: Geochemistry. *in The Encyclopedia of Geochemistry and Environmental Science*, ed. Fairbridge, R. W. Litton Educational Publishing, Inc, New York.

Schwartz, F.W. & Zhang, H., 2003. *Fundamentals of Groundwater*, edn, Vol., pp. Pages, John Wiley & Sons, Inc, New York.

Semkin, R.G., GJeffries, D.S. & Clair, T.A., 1994. Hydrochemical methods and relationships for study of stream output from small catchments. *in Biogeochemistry of small catchments: A tool for environmental research*, eds. Moldan, B. & Cerny, J. John Wiley & Sons Ltd.

Silliman, S.E. & Booth, D.F., 1993. Analysis of timeseries measurements of sediment temperature for identification of gaining vs. losing portions of Juday Creel, Indiana *Journal of Hydrology*, 146**,** 131-148.

Smart, C.C., 1992. Temperature compensation of electrical conductivity in glacial meltwaters, *Journal of Glaciology*, 38**,** 9-12.

Smith, D.G. & Maasdam, R., 1994. New Zealand's National River Water Quality Network 1. Design and physico-chemical characterisation, *New Zealand Journal of Marine and Freshwater Research,* 28**,** 19-35.

Sophocleous, M., 2002. Interactions between groundwater and surface water: the state of science, *Hydrogeology Journal,* 10**,** 52-67.

Steefel, C.I., 2008. 11 Geochemical Kinetics and Transport *in Kinetics of rock-water interaction* pp. 545-589, eds. Brantley, S. L., Kubicki, J. D. & White, A. R. Springer New York.

Stewart, M.K., Hong, T.Y.S., Cameron, S.C., Daughney, C.J., Tait, T. & Thomas, J.T., 2003. Investigation of groundwater in the Upper Motueka River Catchment, Institute of Geological and Nuclear Science (GNS), Lower Hutt.

Storey, R.G., Howard, K.W.F. & Williams, D.D., 2003. Factors controlling riffle-scale hyporheic exchange flows and their seasonal changes in a gaining stream: A three-dimensional groundwater flow model,, *Water Resources Research,* 39.

Stumm, W. & Morgan, J.J., 1996. *Aquatic Chemistry,* edn, Vol., pp. Pages, John Wiley & Sons, Inc., New York.

Taylor, C.B., Wilson, D.D., Brown, L.J., Stewart, M.K., Burden, R.J. & Brailsford, G.W., 1989. Sources and flow of North Canterbury Plains Groundwater, New Zealand, *Journal of Hydrology,* 106.

Thompson, C.S., 1982. The weather and climate of the Wairarapa region. *in New Zealand Meteorological Service* Ministry of Transport, Wellington

Timm, N.H., 2002. *Applied multivariate statistics,*, edn, Vol., pp. Pages, Springer-Verlag Inc., New York.

Todd, D.K. & Mays, L.W., 2005. *Groundwater Hydrology,* edn, Vol., pp. Pages, John Wiley & Sons, Inc, Hoboken.

Toth, J., 1963. A theoretical analysis of groundwater flow in a small drainage basin, *Journal of Geophysical Research,* 68**,** 4795-4812.

Townend, J., 2002. *Practical Statistics for Environmental and Biological Scientists,* edn, Vol., pp. Pages, John Wiley & Sons, Ltd West Sussex

Tranter, M., Brown, G.H., Raiswell, R., Sharp, M.J. & Gurnell, A., 1993. A conceptual model of solute acquisition by Alpine glacial meltwaters *Journal of Glaciology,* 39**,** 573-581.

Tweed, S., Leblanc, M. & Cartwright, I., 2009. Groundwater-surface water interaction and the impact of a multi-year drought on lake conditions in South-East Australia *Journal of Hydrology,* 379**,** 41-53.

von Gunten, H.R., Karametaxas, G., Krahenbuhl, U.m., Kuslys, M., Giovanoli, R., Hoehn, E. & Keil, R., 1991. Seasonal biogeochemical cycles in riverborne groundwater,, *Geochemica et Cosmochimica Acta,* 55**,** 3597-3609.

Venugopal, T., Giridharan, L. & Jayaprakash, M., 2008. Groundwater quality assessment using Chemometric analysis in the Adyar River, South India., *Arch Environ Contam Toxicol,* 55**,** 180-190.

Verhoeven, W., Hermann, R., Eiden, R. & Klemm, O., 1987. A comparison of the chemical composition of fog and rainwater collected in the Fichtelgebirge, Federal Republic of Germany and from the South Island of New Zealand, *Theoretical and Applied Climatology,* 38**,** 210-221.

Vidon, P., Hubbard, L.E. & Soyeux, E., 2009. Seasonal solute dynamics across land uses during storms in glaciated landscape of the US Midwest, *Journal of Hydrology,* 376**,** 34-37.

Ward, J.H., 1963. Hierarchical grouping to optimise an objective function, *Journal of American Statistical Association,* 58**,** 236-244.

Ward, J.V. & Stanford, J.A., 1982. Thermal responses in the evolutionary ecology of aquatic insects *Annual Review of Entomology,* 27**,** 105-111.

Watts, L., 2005. Hydrological monitoring technical report.Greater Wellington Regional Council., Wellington.

Watts, L. & Gordon, M., 2008. Annual hydrology monitoring report for the Wellington region, 2007/2008,Greater Wellington Regional Council, Wellington.

Wilson, L.C. & Rouse, J.V., 1983. Variations in water quality during initial pumping of monitoring wells, *Ground Water Monitoring Review,* 3**,** 103-109.

Winter, T.C., Harvey, J.W., Franke, O.L. & Alley, W.M., 1998. Groundwater and surface water: A single resource, ed Survey, U. G. U.S. Government Printing Office, Denver, Colorado.

Woessner, W.W., 2000. Stream and fluvial plain ground water interactions: Rescaling Hydrogeologic thought, *Ground Water,* 38**,** 423-429.

Wollschlager, U., Ilmberger, J., Isenbeck-Scroter, M., Kreuzer, A.M., vo Rohden, C., Roth, K. & Schafer, W., 2007. Coupling of groundwater and surface water at Lake Willersinnweiher: Groundwater modeling and tracer studies *Aquatic Science***,** 138-152.

Woocay, A. & Walton, J., 2008. Multivariate analyses of water chemistry: surface and groundwater interactions, *Ground Water,* 46**,** 437-449.

Younger, P.L., 2007. *Groundwater in the Environment: an introduction,* edn, Vol., pp. Pages, Blackwell Publishing Ltd, Malden.

Appendix A
Full list of hydrochemical analytes

The hydrochemical database was made up of the following water quality variables:

- Water temperature (°C)
- Lab conductivity (µS/cm)
- Field conductivity (µS/cm)
- E-Coli (cfu / 100mL)
- Alkalinity (mg/L)
- Total chloride (mg/L)
- Total magnesium (mg/L)
- Lab pH (-)
- Total dissolved solids (mg/L)
- Total organic carbon (mg/L)
- Nitrite nitrogen (mg/L)
- Nitrate nitrogen (mg/L)
- Dissolved reactive phosphorus (mg/L)
- Total alkalinity (mg/L)
- Bicarbonate (mg/L)
- Total boron (mg/L)
- Bromide (mg/L)
- Fluoride (mg/L)
- Dissolved reactive silica (mg/L)
- Sulphate (mg/L)
- Total calcium (mg/L)
- Total sodium (mg/L)
- Total hardness (mg/L)
- Total potassium (mg/L)
- Dissolved zinc (mg/L)
- Faecal coliforms (cfu / 100mL)
- Total coliforms (cfu / 100mL)
- Ammoniacal nitrogen (mg/L)
- Field pH (-)
- Field dissolved oxygen (%)
- Lab dissolved oxygen (%)
- Total cations (mg/L)
- Total anions (mg/L)
- Ionic balance error (%)
- Free carbon dioxide (mg/L)
- Dissolved boron (mg/L)
- Dissolved calcium (mg/L)
- Dissolved magnesium (mg/L)
- Dissolved potassium (mg/L)
- Dissolved sodium (mg/L)
- Total oxidized nitrogen (mg/L)
- Dissolved chloride (mg/L)
- Dissolved iron (mg/L)
- Total lead (mg/L)
- Total manganese (mg/L)
- Dissolved manganese (mg/L)
- Dissolved arsenic (mg/L)

Appendix B
Charge balance error results

Table C.1. Ground and surface water monitoring sites Wairarapa valley, New Zealand and associated Charge Balance Error (CBE) and CBE rating. CBE rating is dependent on whether CBE falls within the ±10% range limit. 'No CBE' denotes when a CBE could not be calculated for a particular site due to one or more missing parameters.

Site	Water type	CBE	Is CBE acceptable?
Beef Creek at h	Surface	-3.52	OK
Enaki Stream D/	Surface	No CBE	
Enaki Stream U/	Surface	No CBE	
Huangarua River	Surface	-3.61	OK
Kopuaranga Stre	Surface	-0.84	OK
Lake Wairarapa	Surface	34.91	**High (CBE > ± 10%)**
Lake Wairarapa	Surface	8.92	OK
Lake Wairarapa	Surface	16.43	**High (CBE > ± 10%)**
Lake Wairarapa	Surface	26.15	**High (CBE > ± 10%)**
Mangatarere Riv	Surface	-0.72	OK
Parkvale Stream	Surface	-5.03	OK
Parkvale tribut	Surface	-2.36	OK
Ruamahanga Rive	Surface	No CBE	
Ruamahanga Rive	Surface	-1.13	OK
Ruamahanga Rive	Surface	1.07	OK
Ruamahanga Rive	Surface	1.2	OK
Ruamahanga Rive	Surface	3.81	OK
Ruamahanga Rive	Surface	No CBE	
Tauanui River a	Surface	-4.56	OK
Taueru River at	Surface	-9.2	OK
Tauherenikau Ri	Surface	-4.82	OK
Waingawa River	Surface	-4.79	OK
Waiohine River	Surface	-5.3	OK
Waiohine River	Surface	-4.9	OK
Waiorongomai Ri	Surface	-2.44	OK
Waipoua River a	Surface	-5.43	OK
Whangaehu River	Surface	-0.8	OK
Whangaehu River	Surface	No CBE	
R28/0012	Ground	1.81	OK
S26/0034	Ground	-1.82	OK
S26/0086	Ground	6.44	OK
S26/0092	Ground	11.88	**High (CBE > ± 10%)**
S26/0101	Ground	5.67	OK
S26/0117	Ground	-0.76	OK
S26/0155	Ground	-9	OK
S26/0164	Ground	2.29	OK
S26/0185	Ground	0.14	OK
S26/0188	Ground	No CBE	
S26/0192	Ground	No CBE	
S26/0198	Ground	-3.11	OK
S26/0204	Ground	-1.03	OK
S26/0220	Ground	-1.26	OK
S26/0223	Ground	-2.38	OK
S26/0244	Ground	0.04	OK
S26/0256	Ground	No CBE	

Site	Water type	CBE		Is CBE acceptable?
S26/0259	Ground		-4.59	OK
S26/0267	Ground		-2.18	OK
S26/0299	Ground		1.37	OK
S26/0317	Ground		-3.8	OK
S26/0319	Ground		-4.13	OK
S26/0355	Ground		3.18	OK
S26/0381	Ground		6.65	OK
S26/0386	Ground		16.47	**High (CBE > ± 10%)**
S26/0395	Ground		-3.15	OK
S26/0400	Ground		1.3	OK
S26/0427	Ground	No CBE		
S26/0437	Ground		7.79	OK
S26/0439	Ground		-1.27	OK
S26/0442	Ground	No CBE		
S26/0448	Ground	No CBE		
S26/0449	Ground		0.57	OK
S26/0457	Ground		0.23	OK
S26/0467	Ground		-0.5	OK
S26/0547	Ground		7.61	OK
S26/0562	Ground	No CBE		
S26/0568	Ground		0.8	OK
S26/0573	Ground		-4.44	OK
S26/0576	Ground		0.75	OK
S26/0580	Ground		-1.61	OK
S26/0614	Ground		-4.49	OK
S26/0615	Ground		-4.65	OK
S26/0621	Ground		-3.77	OK
S26/0632	Ground		5.96	OK
S26/0642	Ground		4.83	OK
S26/0657	Ground		-2.37	OK
S26/0660	Ground		-4.49	OK
S26/0662	Ground		-4.52	OK
S26/0675	Ground		-9.14	OK
S26/0705	Ground		0.84	OK
S26/0708	Ground		-5.13	OK
S26/0709	Ground		-6.38	OK
S26/0734	Ground		2.46	OK
S26/0738	Ground		-3.81	OK
S26/0739	Ground		-5.11	OK
S26/0740	Ground		-4.5	OK
S26/0743	Ground		-4.59	OK
S26/0744	Ground		-3.07	OK
S26/0753	Ground		-3.1	OK
S26/0756	Ground		0.38	OK
S26/0758	Ground		-6.05	OK

Site	Water type	CBE		Is CBE acceptable?
S26/0762	Ground		1.92	OK
S26/0768	Ground		-5.96	OK
S26/0774	Ground		-4.62	OK
S26/0788	Ground	No CBE		
S26/0793	Ground		0.88	OK
S26/0803	Ground		16.61	**High (CBE > ± 10%)**
S26/0824	Ground		-0.59	OK
S26/0830	Ground		-4.94	OK
S26/0846	Ground		0.42	OK
S26/0877	Ground		-1.62	OK
S26/0879	Ground	No CBE		
S26/0911	Ground		-2.48	OK
S26/0945	Ground		-1.87	OK
S26/0977	Ground		4.78	OK
S26/0978	Ground		21.73	**High (CBE > ± 10%)**
S26/1034	Ground		1.28	OK
S26/1035	Ground		4.59	OK
S26/1066	Ground		2.39	OK
S26/1069	Ground		7.79	OK
S26/1072	Ground		4.48	OK
S27/0008	Ground		2.27	OK
S27/0009	Ground		-2.34	OK
S27/0059	Ground		-11.72	**Low (CBE > ± 10%)**
S27/0070	Ground		-0.62	OK
S27/0106	Ground		3.13	OK
S27/0136	Ground		-2.23	OK
S27/0141	Ground		4.07	OK
S27/0156	Ground		-0.2	OK
S27/0198	Ground		7.22	OK
S27/0202	Ground		2.13	OK
S27/0268	Ground		2.31	OK
S27/0283	Ground		4.64	OK
S27/0299	Ground		0.21	OK
S27/0330	Ground		0.66	OK
S27/0344	Ground		0.58	OK
S27/0389	Ground		-0.59	OK
S27/0396	Ground		-1.17	OK
S27/0416	Ground	No CBE		
S27/0427	Ground		3.75	OK
S27/0433	Ground		2.61	OK
S27/0435	Ground		-2.03	OK
S27/0442	Ground		-1.98	OK
S27/0495	Ground		1.24	OK
S27/0522	Ground		2.58	OK
S27/0547	Ground		0.75	OK

Site	Water type	CBE		Is CBE acceptable?
S27/0571	Ground		-1.06	OK
S27/0574	Ground		2.88	OK
S27/0585	Ground		0.61	OK
S27/0588	Ground		1.54	OK
S27/0594	Ground		0.52	OK
S27/0602	Ground		-1.84	OK
S27/0607	Ground		0.88	OK
S27/0609	Ground		1.9	OK
S27/0614	Ground		1.49	OK
S27/0615	Ground		-1.18	OK
S27/0621	Ground		-1.22	OK
S27/0640	Ground		-2.33	OK
S27/0681	Ground		-0.53	OK
S27/0717	Ground		-0.46	OK
T26/0003	Ground		-0.98	OK
T26/0011	Ground		4.68	OK
T26/0087	Ground		-0.29	OK
T26/0099	Ground		-1.81	OK
T26/0201	Ground		1.48	OK
T26/0206	Ground		-0.69	OK
T26/0225	Ground	No CBE		
T26/0236	Ground	No CBE		
T26/0237	Ground		71.13	**High (CBE > ± 10%)**
T26/0240	Ground	No CBE		
T26/0242	Ground	No CBE		
T26/0259	Ground		1.27	OK
T26/0264	Ground	No CBE		
T26/0275	Ground	No CBE		
T26/0326	Ground		6.52	OK
T26/0332	Ground		-1.97	OK
T26/0349	Ground	No CBE		
T26/0413	Ground		0.28	OK
T26/0430	Ground		1.92	OK
T26/0465	Ground	No CBE		
T26/0470	Ground	No CBE		
T26/0471	Ground	No CBE		
T26/0472	Ground	No CBE		
T26/0481	Ground	No CBE		
T26/0482	Ground		68.74	**High (CBE > ± 10%)**
T26/0483	Ground	No CBE		
T26/0484	Ground	No CBE		
T26/0487	Ground	No CBE		
T26/0488	Ground		20.05	**High (CBE > ± 10%)**
T26/0489	Ground		1.08	OK
T26/0490	Ground		-6.55	OK

Site	Water type	CBE		Is CBE acceptable?
T26/0492	Ground		1.32	OK
T26/0499	Ground		76.74	**High (CBE > ± 10%)**
T26/0503	Ground		20.6	**High (CBE > ± 10%)**
T26/0504	Ground	No CBE		
T26/0508	Ground		52.92	**High (CBE > ± 10%)**
T26/0509	Ground		72.59	**High (CBE > ± 10%)**
T26/0517	Ground		23.54	**High (CBE > ± 10%)**
T26/0518	Ground	No CBE		
T26/0525	Ground		79.46	**High (CBE > ± 10%)**
T26/0527	Ground	No CBE		
T26/0538	Ground		-1.13	OK
T26/0541	Ground		59.67	**High (CBE > ± 10%)**
T26/0547	Ground		17.4	**High (CBE > ± 10%)**
T26/0552	Ground	No CBE		
T26/0553	Ground	No CBE		
T26/0554	Ground	No CBE		
T26/0555	Ground		64.45	**High (CBE > ± 10%)**
T26/0557	Ground	No CBE		
T26/0561	Ground	No CBE		
T26/0565	Ground	No CBE		
T26/0626	Ground	No CBE		
T26/0643	Ground	No CBE		
T26/0672	Ground	No CBE		
T26/0677	Ground	No CBE		
T26/0690	Ground	No CBE		
T26/0725	Ground	No CBE		
S26/0051	Ground		-0.84	OK
S26/0169	Ground	No CBE		
S26/0705 NGMP	Ground		26.83	**High (CBE > ± 10%)**
S26/0935	Ground	No CBE		
S26/0979	Ground	No CBE		
S26/0980	Ground	No CBE		
S27/0299 NGMP	Ground		46.61	**High (CBE > ± 10%)**
S27/0344 NGMP	Ground		23.5	**High (CBE > ± 10%)**
S27/0607 NGMP	Ground		19.3	**High (CBE > ± 10%)**
T26/0227	Ground		29.86	**High (CBE > ± 10%)**
T26/0232	Ground		84.74	**High (CBE > ± 10%)**
T26/0254	Ground		76.64	**High (CBE > ± 10%)**
T26/0489 NGMP	Ground		20.94	**High (CBE > ± 10%)**
T26/0493	Ground		23.13	**High (CBE > ± 10%)**
T26/0498	Ground		24.48	**High (CBE > ± 10%)**
T26/0505	Ground		31.65	**High (CBE > ± 10%)**
T26/0542	Ground		39.58	**High (CBE > ± 10%)**
S26/0127	Ground	No CBE		
S26/0144	Ground	No CBE		

Site	Water type	CBE		Is CBE acceptable?
S26/0199	Ground	No CBE		
S26/0207	Ground	No CBE		
S26/0263	Ground	No CBE		
S26/0273	Ground	No CBE		
S26/0290	Ground	No CBE		
S26/0300	Ground	No CBE		
S26/0908	Ground	No CBE		
R27/0004	Ground		7.18	OK
R27/0006	Ground		2.36	OK
R28/0001	Ground		1.37	OK
R28/0015	Ground		0.17	OK
S26/0001	Ground		-1.76	OK
S26/0016	Ground		9.22	OK
S26/0030	Ground		6.19	OK
S26/0031	Ground		3.21	OK
S26/0032	Ground		17.6	**High (CBE > ± 10%)**
S26/0045	Ground		-4.19	OK
S26/0060	Ground		3.65	OK
S26/0070	Ground	No CBE		
S26/0071	Ground		-52.7	**Low (CBE > ± 10%)**
S26/0106	Ground		2.79	OK
S26/0113	Ground		-8.31	OK
S26/0122	Ground		8.72	OK
S26/0140	Ground		3.56	OK
S26/0166	Ground		11.85	**High (CBE > ± 10%)**
S26/0178	Ground	No CBE		
S26/0179	Ground	No CBE		
S26/0190	Ground	No CBE		
S26/0213	Ground		-1.03	OK
S26/0229	Ground		-1.09	OK
S26/0236	Ground		5.21	OK
S26/0237	Ground		1.67	OK
S26/0239	Ground		10.81	**High (CBE > ± 10%)**
S26/0243	Ground		16.89	**High (CBE > ± 10%)**
S26/0245	Ground	No CBE		
S26/0248	Ground		9.42	OK
S26/0252	Ground		-5.3	OK
S26/0254	Ground		-10.18	**Low (CBE > ± 10%)**
S26/0265	Ground	No CBE		
S26/0268	Ground		-10.52	**Low (CBE > ± 10%)**
S26/0269	Ground	No CBE		
S26/0271	Ground		5.07	OK
S26/0277	Ground	No CBE		
S26/0288	Ground	No CBE		
S26/0301	Ground		11.49	**High (CBE > ± 10%)**

Site	Water type	CBE		Is CBE acceptable?
S26/0320	Ground		8.33	OK
S26/0326	Ground		2.72	OK
S26/0354	Ground		2.35	OK
S26/0378	Ground		-19.94	**Low (CBE > ± 10%)**
S26/0387	Ground		22.17	**High (CBE > ± 10%)**
S26/0398	Ground		10.36	**High (CBE > ± 10%)**
S26/0399	Ground		-3.61	OK
S26/0401	Ground		-3.17	OK
S26/0403	Ground		-1.31	OK
S26/0432	Ground	No CBE		
S26/0471	Ground		1.8	OK
S26/0480	Ground	No CBE		
S26/0481	Ground	No CBE		
S26/0500	Ground		7.62	OK
S26/0515	Ground	No CBE		
S26/0520	Ground		5.66	OK
S26/0529	Ground		7.94	OK
S26/0540	Ground		5.09	OK
S26/0545	Ground		4.13	OK
S26/0550	Ground		-7.61	OK
S26/0552	Ground	No CBE		
S26/0563	Ground	No CBE		
S26/0582	Ground		6.74	OK
S26/0591	Ground		3.96	OK
S26/0622	Ground		2.86	OK
S26/0624	Ground		-0.93	OK
S26/0629	Ground		4.92	OK
S26/0637	Ground		27.54	**High (CBE > ± 10%)**
S26/0644	Ground		19.62	**High (CBE > ± 10%)**
S26/0646	Ground	No CBE		
S26/0649	Ground		2.9	OK
S26/0651	Ground	No CBE		
S26/0653	Ground		3.7	OK
S26/0658	Ground		12.99	**High (CBE > ± 10%)**
S26/0659	Ground		1.79	OK
S26/0661	Ground		-20.94	**Low (CBE > ± 10%)**
S26/0663	Ground		5.42	OK
S26/0664	Ground	No CBE		
S26/0666	Ground		0.06	OK
S26/0667	Ground		-0.01	OK
S26/0668	Ground		5.33	OK
S26/0669	Ground		-1.59	OK
S26/0672	Ground	No CBE		
S26/0693	Ground	No CBE		
S26/0721	Ground		3.52	OK

Site	Water type	CBE		Is CBE acceptable?
S26/0726	Ground	No CBE		
S26/0730	Ground		13.82	**High (CBE > ± 10%)**
S26/0732	Ground		-54.07	**Low (CBE > ± 10%)**
S26/0736	Ground		3.67	OK
S26/0752	Ground		-99.35	**Low (CBE > ± 10%)**
S26/0779	Ground		4.25	OK
S26/0780	Ground		1.84	OK
S26/0781	Ground		16.97	**High (CBE > ± 10%)**
S27/0006	Ground		26.93	**High (CBE > ± 10%)**
S27/0011	Ground		3.36	OK
S27/0012	Ground		-0.49	OK
S27/0018	Ground		-0.92	OK
S27/0024	Ground		3.49	OK
S27/0031	Ground		7.4	OK
S27/0035	Ground		-14.3	**Low (CBE > ± 10%)**
S27/0043	Ground		2.38	OK
S27/0065	Ground	No CBE		
S27/0096	Ground		3.24	OK
S27/0099	Ground		2.13	OK
S27/0102	Ground		4.17	OK
S27/0107	Ground		-34.21	**Low (CBE > ± 10%)**
S27/0108	Ground		-30.53	**Low (CBE > ± 10%)**
S27/0110	Ground		6.9	OK
S27/0126	Ground		5.15	OK
S27/0133	Ground	No CBE		
S27/0148	Ground		1.4	OK
S27/0163	Ground		0.15	OK
S27/0167	Ground		-19.51	**Low (CBE > ± 10%)**
S27/0169	Ground	No CBE		
S27/0184	Ground		-30.35	**Low (CBE > ± 10%)**
S27/0185	Ground		-19.67	**Low (CBE > ± 10%)**
S27/0188	Ground		0.57	OK
S27/0192	Ground		-0.14	OK
S27/0196	Ground		11.2	**High (CBE > ± 10%)**
S27/0200	Ground	No CBE		
S27/0206	Ground		-11.61	**Low (CBE > ± 10%)**
S27/0209	Ground	No CBE		
S27/0211	Ground	No CBE		
S27/0212	Ground	No CBE		
S27/0248	Ground		13.39	**High (CBE > ± 10%)**
S27/0249	Ground		6.48	OK
S27/0250	Ground	No CBE		
S27/0258	Ground		1.91	OK
S27/0261	Ground		-0.55	OK
S27/0263	Ground		-5.6	OK

Site	Water type	CBE		Is CBE acceptable?
S27/0271	Ground		6.51	OK
S27/0273	Ground		-1.1	OK
S27/0282	Ground		2.38	OK
S27/0293	Ground		-5.59	OK
S27/0304	Ground		2.25	OK
S27/0326	Ground		4.58	OK
S27/0340	Ground		4.59	OK
S27/0343	Ground	No CBE		
S27/0345	Ground		0.13	OK
S27/0351	Ground		2.97	OK
S27/0362	Ground		17.78	**High (CBE > ± 10%)**
S27/0374	Ground		-32.22	**Low (CBE > ± 10%)**
S27/0376	Ground		7.47	OK
S27/0419	Ground		7.42	OK
S27/0420	Ground		1.87	OK
S27/0425	Ground		1.24	OK
S27/0426	Ground		0.36	OK
S27/0428	Ground		1.6	OK
S27/0429	Ground		-3.36	OK
S27/0438	Ground		2.97	OK
S27/0439	Ground		1.48	OK
S27/0440	Ground		-6.04	OK
S27/0441	Ground		-6.67	OK
S27/0443	Ground		1.04	OK
S27/0446	Ground		-0.91	OK
S27/0447	Ground		-0.21	OK
S27/0449	Ground		0.26	OK
S27/0450	Ground		1.64	OK
S27/0461	Ground		5.35	OK
S27/0463	Ground		5.82	OK
S27/0464	Ground		-1.39	OK
S27/0465	Ground		-3.05	OK
S27/0466	Ground		3.12	OK
S27/0473	Ground		-0.72	OK
S27/0478	Ground		1.03	OK
S27/0481	Ground		0.31	OK
S27/0489	Ground		5.01	OK
S27/0502	Ground		1.38	OK
S27/0503	Ground		3.41	OK
S27/0518	Ground	No CBE		
S27/0541	Ground		1.92	OK
S27/0545	Ground		-20.69	**Low (CBE > ± 10%)**
S27/0577	Ground		-3.03	OK
S27/0579	Ground		-5.47	OK
S27/0580	Ground	No CBE		

Site	Water type	CBE		Is CBE acceptable?
S27/0581	Ground		1.65	OK
S27/0582	Ground		0.34	OK
S27/0583	Ground		0.73	OK
S27/0591	Ground		-12.22	**Low (CBE > ± 10%)**
S27/0592	Ground		-50.28	**Low (CBE > ± 10%)**
S27/0593	Ground		5.56	OK
S27/0595	Ground		-0.62	OK
S27/0596	Ground		2.29	OK
S27/0597	Ground		0.56	OK
S27/0599	Ground		-0.79	OK
S27/0600	Ground		-1.66	OK
S27/0601	Ground		-0.58	OK
S27/0603	Ground		3.11	OK
S27/0604	Ground		5.49	OK
S27/0605	Ground		0.73	OK
S27/0606	Ground		2.91	OK
S27/0608	Ground		-1.63	OK
S27/0618	Ground		3.23	OK
S27/0619	Ground		6.12	OK
S27/0620	Ground		5.21	OK
S27/0622	Ground		1.12	OK
S27/0623	Ground		0.78	OK
S27/0624	Ground		0.32	OK
T26/0028	Ground		-17.02	**Low (CBE > ± 10%)**
T26/0039	Ground		8.97	OK
T26/0051	Ground		3.81	OK
T26/0057	Ground	No CBE		
T26/0064	Ground	No CBE		
T26/0071	Ground	No CBE		
T26/0072	Ground	No CBE		
T26/0092	Ground		9.82	OK
T26/0143	Ground		4.1	OK
T26/0159	Ground		0.22	OK
T26/0160	Ground		3.66	OK
T26/0165	Ground		13.94	**High (CBE > ± 10%)**
T26/0172	Ground		6.23	OK
T26/0204	Ground		2.65	OK
T26/0212	Ground	No CBE		
T26/0220	Ground		2.62	OK
T26/0233	Ground		-0.7	OK
T26/0235	Ground		1.28	OK
T26/0238	Ground		14.4	**High (CBE > ± 10%)**
T26/0239	Ground		4.16	OK
T26/0293	Ground		7.9	OK
T26/0294	Ground		-2.88	OK

Site	Water type	CBE		Is CBE acceptable?
T26/0302	Ground	No CBE		
T26/0304	Ground	No CBE		
T26/0305	Ground	No CBE		
T26/0328	Ground	No CBE		
T26/0334	Ground		-5.18	OK
T26/0392	Ground		4.99	OK
T26/0393	Ground	No CBE		
T26/0394	Ground		4.61	OK
T26/0400	Ground		-41.48	**Low (CBE > ± 10%)**
T26/0408	Ground		-13.31	**Low (CBE > ± 10%)**
T26/0412	Ground		6.68	OK
T26/0416	Ground		0.34	OK
T26/0422	Ground		7.21	OK
T26/0424	Ground		4.8	OK
T26/0426	Ground	No CBE		
T26/0428	Ground		-1.02	OK
T26/0429	Ground		1.37	OK
T26/0432	Ground		1.57	OK
T26/0437	Ground		-5.36	OK
T26/0480	Ground		2.35	OK
T26/0500	Ground		1.23	OK
T26/0502	Ground		11.88	**High (CBE > ± 10%)**
T26/0513	Ground		-7.05	OK
T26/0514	Ground		-0.25	OK
T26/0516	Ground		2.23	OK
T26/0530	Ground		23.26	**High (CBE > ± 10%)**
T26/0531	Ground		3.93	OK
T26/0533	Ground		-2.58	OK
T26/0540	Ground		0.84	OK
T26/0622	Ground		12.25	**High (CBE > ± 10%)**
R28/0017	Ground		34.58	**High (CBE > ± 10%)**
S26/0028	Ground		21.04	**High (CBE > ± 10%)**
S26/0168	Ground		29.79	**High (CBE > ± 10%)**
S26/0249	Ground	No CBE		
S26/0253	Ground	No CBE		
S26/0264	Ground	No CBE		
S26/0272	Ground	No CBE		
S26/0276	Ground	No CBE		
S26/0282	Ground	No CBE		
S26/0283	Ground	No CBE		
S26/0284	Ground	No CBE		
S26/0285	Ground	No CBE		
S26/0286	Ground	No CBE		
S26/0287	Ground	No CBE		
S26/0310	Ground	No CBE		

Site	Water type	CBE		Is CBE acceptable?
S26/0311	Ground	No CBE		
S26/0312	Ground	No CBE		
S26/0313	Ground	No CBE		
S26/0315	Ground	No CBE		
S26/0316	Ground	No CBE		
S26/0429	Ground	No CBE		
S26/0930	Ground	No CBE		
S27/0506	Ground	No CBE		
S27/0508	Ground	No CBE		
S27/0543	Ground	No CBE		
S28/0003	Ground		27.58	**High (CBE > ± 10%)**
T26/0200	Ground	No CBE		
T26/0330	Ground	No CBE		
T26/0520	Ground	No CBE		
S26/0094	Ground	No CBE		
S26/0132	Ground	No CBE		
S26/0270	Ground	No CBE		
S26/0274	Ground	No CBE		
S26/0334	Ground	No CBE		
S26/0336	Ground	No CBE		
S26/0337	Ground	No CBE		
S26/0345	Ground	No CBE		
S26/0357	Ground	No CBE		
S26/0362	Ground	No CBE		
S26/0379	Ground	No CBE		
S26/0402	Ground	No CBE		
S26/0408	Ground	No CBE		
S26/0435	Ground	No CBE		
S26/0466	Ground	No CBE		
S26/0574	Ground	No CBE		
S26/0575	Ground	No CBE		
S26/0597	Ground	No CBE		
S26/0654	Ground	No CBE		
S26/0706	Ground	No CBE		
S26/0813	Ground	No CBE		
S26/0936	Ground	No CBE		
S27/0014	Ground	No CBE		
S27/0019	Ground	No CBE		
S27/0023	Ground	No CBE		
S27/0027	Ground	No CBE		
S27/0044	Ground	No CBE		
S27/0076	Ground	No CBE		
S27/0092	Ground	No CBE		
S27/0306	Ground	No CBE		
S27/0659	Ground	No CBE		

Site	Water type	CBE	Is CBE acceptable?
S27/0675	Ground	No CBE	
S27/0680	Ground	No CBE	
S27/0827	Ground	No CBE	
T26/0170	Ground	No CBE	
T26/0461	Ground	No CBE	
R27/0003	Ground	No CBE	
R27/6387	Ground	No CBE	
R27/6389	Ground	No CBE	
S26/0084	Ground	No CBE	
S26/0142	Ground	No CBE	
S26/0147	Ground	No CBE	
S26/0151	Ground	No CBE	
S26/0194	Ground	No CBE	
S26/0294	Ground	No CBE	
S26/0328	Ground	No CBE	
S26/0445	Ground	No CBE	
S26/0486	Ground	No CBE	
S26/0530	Ground	No CBE	
S26/0546	Ground	No CBE	
S26/0548	Ground	No CBE	
S26/0554	Ground	No CBE	
S26/0639	Ground	No CBE	
S26/0697	Ground	No CBE	
S26/0707	Ground	No CBE	
S26/0737	Ground	No CBE	
S26/0796	Ground	No CBE	
S26/0797	Ground	No CBE	
S26/0798	Ground	No CBE	
S26/0800	Ground	No CBE	
S26/0804	Ground	No CBE	
S26/0805	Ground	No CBE	
S26/0806	Ground	No CBE	
S26/0807	Ground	No CBE	
S26/0808	Ground	No CBE	
S26/0811	Ground	No CBE	
S26/0812	Ground	No CBE	
S26/0814	Ground	No CBE	
S26/0815	Ground	No CBE	
S26/0816	Ground	No CBE	
S26/0817	Ground	No CBE	
S26/0838	Ground	No CBE	
S26/0871	Ground	No CBE	
S27/0042	Ground	No CBE	
S27/0174	Ground	No CBE	
S27/0195	Ground	No CBE	

Site	Water type	CBE	Is CBE acceptable?
S27/0221	Ground	No CBE	
S27/0278	Ground	No CBE	
S27/0281	Ground	No CBE	
S27/0300	Ground	No CBE	
S27/0301	Ground	No CBE	
S27/0302	Ground	No CBE	
S27/0375	Ground	No CBE	
S27/0641	Ground	No CBE	
S27/0671	Ground	No CBE	
S27/0672	Ground	No CBE	
S27/0673	Ground	No CBE	
S27/0682	Ground	No CBE	
S27/0683	Ground	No CBE	
S27/0684	Ground	No CBE	
S27/0687	Ground	No CBE	
S27/0693	Ground	No CBE	
S27/0694	Ground	No CBE	
S27/0696	Ground	No CBE	
S27/0700	Ground	No CBE	
S27/0701	Ground	No CBE	
S27/0705	Ground	No CBE	
S27/0772	Ground	No CBE	
S27/0777	Ground	No CBE	
T25/0003	Ground	No CBE	
T26/0034	Ground	No CBE	
T26/0333	Ground	No CBE	
T26/0462	Ground	No CBE	
T26/0633	Ground	No CBE	
T26/0634	Ground	No CBE	
T26/0635	Ground	No CBE	
T26/0637	Ground	No CBE	
T26/0638	Ground	No CBE	
T26/0639	Ground	No CBE	
T26/0642	Ground	No CBE	
T26/0726	Ground	No CBE	
S26/0193	Ground	No CBE	
S26/0279	Ground	No CBE	
S26/0440	Ground	No CBE	
S26/0643	Ground	No CBE	
S26/0677	Ground	No CBE	
S27/0208	Ground	No CBE	
T26/0144	Ground	No CBE	
T26/0433	Ground	No CBE	
S26/0577	Ground	No CBE	
S26/0578	Ground	No CBE	

Site	Water type	CBE	Is CBE acceptable?
S26/0579	Ground	No CBE	
S26/0750	Ground	No CBE	
S27/0487	Ground	No CBE	
S27/0488	Ground	No CBE	
S27/0490	Ground	No CBE	

Appendix C
Monitoring site cluster assignment

Table D.1. Assignment of individual ground and surface water monitoring stations from the Wairarapa valley into six defined clusters (A1-A2, B1-B4). Determined using HCA – Wards linkage method. Total number of sites assigned to each cluster presented in last row. Number of surface water sites is parenthesized.

A1	A2	A2 cont..	B1	B2	B3
Beef Creek at headwaters	Mangatarere River at State Highway 2	T26/0201	Huangarua River at Ponatahi Bridge	S26/0198	S26/0573
Ruamahanga River at McLays	Parkvale Stream at Weir	T26/0430		S26/0400	S26/0740
Tauherenikau River at Websters	Parkvale tributary at Lowes Reserve	S26/0113		S26/0568	S26/0743
Waingawa River at South Rd	Ruamahanga River at Gladstone Bridge	S26/0140		S26/0576	S26/0758
Waiohine River at Bicknells	Ruamahanga River at Pukio	S26/0237		S26/0580	S26/0762
Waiohine River at Gorge	Ruamahanga River at Te Ore Ore	S26/0248		S26/0615	S27/0268
Waiorongomai River at Forest Park	Tauanui River at Whakatomotomo Rd	S26/0320		S26/0621	S27/0435
S26/0034	Waipoua River at Colombo Rd Bridge	S26/0500		S26/0632	S27/0585
S26/0317	S26/0117	S26/0529		S26/0675	S27/0594
S26/0457	S26/0155	S26/0667		S26/0753	S27/0602
S26/0547	S26/0220	S26/0668		S26/0774	S27/0640
S26/0846	S26/0223	S26/0669		S27/0141	S27/0717
S26/0911	S26/0244	S26/0780		S27/0156	S27/0282
S27/0070	S26/0259	S27/0011		S27/0283	S27/0304
S27/0198	S26/0267	S27/0018		S27/0389	S27/0419
S27/0299	S26/0299	S27/0024		T26/0206	S27/0425
S27/0330	S26/0319	S27/0031		T26/0326	S27/0428
T26/0003	S26/0439	S27/0043		T26/0413	S27/0440
T26/0011	S26/0467	S27/0096		S26/0030	S27/0441
T26/0259	S26/0705	S27/0102		S26/0031	S27/0446
S26/0051	S26/0709	S27/0126		S26/0106	S27/0449
S26/0060	S26/0734	S27/0148		S26/0229	S27/0450
S26/0252	S26/0738	S27/0192		S26/0236	S27/0463
S26/0326	S26/0824	T26/0039		S26/0271	S27/0581
S26/0399	S26/0830	T26/0051		S26/0545	S27/0596
S26/0401	S27/0009	T26/0160		S26/0582	S27/0597
S26/0403	S27/0106	T26/0220		S26/0591	S27/0600
S26/0520	S27/0136	T26/0235		S26/0624	S27/0601
S26/0540	S27/0202	T26/0239		S26/0629	S27/0606
T26/0143	T26/0087	T26/0293		S26/0649	S27/0620
T26/0159	T26/0099	T26/0294		S26/0653	
T26/0233		T26/0334		S26/0666	
T26/0392		T26/0394		S26/0721	
WN5		T26/0422			
		T26/0428			
		T26/0432			
		T26/0480			
		T26/0500			
		T26/0513			
		T26/0514			
		T26/0516			
		T26/0533			
		WN3			
		WN4			
Total: 34 (8)		**Total**: 75 (10)	**Total**: 54 (4)	**Total**: 44 (0)	**Total**: 30 (0)

Table D continued…..

B4
R28/0012
S26/0768
S27/0427
S27/0433
S27/0495
S27/0522
S27/0607
S27/0621
R28/0001
R28/0015
S26/0622
S27/0376
S27/0426
S27/0429
S27/0438
S27/0439
S27/0443
S27/0447
S27/0461
S27/0464
S27/0478
S27/0489
S27/0579
S27/0583
S27/0593
S27/0595
S27/0599
S27/0605
S27/0622
S27/0623
S27/0624
Total: 31 (0)

Appendix D
ANOVA analysis outputs

Explanation of Statgraphics CENTURION statistical outputs. Kruskall-Wallis test investigates if a statistical significant difference is presented between sample medians, while a Multiple range test investigates if a statically significant difference is present between sample means.

Kruskall-Wallis tests produce one output table and tests the null hypothesis that the medians of a selected parameter (e.g. conductivity, Ca^{2+}, etc) within each of the 6 levels of Classification (e.g. 6 clusters) are the same. The data from all the levels is first combined and ranked from smallest to largest. The average rank is then computed for the data at each level. If the resulting P-value is less than 0.05, there is a statistically significant difference amongst the medians at the 95.0% confidence level and the null hypothesis is rejected. The Kruskall-Wallis test is presented first for each water quality analyte.

A Multiple range test applies a multiple comparison procedure to determine which means are significantly different from each other. Two output tables are produced. The first table identifies the sample mean for the selected parameter (e.g. conductivity) for each of the six cluster groups. Six homogenous groups are identified in the last column using columns of X's. If X's overlap there is no statistical difference amongst the sample mean between the overlapping groups. The second table investigates the estimated difference between each pair of means. If an asterisk has been placed next to a pair, this indicates that these pairs show a statistically significant difference at the 95.0% confidence interval. The method used to discriminate among the means is Fisher's least significant difference (LSD) procedure. With this method, there is a 5.0% risk of calling each pair of means significantly different when the actual difference equals 0.

Resulting outputs:

Conductivity

Table E.1. Kruskal-Wallis Test for log10(Conductivity) by Classification 6 clusters

Classification 6 clusters	*Sample Size*	*Average Rank*
A1	34	19.3235
A2	75	75.6067
B1	54	180.944
B2	44	130.227
B3	30	213.15
B4	31	252.355

Test statistic = 240.467 P-Value = 0.0

Table E.2. Multiple Range Tests for log10(Conductivity) by Classification 6 clusters
Method: 95.0 percent LSD

Level	*Count*	*Mean*	*Homogeneous Groups*
A1	34	1.88727	X
A2	75	2.13208	X
B2	44	2.29659	X
B1	54	2.47837	X
B3	30	2.62447	X
B4	31	2.98591	X

Table E.3. Multiple Range Tests for log10(Conductivity) by Classification 6 clusters
Method: 95.0 percent LSD

Contrast	*Sig.*	*Difference*	*+/- Limits*
A1 - A2	*	-0.244807	0.0436765
A1 - B1	*	-0.591094	0.0462498
A1 - B2	*	-0.409315	0.0482376
A1 - B3	*	-0.737196	0.0529169
A1 - B4	*	-1.09864	0.0524615
A2 - B1	*	-0.346287	0.0377027
A2 - B2	*	-0.164508	0.0401163
A2 - B3	*	-0.492389	0.045636
A2 - B4	*	-0.853834	0.0451072
B1 - B2	*	0.181779	0.0429037
B1 - B3	*	-0.146102	0.0481046
B1 - B4	*	-0.507547	0.0476032
B2 - B3	*	-0.327881	0.0500188
B2 - B4	*	-0.689326	0.0495368
B3 - B4	*	-0.361445	0.0541038

* denotes a statistically significant difference.

Ca^{2+}

Table E.4. Kruskal-Wallis Test for log10(Calcium) by Classification 6 clusters

Classification 6 clusters	*Sample Size*	*Average Rank*
A1	34	38.2647
A2	75	86.7933
B1	54	180.009
B2	44	129.625
B3	30	173.7
B4	31	245.177

Test statistic = 170.566 P-Value = 0.0

Table E.5. Multiple Range Tests for log10(Calcium) by Classification 6 clusters

Level	*Count*	*Mean*	*Homogeneous Groups*
A1	34	0.811876	X
A2	75	0.953859	X
B2	44	1.07978	X
B3	30	1.25435	X
B1	54	1.29588	X
B4	31	1.62653	X

Table E.6. Multiple Range Tests for log10(Calcium) by Classification 6 clusters

Contrast	*Sig.*	*Difference*	*+/- Limits*
A1 - A2	*	-0.141984	0.0696338
A1 - B1	*	-0.484003	0.0737364
A1 - B2	*	-0.2679	0.0769057
A1 - B3	*	-0.442474	0.0843659
A1 - B4	*	-0.814652	0.0836398
A2 - B1	*	-0.342019	0.0601096
A2 - B2	*	-0.125917	0.0639578
A2 - B3	*	-0.30049	0.0727579
A2 - B4	*	-0.672668	0.0719148
B1 - B2	*	0.216103	0.0684017
B1 - B3		0.0415295	0.0766936
B1 - B4	*	-0.330649	0.0758942
B2 - B3	*	-0.174573	0.0797454
B2 - B4	*	-0.546751	0.0789769
B3 - B4	*	-0.372178	0.0862582

* denotes a statistically significant difference.

HCO_3^-

Table E.7. Kruskal-Wallis Test for log10(Bicarbonate) by Classification 6 clusters

Classification 6 clusters	*Sample Size*	*Average Rank*
A1	34	46.25
A2	75	62.2933
B1	54	166.13
B2	44	158.545
B3	30	209.567
B4	31	244.113

Test statistic = 212.551 P-Value = 0.0

Table E.8. Multiple Range Tests for log10(Bicarbonate) by Classification 6 clusters

Level	*Count*	*Mean*	*Homogeneous Groups*
A1	34	1.4241	X
A2	75	1.47466	X
B2	44	1.95779	X
B1	54	1.97059	X
B3	30	2.17408	X
B4	31	2.36739	X

Table E.9. Multiple Range Tests for log10(Bicarbonate) by Classification 6 clusters

Contrast	*Sig.*	*Difference*	*+/- Limits*
A1 - A2		-0.0505609	0.0683756
A1 - B1	*	-0.546496	0.0724041
A1 - B2	*	-0.533694	0.0755161
A1 - B3	*	-0.749981	0.0828415
A1 - B4	*	-0.943291	0.0821286
A2 - B1	*	-0.495936	0.0590235
A2 - B2	*	-0.483133	0.0628021
A2 - B3	*	-0.69942	0.0714433
A2 - B4	*	-0.892731	0.0706154
B1 - B2		0.0128023	0.0671657
B1 - B3	*	-0.203484	0.0753078
B1 - B4	*	-0.396795	0.0745229
B2 - B3	*	-0.216287	0.0783045
B2 - B4	*	-0.409597	0.0775499
B3 - B4	*	-0.193311	0.0846996

Na^+

Table E.10. Kruskal-Wallis Test for log10(Sodium) by Classification 6 clusters

Classification 6 clusters	*Sample Size*	*Average Rank*
A1	34	24.6324
A2	75	71.9333
B1	54	170.269
B2	44	144.557
B3	30	215.417
B4	31	251.484

Test statistic = 232.777 P-Value = 0.0

Table E.11. Multiple Range Tests for log10(Sodium) by Classification 6 clusters

Level	*Count*	*Mean*	*Homogeneous Groups*
A1	34	0.782123	X
A2	75	1.0284	X
B2	44	1.3199	X
B1	54	1.44272	X
B3	30	1.67098	X
B4	31	2.08577	X

Table E.12. Multiple Range Tests for log10(Sodium) by Classification 6 clusters

Contrast	*Sig.*	*Difference*	*+/- Limits*
A1 - A2	*	-0.24628	0.0612189
A1 - B1	*	-0.660597	0.0648258
A1 - B2	*	-0.537774	0.0676121
A1 - B3	*	-0.88886	0.0741707
A1 - B4	*	-1.30364	0.0735325
A2 - B1	*	-0.414317	0.0528457
A2 - B2	*	-0.291494	0.0562288
A2 - B3	*	-0.64258	0.0639655
A2 - B4	*	-1.05736	0.0632243
B1 - B2	*	0.122823	0.0601357
B1 - B3	*	-0.228263	0.0674256
B1 - B4	*	-0.643047	0.0667228
B2 - B3	*	-0.351086	0.0701086
B2 - B4	*	-0.76587	0.069433
B3 - B4	*	-0.414784	0.0758344

* denotes a statistically significant difference.

Cl^-

Table E.12. Kruskal-Wallis Test for log10(Chloride) by Classification 6 clusters

Classification 6 clusters	*Sample Size*	*Average Rank*
A1	34	29.4412
A2	75	80.8067
B1	54	182.528
B2	44	116.216
B3	30	208.333
B4	31	250.468

Test statistic = 218.302 P-Value = 0.0

Table E.13. Multiple Range Tests for log10(Chloride) by Classification 6 clusters

Level	*Count*	*Mean*	*Homogeneous Groups*
A1	34	0.814977	X
A2	75	1.04062	X
B2	44	1.1857	X
B1	54	1.52293	X
B3	30	1.7179	X
B4	31	2.25979	X

Table E.14. Multiple Range Tests for log10(Chloride) by Classification 6 clusters

Contrast	*Sig.*	*Difference*	*+/- Limits*
A1 - A2	*	-0.225638	0.0773308
A1 - B1	*	-0.70795	0.0818869
A1 - B2	*	-0.37072	0.0854065
A1 - B3	*	-0.902924	0.0936913
A1 - B4	*	-1.44481	0.0928851
A2 - B1	*	-0.482312	0.0667539
A2 - B2	*	-0.145082	0.0710274
A2 - B3	*	-0.677287	0.0808003
A2 - B4	*	-1.21917	0.079864
B1 - B2	*	0.33723	0.0759625
B1 - B3	*	-0.194974	0.085171
B1 - B4	*	-0.736861	0.0842833
B2 - B3	*	-0.532204	0.0885602
B2 - B4	*	-1.07409	0.0877067
B3 - B4	*	-0.541886	0.0957928

* denotes a statistically significant difference.

SO_4^{2-}

Table E.15. Kruskal-Wallis Test for log10(Sulphate) by Classification 6 clusters

Classification 6 clusters	*Sample Size*	*Average Rank*
A1	34	118.426
A2	75	184.44
B1	54	200.306
B2	44	85.7045
B3	30	45.0333
B4	31	72.5161

Test statistic = 149.04 P-Value = 0.0

Table E.16. Multiple Range Tests for log10(Sulphate) by Classification 6 clusters

Level	*Count*	*Mean*	*Homogeneous Groups*
B3	30	-0.0117463	X
B4	31	0.160622	XX
B2	44	0.292261	X
A1	34	0.612779	X
A2	75	0.877062	X
B1	54	1.00266	X

Table E.17. Multiple Range Tests for log10(Sulphate) by Classification 6 clusters

Contrast	*Sig.*	*Difference*	*+/- Limits*
A1 - A2	*	-0.264283	0.144614
A1 - B1	*	-0.389878	0.153134
A1 - B2	*	0.320518	0.159716
A1 - B3	*	0.624525	0.175209
A1 - B4	*	0.452157	0.173702
A2 - B1	*	-0.125594	0.124835
A2 - B2	*	0.584801	0.132826
A2 - B3	*	0.888808	0.151102
A2 - B4	*	0.71644	0.149351
B1 - B2	*	0.710396	0.142055
B1 - B3	*	1.0144	0.159276
B1 - B4	*	0.842035	0.157616
B2 - B3	*	0.304007	0.165614
B2 - B4		0.131639	0.164018
B3 - B4		-0.172368	0.179139

Mg^{2+}

Table E.18. Kruskal-Wallis Test for log10(Magnesium) by Classification 6 clusters

Classification 6 clusters	*Sample Size*	*Average Rank*
A1	34	21.1176
A2	75	78.2867
B1	54	163.981
B2	44	150.136
B3	30	207.433
B4	31	250.726

Test statistic = 218.242 P-Value = 0.0

Table E.19. Multiple Range Tests for log10(Magnesium) by Classification 6 clusters

Level	*Count*	*Mean*	*Homogeneous Groups*
A1	34	0.16752	X
A2	75	0.498086	X
B2	44	0.758073	X
B1	54	0.816214	X
B3	30	0.984185	X
B4	31	1.29396	X

Table E.20. Multiple Range Tests for log10(Magnesium) by Classification 6 clusters

Contrast	*Sig.*	*Difference*	*+/- Limits*
A1 - A2	*	-0.330566	0.0599108
A1 - B1	*	-0.648694	0.0634406
A1 - B2	*	-0.590553	0.0661673
A1 - B3	*	-0.816665	0.0725858
A1 - B4	*	-1.12644	0.0719612
A2 - B1	*	-0.318128	0.0517165
A2 - B2	*	-0.259986	0.0550273
A2 - B3	*	-0.486099	0.0625987
A2 - B4	*	-0.795875	0.0618733
B1 - B2		0.0581413	0.0588507
B1 - B3	*	-0.167971	0.0659848
B1 - B4	*	-0.477748	0.0652971
B2 - B3	*	-0.226112	0.0686105
B2 - B4	*	-0.535889	0.0679494
B3 - B4	*	-0.309776	0.0742139

* denotes a statistically significant difference.

K^+

Table E.21. Kruskal-Wallis Test for log10(Potassium) by Classification 6 clusters

Classification 6 clusters	*Sample Size*	*Average Rank*
A1	34	29.3971
A2	75	106.88
B1	54	174.222
B2	44	96.375
B3	30	197.65
B4	31	240.403

Test statistic = 174.78 P-Value = 0.0

Table E.22. Multiple Range Tests for log10(Potassium) by Classification 6 clusters

Level	*Count*	*Mean*	*Homogeneous Groups*
A1	34	-0.13254	X
B2	44	0.0911872	X
A2	75	0.125491	X
B1	54	0.32697	X
B3	30	0.444295	X
B4	31	0.717977	X

Table E.23. Multiple Range Tests for log10(Potassium) by Classification 6 clusters

Contrast	*Sig.*	*Difference*	*+/- Limits*
A1 - A2	*	-0.25803	0.0754499
A1 - B1	*	-0.45951	0.0798952
A1 - B2	*	-0.223727	0.0833292
A1 - B3	*	-0.576835	0.0914125
A1 - B4	*	-0.850517	0.0906259
A2 - B1	*	-0.20148	0.0651303
A2 - B2		0.0343035	0.0692998
A2 - B3	*	-0.318804	0.078835
A2 - B4	*	-0.592487	0.0779215
B1 - B2	*	0.235783	0.0741149
B1 - B3	*	-0.117325	0.0830994
B1 - B4	*	-0.391007	0.0822333
B2 - B3	*	-0.353108	0.0864062
B2 - B4	*	-0.62679	0.0855735
B3 - B4	*	-0.273682	0.0934629

* denotes a statistically significant difference.

Total reactive P

Table E.24. Kruskal-Wallis Test for log10(Phosphorus) by Classification 6 clusters

Classification 6 clusters	*Sample Size*	*Average Rank*
A1	25	47.52
A2	49	71.7347
B1	31	78.7742
B2	25	111.78
B3	15	112.567
B4	15	83.4667

Test statistic = 33.1336 P-Value = 0.0000035404

Table E.25. Multiple Range Tests for log10(Phosphorus) by Classification 6 clusters

Level	*Count*	*Mean*	*Homogeneous Groups*
A1	25	-1.89146	X
A2	49	-1.68792	XX
B1	31	-1.52043	X
B4	15	-1.46489	X
B2	25	-0.975033	X
B3	15	-0.717428	X

Table E.26. Multiple Range Tests for log10(Phosphorus) by Classification 6 clusters

Contrast	*Sig.*	*Difference*	*+/- Limits*
A1 - A2		-0.203541	0.302039
A1 - B1	*	-0.371026	0.330338
A1 - B2	*	-0.916426	0.347585
A1 - B3	*	-1.17403	0.401356
A1 - B4	*	-0.426568	0.401356
A2 - B1		-0.167485	0.282021
A2 - B2	*	-0.712885	0.302039
A2 - B3	*	-0.970489	0.362628
A2 - B4		-0.223027	0.362628
B1 - B2	*	-0.5454	0.330338
B1 - B3	*	-0.803004	0.386516
B1 - B4		-0.0555419	0.386516
B2 - B3		-0.257604	0.401356
B2 - B4	*	0.489858	0.401356
B3 - B4	*	0.747462	0.44873

* denotes a statistically significant difference.

NO_3^-

Table E.27. Kruskal-Wallis Test for log10(Nitrate) by Classification 6 clusters

Classification 6 clusters	*Sample Size*	*Average Rank*
A1	33	94.2576
A2	75	162.34
B1	47	102.33
B2	34	80.2941
B3	15	48.2333
B4	18	66.8889

Test statistic = 81.6075 P-Value = 0.0

Table E.28. Multiple Range Tests for log10(Nitrate) by Classification 6 clusters

Level	*Count*	*Mean*	*Homogeneous Groups*
B3	15	-1.45797	X
B4	18	-1.15111	X
B2	34	-0.949198	XX
B1	47	-0.640585	X
A1	33	-0.613007	X
A2	75	0.32785	X

Table E.29. Multiple Range Tests for log10(Nitrate) by Classification 6 clusters

Contrast	*Sig.*	*Difference*	*+/- Limits*
A1 - A2	*	-0.940857	0.350805
A1 - B1		0.0275779	0.3814
A1 - B2		0.336192	0.410377
A1 - B3	*	0.844959	0.52295
A1 - B4	*	0.538105	0.492078
A2 - B1	*	0.968435	0.312422
A2 - B2	*	1.27705	0.347204
A2 - B3	*	1.78582	0.474993
A2 - B4	*	1.47896	0.440774
B1 - B2		0.308614	0.378091
B1 - B3	*	0.817381	0.498016
B1 - B4	*	0.510527	0.465493
B2 - B3		0.508767	0.520541
B2 - B4		0.201914	0.489517
B3 - B4		-0.306854	0.587107

* denotes a statistically significant difference.

NH_4^+

Table E.30. Kruskal-Wallis Test for log10(Ammonium) by Classification 6 clusters

Classification 6 clusters	*Sample Size*	*Average Rank*
A1	25	52.12
A2	54	53.2315
B1	34	87.9265
B2	31	120.097
B3	16	150.969
B4	14	137.107

Test statistic = 90.7306 P-Value = 0.0

Table E.31. Multiple Range Tests for log10(Ammonium) by Classification 6 clusters

Level	*Count*	*Mean*	*Homogeneous Groups*
A2	54	-2.02704	X
A1	25	-1.99452	X
B1	34	-1.33653	X
B2	31	-0.751235	X
B4	14	-0.26058	X
B3	16	-0.0315168	X

Table E.32. Multiple Range Tests for log10(Ammonium) by Classification 6 clusters

Contrast	*Sig.*	*Difference*	*+/- Limits*
A1 - A2		0.0325183	0.313212
A1 - B1	*	-0.657989	0.341121
A1 - B2	*	-1.24329	0.348045
A1 - B3	*	-1.96301	0.414528
A1 - B4	*	-1.73394	0.432205
A2 - B1	*	-0.690507	0.283463
A2 - B2	*	-1.27581	0.291759
A2 - B3	*	-1.99552	0.368539
A2 - B4	*	-1.76646	0.388316
B1 - B2	*	-0.585299	0.321535
B1 - B3	*	-1.30502	0.392534
B1 - B4	*	-1.07595	0.411158
B2 - B3	*	-0.719718	0.398566
B2 - B4	*	-0.490655	0.41692
B3 - B4		0.229063	0.473836

* denotes a statistically significant difference

Fe^{2+}

Table E.33. Kruskal-Wallis Test for log10(Iron) by Classification 6 clusters

Classification 6 clusters	*Sample Size*	*Average Rank*
A1	33	89.9394
A2	73	82.226
B1	54	132.898
B2	44	158.989
B3	30	182.65
B4	30	211.933

Test statistic = 93.0186 P-Value = 0.0

Table E.34. Multiple Range Tests for log10(Iron) by Classification 6 clusters

Level	*Count*	*Mean*	*Homogeneous Groups*
A2	73	-1.30558	X
A1	33	-1.15658	X
B1	54	-0.531558	X
B2	44	-0.121224	X
B3	30	0.222328	XX
B4	30	0.572887	X

Table E.35. Multiple Range Tests for log10(Iron) by Classification 6 clusters

Contrast	*Sig.*	*Difference*	*+/- Limits*
A1 - A2		0.148998	0.376032
A1 - B1	*	-0.625021	0.396091
A1 - B2	*	-1.03536	0.412811
A1 - B3	*	-1.37891	0.452212
A1 - B4	*	-1.72947	0.452212
A2 - B1	*	-0.774019	0.321761
A2 - B2	*	-1.18435	0.342133
A2 - B3	*	-1.5279	0.388764
A2 - B4	*	-1.87846	0.388764
B1 - B2	*	-0.410335	0.364066
B1 - B3	*	-0.753886	0.408199
B1 - B4	*	-1.10445	0.408199
B2 - B3		-0.343551	0.424442
B2 - B4	*	-0.694111	0.424442
B3 - B4		-0.350559	0.462854

* denotes a statistically significant difference.

Mn

Table E.36. Kruskal-Wallis Test for log10(Manganese) by Classification 6 clusters

Classification 6 clusters	*Sample Size*	*Average Rank*
A1	33	61.8485
A2	72	70.3333
B1	53	144.557
B2	44	162.943
B3	30	201.95
B4	31	216.823

Test statistic = 148.239 P-Value = 0.0

Table E.37. Multiple Range Tests for log10(Manganese) by Classification 6 clusters.

Level	*Count*	*Mean*	*Homogeneous Groups*
A1	33	-2.17497	X
A2	72	-2.01625	X
B1	53	-0.89913	X
B2	44	-0.500303	X
B3	30	-0.134042	X
B4	31	-0.107272	X

Table E.38. Multiple Range Tests for log10(Manganese) by Classification 6 clusters.

Contrast	*Sig.*	*Difference*	*+/- Limits*
A1 - A2		-0.158714	0.300065
A1 - B1	*	-1.27584	0.316518
A1 - B2	*	-1.67466	0.328705
A1 - B3	*	-2.04093	0.360078
A1 - B4	*	-2.0677	0.357023
A2 - B1	*	-1.11712	0.258342
A2 - B2	*	-1.51595	0.273137
A2 - B3	*	-1.88221	0.310182
A2 - B4	*	-1.90898	0.306631
B1 - B2	*	-0.398827	0.291116
B1 - B3	*	-0.765088	0.326125
B1 - B4	*	-0.791859	0.322749
B2 - B3	*	-0.366261	0.337966
B2 - B4	*	-0.393031	0.334709
B3 - B4		-0.0267705	0.365567

* denotes a statistically significant difference.

pH

Table E.39. Kruskal-Wallis Test for pH by Classification 6 clusters

Classification 6 clusters	*Sample Size*	*Average Rank*
A1	30	102.883
A2	68	79.125
B1	50	134.53
B2	41	147.354
B3	26	154.154
B4	30	163.067

Test statistic = 49.2731 P-Value = 1.95158E-9

Table E.40. Multiple Range Tests for pH by Classification 6 clusters

Level	*Count*	*Mean*	*Homogeneous Groups*
A2	68	6.40963	X
A1	30	6.6235	XX
B1	50	6.8618	XX
B2	41	6.89329	X
B3	26	6.9425	X
B4	30	7.04567	X

Table E.41. Multiple Range Tests for pH by Classification 6 clusters

Contrast	*Sig.*	*Difference*	*+/- Limits*
A1 - A2		0.213868	0.226778
A1 - B1		-0.2383	0.238948
A1 - B2	*	-0.269793	0.248588
A1 - B3	*	-0.319	0.277236
A1 - B4	*	-0.422167	0.267151
A2 - B1	*	-0.452168	0.192755
A2 - B2	*	-0.48366	0.204583
A2 - B3	*	-0.532868	0.238576
A2 - B4	*	-0.636034	0.226778
B1 - B2		-0.0314927	0.217995
B1 - B3		-0.0807	0.250172
B1 - B4		-0.183867	0.238948
B2 - B3		-0.0492073	0.259395
B2 - B4		-0.152374	0.248588
B3 - B4		-0.103167	0.277236

* denotes a statistically significant difference.

Appendix E
ANOVA analysis-cluster differentiation

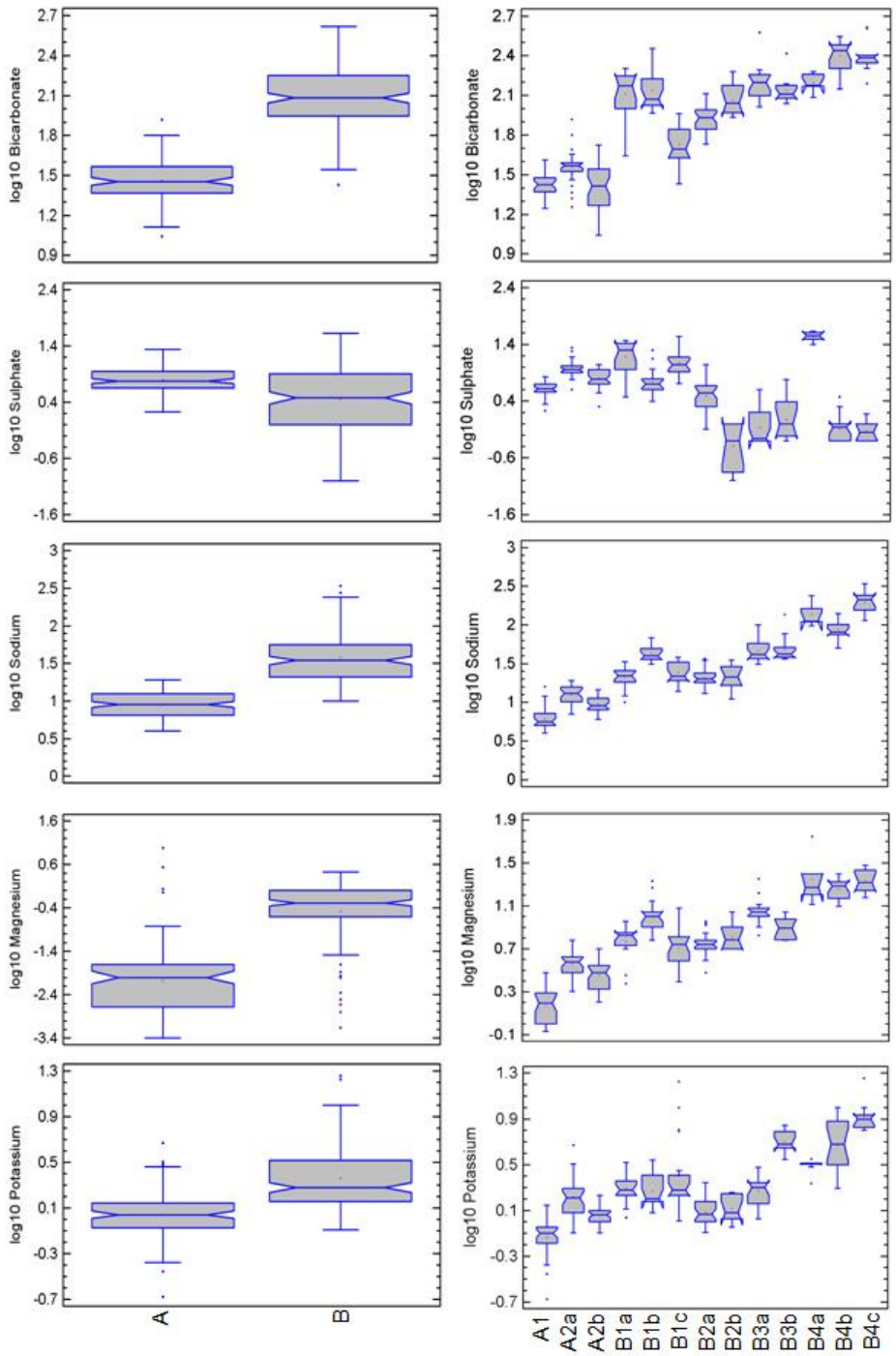

Figure G.1. One-Way ANOVA Box-Whisker plots showing the variation for remaining parameters across the two and 13 cluster thresholds. All parameters are presented in mg/L. The rectangular box identifies the first to the third quartile of the data, separated by a horizontal median line. Median notches are also present around the median line indicating the margin of error surrounding the estimation of the sample median. The vertical whisker lines identify the lowest and highest observations in the sample, except those deemed to be outliers as represented by the dots plotted outside these whiskers

Appendix F
Darcy’s flow calculations

Appendix G
Discharge-stage rating curves

H.1 Mangatarere at Gorge

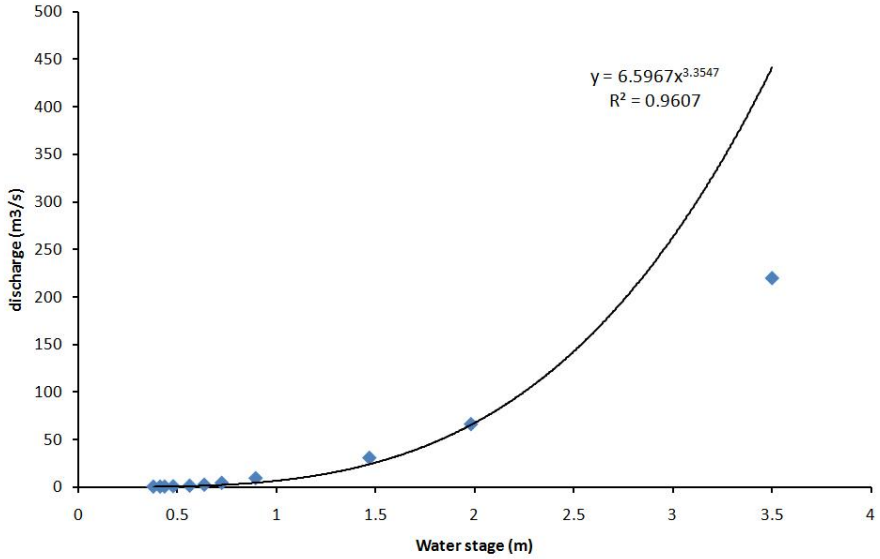

Figure H.1. Fitted power relationship between water stage and corresponding discharge measurements at the Mangatarere at Gorge gauging station. Discharge measurements lie close to the fitted curve as indicated by a high coefficient of determination ($R^2 = 0.96$). However, this relationship breaks down in the higher discharge range (> 150 m^3/s). This is no considered an issue, as this research does not deal with stage and therefore discharge values in this range. Stage values for this research fall within 0.4-2.5m.

Table H.1. Stage and discharge rating data from the Mangatarere gauging station at Gorge. Data provided by GWRC.

Stage (m)	Discharge (m/s)
0.378	0.121
0.412	0.229
0.435	0.303
0.478	0.516
0.561	1.146
0.635	2.189
0.723	4.134
0.894	9.05
1.468	30.535
1.981	66
3.5	220

H.2 Mangatarere at State Highway 2 (SH2)

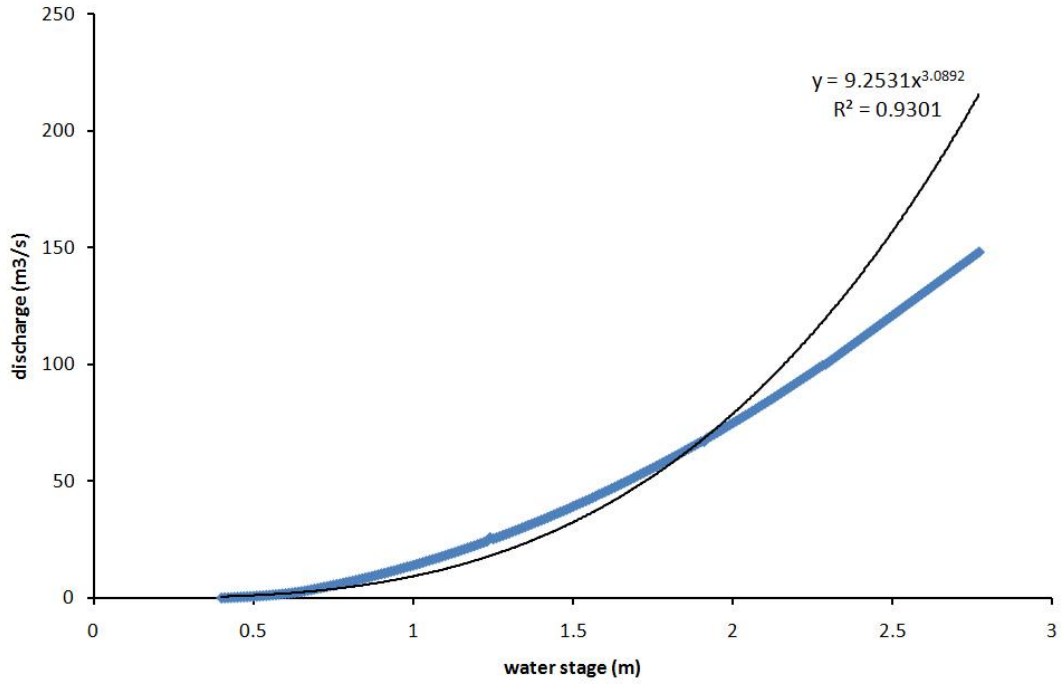

Figure H.2. Fitted power relationship between water stage and corresponding discharge measurements at the Mangatarere stream State Highway 2 (SH2) gauging station. Also known as the downstream gauging station. Discharge measurements lie close to the fitted curve as indicated by a high coefficient of determination (R^2 = 0.96). However, this relationship breaks down in the higher discharge range (> 50 m^3/s). This is no considered an issue, as this research does not deal with discharge values in this range. Stage values for this research fall within 0.4-2.5m.

Table H.2. Stage and discharge (Q) rating data from the Mangatarere at State Highway 2 (SH2), also known as the downstream gauging station. Data provided by GWRC.

Stage (m)	Q (m^3/s)	Stage (m)	Q (m^3/s)	Stage (m)	Q (m^3/s)	Stage (m)	Q (m^3/s)
0.4	0.008	0.89	9.94	1.38	32.2	1.87	64.6
0.41	0.07	0.9	10.3	1.39	32.7	1.88	65.3
0.42	0.134	0.91	10.6	1.4	33.3	1.89	66.1
0.43	0.199	0.92	11	1.41	33.8	1.9	66.9
0.44	0.265	0.93	11.4	1.42	34.4	1.91	67
0.45	0.335	0.94	11.7	1.43	35	1.92	68.5
0.46	0.407	0.95	12.1	1.44	35.6	1.93	69.2
0.47	0.481	0.96	12.5	1.45	36.2	1.94	70
0.48	0.556	0.97	12.9	1.46	36.8	1.95	70.8
0.49	0.633	0.98	13.3	1.47	37.3	1.96	71.6
0.5	0.711	0.99	13.6	1.48	37.9	1.97	72.4
0.51	0.791	1	14	1.49	38.5	1.98	73.3
0.52	0.88	1.01	14.4	1.5	39.2	1.99	74.1
0.53	0.98	1.02	14.8	1.51	39.8	2	74.9
0.54	1.09	1.03	15.2	1.52	40.4	2.01	75.7
0.55	1.2	1.04	15.7	1.53	41	2.02	76.5
0.56	1.31	1.05	16.1	1.54	41.6	2.03	77.4
0.57	1.43	1.06	16.5	1.55	42.2	2.04	78.2
0.58	1.57	1.07	16.9	1.56	42.9	2.05	79
0.59	1.71	1.08	17.3	1.57	43.5	2.06	79.9
0.6	1.86	1.09	17.8	1.58	44.3	2.07	80.7
0.61	2.02	1.1	18.2	1.59	44.8	2.08	81.6
0.62	2.18	1.11	18.7	1.6	45.5	2.09	82.5
0.63	2.35	1.12	19.1	1.61	46.1	2.1	83.3
0.64	2.53	1.13	19.5	1.62	46.8	2.11	84.2
0.65	2.76	1.14	20	1.63	47.4	2.12	85
0.66	3	1.15	20.5	1.64	48.1	2.13	85.9
0.67	3.25	1.16	20.9	1.65	48.8	2.14	86.8
0.68	3.52	1.17	21.4	1.66	49.4	2.15	87.7
0.69	3.8	1.18	21.9	1.67	50.1	2.16	88.6
0.7	4.07	1.19	22.3	1.68	50.8	2.17	89.5
0.71	4.34	1.2	22.8	1.69	51.5	2.18	90.4
0.72	4.62	1.21	23.3	1.7	52.2	2.19	91.3
0.73	4.89	1.22	23.8	1.71	52.9	2.2	92.2
0.74	5.19	1.23	24.3	1.72	53.6	2.21	93.1
0.75	5.47	1.24	25.8	1.73	54.3	2.22	94
0.76	5.76	1.25	25.3	1.74	55	2.23	94.9
0.77	6.05	1.26	25.8	1.75	55.7	2.24	95.8
0.78	6.35	1.27	26.3	1.76	56.4	2.25	96.7
0.79	6.66	1.28	26.8	1.77	57.1	2.26	97.7
0.8	6.97	1.29	27.3	1.78	57.9	2.27	98.6
0.81	7.28	1.3	27.8	1.79	58.6	2.28	99.5
0.82	7.6	1.31	28.4	1.8	59.3	2.29	100
0.83	7.92	1.32	28.9	1.81	60.1	2.3	101
0.84	8.25	1.33	29.4	1.82	60.8	2.31	102
0.85	8.58	1.34	30	1.83	61.5	2.32	103
0.86	8.91	1.35	30.5	1.84	62.3	2.33	104
0.87	9.25	1.36	31.1	1.85	63.1	2.34	105
0.88	9.59	1.37	31.6	1.86	63.8	2.35	106
0.89	9.94	0.89	9.94	1.38	32.2	1.87	64.6
0.4	0.008	0.9	10.3	1.39	32.7	1.88	65.3
0.41	0.07	0.91	10.6	1.4	33.3	1.89	66.1

Appendix H
EC vs water temperature regression

Simple linear regression analysis was conducted for the two high conductivity events experienced at the upstream and downstream surface water gauging stations on JD358 and JD019 respectively. Resulting Statgraphic Centurion (Version 15.2.12) are presented below. Results show a weak relationship between conductivity and water temperature during both events.

Output 1: Upstream surface water conductivity (US EC) vs upstream surface water temperature (US temp) JD358.

Simple Regression - log10(US EC) vs. log10(US Temp)
Dependent variable: log10(US EC)
Independent variable: log10(US Temp)
Linear model: Y = a + b*X

Analysis of Variance

Source	*Sum of Squares*	*Df*	*Mean Square*	*F-Ratio*	*P-Value*
Model	0.0000028813	1	0.0000028813	1.37	0.2452
Residual	0.000146872	70	0.00000209817		
Total (Corr.)	0.000149753	71			

Correlation Coefficient = 0.138709
R-squared = 1.92403 percent
R-squared (adjusted for d.f.) = 0.522946 percent
Standard Error of Est. = 0.00144851
Mean absolute error = 0.00119788
Durbin-Watson statistic = 0.0396199 (P=0.0000)
Lag 1 residual autocorrelation = 0.94153

The output shows the results of fitting a linear model to describe the relationship between log10(US EC) and log10(US Temp). The equation of the fitted model is

log10(US EC) = 1.18707 + 0.998984*log10(US Temp)

Since the P-value in the ANOVA table is greater or equal to 0.05, there is not a statistically significant relationship between log10(US EC) and log10(US Temp) at the 95.0% or higher confidence level.

The R-Squared statistic indicates that the model as fitted explains 1.92403% of the variability in log10(US EC). The correlation coefficient equals 0.138709, indicating a relatively weak relationship between the variables. The standard error of the estimate shows the standard deviation of the residuals to be 0.00144851.

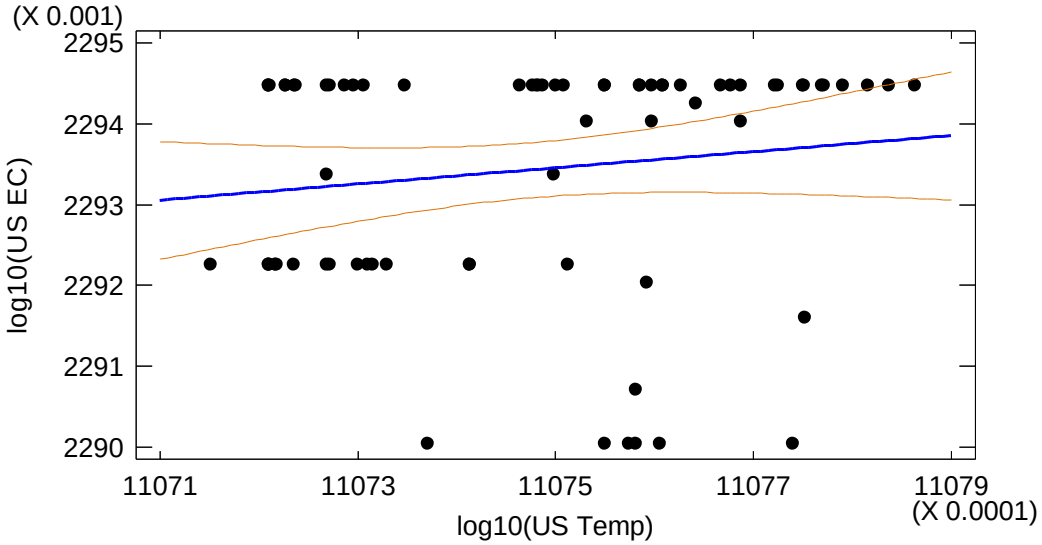

Figure J.2. Fitted linear relationship (blue line) between upstream surface water electrical conductivity (US EC) and water temperature (US temp) JD358. 95% confidence limits are also presented on both sides of the fitted regression (orange lines).

Appendix I
Principal Component Analysis output

Results from Principal Component Analysis suggest a moderate relationship between upstream surface water stage and precipitation (Component 1 – Table K.1, Figure K.1). This is to be expected as precipitation drives increases in surface water stage. The breakdown of this relationship is likely due to the delay of precipitation waters arriving at the stream and initiating an increase in surface water stage. Surface water conductivity is inversely related to surface water stage (Component 1).

Groundwater conductivity was inversely related to groundwater stage, while groundwater stage was slightly correlated to surface water stage (Component 2 – Table K.1). Interestingly groundwater stage has a slight inverse relationship to precipitation.

Table K.1. Individual component loadings for daily average upstream surface and groundwater data JD324-051, Mangatarere catchment. Loadings present the relationship between variables with negative loadings indicate an inverse relationship. 'GW EC' denotes upstream groundwater electrical conductivity, 'GW stage' denotes upstream groundwater stage, 'SW EC' denotes upstream surface water electrical conductivity, 'SW stage' denotes upstream surface water stage and 'Reid Prec' denotes precipitation.

	***Component* 1**	***Component* 2**
GW EC	0.165416	-0.538616
GW Stage	-0.100452	0.748786
SW EC	-0.619201	-0.0537151
SW stage	0.619368	0.338623
Reid Prec	0.442178	-0.177938

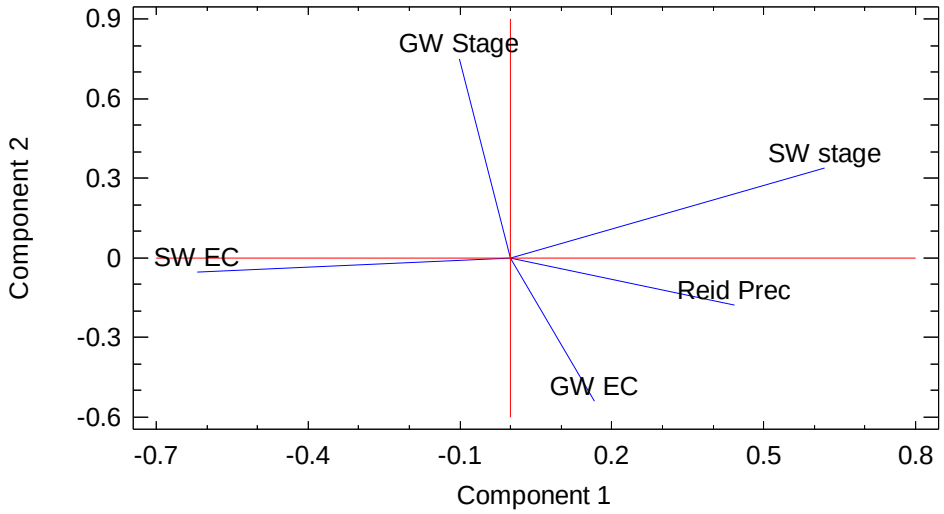

Figure K.1. Principal Component Analysis 2D component plot for average daily upstream ground and surface water stage, electrical conductivity and precipitation data, Mangatarere catchment, New Zealand. Component 1 explains 40% of the total variance while Component 2 explains 27% of the total variance. 'GW EC' denotes upstream groundwater electrical conductivity, 'GW stage' denotes upstream groundwater stage, 'SW EC' denotes upstream surface water electrical conductivity, 'SW stage' denotes upstream surface water stage and 'Reid Prec' denotes precipitation.

Appendix J
Remaining hydrochemical parameters

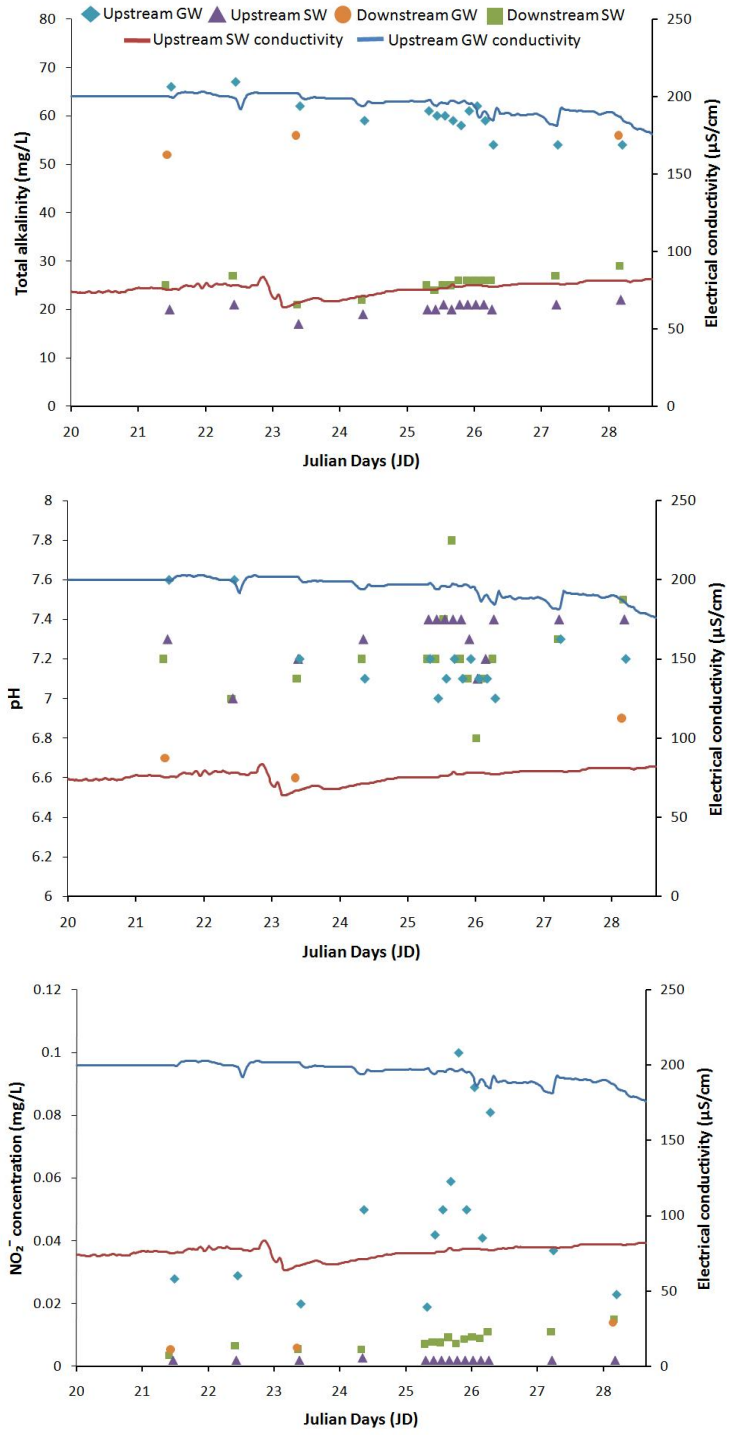

Figure L.1. Temporal variations in Total alkalinity, pH and NO_2^- at the upstream and downstream surface and groundwater stations JD020-028. Upstream surface and groundwater conductivity are also shown on the secondary axis for comparison.